Helsinki University of Technology Water Resources Publications

Teknillisen korkeakoulun vesitalouden ja vesirakennuksen julkaisuja

Espoo 2002 TKK-VTR-5

EFFECTS OF METEOROLOGICAL CONDITIONS AND WATER MANAGEMENT ON HYDROLOGICAL PROCESSES IN AGRICULTURAL FIELDS

PARAMETERIZATION AND MODELING OF ESTONIAN CASE STUDIES

Toomas Tamm

Dissertation for the degree of Doctor of Science to be presented with the permission of the Department of Civil and Environmental Engineering for public criticism in Auditorium R1 at Helsinki University of Technology, Espoo, Finland on the 13th of December, at 12 o'clock noon.

Helsinki University of Technology
Department of Civil and Environmental Engineering
Laboratory of Water Resources Engineering

Teknillinen korkeakoulu
Rakennus- ja yhdyskuntatekniikan osasto
Vesitalouden ja vesirakennuksen laboratorio

Tamm, T. 2002. Effect of meteorological conditions and water management on hydrological processes in agricultural fields: Parameterization and modeling of Estonian case studies.
Water Resources Publications TKK-VTR-5. Espoo 2002, 194 pp.

Distribution:
Helsinki University of Technology
Water Resources Laboratory
B.O.Box 5300
FIN-02015 HUT
Tel. +358-9-451 3821
Fax. +358-9-451 3827
E-mail: contact@water.hut.fi

ISBN 951-22-6207-X (print)
ISBN 951-22-6240-1 (PDF)
ISSN 1456-2596

Otamedia Oy
Espoo

HELSINKI UNIVERSITY OF TECHNOLOGY
Civil and Environmental Engineering

Abstract of Doctoral thesis

Author: Toomas Tamm
Thesis: Effect of meteorological conditions and water management on hydrological processes in agricultural fields: Parameterization and modeling of Estonian case studies.

Date: 13.12.2002 Pages: 194
Professorship: Water Resources Engineering Code: Yhd-12

Supervisor: Professor Tuomo Karvonen

This thesis was a study of the effect of meteorological conditions and water management on hydrological processes in agricultural fields. The emphasis was put on parameterization, validation and critical analysis of the different methods commonly used in field-scale hydrological models.

The study object was a two dimensional soil profile covered with cultivated grass that completely shaded the ground. Both energy and water balance components were estimated and compared with observed values and experimental results. A standard procedure for estimating net radiation was parameterized with new values to get a better fit with observed radiation in Estonia. The commonly used set of parameters were found to systematically overestimate net radiation during the summer months and underestimate in winter months. New equations for the net long-wave radiation that may also be used in the Priestley-Taylor equation were developed.

Soil heat flux was estimated numerically for both bare soil and grass covered soil. The soil heat flux from grass-covered surfaces was less than 10% of the net radiation during the March-September period. The highest soil heat flux, in June (21 MJ m^{-2} $month^{-1}$), was equal to 5.8% of net radiation. The largest relative value, in October (-13.7 MJ m^{-2} $month^{-1}$), was equal to -173.4% of net radiation.

Measured evapotranspiration obtained from the hydraulic pan covered with a clipped grass canopy was used to validate the Penman-Monteith equation in Estonian conditions. In three out of four years the results were very good. The highest coefficient of determination was obtained in May 1985 (r^2=0.922), and the lowest in July 1988 (r^2=0.421). On a monthly basis comprising all years of experimentation the correlation was the best in June (r^2=0.913). It was also shown that vapor pressure deficit correlated well with net radiation both on a daily basis (r^2=0.602) and on a long-term monthly basis (r^2=0.976). These results validate the use of the Priestly-Taylor equation in Estonian conditions. A comparison of the measured and estimated evapotranspiration revealed a higher r^2 with the Penman-Monteith method. However the difference between the two methods was small to negligible in several months.

Water retention curves and soil hydraulic conductivity functions were determined with two methods: 1) Wind's evaporation method and 2) Andersson's method based on the soil particle size distribution. Wind's method yielded a rather smooth curve for $\theta(h)$ and a scattered cloud for K(h). The shape of the water retention curves were unexpectedly of a 'clay'-type, although the clay fraction was small in the samples. Andersson's method resulted in 'loamy soil'-type curves.

The experiment of controlled drainage by raising the water table at a nearby ditch showed that with very simple and low-cost hydraulic structures the water regime in an adjacent field could be affected. The agro-hydrological model, SWAP, developed in the Netherlands, was used to simulate the controlled drainage experiment. Calculated depths of the groundwater table and drainage flux using SWAP and CROPWATN (developed in Finland) were almost identical. The effect of different drainage design parameters, soil properties and different water management strategies was revealed using CROPWATN for continuous simulations over a period of 30 years.

TEKNILLINEN KORKEAKOULU
Rakennus- ja yhdyskuntatekniikan osasto

Väitöskirjan tiivistelmä

Tekijä: Toomas Tamm
Työn nimi: Meteorologisten olosuhteiden ja vesitalouden säädön vaikutus peltoalueiden hydrologisiin prosesseihin: Virolaisten esimerkkitapausten parameterisointi ja mallitaminen.

Päiväys: 13.12.2002 Sivumäärä: 194
Professuuri: Vesitalous ja vesirakennus Koodi: Yhd-12

Valvoja: Prof. Tuomo Karvonen

Tämän työn päätavoitteena oli tutkia meteorologisten olosuhteiden ja pellon vesitalouden säädön vaikutusta hydrologisen kierron komponentteihin. Erityisesti keskityttiin yleisesti käytössä olevien mallien ja menetelmien parametrisointiin, validointiin ja niiden soveltuvuuden arviointiin.

Työssä tutkittiin kaksidimensionaalista profiilia, jossa maanpinta oli yhtenäisen kasvillisuuden peitossa. Tutkimuksessa arvioitiin sekä maanpinnan energia- että vesitaseen komponentit ja estimoituja tuloksia verrattiin koekentillä mitattuihin arvoihin. Työssä määritettiin uudet, paremmin Viron olosuhteisiin soveltuvat parametriarvot nettosäteilyn laskemiseksi. Aiemmin yleisesti käytössä olleet menetelmät yliarvioivat systemaattisesti kesäajan nettosäteilyn ja aliarvioivat sen talvikuukausina. Työssä kehitettiin uudet laskentakaavat pitkäaaltoiselle säteilylle. Tuloksia voidaan käyttää laskettaessa potentiaalista evapotranspiraatiota Priestley-Taylorin menetelmällä.

Maan lämmönvaihdon osuus koko säteilytaseesta arviotiin numeerisilla malleilla sekä paljaalle, että ruohopeitteiselle pinnalle. Maan lämmönvaihdon osuus ruohopeitteisen pinnan energiataseesta oli pienempi kuin 10 % nettosäteilystä maalis-syyskuun välisenä ajanjaksona. Maan lämmönvaihdon absoluuttinen arvo oli suurin heinäkuussa (21 MJ m^2 kk^{-1}, 5.8 % nettosäteilystä) ja suhteellinen arvo oli korkein lokakuussa (-13.7 MJ m^2 kk^{-1}, -173.4 % nettosäteilystä).

Ruohopeitteisestä, punnitsevasta haihdunta-astiasta mitattua todellista evapotranspiraatiota käytettiin validoitaessa Penman-Monteithin menetelmää Viron olosuhteisiin. Kolmena vuotena neljästä menetelmän antamat tulokset olivat erittäin hyviä. Vuorokausiarvojen korrelaatio oli paras toukokuun 1985 mittauksille (r^2=0.922) ja huonoin kesäkuun 1988 aineistolle (r^2=0.421). Kuukausitasolla paras selitysaste saatiin kesäkuun havainnoille (r^2=0.913). Työssä osoitettiin myös, että Priestley-Taylorin kehittämä potentiaalisen haihdunnan laskentakaava soveltuu hyvin Viron olosuhteisiin. Tämä perustuu siihen, että kyllästysvajauksen ja nettosäteilyn välillä oli hyvä korrelaatio sekä vuorokausitasolla (r^2=0.602), että kuukausiarvoilla (r^2=0.976). Penman-Monteithin ja Priestley-Taylorinin menetelmillä laskettuja haihdunnan arvoja verrattiin mitattuihin ja ensin mainittu antoi hieman parempia tuloksia, mutta erot olivat melko pieniä.

Vedenpidätyskäyrä ja kyllästymättömän maan hydraulinen johtavuus arvioitiin kahdella eri menetelmällä: 1) Windin haihduntamenetelmällä ja 2) Anderssonin kehittämällä menetelmällä, joka perustuu rakeisuuskäyrän käyttöön. Windin menetelmän antaman pF-käyrän keskihajonta oli pieni, mutta K(h)-käyrä tulostui pisteparvena. Vedenpidätyskäyrä muistutti tyypillistä saven käyrää vaikka näytteiden saven osuus oli hyvin pieni. Anderssonin menetelmä antoi tulokseksi hiesumaan tyypillisen vedenpidätyskäyrän.

Säätösalaojituskoe osoitti, että pellon vesitalouteen voidaan vaikuttaa yksinkertaisella ja halvalla patorakenteella, jolla nostettiin vedenpintaa läheisessä valtaojassa. Hollannissa kehitettyä SWAP-mallia käytettiin simuloitaessa säätösalaojituskokeen vaikutuksia pellon vesitalouteen. SWAP-mallilla ja Suomessa kehitetyllä CROPWATN-mallilla lasketut pohjavedenpinnan syvyyden ja salaojavalunnan tulokset olivat lähes identtisiä. Kuivatuksen suunnitteluparametrien, maalajin ja eri säätövaihtoehtojen vaikutus hydrologisiin prosesseihin pitkällä aikavalillä arvioitiin käyttäen 30 vuoden meteorologista havaintojaksoa ja CROPWATN-mallia.

HELSINKI TEHNIKAÜLIKOOL
Ehitus- ja keskkonnatehnika osakond

Doktoritöö kokkuvõte

Autor: Toomas Tamm
Pealkiri: Meteoroloogiliste tingimuste ja veemajanduslike meetmete mõju põllumajanduslike maade hüdroloogilistele protsessidele: parameetrite määramine ja modelleerimine Eesti näidetel.

Kuupäev: 13.12.2002 | Lehekülgi: 194
Professuur: veemajandus ja vesiehitus | Kood: Yhd-12

Juhendaja: prof. Tuomo Karvonen

Käesoleva töö eesmärk oli uurida meteoroloogiliste tingimuste ja veemajanduslike meetmete mõju põllumajandusliku maa hüdroloogilistele protsessidele. Põhitähelepanu pöörati põllutasandi hüdroloogiliste mudelite parameteriseerimisele, kontrollimisele ja kriitilisele analüüsile.

Uurimisobjektiks oli kahedimensionaalne pinnaseprofiil maapinda täielikult katva kultuurrohumaaga. Arvutustega leiti energia ja veebilansi komponentide väärtused, mida võrreldi vaatlus- ning eksperimentaaltulemustega. Netokiirguse (kiirgusbilansi) arvutamise standardmeetodi jaoks leiti Eesti oludesse sobivad uued väärtused, sest standardparameetrid ülehindasid süstemaatiliselt netokiirgust suvekuudel ja alahindasid talvekuudel. Priestley-Taylori meetodi jaoks pakuti välja uued lihtsad pikalainelise kiiruse arvutamise valemid.

Rohumaa ja taimkatteta ala pinnases neeldunud kiirgus arvutati mitmete meetoditega. Rohumaa puhul moodustas neeldunud kiirgus perioodil märts kuni september vähem kui 10% netokiirgusest, olles suurima absoluutväärtusega juunis (21 MJ m^{-2} kuu^{-1}, võrdne 5,8% netokiirgusest) ja suhteliselt suurim oktoobris (-13,7 MJ m^{-2} kuu^{-1}, võrdne -173,4% netokiirgusest).

Hüdraulilise aurumismõõtlaga saadud evapotranspiratsiooni mõõtmistulemusi kasutati Penman-Monteith'i valemi kontrollimiseks Eesti tingimustes kultuurrohumaaga kaetud pinnalt. Kolmel aastal neljast olid tulemused väga head. Suurim korrelatsioonikoefitsient oli 1985 aasta mais (r^2=0,922) ja väikseim 1988 aasta juulis (r^2=0,421). Kõiki eksperimendiaastaid hõlmavas kuudearvestuses oli suurim korrelatsioon juunis (r^2=0,913). Veeaurudefitsiit korreleerus väga hästi netokiirguse ööpäevaste andmetega (r^2=0,602) ja veelgi paremini pikaajaliste kuuandmetega (r^2=0,976), mis omakorda viitab põhjustele, miks Priestley-Taylor'i meetod on Eesti tingimustes kasutatav. Korrelatsiooniga mõõdetud aurumise ja Penman-Monteith'i meetodiga arvutatud aurumise vahel oli veidi parem kui Priestley-Taylor'i meetodiga, kuid mitmel kuul erinevus praktiliselt puudus.

Mullaveepinge ja hüdraulilise juhtivuse kõverad leiti kahe meetodiga: 1) Wind'i aurumismeetodi ja 2) Anderssoni meetodiga, mis kasutab pinnase sõelkõverate andmeid. Wind'i meetod andis väga väikese hajuvusega mullaveepingekõvera ja hajusa pilve K(h)-punktipaaride korral. Leitud mullaveepingekõver osutus vastu ootusi sarnaseks tüüpilisele savimullale, kuigi tegelik savifraktsiooni sisaldus oli väike. Anderssoni meetodiga leitud mullaveepingekõver vastas rohkem saviliivale.

Kontrolldrenaažieksperiment näitas, et kraaviga piirneva põllu veerežiimi võib mõjutada väga väikeste kulutustega teostatava regulaatoriga äravoolukraavil. Kontrolldrenaaži modelleerimiseks kasutati Hollandis väljatöötaud mudelit SWAP. SWAP'i ja Soomes väljatöötatud mudeli CROPWATN võrdluses osutusid arvutatud põhjaveetasemed ja dreeniäravoolu väärtused praktiliselt identseteks. CROPWATN'i kasutati 30 aastat hõlmavateks pikaajalisteks arvutusteks, et uurida kuivendussüsteemi parameetrite, mullaomaduste ja erinevate kuivendusmeetmete mõju põllu hüdroloogilistele protsessidele.

Acknowledgements

This work had been conducted while the author worked as a lecturer at the Estonian Agricultural University, Institute of Water Management in Tartu, Estonia, simultaneously visiting Finland to complete postgraduate studies at the Helsinki University of Technology and at the Helsinki University. I wish to express my gratitude towards all three Universities and the people working in them who were teaching and helping me.

I am most grateful to my supervisor Professor Tuomo Karvonen from the Laboratory of Water Resources for the teaching, discussions and criticism, and for helping to arrange oversea studies.

I want to thank the people working at the division of the Soil Chemistry and Physics at the University of Helsinki where I started my studies in Finland, also the students' affairs secretary of the Faculty of Agriculture and Forestry, University of Helsinki, Jaakko Hannula, who kindly helped me enter into university life. Also, I want to thank the people working at the Laboratory of Water Resources, especially Professor Pertti Vakkilainen for long debates concerning the evaporation phenomena. Professor Erkki Aura and Docent Risto Lemmelä are gratefully acknowledged for their pre-examination of the manuscript of my thesis.

I am also indebted to numerous people for helping to arrange field experiments, especially Mr. Toomas Timmusk together with whom the control drainage experiment was established, Mr. Väino Tamm, my father, for supplying the data of the lysimeter evapotranspiration experiments and to Mr. Ain Kallis from the Actinometric Station of Tõravere of the Estonian Institute of Meteorology and Hydrology for providing necessary data.

This study was partly financially supported by the Estonian Science Foundation (Grant No 2074), the Research Foundation of the Helsinki University of Technology and the Foundation of the Finnish Field Drainage Center. I also want to thank Mr. Rauno Peltomaa and Mr. Jussi Saavalainen for their personal support. I also express my gratitude to Mrs. Ester Jaigma (Tartu) and Mr. Jaak Järve (Toronto) for the English language revision of my thesis.

Finally, I thank my parents for their continuing support. Most of all, I am grateful to my wife Egle and our daughter Agnes for enduring my long trips away in Finland.

Tartu, Estonia, May 23, 2002

Toomas Tamm

Table of contents

List of Symbols

Roman alphabet

$a_{c'}$	empirical cloudiness coefficient [-]
a_e	empirical emissivity coefficient [-]
a_s	empirical solar coefficient [-]
A_0	amplitude of the surface temperature fluctuation [K]
A	area of cross-section of the monolith [m^2]
b_c	empirical cloudiness coefficient [-]
b_e	empirical emissivity coefficient [-]
b_s	empirical solar coefficient [-]
c	bulk specific heat [J kg^{-1} K^{-1}]
c_p	specific heat of moist air (= 1.013 kJ kg^{-1} $°C^{-1}$)
c_s	specific heat of dry soil [J kg^{-1} K^{-1}]
C	differential soil water capacity ($d\Theta/dh$) [cm^{-1}]
C'	bulk specific heat capacity [J kg^{-1} K^{-1}]
C_S	volumetric specific heat capacity [J m^{-3} K^{-1}]
d	zero plane displacement height [m]
d_d	*damping depth*, at which the temperature amplitude decreases to the fraction 1/e of the amplitude at the soil surface A_0 [m]
d_{eq}	equivalent depth from the drain level to the impervious layer
D_a	thermal diffusivity [m^2 s^{-1}]
e_a	vapor pressure [kPa]
$e_s(T)$	saturated vapor pressure at temperature T [kPa]
E	evaporation rate [mm d^{-1}]
ET	evapotranspiration rate [mm d^{-1}]
f	adjustment for cloud cover
G	soil heat flux [MJ m^{-2} d^{-1}]
h	soil water pressure head [cm]
h_{drain}	the height of the water table above water level in the drain [m]
k	von Karman's constant (=0.41)
K	hydraulic conductivity [cm d^{-1}]
K_{sat}	saturated hydraulic conductivity [cm d^{-1}]
K_T	thermal conductivity [J m^{-1} s^{-1} K^{-1}]
l_{lys}	sinking depth of hydraulic pan [cm]
L_{drain}	drain spacing [m]
LAI_{active}	active (sunlit) leaf area index [m^2 (leaf area) m^{-2} (soil surface)]
m	empirical shape factor [-]; mass of the monolith [kg]
n	duration of bright sunshine [h]; empirical shape factor [-]
N	total day length [h]
P	precipitation [mm d^{-1}]
q	soil water flux density [cm d^{-1}]
q_{drain}	drainage flux density [cm d^{-1}]
q_{surf}	surface runoff [mm d^{-1}]
q_{bot}	bottom flux [mm d^{-1}]
r_a	aerodynamic resistance [s m^{-1}]
r_c	canopy resistance [s m^{-1}]
r_s	bulk stomatal resistance of the well-illuminated leaf [s m^{-1}]
R_a	extraterrestrial radiation [MJ m^{-2} d^{-1}]
$R_{s,c'}$	clear day irradiance [MJ m^{-2} d^{-1}]

R_D diffuse radiation [MJ m^{-2} d^{-1}]
RH relative humidity [%]
R_I direct solar radiation [MJ m^{-2} d^{-1}]
R_n incoming net radiation [MJ m^{-2} d^{-1}]
R_{nl} long-wave radiation [MJ m^{-2} d^{-1}]
R_s total incoming short-wave radiation [MJ m^{-2} d^{-1}]
t day number [-]
T temperature [°C]
T_{ave} average temperature [°C]
T_p potential transpiration [cm d^{-1}]
u_z wind speed at height z [m s^{-1}].
u_{drain} wet perimeter of drain [m]
VPD vapor pressure deficit [kPa]
W total soil water content in the soil profile [mm]
x volumetric fraction [m^3 m^{-3}]
z gravitational head [cm]; vertical coordinate [m]
z_m height of wind measurements [m]
z_h height of humidity measurements [m]
z_{om} roughness length governing momentum transfer [m]
z_{oh} roughness length governing transfer of heat and vapor [m]

Greek alphabet

α albedo [-]; empirical coefficient [-]
α_{rw} reduction coefficient for root water uptake, [-]
Δ slope of the vapor pressure curve [kPa °C^{-1}]
ε' net emissivity
ϕ_0 phase constant [rad]
ϕ_{GWL} groundwater level [cm]
ϕ_{drain} the drain level [cm]
γ psychrometer constant [kPa °C^{-1}]
γ^* apparent value of psychrometer constant $=\gamma(r_a+r_c)/r_a$
γ_{tot} total drainage resistance [d]
γ_{drain} drainage resistance [d]
γ_{entr} entrance resistance [d]
λ latent heat of vaporization [MJ kg^{-1}]; empirical shape factor [-]
Θ volumetric water content [cm^3 cm^{-3}]
Θ_{sat} saturated water content [cm^3 cm^{-3}]
Θ_{res} residual water content [cm^3 cm^{-3}]
ρ density [kg m^{-3}]
ρ' soil bulk density [kg m^{-3}]
σ Stefan-Boltzmann constant [4.903×10^{-9} MJ m^{-2} °K^{-4} d $^{-1}$]
τ time in seconds from the beginning of the year [s]
ϖ radial frequency [s^{-1}]

Other subscripts

s, l, g solid, liquid and gaseous component, respectively
i enumerates node i

List of Tables

List of figures

Chapter 1

INTRODUCTION

1.1 Conceptual framework of water balance modeling

The hydrologic processes of precipitation, runoff, evaporation, transpiration, infiltration and drainage are of great importance. An understanding of these hydrological processes has both an academic and practical value. This understanding enables society to better manage food production, to reduce the pollution of ground and surface waters, and to anticipate the risks of drought or flooding that would arise with global climate change. These processes have been studied at different scales, embracing global scenarios, watersheds and small pot experiments. However, one important scale is a field with a relatively homogeneous canopy cover, homogeneous soil properties and which has measures to control the water regime (e.g. a typical agricultural field of cultivated grassland or cereal crops). Hydrological processes occurring at this scale are very often described in quasi-two-dimensional models that consider the vertical soil profile with vertical fluxes within it and with certain rules to consider lateral fluxes. This kind of soil profile has permeable boundaries though which the domain interacts continually with its surroundings (Fig. 1.1). Between upper and lower boundary lies the flow domain – a soil matrix where the liquid water containing dissolved substances and gaseous compounds are moving. In fact, the field is a very complex system: plants are growing at the top of this profile and depend on the available energy, water and nutrients; available energy and water influence the complicated turnover processes from organic matter to mineral compounds; the soil matrix has more or less constant hydro-physical properties; the natural or artificial groundwater regime depends on changing meteorological conditions. All these processes, both the abiotic and biotic factors, often imperfectly understood interactions have been used to formulate mathematical equations. Thus, the contemporary soil-plant-atmosphere models may consist from dozens to hundreds of differential equations, which have to be solved and parameterized. Although numerical models have become more and more sophisticated, their success and reliability are critically dependent on accurate information of hydrological system parameters (Schaap and Leij 2000).

The author believes that it is worth once again to check how common procedures and 'standard' parameters fit with reality, particularly in that local environment where the problems must be solved. If model parameters are drawn from diverse sources, as they usually are, then it is difficult to assess how compatible these parameters are and to foresee how these possible incompabilities affect the model's results. Also, it is often implicitly assumed that these parameters, particularly empirical constants, refer to 'true' values, missing the fact these values may be measured in completely different conditions and that all measurements contain measurement errors. In worst cases these parameters are altered and used in impossible combinations in an attempt to model incremental scenarios in climate change studies. This situation became particularly apparent when the author attempted to resolve water balance problems in Estonian agricultural fields.

Although Estonian soils are terminologically and pedologically well studied (Reintam 1995, Kask 1996), no information was found about soil hydraulic functions. Although there are more than twenty meteorological stations, but radiation is measured only in two and, thus, it must be estimated from meteorological parameters. Although more than 750 thousand of hectares have been drained no database is available to validate the model made in Holland or Finland with Estonian experimental data. This list can be extended. Thus, the purpose of this study is to fill several gaps in Estonian environmental studies.

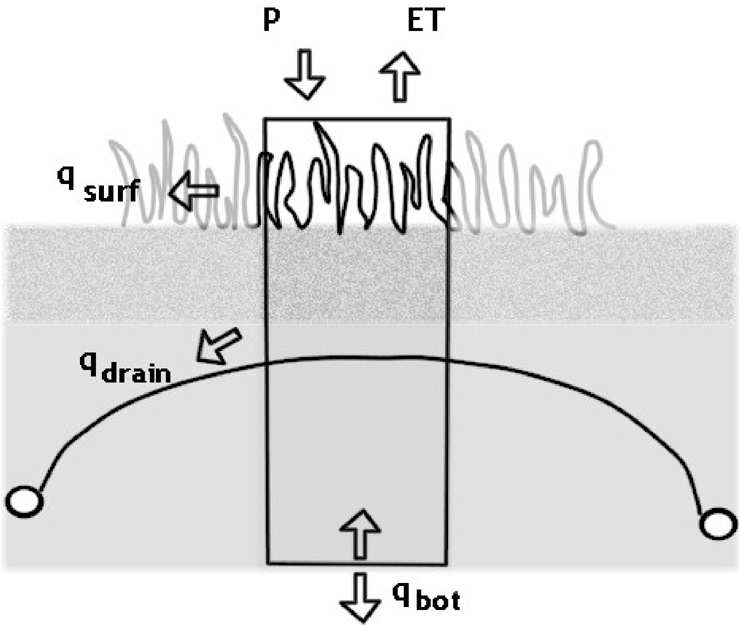

Figure 1.1. Hydrological flow processes at the field scale level. *P* - precipitation, *ET* - evapotranspiration, q_{surf} - surface runoff, , q_{drain} - drainage runoff, q_{bot} - bottom flux.

1.2 The scope and objectives of this study

In this study the hydrological processes in agricultural fields, their estimation procedures and then parameterization are investigated. Both energy and water balance components are estimated and compared with observed or experimental values based on Estonian case studies (Fig. 1.2). The study object is a two dimensional soil profile covered with cultivated grass that completely shades the ground. The soil moisture regime is influenced by meteorological conditions, soil and canopy properties, and by natural or controlled drainage. The soil profile is viewed as a flow domain, which is bounded with upper and lower boundaries through which the domain receives and loses water and energy. It must be emphasized that the definition of boundaries here is broader than usual. The upper boundary is located just above the vegetation for energy partitioning and for receiving-loosing water by precipitation-evapotranspiration. In the case of the lower boundary, both bottom flux and drainage flux are considered together. In the next chapters the various elements of the energy and water balance are described in more detail starting with the upper boundary processes, then dealing with physical properties of the flow domain, and finally the effect of a fluctuating groundwater table at the lower part of the soil profile is studied.

The main emphasis in this study is to validate the common equations and procedures in water balance models, to calibrate these methods, and if necessary, to critically evaluate these methods.

The specific objectivities were to:

1. Validate and calibrate, if necessary, the estimation procedures of net radiation and soil heat flux using Estonian observations.

2. Validate the Penman-Monteith and Priestley-Taylor methods with data of actual evapotranspiration measured at Tartu, Estonia.

3. Measure and estimate water retention curves and unsaturated hydraulic conductivity functions of typical South-Estonian soil. Assess the problems occurring when these curves are described with van Genuchten equations.

4. Assess the effect of water table management on soil water conditions using experimental data.

5. Validate and assess the agro-hydrological model SWAP with experimental data.

6. Compare agro-hydrological models SWAP and CROPWATN in assessing the effects of climatic variability on the soil water balance in conditions of different drainage strategies and using long-term meteorological dataset.

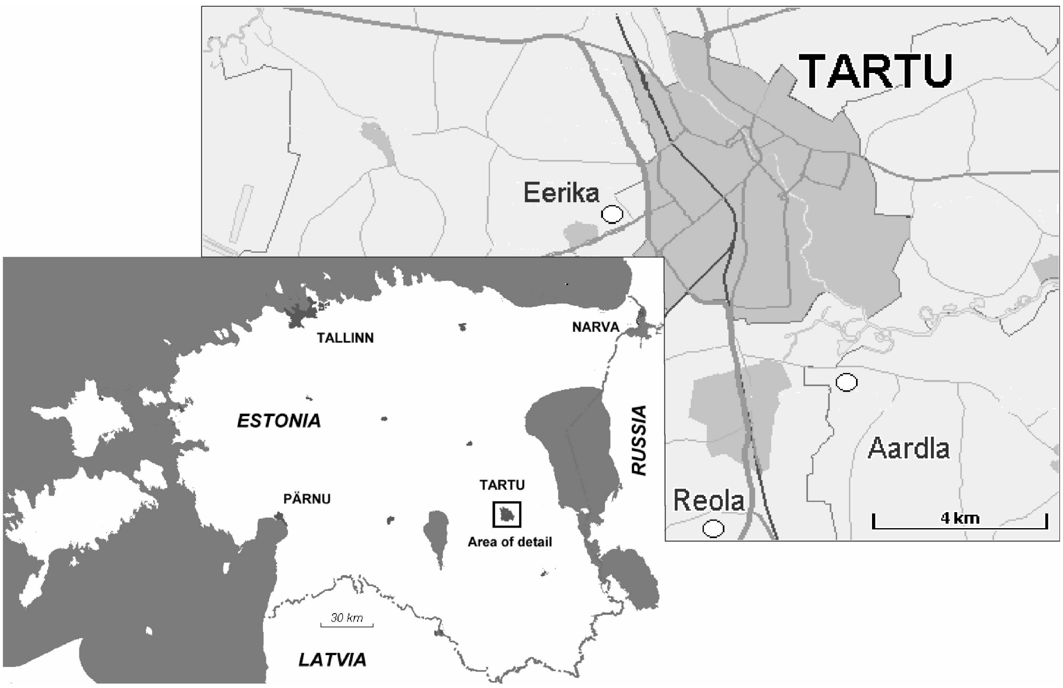

Figure 1.2. Location of the three case studies: lysimeter experiments at Eerika and at Polder of Aardla (Chapter 3), and the control drainage experiment at Reola (Chapter 5 and 6).

1.3 Organization of the thesis

The thesis is organized into eight chapters:

Chapter 1 is a short introduction to the subject and outline of the study.

Chapter 2 describes energy partitioning at the upper boundary. The main approaches of measurement and estimation of evapotranspiration are reviewed. The common procedures to estimate net radiation and its components are described with a comparison of observed values. Soil heat flux is calculated with a numerical model and its importance in energy partitioning is analyzed.

Chapter 3 is a case study of an evapotranspiration measurement with a hydraulic evaporation pan. Two widely known evapotranspiration methods, Penman-Monteith and Priestley-Taylor, are validated with measured evapotranspiration. Actual canopy resistance is estimated by backward calculation. The possibility of using the simpler Priestley-Taylor method instead of the Penman-Monteith method is analyzed. Finally, the theoretical problems arising from the character of the Penman-Monteith method are discussed.

Chapter 4 describes the problems when the soil hydraulic properties are measured and estimated. Wind's evaporation method is used to measure water retention curves and hydraulic conductivity functions. Andersson's method is used to predict the water retention function. The problematic character of the van Genuchten equations in near-saturation conditions is discussed.

Chapter 5 describes the case study of controlled drainage and its effect on the water regime in the soil. The soil moisture profiles of three study plots are compared to find differences in soil moisture content depending on the distance and elevation from the raised water level at the adjacent drainage ditch. Complementary soil moisture estimation methods, tensiometers and nylon blocks are described and their reliability is discussed.

Chapter 6 evaluates the agro-hydrological model SWAP by comparing the measured soil moisture values and the groundwater table with and without controlled drainage. Experimental data obtained from the controlled drainage experiment (Chapter 5) is used to calibrate and to evaluate SWAP in Estonian conditions.

Chapter 7 compares agro-hydrological models SWAP and CROPWATN and analyses the effect of long-term meteorological conditions on the soil water balance.

Chapter 8 presents the summary.

Chapter 2

UPPER BOUNDARY

2.1 Introduction

Considering the soil profile as a flow domain, the upper boundary of this domain is defined as a contact layer between the soil, covered with canopy, and the atmosphere. This definition is broader than usually understood ('a thin skin of air in contact with the surface' by Monteith and Unsworth 1990). It includes all of the complex mass and energy transfer processes at the upper end of the flow domain. That complexity is caused by the interactive manner of the flows of water and of thermal energy, as the temperature gradients affect the liquid and vapor movement and, at the same time, the moisture gradients in the soil move water, which in turn carries heat. The example of the combined transport of heat and moisture process is an evaporation phenomenon. Its importance in the water cycle is well known for all environmental modelers as well as are problems arising in development of simulation and predictive models. Moreover, its importance is also well known for crop production modelers, as there is often a direct relation between the ratio of actual to potential evapotranspiration and the actual to potential crop yield (Feddes 1986, Feddes et al. 1997). The less considered phenomena is the soil heat flux where soil temperature varies in response to changes in the radiant, thermal, and latent energy exchange processes that take place primarily through the soil surface. However, by far the most interesting issue for agronomists and for environmental studies has been the water balance of the soil.

Upper boundary processes have a crucial effect on the water balance of the soil profile because the upper boundary receives all of the input water (except for capillary fringe from shallow groundwater aquifers) and loses a significant part of it. Both the properties of the topsoil and vegetation determine the distribution of rainfall into evaporation, transpiration, and percolation. Part of precipitation may also flow laterally towards a depression or a pond temporarily. Numerous physical, chemical and biological processes in topsoil are substantially influenced by water conditions and by available energy at the upper boundary. Therefore, the correct understanding of the complex processes at the upper boundary is essential for agricultural, environmental and climatic studies.

In general, downward and upward mass and energy fluxes can be distinguished and may be described by balance equations. The main components of the energy exchange of the upper boundary comprise radiative transfer, i.e. net radiation, R_n (the difference of incoming short-wave radiation and terrestrial long-wave radiation) [MJ m^{-2} d^{-1}], the sensible heat transfer H [MJ m^{-2} d^{-1}], transfer to or from surface, i.e. soil heat flux, G [MJ m^{-2} d^{-1}], and latent heat transfer, λE [MJ m^{-2} d^{-1}], i.e. a product of the evaporation rate E [mm d^{-1}] and the latent heat per unit quantity of water evaporated, λ [J kg^{-1}]:

$$R_n = H + G + \lambda E \tag{2.1}$$

Water balance is defined as any change that occurs in the water content ΔW of a soil profile during a specified period and it may have different components depending on the spatial and temporal scale (e.g. root zone only, whole soil profile from soil surface to impervious layer, all watershed etc.). A simple formula for the soil profile (Fig. 1.1) is as follows:

$$\Delta W = P_e - E - q_{surf} - q_{dr} - q_{bot} \tag{2.2}$$

where ΔW – is the change in soil water content in the soil profile [mm d^{-1}]
P_e – is effective precipitation, i.e. precipitation *minus* interception [mm d^{-1}]
E – is evaporative flux [mm d^{-1}]
q_{surf} – is surface runoff [mm d^{-1}]
q_{dr} – drainage outflow or inflow [mm d^{-1}]
q_{bot} – is bottom flux [mm d^{-1}]

In Eq. (2.2) two processes at the upper boundary, occurring in opposite directions – precipitation P end evaporation E – are influencing the direction of in the soil profile. In general, in excess periods when precipitation exceeds the evaporative flux, water infiltrated into the soil percolates downward causing the rise of groundwater level and drainage flux, whereas in dry periods when atmospheric demand exceeds precipitation, the upward flux, contributed by the groundwater table, is generated. Such a description is certainly simplified, but it points to the general flux pattern in the flow domain. In reality, the specific properties of the upper boundary, including surface cover and soil, determine the actual pattern of wetting and drying in the soil profile.

In Estonia only a few studies have been focused either on the theoretical analyses or practical measurements of evapotranspiration. The oldest and probably the most outstanding study was carried out by E. Oldekop who published the book 'On the evaporation from river watersheds' (*in Russian*) in 1911, where he proposed, after analyzing available hydrological data, the function of the hyperbolic tangent to estimate monthly actual evaporation from precipitation and from 'possible maximum' evaporation: $z = z_0\, tgh\left(\frac{x}{z_0}\right)$ where (original symbols) z_0 denoted possible maximum evaporation [mm], x denoted precipitation [mm], and z actual evaporation [mm]. Possible maximum evaporation was estimated empirically from vapor pressure deficit. A comprehensive theoretical study on the modeling of transpiration and photosynthesis was published by Z. Bihele, H. Moldau and J. Ross in 1980, unfortunately without experimental evidences. In the 70'ies H. Roostalu experimented with chamber systems (personal communication), V. Tamm (1975) studied evapotranspiration from irrigated agricultural crops and established a hydraulic lysimeter experiment in the 80'ies (Tamm 1994). Stomatal conductance and sap flow of forest canopies has been measured by Niinemets et al. (1999a, b). In neighboring countries, for example, the following studies have been conducted: in Finland Vakkilainen (1982), in Sweden (Sandsborg and Olofsson 1980, Halldin 1988).

Main emphasis in Chapter 2 was placed on the correct estimation of the components of the energy balance and on calibrating the existing component models with measurements made in Estonia. The sensitivity of the parameter was also considered. It should be emphasized that hereafter evapotranspiration is analyzed only in the context of relatively dense field canopies excluding sparse canopies and forest. The basic concepts and definitions in the next chapters are followed by Jensen et al. (1990), Burman and Pochop (1994), and Pereira et al. (1999).

2.2 Measurement approaches to evapotranspiration

Since evapotranspiration is included both in the water and energy balance, it is obvious how important it is to measure or estimate it correctly. In numerous studies where evapotranspiration is considered explicitly, the methods used to measure it vary considerably with respect to the evaporative area and time scale with certain implications for the accuracy of the experiment. These methods may be divided into different categories depending on the objectivity, and on the physical basis of the measurement technique or scale, e.g. from a single leaf to the entire watershed. According to the main approach or method the following groups can be distinguished (Rose and Sharma 1984): 1) hydrological approaches (*soil water balance*, *weighing lysimeters*), 2) micrometeorological approaches (*energy balance and Bowen ratio*, *aerodynamic method*, *eddy correlation*), and 3) plant physiology approaches (*sap flow method*, *chamber system*). The first group is hereafter extended to hydraulic evaporation pan described in Chapter 3, the second and third groups are only briefly mentioned.

Hydrological approaches

Soil water balance is an indirect method where evapotranspiration is determined as the residual of water balance (see Eq. 2.2) instead of measuring it directly. There exists a wide range of experiments: watershed studies, agricultural plots on which evaporation is estimated from changes in soil moisture content (TDR-based water balance, tensiometer readings, soil sampling, etc.), lysimeters of different size, and small scale laboratory column experiments. The common disadvantage of approaches to soil water balance is that all components of the balance equation are rarely measured, or even cannot be measured, and therefore, evaporation is not the only estimated value. For example, capillary upward flux into the soil profile may contribute substantially to the water balance, but it cannot be directly measured. Natural drainage flux or deep percolation is also rather difficult to measure. Precipitation is directly measurable with rain gauges. However, it is also known that precipitation records may involve systematic errors (Halldin 1988). Also, drainage flux may be measured as discharging from subsurface drainage pipes. Depending on the objectivity of the study, and on the spatial and time scale, a number of simplifications may occur, e.g. even the soil water storage term ΔW can be neglected in the case of long-term calculations. For example, at the watershed-scale evapotranspiration is obtained as the residual from difference between precipitation and runoff. These simplifications reduce the accuracy of evapotranspiration estimation. Thus, the *soil water balance* method is better applicable for small systems with controlled boundaries like lysimeters, while *water balance* method is suitable large-scale and long-term watershed studies.

Other approaches

The most direct method to measure the rate of evaporation is the *eddy correlation method* (WMO 1966). *Bowen ratio energy balance method* is based on the ratio of sensible to latent heat ($\beta = H/\lambda E$), where β is measured by the ratio of the air temperature difference between two levels to the vapor pressure difference at same levels ($\beta = \gamma \Delta T/\Delta e$). This method is used and analyzed in a number of studies using different climate and surface cover conditions (e.g. Revheim and Jordan 1976). *Aerodynamic method*, based on wind velocity and temperature profile measurements, is less used than the Bowen ratio method (Saugier and Ripley 1978, Ortega-Farias et al. 1996). Plant physiology approaches deal with a single plant or a group of plants where *sap flow method* is based either on determination of heat pulse or heat balance, *chamber systems* are applicable only in a fast measurement of evapotranspiration, where the rate of evapotranspiration is calculated from the vapor density difference before the chamber is placed on the surface and a short time after this period (e.g. 1 minute) (Reicosky and Peters 1977).

2.3 Computational approaches to evapotranspiration

For practical use, instead of measuring evapotranspiration, it is more applicable to calculate it using meteorological data collected at or near the study site. All methods more widely used in estimation of evaporation and evapotranspiration can be roughly divided into two groups: physically based (derived from the energy balance and resistance network, but may still involve slightly empirical approach) and more or less empirical methods. Some of the empirical methods are simplifications of physically based methods, demanding less input parameters and introducing empirical relationships between meteorological variables and evaporation, often with a local character. Empirical methods are not considered in the present paper with the exception of the semi-empirical Priestley-Taylor method.

The first group contains so called *combination equations*, more commonly known as Penman-based methods.

H.L.Penman (1948) was the first to derive an equation which combines the energy balance and the empirical description of the diffusion mechanism by which energy is removed from the surface as water vapor (Shuttleworth 1992). Hence it is known as a *combination equation*. The general form of the Penman equation is:

$$\lambda E = \frac{\Delta}{\Delta + \gamma}(R_n + G) + \frac{\gamma}{\Delta + \gamma} f(u) f(e) \tag{2.3}$$

where λE – is outgoing energy as evaporation [MJ m^{-2} d^{-1}]
λ – is latent heat of vaporization [MJ kg^{-1}]
R_n – is incoming net radiation [MJ m^{-2} d^{-1}]
G – is outgoing heat energy into the soil [MJ m^{-2} d^{-1}]
γ- is psychrometric constant [kPa °C^{-1}]
Δ - is slope of the vapor pressure curve [kPa °C^{-1}]
(u) – is empirical aerodynamic wind function [m s^{-1}]
f(e) – is function of vapor pressure deficit [kPa]

The empiricism involved in the description of the aerodynamic term was found to be beneficial due to the fact that the seasonal and local adjustments can be easily taken into account when deriving Penman-based equations for different locations. To this group belong several modifications based on experimental work conducted at Kimberly, Idaho, (Wright and Jensen 1972, Wright 1982, Jensen et al. 1990). Besides the wind function, differences are in the calculation of vapor pressure deficit (either at mean air temperature or as the average of saturation vapor pressure at maximum and minimum temperatures). Also, the Penman's original equation (1948) neglected the soil heat term G.

Another modification is known as the FAO-24 Penman equation (Doorenbos and Pruitt 1977) that was calibrated with data from several locations, but mainly influenced by the data set obtained from Davis, California.

All of the Penman combination type equations assume indirectly that surface resistance is zero and that aerodynamic resistance is included within the wind function itself (Howell et al. 1988). Monteith (1965) (also Rijtema 1965) improved the Penman's equation substantially by introducing canopy resistance and a more general use of aerodynamic resistance. The first term determines the resistance that the canopy opposes to the diffusion of water vapor from the 'big leaf' toward the atmosphere, and the latter describes the resistance of the aerial boundary layer to water vapor transfer. The principal advantage of Eq. (2.4) is that the physiological control of evaporation rate is concentrated in one parameter, r_c (Wallace 1995). Many studies have proved that the Penman-Monteith method (P-M) estimates evapotranspiration realistically from various surfaces, climatic conditions and at different scales (e.g. grass in central Sudan – Hussein 1999, spring cereals with and without Italian rye grass, Lewan 1993, winter wheat – Howell et al. 1995, cattails – Abtew and Obeysekera 1995, arctic coastal wetland – Mendez et al. 1998, watershed scale - Vörösmarty et al. 1998, potato - Kashyap and Panda 2001). Jensen et al. (1990) found that the P-M equation performed well in comparison with the lysimeter data of 11 locations. Jensen et al. (1990) ranked the Penman-Monteith equation as the best method among twenty different methods and modifications. Also, relatively sophisticated multilayer models based on the P-M equation have been developed for simulating evaporation and transpiration from partial cover crops (Shuttleworth and Wallace 1985, Shuttlewoth and Gurney 1990).

The Penman-Monteith equation (Monteith and Unsworth 1990):

$$\lambda E = \frac{\Delta(R_n - G) + \rho\, c_p \{e_c(T(z)) - e(z)\}/\, r_a}{\Delta + \gamma^*} \tag{2.4}$$

where λE – is outgoing energy as evaporation [MJ m^{-2} d^{-1}]
λ – is latent heat of vaporization [MJ kg^{-1}]
R_n – is incoming net radiation [MJ m^{-2} d^{-1}]
G – is outgoing heat energy into the soil [MJ m^{-2} d^{-1}]
ρ - is density of water [kg m^{-3}]
c_p – is specific heat of moist air [MJ kg^{-1} $°C^{-1}$]
$e_s(T(z))$ – is saturated vapour pressure at temperature T at reference height z [kPa]
$e(z)$ – is vapour pressure at the reference height z [kPa]
γ – is psychrometric constant [kPa $°C^{-1}$]
γ^* – is the apparent value of psyhrometer constant $\gamma(r_a+r_c)/r_a$
Δ – is the slope of the vapor pressure curve [kPa $°C^{-1}$]
r_a – is aerodynamic resistance [s m^{-1}]
r_c – is canopy resistance [s m^{-1}]

Priestley and Taylor (1972) published a simplified form of the Penman's equation which was classified as a radiation-based equation. They suggested that the air moving over an extensive area of uniform surface wetness should reach an equilibrium with the surface when saturation vapor pressure deficit equals with the so called equilibrium deficit of the surface, yielding an equilibrium rate of evaporation (Monteith and Unsworth 1990):

$$\lambda E_q = \alpha \frac{\Delta R_n}{\Delta + \gamma} \tag{2.5}$$

where λE_q – is latent heat of evaporation from well watered vegetation or water [MJ m^{-2} d^{-1}]
α – is the empirical coefficient equal to 1.26 for areas defined above

Thus, the coefficient α lumps several physical processes into one parameter, which makes it easier to use the Priestley-Taylor (P-T) equation, but definitely oversimplifies the nature of evaporation. Several authors have tried to develop α as a function of vapor pressure deficit (Steiner et al. 1991) or soil moisture (Crago 1996). In literature a number of articles can be found which prove (Davies and Allen 1973, Stewart and Rouse 1977), or disprove the applicability of the Priestley-Taylor equation. The main problem lies in the 'true value' of the constant α. Several authors have shown that P-T approach is theoretically ambiguous (Monteith and Unsworth 1990, Linsley et al. 1997), however new papers dealing with the P-T equation are still being published. Kustas et al. (1996) found that the midday values of α are less than 1.0 (r_c=100…200 s m^{-1}) and α varies between 1 and 0.6, in overall. Mendez et al. (1998) found at arctic conditions that α is 0.95…0.91 (r_c=58…70 s m^{-1}) for upland tundra and α is 1.15…1.1 (r_c=25…30 s m^{-1}) for wetland. Abtew and Obeysekera (1995) determined that α is 1.18 for cattail march and that the P-M equation yielded better correlation (r^2=0.86) than the P-T equation (r^2=0.79) with estimated r_c=25 s m^{-1}. Crago (1996) found that midday values significantly differ from the daytime averages due to the concave-up shape of the diurnal progression of the parameter α.

In many cases when estimated evapotranspiration is considered, it is simply mentioned that the Penman-Monteith, Priestley-Taylor or other method was used, but the exact way of implementation of the parameters and alternative equations possible for energy or resistance components have not always been described. Thus, it can be assumed that it was done with 'standard' parameters found in every textbook of hydrology. In the best case all calculation equations are clearly described, however, commonly it is only noted that *ET* was estimated as, for example, presented by Allen et al. (1989) or Allen et al. (1998). In fact, these so called 'methods' are actually a set of equations, including a variety of different parameters, which may strongly influence estimated *ET* and, hence, the energy and water balance of the surface. Among the physically based parameters the procedures of radiation and aerodynamic estimation include several empirical 'local' parameters. These are mostly the so called 'recommended' values tabulated on yearly or monthly basis, depending more or less on the surface type and latitude. Unfortunately, corresponding references for northern latitudes are lacking.

2.4 Irradiance

Solar radiation has an enormous importance for plant growth processes, either directly playing the leading role in photosynthesis, or indirectly, influencing the rate of evapotranspiration and warming up the soil surface, e.g. speeding up germination. The fraction of net radiation is allocated to sensible heat, soil heat, and the complementary fraction is allocated to latent heat (Eq. 2.1). Detailed equations distinguish also the net rate of heat storage in metabolic reactions, i.e. photosynthesis and respiration, but in ordinary conditions this part forms less than 1-2% of the energy balance (Hillel 1998). The proportionate allocation of R_n between H and λE depends on the availability of water for evaporation (Hillel 1998). The energy partitioning close to Estonian conditions has been studied in Finland (Vakkilainen 1982). Approximately 50% of evapotranspiration from canopy may be caused by net radiation whereas the rest is attributed to aerodynamic processes (see Section 3.7.3).

The observed radiation is rarely available (e.g. Thornton and Running 1999) and the daily estimates of the radiation term for evapotranspiration equations are usually derived from meteorological data. In Estonia detailed meteorological data required for the

Penman-Monteith equation are recorded at more than 23 stations, however solar radiation is measured only at the Tõravere Actinometric Station and Tiirikoja Lake Station. An analogous situation is rather common in most countries and to overcome the paucity of data there is formed a set of equations to estimate unobserved data.

It is evident that measured irradiance is the best source for R_n-term in the Penman-Monteith method, but it can be replaced by estimated values and usually the following options are used: 1) net radiation is estimated from recorded sunshine hours, or, 2) from sky cover observations, or, 3) from purely empirical relationships based only on the daily temperature difference (T_{max}-T_{min}) and extraterrestrial radiation (Hargreaves and Samani, 1982). In Estonian conditions the first option is the only reasonable choice as the duration of bright sunshine hours is recorded in most of the meteorological stations. Lindsey and Farnsworth (1977) have extensively compared the monthly estimates of solar radiation with those of observations. They found that the sky cover estimates were about 10% lower than those based on pyranometer observations, whereas the sunshine-hour-based estimates yielded close average values.

Among the studies concerning evapotranspiration, determined with the P-M or similar methods, it is very common to estimate net radiation from the following meteorological variables: temperature, T, vapour pressure, e_a, and sunshine hours, n. The estimation procedures include also location-specific empirical parameters (see Sections 2.4.1- 2.4.3). Due to the findings that there exist long-term trends in atmospheric transmittance and, hence, changes in radiation regime (Russak 1998), the need to calibrate or recalibrate the location-specific parameter is obvious, which was done in the present paper.

2.4.1 Short-wave radiation

As the solar beam penetrates the earth's atmosphere, some of the radiation reaches the canopy surface as the direct solar beam, some is scattered, reflected or absorbed by the atmospheric gases (e.g. water vapor), clouds and dust. The solar irradiance received by the unit area of a horizontal surface is known as the *total incoming short-wave radiation* R_s. It is commonly estimated from *extraterrestrial radiation* R_a and from the relative duration of sunshine by the Ångström-Prescott equation (Prescott 1940):

$$R_s = R_a\left(a_s + b_s\frac{n}{N}\right) \quad [\mathrm{MJ\ m^{-2}\ d^{-1}}] \tag{2.6}$$

where R_a – is extraterrestrial radiation [MJ m^{-2} d^{-1}]
a_s – is the fraction of extraterrestrial radiation on overcast days (n=0)
a_s+b_s – is the fraction of extraterrestrial radiation on clear days
n – is duration of bright sunshine [h]
N – is total day length [h]
n/N – cloudiness fraction

Originally this equation, proposed by Ångström (1924), included *clear day irradiance* $R_{s,c}$ instead of extraterrestrial radiation R_a , $R_s/R_{s,c}=a_s+b_s$ (n/N). He also suggested that $a_s+b_s=1$. The disadvantage of the Ångström function is that $R_{s,c}$ is time and location specific, i.e. it can be found from long-term observations.

Extraterrestrial irradiance R_a is more convenient to use, because it can be estimated by the solar constant and the other astronomical parameters, i.e. latitude and day of the year. This replacement in Ångström's equation, proposed by Prescott (1940), made this simple linear relationship very popular for studies dealing with evaporation.

The value of $1\text{-}(a_s\text{+}b_s)$ on a given day can be interpreted as the value for the atmospheric attenuation of extraterrestrial irradiance in the absence of clouds due to atmospheric path length and atmospheric composition, such as water vapor content and presence of particles that absorb or scatter radiation as it passes trough the atmosphere. The physical meaning of a_s in Eq. (2.6) corresponds to the solar radiation of a completely overcast day (n=0). In reality, it does not hold, as total radiation on days with no recorded sunshine can vary considerably (Revfeim 1997, see also Fig. 2.2). Where no actual solar radiation data are available and no calibration has been carried out for parameters a_s and b_s, the values $a_s = 0.25$ and $b_s = 0.50$ are recommended (Allen et al. 1998).

The purpose of numerous publications has been to generalize the physical meaning of a_s and b_s, to find the effect of latitude (Glover ad McCulloch 1958, Persaud et al. 1997), altitude (Neuwirth 1980, Rosset et al. 1997), and seasonal or time dependence (Mustonen 1964, Persaud et al. 1997). More physically based are attempts to introduce atmospheric conditions, i.e. the attenuation of solar radiation by aerosol and water vapor (Revfeim 1997). Unfortunately, all these improvements have been made for the sake of simplicity and without relevant advantages. Perhaps, local atmospheric characteristics will override the other factors. An extensive overview on the historical evolution and parameter values was given by Martinez-Lozano et al. (1984) where around 200 different sources of Ångström-Prescott coefficients were presented, but only three of them in Nordic countries, i.e. the original Ångström coefficient, Spinnanger (1968) and Stokmans (1971) (cited in Rietveld 1978). These and other selected samples of proposed coefficients are given in Table 2.1.

Table 2.1. Recommended and calibrated values of Ångström's coefficients.

a_s	b_s	Comment	Source
0.25	0.50	Recommended for average climates	Allen et al. (1998)
0.25	0.75	a_s=0.25, b_s=1-a Sweden [a)]	Ångström (1924)
0.15	0.73	Sweden , 5 stations[a)]	Stokmans (1971)
0.20	0.70	Norway, 2 stations [a)]	Spinnanger (1968)
0.24	0.58	Finland, May	Mustonen (1964)
0.23	0.59	Finland, June	Mustonen (1964)
0.23	0.59	Finland, July	Mustonen (1964)
0.23	0.56	Finland, August	Mustonen (1964)
0.23	0.54	Finland, September	Mustonen (1964)
0.23	0.52	Finland, October	Mustonen (1964)
0.18	0.55	England (Rothamsted), 10-year period average [a)]	Penman (1948)
0.19	0.62	England (Eskadlemuir), 10-year period average	Hanna and Siam (1981)
0.21	0.67	Ireland, 6 stations, 8-year period average [a)]	McEntee (1980)
0.26	0.42	Austria, 19 stations [a)]	Neuwirth (1980)
0.22	0.50	France (Versailles), 33-year period average	Durand (1975)

[a)]Calculated from monthly values

The fraction of the incident short-wave radiation captured at the ground is called *net short-wave radiation* R_{ns} and is found as:

$$R_{ns} = R_s\,(1-\alpha) \quad [\text{MJ m}^{-2}\ \text{d}^{-1}] \tag{2.7}$$

where α – *is* albedo.

2.4.2 Long-wave radiation

The rate of long-wave energy emission is proportional to the absolute temperature of the surface, raised to the fourth power (Stefan-Boltzmann law). The net energy flux leaving the earth's surface is, however, less than that emitted and is given by the Stefan-Boltzmann law due to absorption and downward radiation from the sky (Allen et al. 1998). The net outgoing flux is corrected by humidity and cloudiness, as the water vapor and carbon dioxide are the main absorbers and emitters of long-wave radiation (Monteith and Unsworth 1990). Thus, terrestrial radiation or *net long-wave radiation* is the difference between incoming and outgoing long-wave radiation:

$$R_{nl} = R_{nl}\downarrow - R_{nl}\uparrow = -f\varepsilon'\sigma(T+273.2)^4 \quad [\text{MJ m}^{-2}\ \text{d}^{-1}] \tag{2.8}$$

where $R_{nl}\downarrow$ – is incoming long-wave radiation [MJ m^{-2} d^{-1}]
$R_{nl}\uparrow$ – is outgoing long-wave radiation [MJ m^{-2} d^{-1}]
f – is adjustment for cloud cover
ε' – net emissivity between the atmosphere and the ground
σ – Stefan-Boltzmann constant [4.903×10^{-9} MJ m^{-2} ^{o}K^{-4} d^{-1}]
T – mean air temperature [^{o}C]

The *net emissivity* ε' can be estimated from the following equation (Allen et al. 1989):

$$\varepsilon' = a_e + b_e\sqrt{e_a} \tag{2.9}$$

where a_e , b_e – are emissivity coefficients
e_a – is vapor pressure [kPa]

The proposed ranges for coefficients are 0.34 to 0.44 for a_e and –0.14 to –0.25 for b_e (Shuttleworth 1992). For average conditions the following values are suggested: $a_e=0.34$ and $b_e=-0.14$ (Allen et al. 1998).

The *cloudiness factor* f can be estimated from solar radiation data (Wright and Jensen 1972):

$$f = a_c\frac{R_s}{R_{s,c}} + b_c \tag{2.10}$$

where a_c , b_c – are cloudiness coefficients

The recommended values for humid areas are $a_c=1.00$ *and* and $b_e=0.00$.

The disadvantage of Eq. (2.10) is that $R_{s,c}$ must be known. It can be found from long-term observations, which are rarely available. To overcome this problem, substituting Eq. (2.6) into (2.10), adjustment for the cloud cover can be found (Shuttleworth 1992):

$$f = \left(a_c \frac{b_s}{a_s + b_s} \right) \frac{n}{N} + \left(b_c + \frac{a_s}{a_s + b_s} a_c \right) \tag{2.11}$$

where n – is duration of bright sunshine [h]
N – is total day length [h]

2.4.3 Net radiation

The correct determination of net radiation is a problem of great importance, as errors in R_n are reflected in calculated evapotranspiration rate. The net amount of radiation received by surface can be found from the following equation:

$$R_n = R_s(1-\alpha) + R_{nl}\downarrow - R_{nl}\uparrow \quad [\mathrm{MJ\ m^{-2}\ d^{-1}}] \tag{2.12}$$

where R_s – is total incoming short-wave radiation [MJ m^{-2} d^{-1}]
α – is albedo [-]
$R_{nl}\downarrow$ – is incoming long-wave radiation [MJ m^{-2} d^{-1}]
$R_{nl}\uparrow$ – outgoing long-wave radiation [MJ m^{-2} d^{-1}]

Net long-wave radiation yields R_{nl} = $R_{nl}\downarrow$ - $R_{nl}\uparrow$. Total incoming short-wave radiation consists of *direct radiation* R_I and *diffuse radiation* R_D which are measured on a horizontal surface. Under typical weather conditions the R_{nl} is negative, i.e. surface acts as a net long-wave emitter.

2.4.4 Observed radiation data

The dataset of measured radiation for the 11-year period (1986-1996) was available for the current study. Thus, more than 4000 days were used for validation of Eqs. (2.6-2.12). All data were measured at the Tõravere Actinometric Station of the Estonian Meteorological and Hydrometrical Institute (Estonia, 58.3° N, 26.5° E, H=70 m a.s.l.). Besides observed radiation, the meteorological parameters measured at the same station were used in the following analysis. All meteorological measurements were taken at 3.00 a.m., 9.00 am, 15.00 p.m. and 21.00 p.m. The mean value of these four measurements was treated as a daily average. All radiation parameters were observed on an hourly basis and used as a cumulative value for a day. The data were not screened and a few outliers are seen in following figures.

The direct solar radiation R_I was measured with the Yanishevsky thermoelectric actinometer M-50. Diffuse radiation R_D was measured with the Yanishevsky pyranometer M-80. Reflected short-wave radiation $R_s\uparrow$ was measured with the same apparatus. Net radiation R_n was measured with the Yanishevsky net radiometer. All other terms of Eq. (2.12) were found from the observed values:

$$R_s = R_I + R_D \quad [\mathrm{MJ\ m^{-2}\ d^{-1}}] \tag{2.13}$$

$$R_{sn} = R_s - R_s\uparrow \quad [\mathrm{MJ\ m^{-2}\ d^{-1}}] \tag{2.14}$$

$$\alpha = \frac{R_s\uparrow}{R_s} \quad [\mathrm{MJ\ m^{-2}\ d^{-1}}] \tag{2.15}$$

$$R_{nl} = R_n - R_s(1-\alpha) \quad [\mathrm{MJ\ m^{-2}\ d^{-1}}] \tag{2.16}$$

The most inaccurate measurement apparatus is the net radiometer, in which case the observation error can reach up to 10%, whereas in the case of the pyranometer it is 5% and in the case of actinometer only 3% (Sulev 1990). These possible errors must be considered in the evaluation of estimated values, e.g. when the maximum net radiation is about to 20 MJ m^{-2} d^{-1} then maximum error is of the order of 2 MJ m^{-2} d^{-1}.

Measured meteorological parameters were: air temperature T (C^0), vapor pressure e_a (kPa), wind speed u (m s^{-1}), duration of sunshine hours n (h), and precipitation P (mm). Monthly mean averages and standard deviations based on daily data are given in Table 2.2.

The average values for the present data set of 11 years (from 1986 to 1996) were close to those obtained for more than 30-year averages (1955-1986 for radiation and 1955-1989 for meteorological observations, Climate of Tartu…, 1990). The duration of sunshine hours was slightly but systematically longer, deviating in the worst case by 0.9 hours (in May), and ranging from 0.1 to 0.6 hours in other months. The average temperature of the 11-year period was closer to the corresponding values of long-term average, except for warmer winter months (around +2.2 C^0), whereas in the summer months it was only 0.3 C^0 degrees higher. The observed total radiation did not reveal systematic deviations.

Observed total radiation forms a symmetric cloud (Fig. 2.1), with a top in mid-June. The upper edge of the distribution of the observed values correspond to clear day irradiance $R_{s,c}$ which was used in the original Ångström's equation (see Fig. 2.11). The difference between maximum values of R_s in June (up to 30 MJ m^{-2} d^{-1}) and in January (up to 2.5 MJ m^{-2} d^{-1}) is 12-fold. In midsummer R_s can deviate as much as 6-fold, which must considerably influence of plants development and evapotranspiration.

When the data of completely overcast days (n=0) were plotted (Fig. 2.2) it was evident that the first empirical parameter, a_s, cannot meet its character in Ångström-Prescott equation, as the observations showed a significant scattering of total radiation on these particular days. The same type of problems my arise also on almost clear days (n/N≈1), when total irradiation can exceed the flux beneath a cloudless sky by 5 to 10% if a few isolated cumula will appear in the sky (Monteith and Unsworth 1990).

Figure (2.3) represents the scattering of net radiation explicitly included in evapotranspiration methods during the year. A few outliers are seen extending outside the cloud of observed values.

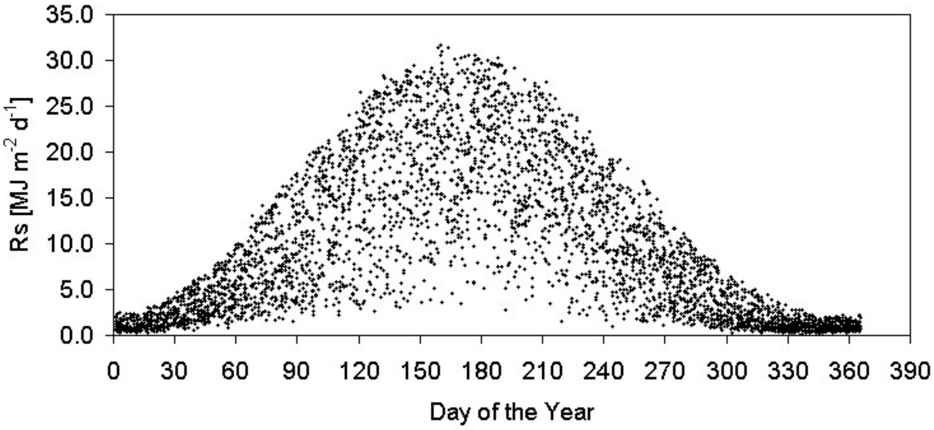

Figure 2.1. Observed solar radiation R_s at the Tõravere Actinometric Station for the period 1986-1996.

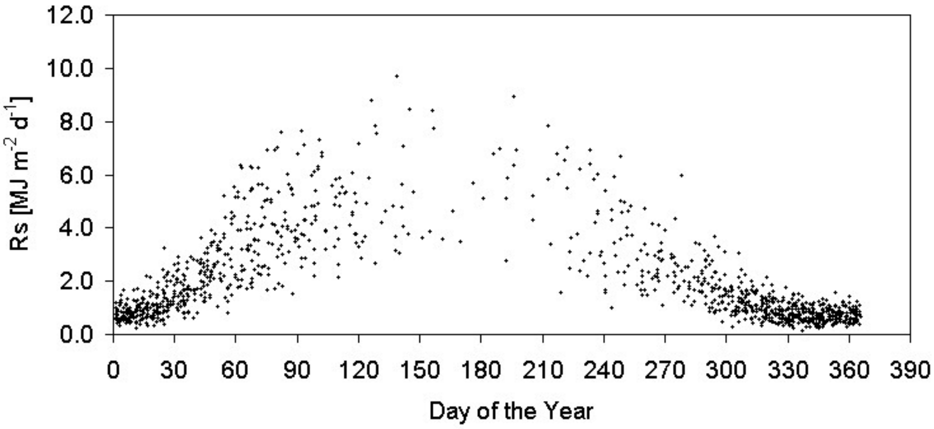

Figure 2.2. Observed solar radiation on completely overcast days (n=0) at the Tõravere Actinometric Station for the period 1986-1996.

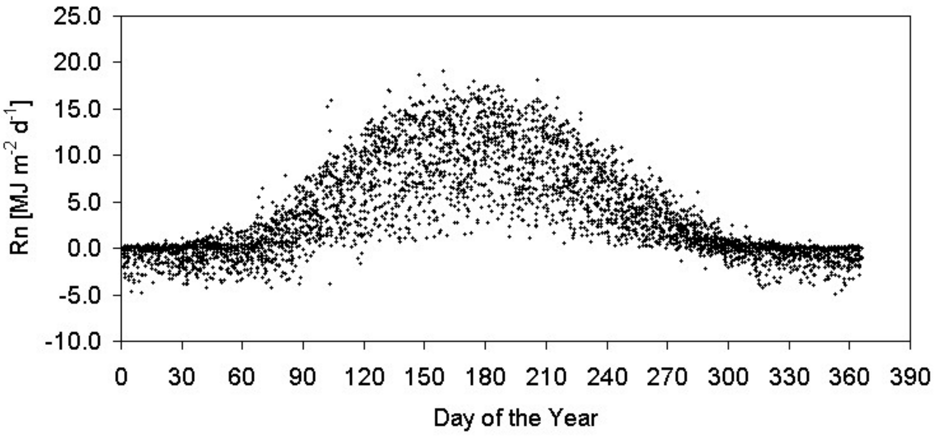

Figure 2.3. Observed net radiation R_n at the Tõravere Actinometric Station for the period 1986-1996.

Table 2.2. Observed monthly average values of total short-wave radiation R_s , net short-wave radiation R_{ns} , net long-wave radiation R_{nl} , duration of sunshine hours n, daylight hours N, relative sunshine duration n/N and temperature T at Tõravere Actinometric Station for the period 1986-1996. Standard deviation is denoted with ±. The sum of R_{ns} and R_{nl} yields net radiation R_n.

Month	R_s MJ m^{-2} d^{-1}	R_{ns} MJ m^{-2} d^{-1}	R_{nl} MJ m^{-2} d^{-1}	n h	N h	n/N %	T C°
January	1.5±0.9	0.7±0.5	-1.3±1.2	1.1±1.9	6.9±0.52	16±27	-4.3±6.9
February	3.8±2.0	1.5±1.0	-1.9±1.4	2.3±2.9	9.1±0.68	25±32	-4.5±6.7
March	7.7±3.9	4.2±3.0	-3.0±2.0	3.6±4.0	11.6±0.77	31±34	-0.6±4.4
April	12.8±5.8	9.8±4.7	-4.3±2.3	5.8±4.7	14.2±0.72	41±33	5.3±4.7
May	18.2±7.1	14.4±5.6	-5.2±2.0	8.5±5.2	16.5±0.60	52±32	11.5±3.8
June	19.8±6.6	15.5±5.2	-4.9±1.6	8.8±4.8	17.8±0.14	50±27	15.4±3.5
July	18.9±6.4	14.9±5.0	-4.8±1.6	8.7±5.0	17.2±0.47	51±29	17.2±3.0
August	14.3±5.7	11.2±4.4	-3.8±1.4	6.9±4.5	15.1±0.69	46±30	15.7±2.9
September	8.5±4.1	6.7±3.2	-2.9±1.3	4.2±3.8	12.6±0.72	33±29	10.1±3.3
October	4.6±2.7	3.6±2.0	-2.5±1.5	3.0±3.3	10.1±0.75	30±32	5.6±3.9
November	1.7±1.2	1.1±0.8	-1.5±1.4	1.2±2.2	7.7±0.62	16±28	-0.1±4.8
December	1.0±0.5	0.5±0.3	-1.3±1.2	0.9±1.7	6.3±0.17	15±26	-3.6±5.5

2.4.5 Albedo

Part of short-wave radiation is reflected depending on various influencing factors: direction of the solar beam, proportion of diffuse radiation, and properties of land cover (Shuttleworth 1992). The reflection coefficient of natural surfaces, also known as *albedo* α, can be calculated from the observed values:

$$\alpha = \frac{R_s - R_{ns}}{R_s} \tag{2.17}$$

where R_s – is total incoming short-wave radiation [MJ m^{-2} d^{-1}]
R_{ns} – is net short-wave radiation [MJ m^{-2} d^{-1}]

Bare soil's albedo depends on soil moisture conditions, ranging from 0.10 to 0.35, for wet and dry soil, respectively. In case of snow cover the reflection coefficient is reduced with the age of snow, where 0.8 is appropriate for a fresh snow cover and 0.2 for an old one (Shuttleworth 1992). For grass and pasture the albedo ranges from 0.2 to 0.26, with an indicative value of 0.23 (Shuttleworth 1992) or 0.24 (Gates 1980). A very comprehensive table of different natural surfaces has been provided by Gates (1980).

According to the present dataset the average albedo for all period from April to October was around 0.21, deviating only in April (α=0.23) (Table 2.3, Fig. 2.4). During the cold period, from November to March, the albedo varies significantly, which must be definitely considered in all predictive calculations, e.g. in global climate change studies. It was also found that albedo and mean monthly temperature (T_{month}) are weakly correlated, r^2=0.514 ($\alpha = -0.0399T_{month} + 0.346$) for the temperature range from +5 ^{0}C to –10 ^{0}C. When the mean monthly temperature was below -10 °C, then the albedo was around 0.75 indicating a stable and complete snow cover.

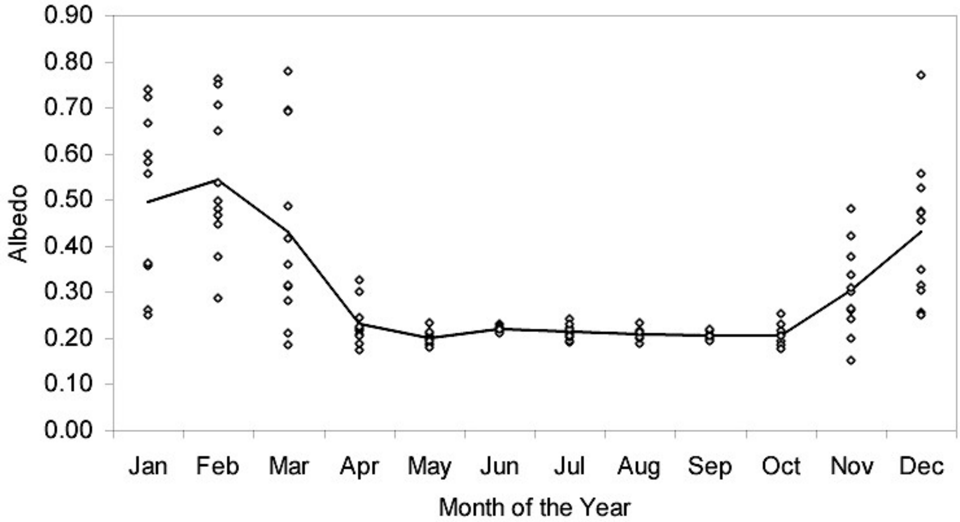

Figure 2.4. Observed monthly albedo (diamonds) and annual trend curve (line) at the Tõravere Actinometric Station for the period 1986-1996.

Table 2.3. Monthly albedos observed at the Tõravere Actinometric Station for the period 1986-1996. Standard deviation is denoted by ±.

Month	Albedo	Month	Albedo
January	0.50±0.18	July	0.21±0.02
February	0.54±0.16	August	0.21±0.01
March	0.43±0.21	September	0.21±0.01
April	0.23±0.05	October	0.21±0.02
May	0.20±0.01	November	0.30±0.10
June	0.22±0.01	December	0.43±0.16

2.4.6 R_n estimated with standard parameters

According to equations (2.6-2.12) net radiation R_n was calculated with a standard set of parameters (Shuttleworth 1992), where $a_s=0.25$, $b_s=0.50$, $a_e=0.34$, $b_e=-0.14$, $a_c=1.00$, $b_c=0.00$. The calculation was carried out with daily values after which monthly cumulative values were found. The results in Fig. (2.5) represent the monthly average values for the period of 1986-1996.

According to comparison of the observed and estimated values, the calculated values of R_n exceeded systematically the measured values during the summer season and were underestimated in winter months, whereas in early spring and late fall the standard set of parameters performed well (Fig. 2.3). The biggest difference was in July, when the $R_{n,cal}$ overestimated the mean observed value by 39 MJ m^{-2} month^{-1}. This corresponds to around 4 mm of evaporated water, which is approximately 5% of monthly *ET* in July. Residuals (observed *minus* estimated) plotted against a month of the year confirmed the systematic character of estimation error. Figure (2.6) reveals an overestimation of both total and net radiation, peaking in June, and an underestimation of net radiation in the winter months. The detected discrepancy between the observed and estimated values gave occasion to analyze the empirical parameters used in the estimation procedure.

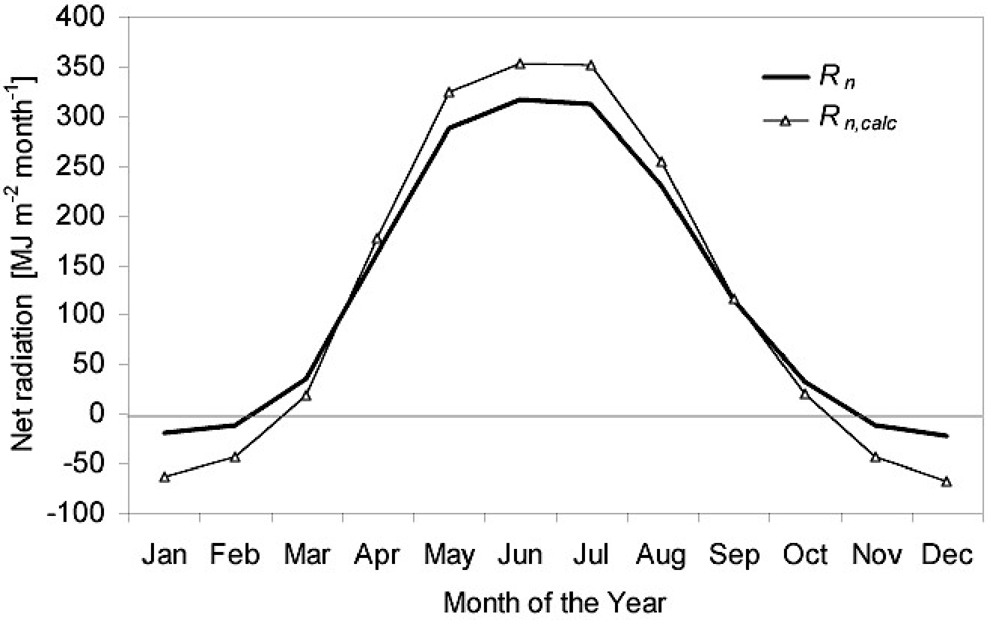

Figure 2.5. Observed R_n and calculated R_{n_calc} monthly mean cumulative net radiation (MJ m^{-2} month^{-1}) at Tõravere using a standard set of parameters for the period 1986-1996.

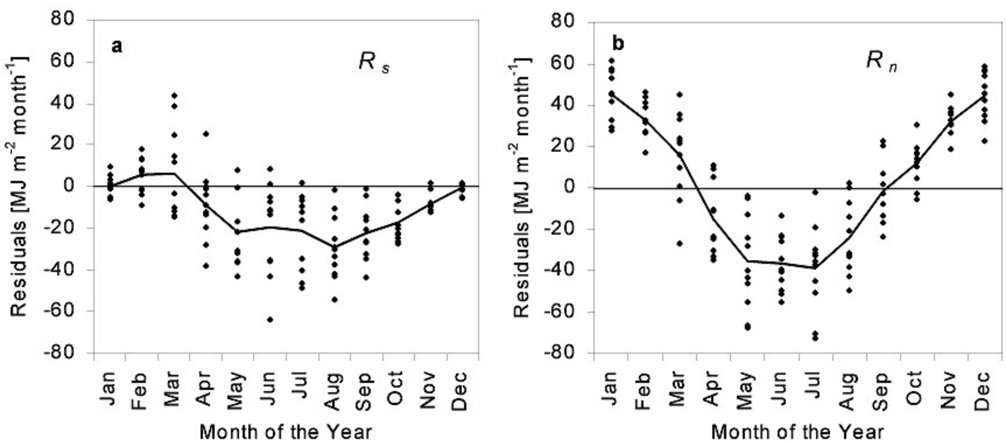

Figure 2.6. Residual plot (observed *minus* estimated) of a) total radiation R_s and b) net radiation R_n calculated with standard parameters. Mean residual is denoted by the line.

To evaluate the model's performance several criteria were used: 1) coefficient of determination (r^2) as a measure of correlation, 2) root-mean-square error (RMSE), and, 3) mean residual error (ME) as the measure of the difference and bias:

$$RMSE = \sqrt{\frac{\sum_{i=1}^{n}(O_i - P_i)^2}{n}} \tag{2.18}$$

$$ME = \frac{\sum_{i=1}^{n}(O_i - P_i)}{n} \tag{2.19}$$

where O_i – is the observed data
P_i – is the predicted data
n – is the number of samples

The regression coefficient has been widely used as a quantitative index of a correlation between the observed and predicted values. RMSE measures the spread of the *y* (predicted) values around the average, i.e. it can usually be expected that 68% of y values are within one RMSE. Thus, RMSE is measured on the same scale and with the same units as *y*, and low values indicate little scatter. Mean residual error describes the average absolute deviation between the observed and predicted data, i.e. it represents a measure of the bias in the simulated results.

Statistical analysis revealed that total radiation is better estimated by proposed models compared with long-wave radiation, i.e. the latter reduces the quality of the prediction of net radiation (Table 2.4). For example, in May R_s (r^2 =0.94), R_{nl} (r^2=0.78), and R_n (r^2=0.84). ME showed systematic over- or underestimation of the predicted values. The RMSE was relatively higher in conditions of low irradiance, i.e. in the winter period.

Table 2.4. Results of statistical analyses of the data for total radiation R_s, net long-wave radiation R_{nl}, and net radiation R_n performed by the standard set of parameters.

Month	Total radiation MJ m^{-2} d^{-1}				Net long-wave radiation MJ m^{-2} d^{-1}				Net radiation MJ m^{-2} d^{-1}			
	Mean	r^2	RMSE	ME	Mean	r^2	RMSE	ME	Mean	r^2	RMSE	ME
Jan	1.48	0.75	0.45	0.01	-2.80	0.49	1.77	1.50	-2.06	0.40	1.68	1.45
Feb	3.64	0.84	0.84	0.20	-3.19	0.66	1.51	1.25	-1.56	0.49	1.48	1.15
Mar	7.51	0.87	1.41	0.19	-3.59	0.67	1.28	0.55	0.60	0.54	1.62	0.51
Apr	13.05	0.91	1.82	-0.31	-4.14	0.69	1.32	-0.21	5.91	0.63	2.00	-0.51
May	18.86	0.94	2.13	-0.70	-4.62	0.78	1.08	-0.54	10.43	0.84	2.00	-1.15
Jun	20.47	0.92	2.12	-0.69	-4.20	0.69	1.14	-0.71	11.77	0.86	1.95	-1.21
Jul	19.61	0.88	2.30	-0.69	-4.10	0.60	1.24	-0.70	11.32	0.81	2.06	-1.25
Aug	15.21	0.92	1.94	-0.95	-3.83	0.67	0.82	-0.01	8.18	0.84	1.53	-0.79
Sep	9.27	0.90	1.53	-0.80	-3.49	0.63	1.02	0.59	3.87	0.72	1.18	-0.06
Oct	5.13	0.90	1.01	-0.56	-3.43	0.65	1.29	0.88	0.65	0.44	1.03	0.39
Nov	1.98	0.85	0.54	-0.30	-2.83	0.68	1.53	1.30	-1.47	0.44	1.30	1.07
Dec	1.05	0.70	0.29	-0.02	-2.77	0.48	1.75	1.49	-2.18	0.42	1.65	1.43

2.4.7 R_n estimated with improved parameters

Basing on the analysis performed in Section 2.4.6 it was evident that the standard set of parameters used in the estimation of radiation yielded biased predictions for Estonian conditions. Monthly total radiation was overestimated in the summer months by around 20-30 MJ m^{-2}, which accounts approximately for 4-8% of monthly values. Therefore, to improve the estimation of R_n following calibration was carried out in two steps: at first for the short-wave component (i.e. for Ångström coefficients a_s and b_s), and secondly for long-wave radiation R_{nl} (i.e. emissivity and cloudiness factor).

Calibration

Total radiation estimated by the Ångström-Prescott equation depends on extraterrestrial radiation and on atmospheric transmittance. The latter may influence local empirical parameters either on short or long-term basis. The atmosphere is the clearest in winter, while low transmittance is characteristic of the summer months (Russak et al. 1997). Relatively short-time variations in atmospheric transmittance are in good agreement with the greatest volcanic eruptions (Russak 1990).

Least-square-method was used in the calibration of the monthly empirical Ångström's coefficients. Each data set consisted of around 330 days (11-years, 28-31 days). It was found that the Ångström's coefficients differed from standard values in Estonian conditions. Negative coherence exists in the monthly time series (Fig. 2.7) where the values of the intercept a_s in Ångström-Prescott equation are mirrored by the corresponding value of the slope b_s. This finding has been reported also in other studies (e.g. Presaud et al. 1997). In general, two distinctive seasons were found with the following recommended values: a_s=0.20 and b_s=0.56 (April-November) and a_s=0.25 and b_s=0.50 (December-March).

The physical interpretation of the new coefficients indicates lower cloud transmission during the April-November period which is in good agreement with the findings obtained at the Tõravere Actinometric Station over 1955-1995 (Russak et al. 1997). The annual pattern of attenuation found by Russak et al. (1997) is different in the first part of the year (from February to June) when extinction by aerosol predominates over extinction by water vapor, whereas during the second half of the year the influence of precipitation as the factor cleaning the atmosphere increases and the role of water vapor becomes dominant. The possible part of extraterrestrial radiation at the earth's surface (a_s+b_s) is the same ~75% as proposed by Ångström-Prescott equation.

Long-wave radiation is more difficult to estimate compared with short-wave radiation. The calibration of R_{nl} revealed that there does not exist a single set of constant values, but several sets of almost equally good parameter combinations depending on how the calibration was carried out. The net emissivity coefficients did not show clearly seasonal character. For the summer months, slightly smaller values a_e=0.30 and b_e=-0.10 could be suggested, but for simplicity's sake the standard values of a_e=0.34 and b_e=-0.14 are also acceptable. For bigger changes must be made in the case of cloudiness coefficients. In literature (Shuttleworth 1992) it is supposed that a_c+b_c=1. Performed calibration revealed that a_c+b_c forms a symmetric parabola with a peak in midsummer (Fig. 2.9), and that the sum of the cloudiness coefficients deviates significantly from 1.0. It should be noted that in spite of the selected calibration variant (a_c free and b_c free, a_c free and b_c constant, a_c constant and b_c free) the sum of a_c and b_c was approximately the same, deviating from 1.0 more at the beginning and at the end of the year (0.5-0.6), and reached 1.2 in midsummer. It is difficult to draw up the physical interpretation of that finding when the cloudiness factor f is higher than 1.0 (Eq. 2.10 and 2.11), most probably it compensates for the model errors, particularly those that were made also in emissivity coefficients.

Statistical analysis showed that the improved set of empirical parameters (Table 2.6) reduced systematic errors in radiation estimates. Mean residual error dropped significantly close to zero values whereas the changes in RMSE were less significant. Calibration improved the coefficient of determination r^2 and RMSE relatively more in the months with low radiation. Daily estimates of both total radiation and net radiation have better correlation in summer months (R_s, r^2 >0.9, R_n, r^2 >0.8, Table 2.5) while winter months reveal a lower correlation (R_s, r^2 ≈0.8, R_n, r^2 ≈0.35, Table 2.5).

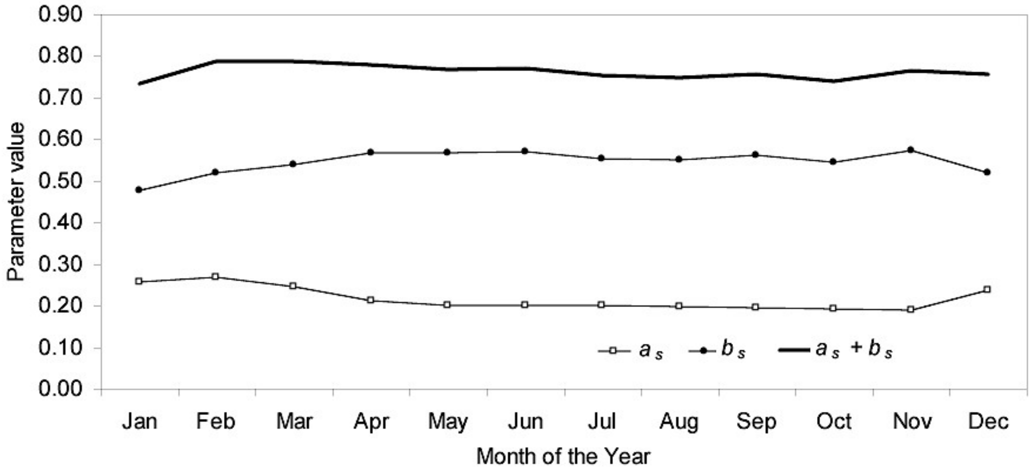

Figure 2.7. Calibration results for the Ångström a_s and b_s coefficients.

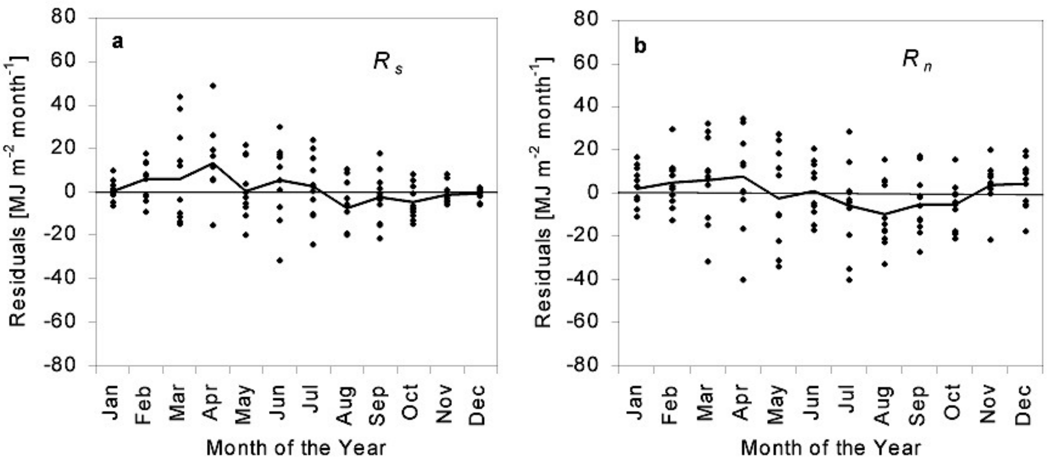

Figure 2.8. Residual plot (observed *minus* estimated) of a) total radiation R_s and b) net radiation R_n calculated with improved parameters. Mean residual is denoted by the line.

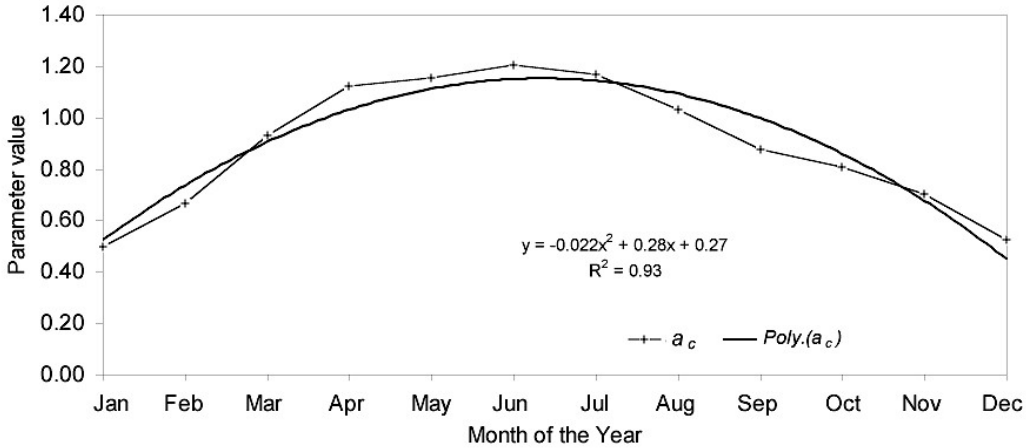

Figure 2.9. Calibration results for the values of cloudiness coefficient a_c (b_c=0) and fitted empirical function.

Table 2.5. Results of statistical analyses of the data for total radiation R_s, net long-wave radiation R_{nl}, and net radiation R_n performed by the improved set of parameters.

Month	Total radiation MJ m^{-2} d^{-1}				Net long-wave radiation MJ m^{-2} d^{-1}				Net radiation MJ m^{-2} d^{-1}			
	Mean	r^2	RMSE	ME	Mean	r^2	RMSE	ME	Mean	r^2	RMSE	ME
Jan	1.48	0.75	0.45	0.01	-1.40	0.49	0.93	0.09	-0.68	0.33	0.86	0.07
Feb	3.64	0.84	0.84	0.20	-2.12	0.66	0.88	0.18	-0.57	0.51	0.93	0.16
Mar	7.51	0.87	1.41	0.19	-3.34	0.67	1.21	0.29	0.92	0.74	1.32	0.20
Apr	12.33	0.92	1.74	0.45	-4.33	0.69	1.27	-0.02	5.16	0.76	1.57	0.24
May	18.15	0.94	1.78	0.01	-5.08	0.78	0.97	-0.08	9.37	0.85	1.58	-0.08
Jun	19.64	0.92	1.87	0.19	-4.78	0.70	0.95	-0.12	10.53	0.87	1.46	0.02
Jul	18.84	0.88	2.22	0.07	-4.56	0.60	1.14	-0.25	10.25	0.81	1.63	-0.19
Aug	14.49	0.92	1.65	-0.23	-3.72	0.67	0.88	-0.12	7.71	0.86	1.27	-0.31
Sep	8.61	0.91	1.27	-0.10	-2.80	0.63	0.82	-0.10	3.99	0.77	1.07	-0.17
Oct	4.72	0.91	0.83	-0.16	-2.51	0.65	0.91	-0.04	1.20	0.51	0.91	-0.16
Nov	1.74	0.86	0.43	-0.04	-1.72	0.68	0.85	0.19	-0.52	0.35	0.81	0.13
Dec	1.05	0.70	0.29	-0.02	-1.46	0.48	0.92	0.17	-0.88	0.34	0.85	0.13

Table 2.6. Results of calibration of the empirical coefficients in radiation estimation equations.

Month	a_s	b_s	a_e	b_e	a_c	b_c
January	0.26	0.48	0.340	-0.140	0.50	0.0
February	0.27	0.52	0.340	-0.140	0.66	0.0
March	0.25	0.54	0.340	-0.140	0.93	0.0
April	0.21	0.57	0.340	-0.140	1.12	0.0
May	0.20	0.57	0.340	-0.140	1.15	0.0
June	0.20	0.57	0.340	-0.140	1.20	0.0
July	0.20	0.55	0.340	-0.140	1.17	0.0
August	0.20	0.55	0.340	-0.140	1.03	0.0
September	0.20	0.56	0.340	-0.140	0.88	0.0
October	0.19	0.55	0.340	-0.140	0.80	0.0
November	0.19	0.57	0.340	-0.140	0.70	0.0
December	0.24	0.52	0.340	-0.140	0.53	0.0

Sensitivity analysis

Sensitivity analysis is an important tool to evaluate the sensitivity of simulation models, i.e. to identify the impact of input parameters on model predictions. The results of sensitivity analysis must reveal the input parameters which should be more carefully estimated. Consequently, the sensitivity of input variables will determine the required accuracy in measurements or parameter selection.

Variations in the output values can be quantified on a) a percentage basis, using the maximum absolute difference between the modified and the output base values (e.g. Mahdian and Gallichand 1995, McKenney and Rosenberg 1993), or, b) relative sensitivity coefficients can be determined (Beven 1979, Haan et al. 1995, Qiu 1998). The latter method was selected for the present study.

The relative sensitivity coefficient is defined as:

$$S_r = \frac{\partial O}{\partial I}\frac{I}{O} \tag{2.20}$$

where S_r – is relative sensitivity coefficient [dimensionless]
I – is particular input
O – is particular output

Coefficient S_r represents the fraction of the change in I which is transmitted to a change in O, i.e. the result S_r=0.1 suggests that the 10% increase in I would cause the 1% increase in O. Negative coefficients would indicate a decrease in O, respectively. The benefit from the use of relative sensitivity coefficient is that it is dimensionless, which allows to rank all necessary model parameters.

A sensitivity analysis was performed using the standard set of empirical parameters and all available data for June which was selected due to its highest absolute values as well as the highest absolute deviation between the minimum and maximum values. At first, the sensitivity analysis of empirical parameters was determined changing one parameter at a time by 10%. Secondly, the input values of temperature, vapor pressure, duration of bright sunshine were also changed by 10%. Additionally, the albedo was increased by 10% even though it was actually calculated from the measured data. The results of sensitivity analysis are summarized in Table 2.7.

Total radiation was equally sensitive to both Ångström's parameters, i.e. 10% change in the parameter value changed the output by 8.7% (Table 2.7). The same parameters were also the most sensitive in the case of net radiation whereas the influence of the cloudiness parameter b_c seemed to be negligible with present dataset, which confirms the results received in calibration procedure. Among the measured input data the most sensitive was duration of bright sunshine where 10% error may cause around 5% error in estimated net radiation.

Table 2.7. Relative sensitivity of parameters in equations of total and net radiation.

Parameter	a_s	b_s	a_e	b_e	a_c	b_c
Base value	0.25	0.5	0.34	-0.14	1	0[a)]
Relative sensitivity S_r						
R_s	0.87	0.87	-	-	-	-
R_n	0.62	0.73	-0.64	0.30	-0.36	-0.06

Parameter	T	e_a	n	*albedo*
Base value	15.4	1.2	8.8	0.22
Relative sensitivity S_r				
R_s	-	-	0.87	-
R_n	-0.08	0.15	0.50	-0.38

[a)] for b_c sensitivity the base value was 0.1

Probability analysis

The uncertainty both in model input and output can be quantified in the form of a probability density (or distribution) function (pdf) or a cumulative probability distribution function (cdf). The area bounded by the pdf-curve and the x-axis is equal to 1. The probability that the parameter X falls within a certain interval (a, b) is:

$$P(a \leq X \leq) = \int_a^b f_X(X)dx \tag{2.21}$$

where, for instance, a and b may be the confidence intervals (CI).

A probability analysis was performed using the same dataset as in sensitivity analysis, i.e. for all days in June during the eleven years. Figure 2.10 reveals that the probability density function of measured net radiation forms an unsymmetrical curve with a median of 10.9 MJ m^{-2} d^{-1} (Fig. 2.10a) and estimated net radiation forms a symmetrical curve with a median of 10.8 MJ m^{-2} d^{-1} (Fig. 2.10b), i.e. the medians were very close but estimated net radiation omitted both very low and very high values. Thus, probability analysis revealed that estimated net radiation yielded a probability density function different from the one based on measured values. However, it must be mentioned that the observed net radiation was measured with an error of the order of ±10% and net long-wave radiation was obtained as the residual of net radiation *minus* net short-wave radiation.

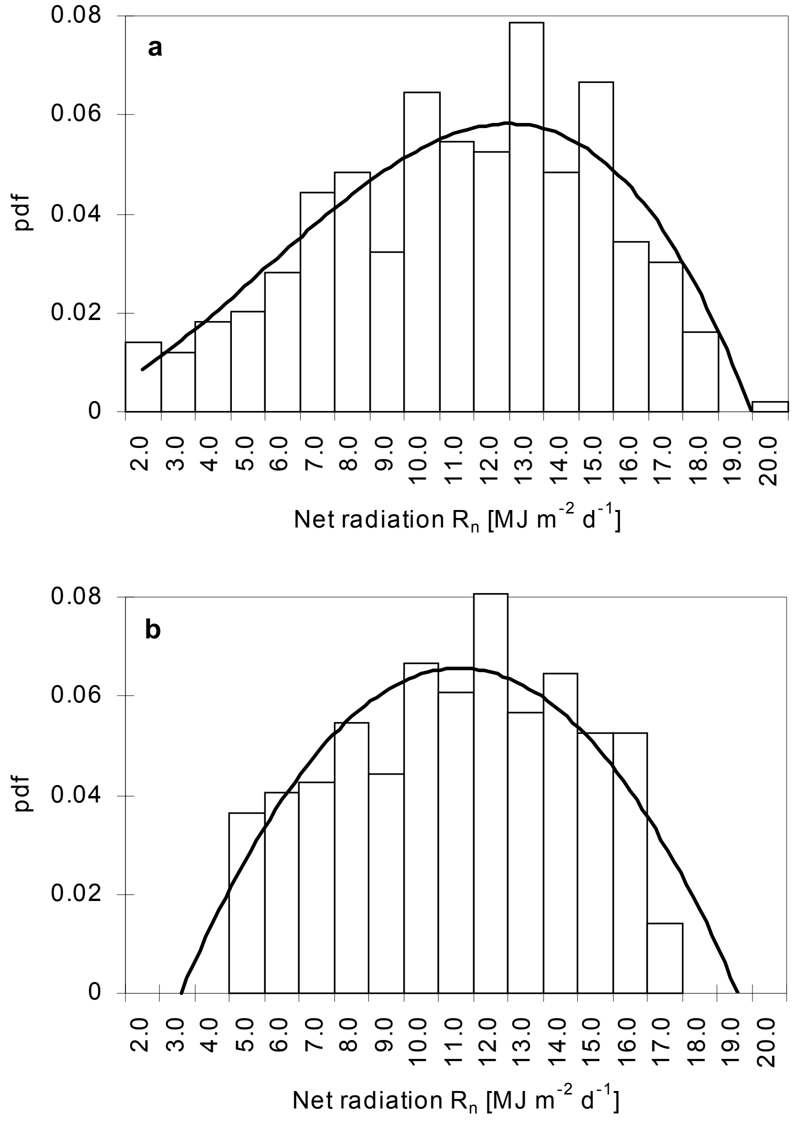

Figure 2.10. The probability density functions (bars) and fitted pdf (lines) of the a) measured and b) estimated net radiation based on the data of June for the period 1986-1996.

2.4.8. New simple empirical methods to estimate clear day solar radiation and R_n

Total radiation of days without clouds forms a sinusoidal curve which depends on latitude and local atmospheric properties. This curve is also called the solar radiation envelope curve, which indicates the maximum solar radiation that can occur on a given day, and it can be estimated from the upper envelope of all measurements (see Fig. 2.1). There are not very many days when the ratio n/N=1.0, particularly in a cold period and, therefore, it is difficult to draw the function from the measured values and, perhaps for this reason, it is also difficult to find these curves from literature. In fact, that curve may be very useful in studies concerning the effect of total radiation. For example, the original Ångström equation includes daily short-wave radiation, determined by clear day irradiance and relative duration of bright sunshine.

The dataset of eleven years for observed total radiation (see Section 2.4.4) was used to determine the function $R_{s,c}$,$=f(t)$. The constraint $n/N > 0.95$ was applied to select days with conditions very close to cloudless days. More strict constraint yielded too few data pairs, particularly for the cold season. Also, above this constraint the measured values and the n/N-ratio were not correlated, i.e. days with the highest radiation were not always characterized by the highest n/N-ratio. A total of 118 out of more that 4000 days were used to calibrate the coefficients for the selected function. It was found that the sinusoidal curve (Eq. 2.22) fitted better than the fifth or higher order polynomials. The coefficient of determination r^2 was 0.994 and RMSE=0.67. However, Fig. (2.11) reveals that Eq. (2.22) slightly underestimated peak values in June and low radiation days in the cold period:

$$R_{s,c} = 15.39 + 14.63 \sin\left(\frac{2\pi t}{365} + 1.56\pi\right) \tag{2.22}$$

where t – is day number

The original Ångström equation was parameterized applying Ångström's assumption that $a_s+b_s=1.0$. The calibrated equation is given in Eq. (2.23). It must be emphasized that Eq. (2.23) is more empirical than the Ångström-Prescott equation (Eq. 2.6) which includes latitude-specific extraterrestrial radiation:

$$R_s = R_{s,c}\left(0.29 + 0.71\frac{n}{N}\right) \tag{2.23}$$

The measured 11-year dataset of total radiation was compared with the estimated values of Ångström-Prescott equation (Eq. 2.6) and the calibrated Ångström equation (Eq. 2.23). Statistical analysis revealed that the Ångström-Prescott equation yielded slightly higher r^2 and RMSE than with Equations (2.22) and (2.23) (Table 2.8). Therefore, considering the results of statistical analysis and the fact that Ångström-Prescott equation is less empirical, it is suggested to prefer Eq. (2.6).

The empiricism involved in the standard procedures of estimation of long-wave radiation, described in Sections 2.4.1. and 2.4.2, raised the question if the number of the input parameters can be reduced. For example, the Priestley-Taylor method (Eq. 2.5) needs only temperature to calculate Δ and γ, while standard procedures for to estimation of R_n (Eq. 2.8-2.11) include also actual vapor pressure e_a. In fact, the Priestley-Taylor method is usually used particularly due to missing of e_a data. Therefore, simpler equations are needed to estimate net long-wave radiation.

Net long-wave radiation found with Eq. (2.8-2.11) was compared with simpler empirical equations listed in Table 2.8. The comparison was performed for June only and for all available data which comprised the full year. Improved parameters found in Section 2.4.7 were applied for a standard set of equations (Eq. 2.8-2.11). Different empirical equations were analyzed of which only the best are listed in Table 2.8. In general, the proposed simple equations showed a comparably good correlation with the measured data. For functional relationship $R_{nl}=f(R_s)$ in case of the data of June r^2 was 0.688 in comparison with 0.696 in Equations (2.8-2.11), but in the case of using all data the simple equation yielded even a better result, r^2 was 0.707 and 0.666, respectively (Table 2.8). Adding temperature, $R_{nl}=f(R_s, T)$ the correlation was slightly poorer in the case of June data, but in the case of all data the coefficient of determination was improved to 0.738. The first proposed equation can be more easily interpreted, i.e. $R_{nl}=f(R_s)$ reveals the proportion of incoming short-wave radiation and outgoing net long-wave radiation. Other combinations of empirical relationships were $R_{nl}=f(n)$, where n was duration of bright sunshine, $R_{nl}=f(n/N)$, where the ratio n/N was relative duration of bright sunshine, and $R_{nl}=f(R_s, e_a)$. The last equation revealed that the role of vapor pressure in estimation of net long-wave radiation was small. Thus, in the cases where e_a is not known, much simpler empirical equations may be used to estimate the net long-wave radiation in Estonian conditions.

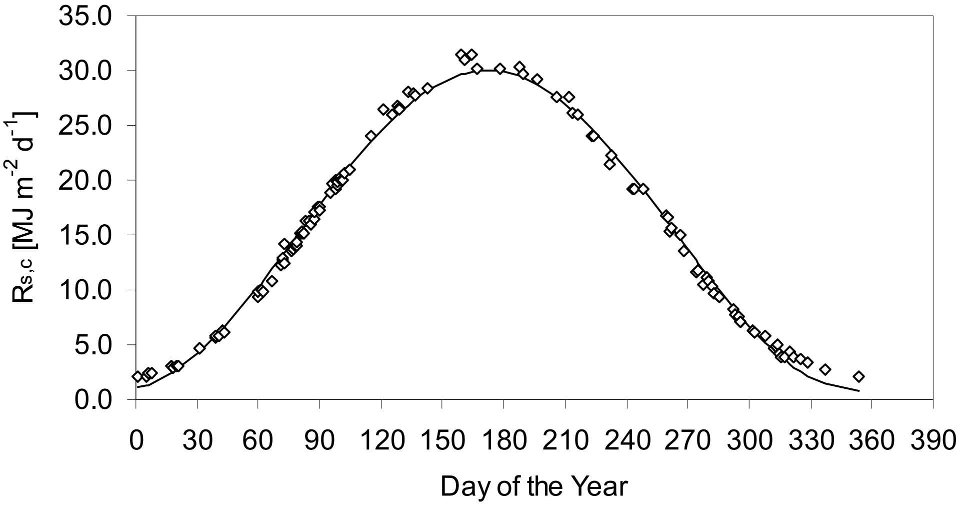

Figure 2.11. Total radiation of days very close to clear day conditions (n/N>0.95) measured at the Tõravere Actinometric Station for the period 1986-1996. Diamonds – measured values, line – estimated sinusoidal function.

Table 2.8. Comparison of different equations to calculate total short-wave radiation and net long-wave radiation (MJ m^{-2} d^{-1}) based on the measured data from Tõravere Actinometric Station for the period 1986-1996.

Equation		r^2	RMSE
Total radiation – All data			
Ångström-Prescott Eq. (2.6)			
$R_s = R_a\left(a_s + b_s\frac{n}{N}\right)$	a_s=0.20, b_s=0.56	0.974	1.34
Original Ångström equation with calibrated parameters			
$R_s = R_{s,c}\left(0.29 + 0.71\frac{n}{N}\right)$		0.972	1.40
Net long-wave radiation – June			
R_{nl} estimated with Eq. (2.8-2.11)		0.696	0.950
New functions:			
R_{nl}= -0.2437 R_s		0.688	0.924
R_{nl}= -0.2242 R_s -0.02681 T		0.683	0.916
R_{nl}= -0.4911 n		0.689	1.48
R_{nl}= -8.7539 n/N		0.691	1.47
R_{nl}= -0.2323 R_s -0.2004 e_a		0.682	0.919
Net long-wave radiation – All data			
R_{nl} estimated with Eq. (2.8-2.11)		0.666	1.25
New functions:			
R_{nl}= -0.2874 R_s		0.707	1.36
R_{nl}= -0.3378 R_s+0.0733 T		0.738	1.27
R_{nl}= -0.5250 n		0.754	1.45
R_{nl}= -7.3478 n/N		0.660	1.56
R_{nl}= -0.2617 R_s-0.4135 e_a		0.682	1.34

2.5 Soil heat flux

2.5.1 Introduction

The soil surface is a very important boundary as it forms the barrier where irradiant energy is partitioned and transformed into different fluxes according to heat/energy balance. The amount of heat absorbed by the soil is determined by available solar energy and the properties of the surface. Entering energy, called soil heat flux G, changes soil temperature, which significantly affects the physical, chemical, and biological processes occurring in the soil. For example, the oxidation of nitrogen into the nitrate form (*nitrification*) does not begin in spring before soil temperature reaches about 5 ^{0}C (Brady 1984), seed germination and root development start above certain critical temperatures, etc.

In spite of the smaller magnitude compared with net radiation and latent heat flux, the soil heat flux plays a substantial role in soil thermal regime. If there were no perturbations then two regular cycles would describe the warming and cooling of the soil: 1) diurnal cycle caused by interchange of daytime heating and nighttime cooling, and 2) annual cycle caused by the rhythm of short-wave radiation (see Section 2.4). At higher latitudes, e.g. in Estonia, the average total radiation in June is around 20 MJ m^{-2} d^{-1} (max values reach up to 30 MJ m^{-2} d^{-1}) whereas in December the average total radiation is only 1.0 MJ m^{-2} d^{-1}. Of course, these 'ideal' cycles are perturbed by meteorological conditions like cloudiness, advective warming and cooling, etc. Secondly, the soil properties, soil moisture regime, canopy cover and human activities influence soil thermal regime, making it difficult to model the rate of soil heat flux. Therefore, G is often neglected in evapotranspiration estimations, or is more seldom empirically estimated from net radiation.

Basically, the methods of soil heat flux estimations can be divided into 4 groups: 1) a simple empirical relationship between G and temperature (Kincaid and Heermann 1974, Wright 1982), 2) an empirical relationship between G and net radiation (Souch et al. 1996), 3) physically based, but idealized models using harmonious oscillation around average temperature (Carslaw and Jaeger 1959, Kirkham and Powers 1972), and, 4) a numerical solution of the partial differential equation of heat balance (e.g. Vakkilainen 1982). The last one, coupled with numerical models of water fluxes through the porous medium is preferred today, allowing to take into account both three-dimensional heterogeneity and temporal variations.

2.5.2 Soil thermal properties and heat flux

The *specific heat capacity* per unit volume of a substance C_S is defined as the quantity of heat required to raise a unit volume of the substance by one degree of temperature (Jury 1991). The specific heat capacity C_S can be estimated from the volume fraction of solids, water and air. The bulk specific heat C' of clay minerals, organic matter and water are 0.9, 1.92 and 4.18 J g^{-1} K^{-1} , respectively (van Wijk and de Vries 1963, Table 2.9). As the bulk specific heat of water is around fourfold higher than that of clay minerals then the changing water content in the soil affects the value of specific heat considerably. In typical mineral soils C_S values range from about 1 MJ m^{-3} K^{-1} in the dry state to about 3 MJ m^{-3} K^{-1} in the water-saturated state (Hillel 1998), Monteith and Unsworth (1990) propose values between 2.0 and 2.5 MJ m^{-3} K^{-1}.

Soil thermal properties are dependent on water content and on soil matrix composition, therefore, the effect of soil moisture changes on specific heat is determined by analyzing volumetric heat capacity:

$$C_S = \rho C' = \rho_m c_m x_m + \rho_o c_o x_o + \rho_l c_l x_l + \rho_g c_g x_g \tag{2.24}$$

where C_S – is vol. specific heat capacity [J m^{-3} K^{-1}]
ρ – is bulk density [kg m^{-3}]
C' – is bulk specific heat capacity [J kg^{-1} K^{-1}]
x – is the volumetric fraction [m^3 m^{-3}]
c – is bulk specific heat [J kg^{-1} K^{-1}]
indices *m*, *o*, *l*, *g* denote mineral matter, organic matter, and liquid and gaseous components, respectively

Thermal conductivity K_T is defined as the quantity of heat transferred through a unit area of the conducting body in unit time under a unit temperature gradient (Marshall et al. 1996). A small amount of water added into very dry soil may increase thermal conductivity by an order of magnitude, whereas the conductivity of very wet soils is almost independent of water content (Monteith and Unsworth 1990). *Thermal diffusivity* D_a is a product of specific heat, thermal conductivity and density, $D_a = K/\rho C'$. Thermal properties of soil constituents and indicative values for sandy and clay soils are given in Table 2.9.

In topsoil, organic substances may influence heat transfer conditions. The humus percentage of the typical Estonian soils is around 2%. The soil bulk density in topsoil is 1.2-1.4 g cm^{-3}. Root dry matter for grasslands is around 4 t ha^{-1} in the upper 10 cm layer and 0.3-1 t ha^{-1} in the 10-20 cm layer (Viiralt 1996). Thus the root mass is 0.004g DM cm^{-3} in the upper 10 cm layer or around 0.3% of bulk mass, for living roots around 30% higher, i.e. 0.4%.

Calculation of the heat flux is carried out using the following equation:

$$q_H = G = -K_T \frac{\partial T}{\partial Z} \tag{2.25}$$

where G – is heat flux density into the soil [J m^{-2} s^{-1}]
K_T – is thermal conductivity [J m^{-1} s^{-1} K^{-1}]
$\partial T/\partial Z$ - is the temperature gradient [K m^{-1}]

Soil moisture conditions may change greatly, from almost dry soil in the top layer after a warm and dry period, to saturated conditions, more likely to occur in deeper layers (e.g. shallow groundwater is typical for Estonian conditions) or in topsoil after heavy rainfall. Thus, according to Eq. (2.24) the thermal properties of soils may considerably vary spatially and temporally. The following analysis attempts to assess how well the soil heat flux is estimated using the average thermal properties and what kind of role it plays in the energy balance, e.g. compared with latent heat flux. For that purpose the numerically found G-values (see Section 2.5.4 *numerical model*) were used as a reference to assess the other models described in section 2.5.4.

Table 2.9. Thermal properties of soils and their components (after van Wijk and de Vries 1963).

	Density ρ 10^6 g m^{-3}	Specific heat C_S J g^{-1} K^{-1}	Thermal conductivity K_T W m^{-1} K^{-1}	Thermal diffusivity D_a 10^{-6} m^2 s^{-1}
Quartz	2.66	0.80	8.80	4.18
Clay minerals	2.65	0.90	2.92	1.22
Organic matter	1.30	1.92	0.25	0.10
Water	1.00	4.18	0.57	0.14
Air (20°C)	1.20x10^{-3}	1.01	0.025	20.5
Dry sandy soil	1.60	0.8	0.3	0.24
Saturated sandy soil	2.00	1.48	2.20	0.74
Dry clay soil	1.60	0.89	0.25	0.18
Saturated clay soil	2.00	1.55	1.58	0.51

2.5.3 Experimental data on soil temperatures

Experimental data for soil heat flux estimation were obtained from the Tõravere Actinometrical Station. Deep thermometers were installed in 1998 and a full dataset was obtained for 1999 only. The soil temperature was measured from bare soil (from the 1st of May to the 10th of October, at depth of 5, 10, 15 and 20 cm) and from clipped grass (from the 1st of January to the 31st of December, at depth of 20, 40, 80, 120, 160, 240 and 320 cm). Unfortunately, there was no data for clipped grass from the uppermost 20 cm.

Annual changes of soil temperature were more evident in subsoil, where the deeper layers were characterized by a more harmonious oscillation, a smaller amplitude and a longer time lag from the annual cycle of air temperature compared with topsoil (Fig. 2.12). The recorded maximum temperatures at different depths were as follows: bare soil at 5 cm 26.7 C^0 and at 20 cm 23.7 C^0, grass at 20 cm 20.9 C^0, at 120 cm 15.1 C^0 and 320 cm 10.7 C^0. The annual differences between the maximum and minimum recorded values for grassland were 23.8 C^0, 13.9 C^0, 6.8 C^0 at 20 cm, 120 cm and 320 cm, respectively. On a long term basis the average temperature of different layers should not deviate, e.g. in the present dataset the yearly average temperature at 20cm was 7.59 C^o, at 120cm 7.33 C^o, and at 320cm 7.25 C^o.

Due to the difference in the albedo and the other surface dependent variables of bare soil and grass-covered soil, soil temperatures at the same depths were different (Fig. 2.13). At the beginning of May the soil under the grass cover was warmer than the bare soil. Further the temperature of bare soil increased more than that of the soil under the plant cover, and during the summer months it was a couple of degrees higher. In October, the temperatures were equal.

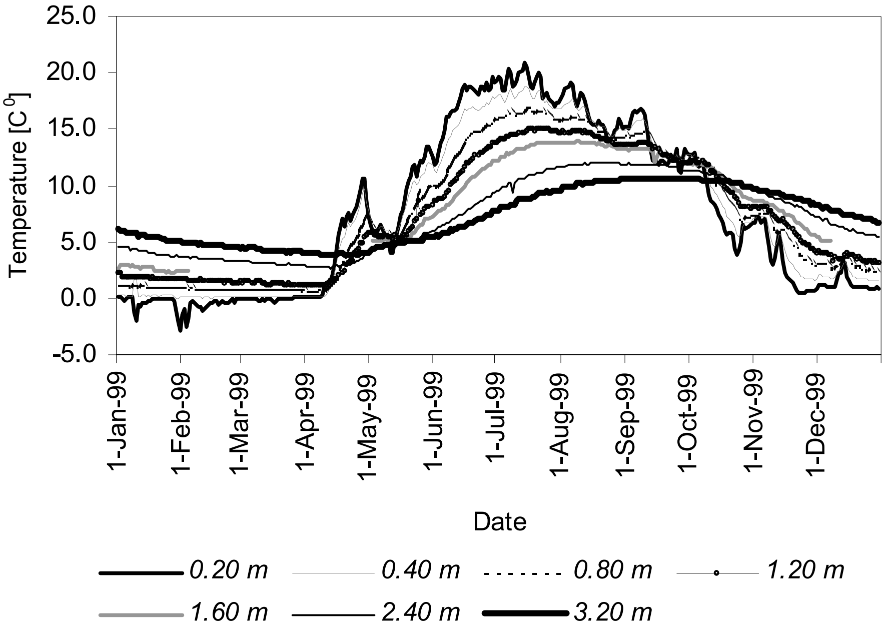

Figure 2.12. Annual temperature change in grassland recorded at different depths at the Tõravere Actinometric Station in 1999.

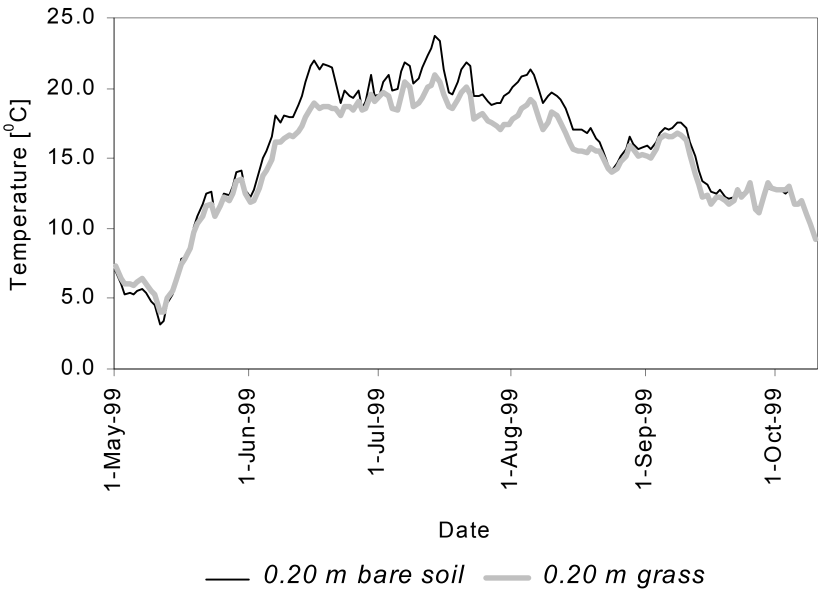

Figure 2.13. Soil temperature changes in bare soil and grass-covered soil at a depth of 0.20 m.

2.5.4 Models for calculation of soil temperature and soil heat flux

For the following analysis the numerically found G-values (see *numerical model*) were used as a reference dataset (G_{ref}) to assess the usefulness of empirical models to predict the soil heat flux.

Empirical daily model

In literature a few empirical methods can be found for estimation of daily soil heat flux for the root zone (e.g. Kincaid and Heermann 1974, Wright 1982), based on mean air temperature and on rough assumptions of average conditions:

$$G = 0.3768\left[\overline{T}_t - \left(\overline{T}_{t-1} + \overline{T}_{t-2} + \overline{T}_{t-3}\right)/3\right] \tag{2.26}$$

where G – is daily soil heat flux [MJ m^{-2} d^{-1}]
T – is daily average temperature [^{0}C]
t – is the index that corresponds to current day (t), previous day (t-1), etc.

In the present analysis this model completely failed because the coefficient of determination between the reference and estimated G was negligible (r^2=0.23) for the April-October period. At the same time, the linear correlation between air temperature and G_{ref} was higher (r^2=0.438) for the same period.

Radiation based model

Camuffo and Bernardi (1982) proposed a model of a simple fraction of the net radiation:

$$G = a_1 R_n + a_2 \frac{\partial R_n}{\partial t} + a_3 \tag{2.27}$$

where a_1, a_2 and a_3 are empirical coefficients
R_n – is net radiation [MJ m^{-2} d^{-1}]
t – is time [d]

The parameter a_1 indicates the overall strength of the dependence of the storage heat flux term on net radiation, the parameter a_2 describes the degree and direction of phase shift, and a_3 is an intercept term. Souch et al. (1996) calculated the wetland's soil heat flux from hourly data where the radiation gradient was estimated from $\partial R_n/\partial t=(R_n^{t+1}-R_n^{t-1})/2$, and they obtained high correlations for Eq. (2.27) r^2=0.977 and for the fitted linear model ($\partial R_n/\partial t$ omitted in Eq. 2.27) r^2=0.961. Analogous estimation was performed with the present dataset of daily measured net radiation and reference soil heat flux. The results revealed a much lower correlation for Eq. (2.27), r^2=0.547, while for a simple linear relationship r^2=0.479. Comparison of the cumulative curves of the reference soil heat flux and both calculated soil heat fluxes (Fig. 2.14) revealed that the gradient term may be omitted in Eq. (2.27) as it was proposed by Souch et al. (1996).

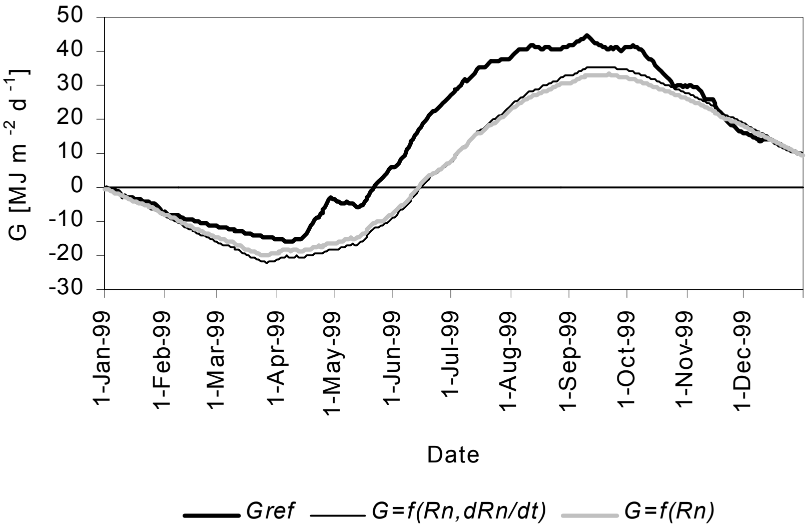

Figure 2.14. Cumulative curves of reference and estimated soil head fluxes estimated with Camuffo and Bernardi (1982) model.

Analytical solution

A rather rough approximation of the yearly fluctuation of soil temperature can be calculated from a sinusoidal function of time around an average value equal for all depths (Hillel 1998):

$$T(z,t) = T_{ave} + A_0\left[\sin\left(\varpi t + \phi_0 - \frac{z}{d}\right)\right]e^{-\frac{z}{d}} \tag{2.28a}$$

$$d = \left(\frac{2D_a}{\varpi}\right)^{\frac{1}{2}} \tag{2.28b}$$

$$D_a = \frac{K_T}{C'\rho} = \frac{K_T}{C_S} \tag{2.28c}$$

$$\varpi = \frac{2\pi}{86400 \cdot 365} \tag{2.28d}$$

where T_{ave} – is average temperature of the surface [K]
t – is time in seconds from the beginning of the year [s]
A_0 – is amplitude of the surface temperature fluctuation [K]
ϖ - is radial frequency [s^{-1}]
ϕ_0 – is phase constant [rad]
z – is depth [m]
d – is damping depth, at which the temperature amplitude decreases to the fraction 1/e of the amplitude at the soil surface A_0 [m].
D_a – is thermal diffusivity [m^2 s^{-1}]
K_T - is thermal conductivity [W m^{-1} K^{-1}]
ρ – is density [kg m^{-3}]
C_S – is volumetric specific heat [J m^{-3} K^{-1}]
C' – is bulk specific heat capacity [J kg^{-1} K^{-1}]

The yearly variation of soil temperature estimated from Eq. (2.28) yielded sinusoidal curves that were similar to those of measured soil temperatures (Fig. 2.15) and where the results improved towards depth. The calibrated phase constant was found to be -1.92 rad. Actually, the yearly variation of soil temperature did not follow the harmonious sinusoidal curve and the analytical method was not capable to take into account all temporal and spatial variations in soil thermal properties, the effect of snow cover, etc. The soil heat flux estimated from analytical temperature fluctuation according to Eq. (2.25) would have the same disadvantages as the estimated temperature. In case of atmosphere-plant-soil models this kind of solution may be too crude especially for topsoil and, therefore, the numerical methods need to be used instead of analytical ones.

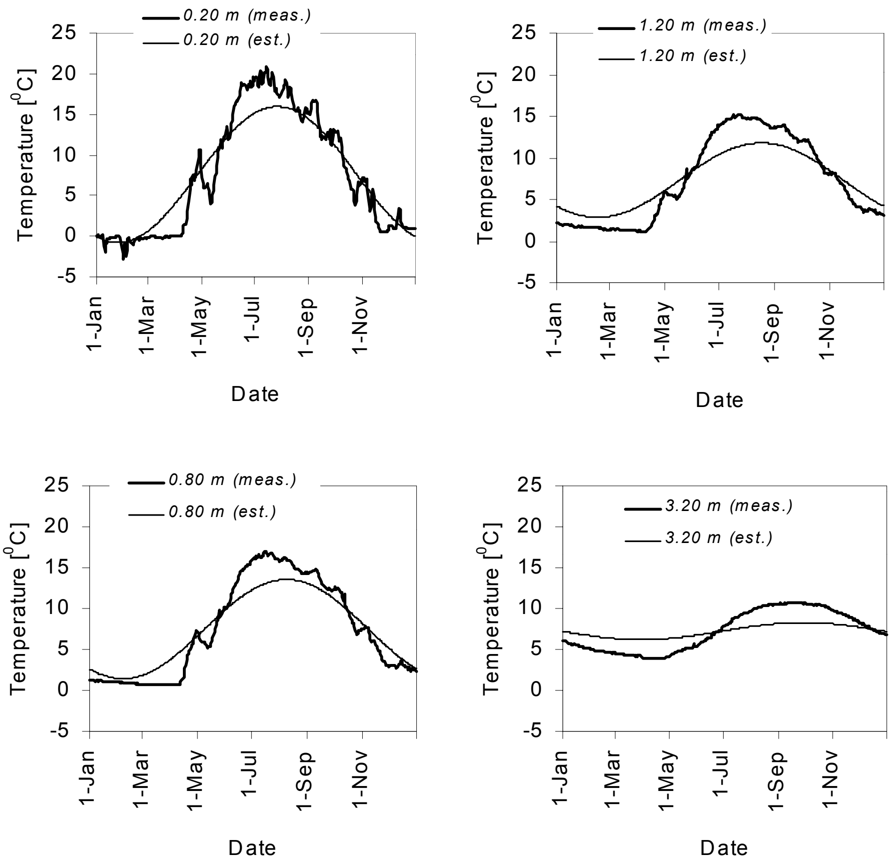

Figure 2.15. Measured and analytically calculated soil temperature at depths of 0.2 m, 0.8 m, 1.2 m and 3.2 m at the Tõravere Actinometric Station in 1999.

Numerical model

Soil temperature and heat flux can be estimated either for the Neuman-type boundary (flow boundary condition) or Dirichlecht-type boundary (state boundary condition), where heat flow into the soil surface or soil temperature is known, respectively. Accordingly, the lower boundary conditions must be set. In the present study the Dirichlecht-type boundaries were selected for the upper and lower boundaries.

Heat flux into or out of the soil can be numerically determined from the following heat conduction equation:

$$C_S \frac{\partial T}{\partial t} = K_T \frac{\partial^2 T}{\partial Z^2}; T(Z,0) = T_{Z0}; T(0,t) = T_0(t); T(Z_{max}, t) = T_{max}(t) \qquad (2.29)$$

where $T(Z,t)$ – is soil temperature [^{0}C]
t – is time [d]
Z – is coordinate [cm]
C_S – is specific heat capacity [J cm^{-3}]
K_T – is thermal conductivity of soil [J cm^{-1} d^{-1} ^{0}C^{-1}]
T_{Z0}– is initial condition [^{0}C]
$T_0(t)$ – is upper boundary condition [^{0}C]
$T_{max}(t)$ – is lower boundary condition [^{0}C]

Eq. (2.29) was solved numerically using the finite difference method by approximating the derivatives ∂T/∂t and ∂^{2}T/∂Z^2 :

$$C_S \frac{T_i^{n+1} - T_i^n}{\Delta t} = K_T \left\{ \Theta \left[\frac{T_{i-1}^{n+1} - 2T_i^{n+1} + T_{i+1}^{n+1}}{(\Delta Z)^2} \right] + (1-\Theta) \left[\frac{T_{i-1}^n - 2T_i^n + T_{i+1}^n}{(\Delta Z)^2} \right] \right\} \qquad (2.30)$$

where Θ is the coefficient of implicity (0.5…1.0), subscript i refers to the node and superscript n refers to the time step (values at level n are known and at level n+1 will be solved). Δt and ΔZ are the time step, and the nodal distance, respectively. The purpose of the calculation was to estimate the specific heat C_S and thermal conductivity K_T by using the least square error technique.

The unknown temperature at the node i and at the time step $n+1$ can be found after rearranging Eq.(2.30):

$$\left[\frac{C_S}{\Delta t} + 2K_T \frac{\Theta}{(\Delta Z)^2} \right] T_i^{n+1} = \frac{C_S}{\Delta t} T_i^n + K_T \left\{ \Theta \left[\frac{T_{i-1}^{n+1} + T_{i+1}^{n+1}}{(\Delta Z)^2} \right] + (1-\Theta) \left[\frac{T_{i-1}^n - 2T_i^n + T_{i+1}^n}{(\Delta Z)^2} \right] \right\} \qquad (2.31)$$

$$T_i^{n+1} = \frac{\frac{C_S}{\Delta t} T_i^n + K_T \left\{ \Theta \left[\frac{T_{i-1}^{n+1} + T_{i+1}^{n+1}}{(\Delta Z)^2} \right] + (1-\Theta) \left[\frac{T_{i-1}^n - 2T_i^n + T_{i+1}^n}{(\Delta Z)^2} \right] \right\}}{\left[\frac{C_S}{\Delta t} + 2K_T \frac{\Theta}{(\Delta Z)^2} \right]} \qquad (2.32)$$

The upper and lower boundary temperatures must be known and the other known temperatures between these depths are used for calibration of specific heat and thermal conductivity. For bare soil, the measured temperatures at 0 cm and 20 cm were set for the upper and lower boundaries, respectively. The measured temperatures at 5 cm, 10 cm and 15 cm were used for calibration of the specific heat C_S and thermal conductivity K_T. For grass-covered surfaces, temperatures at 20 cm and 120 cm were set for the upper and lower boundaries, respectively. The measured temperatures at 40 cm and 80 cm were used for calibration purposes. The diffusivity D_a was calibrated instead of specific heat and thermal conductivity. Specific heat was estimated from average soil conditions by the volumetric fraction using Eq. (2.24) and Table (2.9). Indicative value for partly saturated (50% pore space) soil was 2.12 J cm^{-3} K^{-1}. Equation (2.31) was solved using a spreadsheet program.

Even though the bare soil and grass-covered soil have the same physical properties, the different moisture regimes may influence the soil thermal properties. It was expected that D_a is temporarily variable, especially during the summer period, and towards depth. For bare, soil the calibration revealed the thermal diffusivity value of 0.22x10^{-6} m^2 s^{-1} for upper 20 cm during the investigation period (May-September). The statistical parameters for 5 cm depth were r^2=0.989, RMSE=1.16 ^{0}C, ME=-0.81 ^{0}C (Fig. 2.16) and for 15 cm depth r^2=0.997, RMSE=0.45 ^{0}C, ME=-0.30 ^{0}C. For grass-covered soil the calibrated thermal diffusivity value was 0.47x10^{-6} m^2 s^{-1} for deeper layers throughout the year. Statistical parameters for the 40 cm depth were r^2=0.998, RMSE=0.064 ^{0}C, ME=-0.06 ^{0}C (Fig 2.17). Statistical parameters for the 80 cm depth were r^2=0.998, RMSE=0.28 ^{0}C, ME=0.06 ^{0}C. These results are similar to findings of Kolyasev and Gupalo (1958), where they showed that the dynamics of diffusivity depends on soil water content and on the bulk density of loamy soil. The estimated thermal conductivity for upper soil was around K_T=300 J cm^{-1} d^{-1} °C^{-1} and increased towards the deeper layers yielding around K_T=860 J cm^{-1} d^{-1} °C^{-1} for the 1 m depth when constant specific heat was assumed.

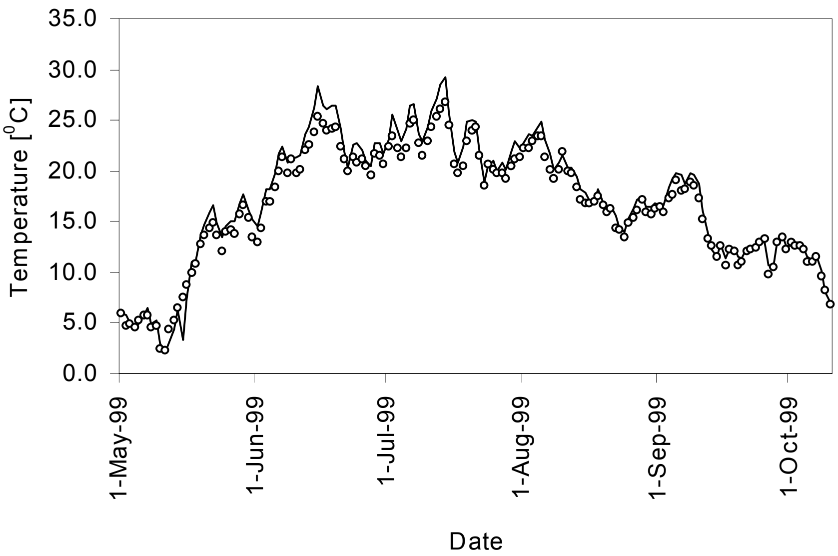

Figure 2.16. Measured (line) and estimated (circles) soil temperature of bare soil at a depth of 5 cm in 1999 at the Tõravere Actinometry Station.

Thus, it can be concluded that the numerical method performed successfully in estimation of temperature changes, but the practical problem for modelers is that measured soil temperature on soil surface as an upper boundary condition is rarely available and, therefore, should be estimated. The simplest solution for this problem is to use air temperature instead of surface temperature (e.g. Gupta et al., 1981, Thunhol, 1990), which is physically ambiguous because it is more stable than air temperature which may be fast affected by advected heat. On days with high net radiation, air temperature deviates considerably from soil surface temperature, by 5 or even more degrees (Fig. 2.18). A high temperature variance is also observed on days with fast advective warming or cooling (see 1st of September 1999 in Fig. 2.18). Generally, in spring and early summer, soil surface temperatures tend to be lower than air temperatures whereas in summer and autumn it is vice versa. In case of the snow cover its thermal conductivity, depending on age and depth, is to be taken into account.

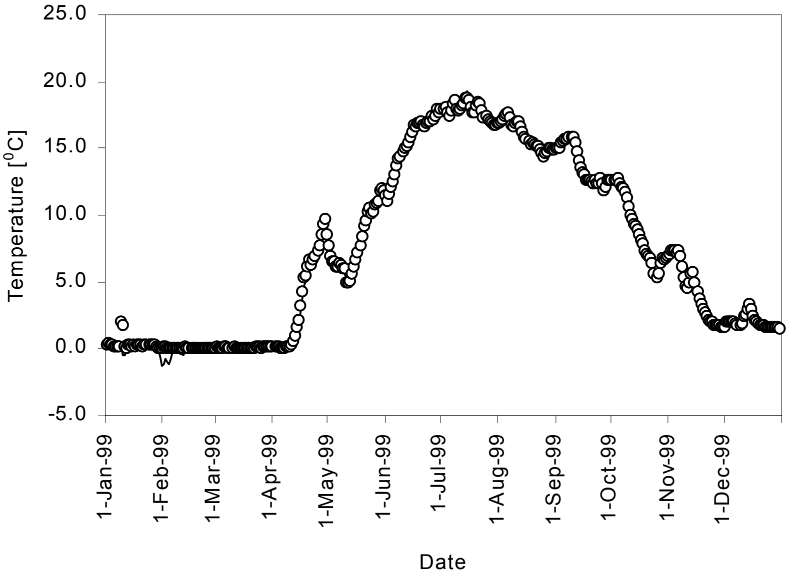

Figure 2.17. Measured (line) and estimated (circles) soil temperatures of grass-covered soil at a depth of 40 cm in 1999 at the Tõravere Actinometric Station.

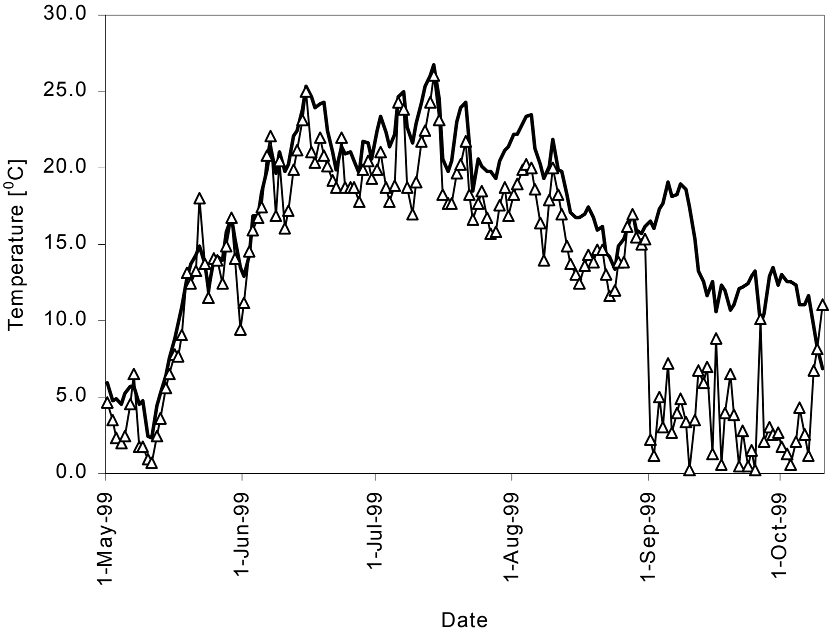

Figure 2.18. Measured air temperatures (thick line) and surface temperatures (line with triangles) in bare soil conditions at a depth of 5 cm depth at the Tõravere Actinometric Sataion in 1999.

The lower boundary condition can be given by sinusoidal temperature variation based on mean temperature and the annual amplitude at the soil surface as described above (*analytical method*). For example, for lower boundary conditions Thunholm (1990) selected the depth of 10 m in the conditions of northern Sweden.

Sensitivity analysis

Although theoretical analysis revealed a high dependence of soil thermal properties on water content (Section 2.5.2), which implies that transport of heat cannot be estimated by the average values of thermal conductivity and specific heat, the numerical modeling showed a relatively good agreement between the measured and modeled soil temperatures. Moench and Evans (1970) found that the diffusivity of the soil was relatively constant when the degree of saturation was higher than 30 per cent.

A sensitivity analysis was carried out to find the relative sensitivity coefficients for C_S and K_T. The analysis was performed for two periods, June and for the whole year, both for grass-covered surfaces at a depth of 40 cm, by changing C_S and K_T base value by 10%. The results are given in Table 2.10. Generally, predicted soil temperature has low sensitivity, whereas the estimated soil heat flux showed significantly higher sensitivity with changes in soil thermal properties, e.g. 10% higher thermal conductivity produced around 9% larger yearly average soil heat flux. Analysis revealed also the nonlinear character of sensitivity where different base values yielded different S_r coefficients. For example, at K_T=300 J cm^{-1} d^{-1} ^{0}C^{-1} the relative sensitivity coefficient for the yearly soil heat flux appeared to be 0.66 instead of 0.89 obtained with K_T=300 J cm^{-1} d^{-1} ^{0}C^{-1} (Table 2.10).

Table 2.10. The results of relative sensitivity analysis of the numerical soil heat flux model.

Parameter	C_S	K_T
Base value	2.12 J cm^{-3} K^{-1}	860 J cm^{-1} d^{-1} ^{0}C^{-1}
Relative sensitivity S_r		
T_{June}	-0.03	0.02
T_{Year}	-0.001	0.001
G_{June}	0.30	0.70
G_{Year}	0.12	0.89

2.5.5 Cumulative soil heat flux

There are two questions to ask: what is the amount of heat flowing into or out of the soil, and what proportion does G make up from the energy balance in Estonian conditions?, i.e. how much it influences the energy available for evapotranspiration? To answer these questions, the soil heat fluxes through a thin layer at top surface were estimated.

Unfortunately, the measured temperature for soil surface was available only for bare soil whereas in the case of grass-covered soil the measured temperatures started only from a depth of 20 cm. Two thin layers for the bare soil, 0-2.5 cm and 17.5-20 cm, were selected and the corresponding soil heat fluxes were calculated. The diurnal variation of soil temperature at the soil surface was evidently higher than at a depth of 20 cm (Fig. 2.19), reflecting the daily cycle of heating and cooling. When the cumulative values of the soil heat flux of both layers were calculated, it revealed that the cumulative heat flux was nearly the same at the end of the period (Fig. 2.20), however, the flux in the deeper layer delayed around one week. This allowed to assume that the selected layer of 20-25 cm in case of grass-covered surface reflects approximately the correct amount of heat penetrating the top surface.

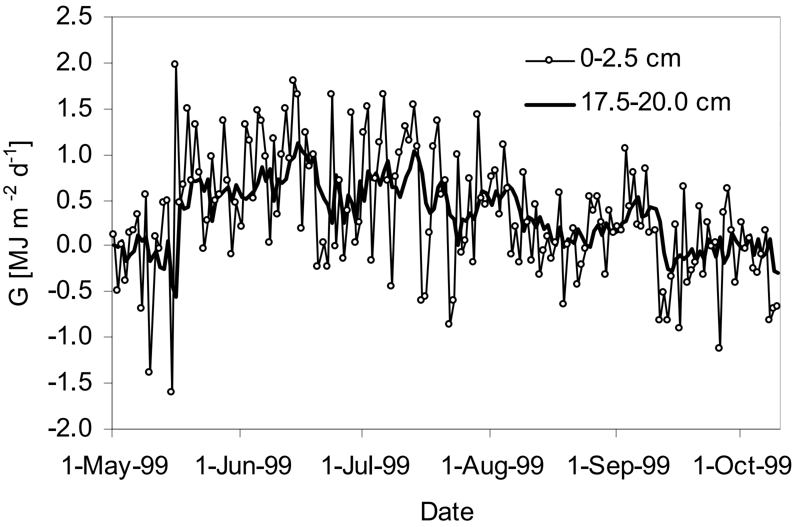

Figure 2.19. The soil heat flux through a 2.5 cm thick layer at two different depths of bare soil.

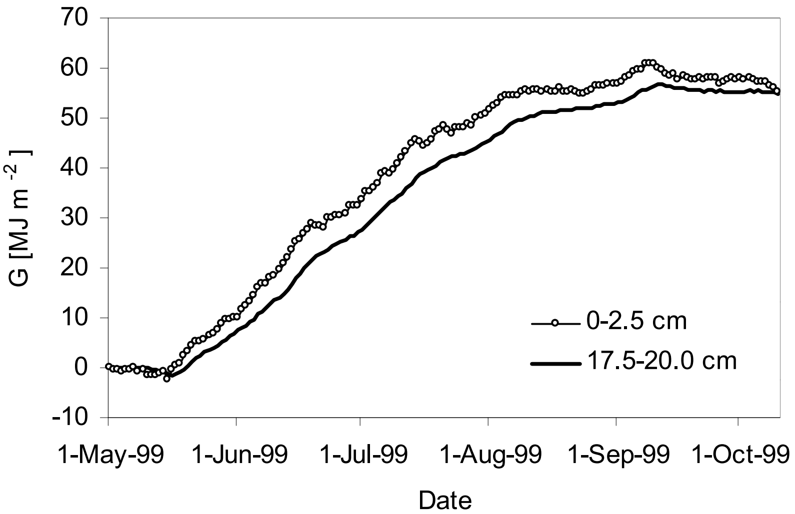

Figure 2.20. Cumulative soil heat fluxes through two thin soil layers of bare soil.

Cumulative heat fluxes were calculated for both bare and grass-covered surfaces. The amount of heat flowing through the surfaces was different due to the effect of shading and aerodynamic properties. During the season when G was positive, i.e. heat was flowing into the soil, the sum of the heat fluxes was approximately 172 MJ m^{-2} for bare soil, and only 60 MJ m^{-2} for grass-covered surface (Fig. 2.21). For the respective periods and surfaces the cumulative net radiation was of 1195 and 1415 MJ m^{-2}. Thus the amount of the heat absorbed by the soil was around 14% in case of bare soil and only around 4% in case of grass-covered surface.

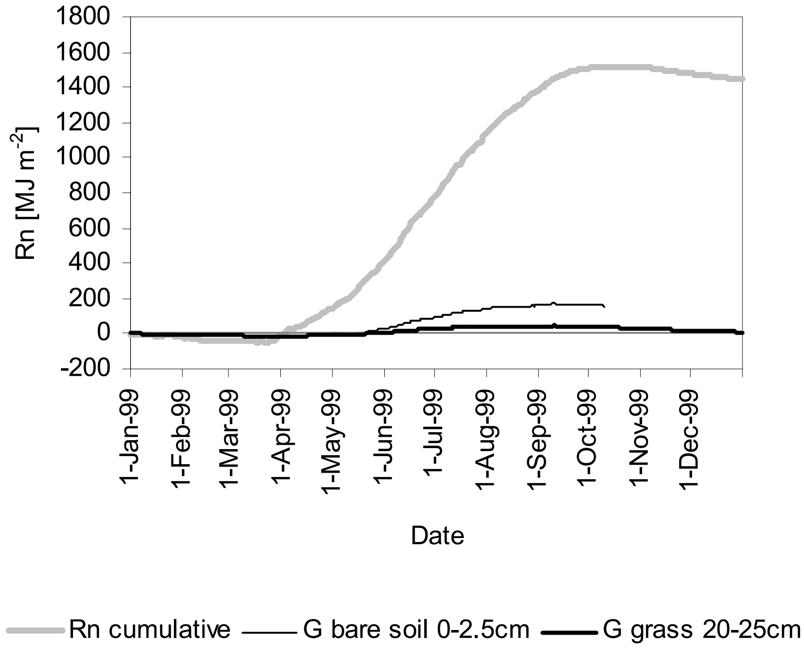

Figure 2.21. Cumulative fluxes of net radiation and soil heat fluxes in grass-covered soil and bare soil in 1999.

2.5.6 Effect of soil heat flux on energy balance

Part of the net radiation received by the soil surface is stored in the soil to be released later. Thus, available energy for evapotranspiration, e.g. in Eq. (2.4), depends also on the soil heat flux (i.e. R_n-G), but in many cases G is neglected due to estimation difficulties, and due to its small magnitude compared to net radiation. When both R_n and G are plotted on the same figure, the assumption of neglecting the soil heat flux becomes evident, as in the winter period, when G may increase the *ET*, the actual rate of *ET* is very low in Estonian conditions and the corrected energy level (R_n-G) will not influence considerably absolute *ET* rate. However, the situation may be different during the spring, summer and fall months with higher absolute evapotranspiration rate. According to the measurement results of one year together with estimated value of the soil heat flux (Section 2.5.5), the total soil heat flux forms only 0.7% of the total energy balance (Table 2.11). During the period from April to August the soil heat flux reduces net radiation by 56.7 MJ m^{-2} which makes up 4.1% of total available R_n for the same period. When analyzing the monthly data then in 1999 G formed 7.7% of R_n in April and only 1.5% of R_n in August. After this stored heat started to increase available energy. For example, Vakkilainen (1982) estimated in South-Finland, similar to Estonian conditions, the following soil heat fluxes: 16.04-20.05.1973 9.1%, 14.05-04.06.1974 5.7%, 07.06-26.06.1973 6.6%, 13.08.-26.08.1974 3.7%. Thus, the above results are in a rather good agreement with the results presented in Table 2.11.

Considering that the energy term in the Penman-Monteith equation (Eq. 2.4) accounts for approximately 50% of *ET* (the rest is caused by the aerodynamic term, see section 3.7.3) then neglecting soil heat flux in mid summer when G might be approximately 6% of R_n causes overestimation of evapotranspiration around 3%. In fact, this is comparable with possible error in radiation measurements, but it has a systematic character. It can be concluded that the soil heat flux does not play a crucial role in *ET* estimation, but due to its systematic effect on available energy it can be suggested to couple the soil heat flux model with detailed water balance models.

Table 2.11. Measured monthly net radiation R_n, estimated soil heat flux G, corrected available energy for evapotranspiration and sensible heat (R_n-G) and the percentage of soil heat from net radiation at the Tõravere Actinometric Station in 1999.

Month	R_n MJ m^{-2} month^{-1}	G MJ m^{-2} month^{-1}	R_n-G MJ m^{-2} month^{-1}	G abs. %
January	-22.6	-7.5	-15.0	33.3
February	-20.2	-4.0	-16.3	19.7
March	31.2	-3.7	35.0	12.0
April	154.6	11.9	142.7	7.7
May	260.0	9.3	250.6	3.6
June	362.5	21.0	341.4	5.8
July	361.3	10.8	350.5	3.0
August	249.3	3.7	245.6	1.5
September	132.7	-0.5	133.2	0.4
October	6.6	-11.4	17.9	173.4
November	-34.6	-13.7	-20.9	39.5
December	-36.9	-6.6	-30.3	17.8
Total	1444	9.4	1434	0.7

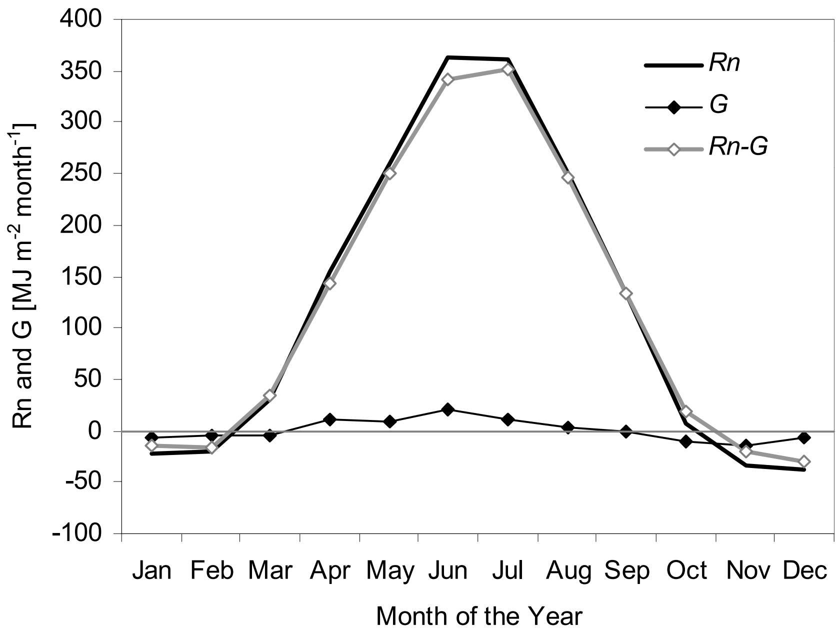

Figure 2.22. Observed monthly net radiation R_n, calculated soil heat flux G and corrected net radiation at the Tõravere Actinometric Station in 1999.

2.6 Conclusions

Upper boundary processes have a crucial effect on the water balance of the soil profile. Different measurement and estimation methods of evapotranspiration were reviewed. It was recognized that available energy (i.e. R_n in evapotranspiration methods) plays an essential role in evapotranspiration phenomena. Both energy and water balance components were estimated and compared with observed values and experimental results.

1. The standard procedure for estimating net radiation was parameterized with new values to improve the fit of the measured and estimated radiation in Estonian conditions. It was found that the standard set of parameters caused systematical overestimation of net radiation during the summer months and underestimation in the winter months. New calibrated coefficients remarkably improved the fit of the measured and the estimated data. The 11-year mean values of R_n, for June with measured, estimated with a standard set and with the improved coefficients were 10.6, 11.77 and 10.53 MJ m^{-2} d^{-1}, respectively. Calibration improved the coefficient of determination r^2 and RMSE relatively more in the months with low radiation.
2. The standard set of radiation equations predicted net long-wave radiation relatively poorly compared with short-wave radiation. New equations for net long-wave radiation, based only on R_s, n, or n/N, were developed. These equations may also be used in the Priestley-Taylor equation.
3. Probability analysis, based on the data of June revealed that the estimated net radiation yielded a probability density function different from obtained with measured radiation due to the missing of low and high values of R_n.
4. The surface cover influences significantly the cumulative soil heat flux, e.g. in 1999 in case of bare soil and grass-covered surface G accounted for 14% and only 4% of R_n, respectively.
5. Different empirical, analytical and numerical methods for estimating the soil heat flux were reviewed and compared with the estimated values obtained from the Tõravere Actinometric Station. The soil heat flux from grass-covered surfaces was less than 10% of the net radiation during the March-September period. The highest soil heat flux, in June (21 MJ m^{-2} $month^{-1}$), was equal to 5.8% of the the net radiation. The largest relative value, in October (-13.7 MJ m^{-2} $month^{-1}$), was equal to -173.4% of the net radiation.

Chapter 3

UPPER BOUNDARY: Case study – Lysimeter evapotranspiration

3.1 Introduction

Among the different methods for evapotranspiration measurements weighing lysimeters have been widely used. Belonging to the group of hydrological approaches (see Chapter 2), evapotranspiration is measured directly from the mass change of the lysimeter, which distinguishes this method from the other hydrological approaches, e.g. from non-weighing lysimeters based on indirect volume balance approach. In general, the weighing lysimeter is a container, which is filled with a sample of disturbed or undisturbed soil cultivated in the same manner as the surrounding field. To determine the mass change of a lysimeter it is weighed.

A number of experiments have been carried out with weighing lysimeters of different evaporative area and soil column depth, starting from heavy lysimeters and ending with small scale laboratory column experiments. Howell et al (1995) reported experiments where weighing lysimeters containing undisturbed monoliths of 3x3x2.3 m were used. Liu et al. (2002) employed weighing lysimeters with a designed size of 2.0x2.5x2.5 m with a weight of about 12000 kg. Qiu et al. (1998) used a weighing lysimeter of 1.5 m in diameter and 1.5 m in depth, which had a resolution of 50 g, corresponding to 0.028 mm of water depth. Todd et al. (1991) carried out evapotranspiration experiments in the mini-lysimeters which were constructed from a PVC irrigation pipe and were 0.225 m deep with an inside diameter of 0.150 m and a wall thickness of 3.2 mm. In fact, both surface area and depth play an important role in experimental setup, and hence also, on results. The border effect (i.e. flow between the lysimeter wall and the soil core) is more substantial in the case of small lysimeters. However, the dimensions of weighing lysimeter are limite by the capacity to measure its weight with necessary accuracy.

The data obtained by the weighing lysimeter may not be representative for the whole field due to several reasons. Differences in canopy properties inside and outside the lysimeter (i.e. density and height) affect the aerodynamic and radiative transfer processes. If the surrounding area is drier than that of the lysimeter, an oasis effect occurs as radiation energy partitioning outside the lysimeter distributes more sensible heat, which is advected toward the lysimeter causing overestimation of the lysimeter evapotranspiration. In fact, the soil inside the lysimeter may also be drier, especially in shallow groundwater areas and with short soil column lysimeters, where the bottom of the lysimeter cuts the pathway of the capillary fringe. It can be avoided with investigation of the soil water content inside and outside the container, and by adding water into the lysimeter bottom, if necessary. Also, the metallic lysimeter rim, heated by radiation energy, can cause advection of additional sensible heat toward the lysimeter. In the early stages of canopy development the rim extending over the vegetation may affect the aerodynamic properties.

The present analysis of evapotranspiration is based on experiments with a hydraulic evaporating pan, conducted by V. Tamm. He compared the original Penman equation (1948) with the measured evapotranspiration values during the four growing seasons (Tamm 1994). The aim of the present chapter was to validate the Penman-Monteith equation with experimental data, to study the dependency of canopy resistance from meteorological parameters and to compare the Penman-Monteith equation with the Priestley-Taylor equation.

3.2 Instrumentation

Unlike experiments referred to previously, the present lysimeter study was conducted with a hydraulic evaporation pan GR-17 (*made in* Russia) where instead of weighing the lysimeter, another physical principle was used (Fig. 3.1). It is based on the law of Archimedes where the change of weight, expressed as a change of water content in the monolith, is determined by the monolith's sinking depth. The hydrostatic balance is described as:

$$\Delta m = \Delta l\ A\ \rho \tag{3.1}$$

where Δm – is mass change of the monolith [kg]
Δl – is change of sinking depth caused by mass change of the monolith [m]
A – is area of cross-section of the monolith [m^2]
ρ – is density of liquid in which monolith with the pontoon is floating [kg m^{-3}]

The cylinder was filled by pressing it into the soil with a special mechanical device. Then it was excavated and the bottom was fixed to the base to retain the soil. The husk was inserted into the floating pontoon and balanced with ballast weights at three shafts in the pontoon and the proper sinking depth was obtained using heavy weights under the center of the pontoon. Both the pontoon and the water level gauge were freely floating inside the water tank. They were kept in the right position under the micrometric gauges within a space determined by wire and rubber threads. Three micrometric electric gauges were used to measure the sinking depth and one gauge was used to measure the water level. The relative change in vertical direction was determined by establishment of the electrical contact with mercury inside the small vessels, after which the readings from micrometric gauges were taken. The average of the three gauges was used as a daily reading. There was no considerable loss of water from the tank of the pan, because a thin film of oil covered water surface, and the roof of the hydraulic pan was covered with a soil layer with growing grass, which prevented direct sunlight from reaching the water surface of the tank.

Two rain gauges (GGI-500, made in Russia) with an area of 500 cm^2 were installed nearby the hydraulic pan. Wind corrections were not made as the precipitation was measured *in situ* at the same level as the hydraulic pan. As the vertical movement of the pan was caused both by evaporated water and precipitation, the daily *ET* values were corrected by measured precipitation. The hydraulic evaporation pan GR-17 enables to measure evapotranspiration in a soil monolith with a height of 1.5 m and an area of 2000 cm^2.

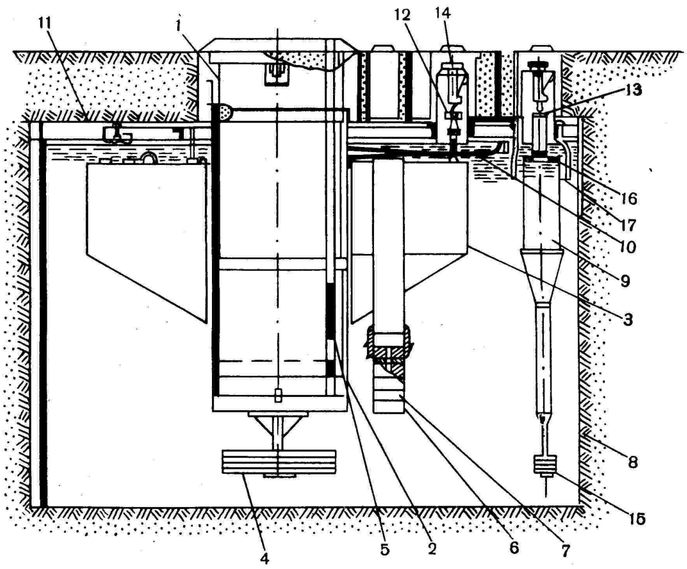

Figure 3.1. Scheme of the hydraulic evaporation pan GR-17.
1 – soil monolith within cylinder, 2 – outer husk, 3 – ring pontoon, 4 – heavy weights, 5 – piezometer to monitor the water level inside the monolith, 6 – shaft of floating pontoon, 7 – ballast weights, 8 – water tank of the hydraulic evaporation pan, 9 – floater of water level gauge, 10 – wire to fix the position of floating pontoon, 11 – roof of the hydraulic pan, 12 – vessel with mercury on floating pontoon, 13 - vessel with mercury on water level meter, 14 – micrometric electric gauges, 15 – light weights, 16 – regulating weights, 17 – rubber threads to fix the water level meter.

Sources of error

The accuracy of the hydraulic pan to measure the vertical shift of the pontoon was ±0.1 mm. In fact, it was probably lower than possible errors occurring from the measurements of precipitation. Daily measured evapotranspiration was calculated from the vertical shift of the pontoon and the measured precipitation:

$$ET_a = \Delta l + P \tag{3.2}$$

If actual precipitation into the lysimeter was different from that measured at rain gauges, then the calculated value of ET_a was erroneous by the difference between actual and recorded precipitations.

3.3 Description of the experiment

The hydraulic evaporating pan was installed at two sites near Tartu (Fig. 1.2). In 1984 and 1985 the experiment was carried out at Eerika (58° 22’ N, 26° 40’ E) on study fields belonging to the Institute of Grassland Husbandry at the Estonian Agricultural University. Measurements started on the 4th of July and took place until the end of September. In 1985 the experiment lasted from the 1st of May to the 10th of August. New financing allowed restarting the experiment in another location, at Polder of Aardla (58° 19’ N, 26° 44’ E), 6.6 km from the Eerika site. The Polder of Aardla is a typical cultivated grassland area, where experiments were conducted from the 6th of July to the 30th of September in 1988 and from the 1st of May to the 30th of September in 1989.

The soil profile at the Eerika site consists of an upper layer (0-70 cm) of sandy loam and a denser lower layer of sandy clay loam (70-150 cm). The soil is classified as light pseudopodzolic soil (FAO/ISRIC *Planosol*) (Reintam 1995). The soil profile at Aardla site consists of two distinct layers, sand (0-90 cm) and silty clay loam (90-150 cm), where the lower layer forms a barrier. The soil is classified as Gley-alluvial soil (FAO/ISRIC - *Eutric Fluvisol*) (Reintam 1995). Main species growing in the lysimeter and in the surrounding field were the following: at Eerika – *Trifolium repens L.*, *Lolioum perenne L.*, *Phleum pratense L.*, *Poa pratensis L.*, and at Polder of Aardla – *Dactylis glomerata L.*, *Phleum pratense L.*, *Phalaris arundinacea L.*, *Alopecurus pratensis L.*

After installation in early spring, the roof of the hydraulic pan was covered with an undisturbed topsoil layer taken from the same place prior to installation of the pan (Fig. 3.2). This ensured that the canopy cover conditions were the same as those of the surrounding area. To improve the quality of grass, the surrounding area of the experiment was seeded by a species of grass. The lysimeter experiment was started after the ground surface was fully covered by canopy, i.e. in 1994 and 1988 the sampling period was shorter than in the second years of the experiment. During the vegetation period, the grass was clipped three times, so that the average estimated canopy height was around 15 cm over the lysimeter and the surrounding area. The readings of the micrometric gauges and precipitation were taken every day at 8 pm. All other meteorological data was received from the Tartu Meteorological Station.

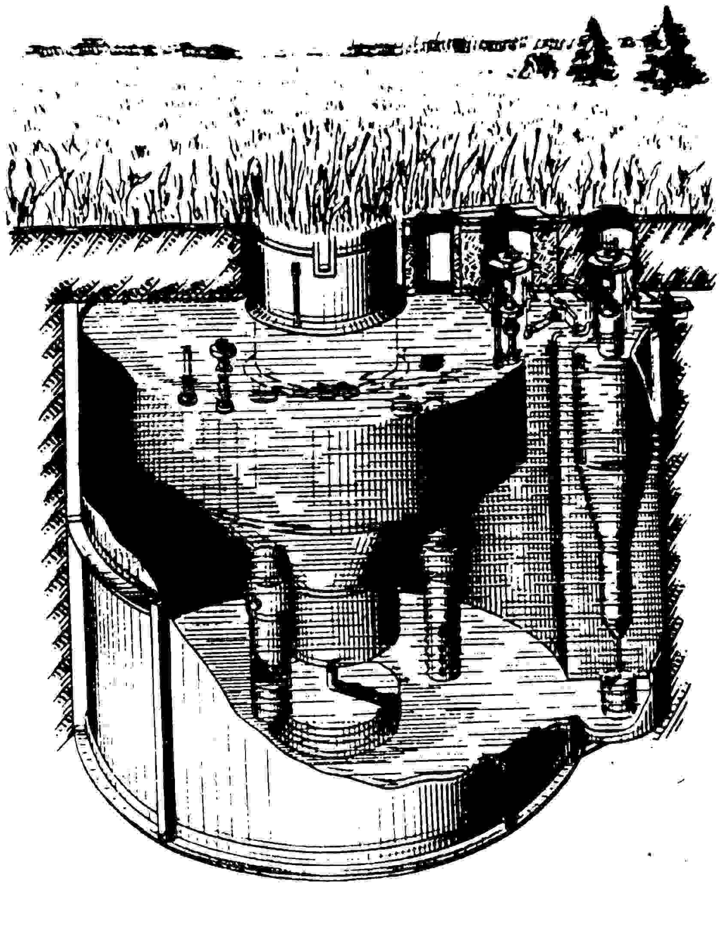

Figure 3.2. Illustration of the hydraulic pan.

Table 3.1. Measured soil properties at Eerika and Aardla experimental sites.

Layer cm	Sand %	Silt %	Clay %	Bulk density g cm^{-3}	Organic matter %	Soil type
			Eerika			
0-20	48.7	38	5.9	1.59	2.7	Sandy loam
20-30	54.9	37.2	7.9	1.64	1.16	Sandy loam
30-50	34.8	38.8	26.4	1.71	0.81	Loam
50-70	60.4	26.3	13.3	1.86	0.35	Sandy loam
70-100	47	24.8	28.2	1.88	0.2	Sandy clay loam
100-150	58.1	23.1	18.8	1.88	0.06	Sandy clay loam
			Aardla			
0-20	86.8	6.2	2	1.20	4.6	Sand
20-30	86.2	12.2	1.6	1.37	4.2	Sand
30-40	89	9.9	1.1	1.47	2.1	Sand
40-70	92	7	1	1.62	0.15	Sand
70-90	85.1	10.7	4.2	1.74	0.150	Sand
90-100	22.2	51.7	26.1	1.76	0.03	Clay loam
100-150	15.1	58.8	26.1	1.80	0.01	Silty clay loam

3.4 Meteorological conditions

Meteorological conditions in the years of the experiments during the vegetation period were different, but close to long time average conditions, except for 1985. For reference conditions, long term average monthly precipitation, air temperature and duration of bright sunshine at Tartu Meteorological Station, located around 10 km from the experimental fields, were used. Total precipitation during the April-September period was 354 mm, 619 mm, 353 mm, and 349 mm in 1984, 1985, 1988, and 1989, respectively. The corresponding long-time average value (1955-1989) was 368 mm. The second year of the experiment was classified as very rainy, as the long-time average yearly precipitation (591 mm) was less than it was recorded merely during the April-September period in 1985. All the years, except for 1985 again, were warmer than the long-term average, particularly 1988, and the total duration of bright sunshine exceeded the average by 2-8%. Variation of the meteorological conditions during the experiments, which caused water shortage or excess periods, is discussed below.

In 1984, the spring was dry and warm (Fig. 3.3 and 3.4) and, especially in April, precipitation was very low. When the experiment was started no ground water level was observed at the soil monolith. However, during the following months actual evapotranspiration corresponded to estimated potential rate (Table 3.2). The total balance of actual evapotranspiration and recorded precipitation was 52 mm in excess of rainfall due to extensive precipitation and low evapotranspiration in September.

In 1985 precipitation exceeded the long-term average values in all months except for April, and measured cumulative evapotranspiration was 80 mm less than recorded precipitation. Groundwater level was found at the bottom of the soil profile, but unfortunately no exact readings were taken. It is quite evident that there was no root water uptake reduction due to water shortage (i.e. ET_a was close to ET) in 1985 (Table 3.2).

In 1988, when the experiment was transferred to the Polder of Aardla area, the climatic conditions were similar to those in the first year of the experiment at Eerika site when precipitation was very low in April. Also, following May and June were very dry. When precipitation was compared with actual evapotranspiration it appeared that ET_a was only slightly higher than P in July and around 70 mm lower than precipitation in August. Therefore, reduction of evapotranspiration due to water shortage could have occurred most probably in July 1988, especially when high average temperature is considered. In all other months evapotranspiration reached potential rate or was close to it.

The last year of the experiment, 1989, differed from the previous ones in a negative water balance, i.e. evapotranspiration was 43 mm higher than precipitation. Reduction in evapotranspiration could be expected in May and July (Table 3.), but probably the water stored in the soil profile compensated for the difference between *ET* and *P*. In fact, very dry and very rainy months alternated so that after high precipitation in June, the July was dry, August was rainy and September was dry again.

Figure 3.5 explains why the highest actual evapotranspiration and potential evapotranspiration were found in July 1989 instead of a very warm July 1988. In 1989 the cumulative recorded duration of sunshine hours was around 6% higher than in 1988. Hence, the energy available for evaporation was also higher.

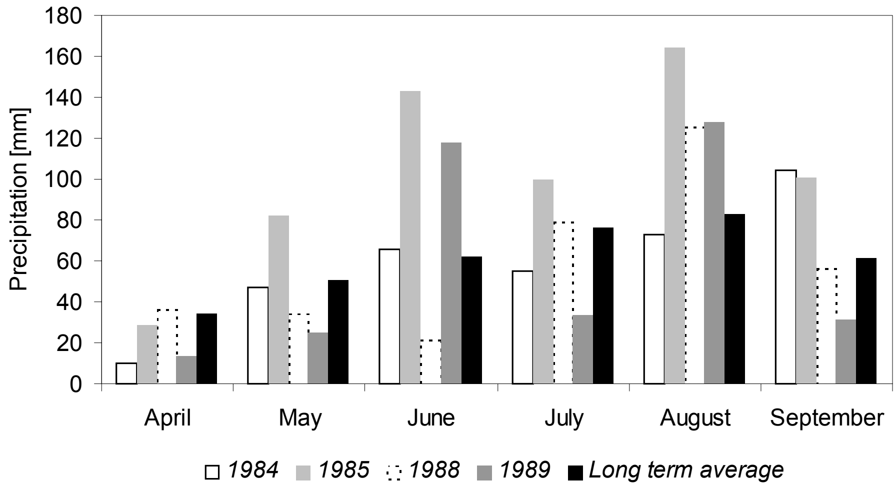

Figure 3.3. Monthly precipitation at the Tartu Meteorological Station.

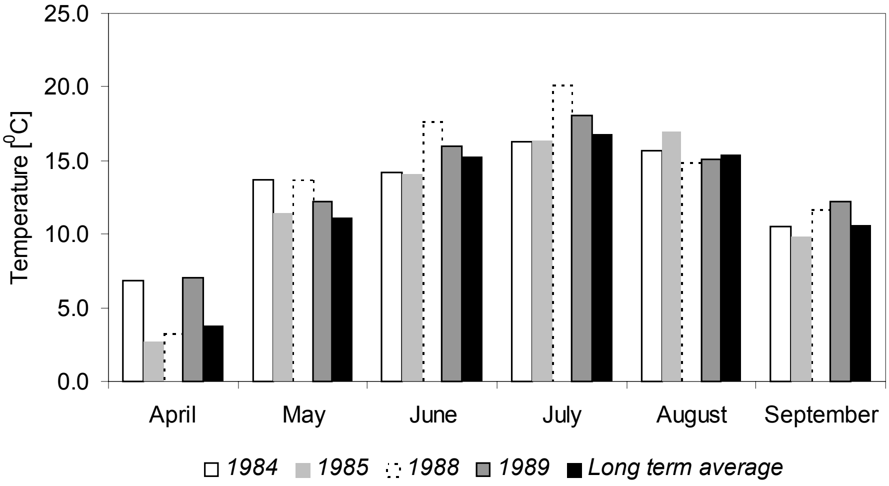

Figure 3.4. Monthly average air temperature at the Tartu Meteorological Station.

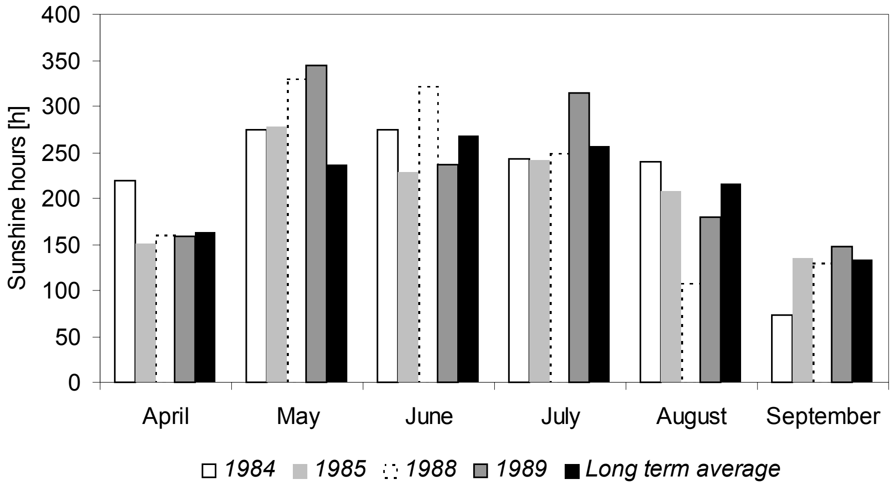

Figure 3.5. Bright sunshine hours at the Tartu Meteorological Station.

3.5 Comparison of measured and calculated evapotranspiration using the Penman-Monteith method

The measurements of evapotranspiration made with the aid of the hydraulic lysimeter were used to validate the Penman-Monteith method in Estonian conditions. The following assumptions were made for all calculation periods: 1) average canopy height was 0.15 m, 2) soil heat flux was set at 0 (the consequences are discussed later), 3) net radiation was estimated with the new empirical parameters found in Section 2.4. Aerodynamic resistance and canopy resistance were estimated according to Monteith (1965) and Allen et al. (1989), respectively (see also Section 3.6). It should be emphasized that the experimental data were not screened nor modified, and no calibration was done in the estimation of evapotranspiration. As it was described in Section 3.4, precipitation was measured on-site, while all other necessary meteorological parameters were obtained from the Tartu Meteorological Station located approximately 10 km from both the Eerika and Aardla experimental sites.

Table. 3.2. Cumulative monthly precipitation *P*, measured ET_a and calculated $ET_{P\text{-}M}$.

	Eerika 1984			Eerika 1985			Aardla 1988			Aardla 1989		
Month	*P*	ET_a	$ET_{P\text{-}M}$	*P*	ET_a	$ET_{P\text{-}M}$	*P*	ET_a	$ET_{P\text{-}M}$	*P*	ET_a	$ET_{P\text{-}M}$
May				82	89	85				25	92	93
June				143	86	80				118	85	81
July	47*	80*	78*	100	86	82	79***	84***	79***	34	105	102
Aug.	73	71	77	44**	27**	26**	126	55	48	128	66	60
Sept.	104	22	27							31	31	35
Total	224	172	183	368	288	272	204	139	126	336	379	372

* 4.07.1984-30.07.1984
** 1.08.1985-10.08.1985
*** 6.07.1988-30.07.1988

In 1984, measurements of ET_a started at the beginning of July when it was decided that the canopy at the hydraulic evaporative pan and in the surrounding area was developed enough to fully cover the ground. Measured and estimated evapotranspiration showed a good correlation (r^2=0.832, RMSE=0.57 mm), but the calculated values slightly overestimated the 'true' values (ME=-10.5 mm) (Table 3.3). The measured peak values of ET_a reached 5.3 mm d^{-1} in July, 4.9 mm d^{-1} in August and 3.2 mm d^{-1} in September (Fig. 3.6). The monthly average values were 2.8, 2.5 and 0.9 mm d^{-1}, respectively. Generally, the maximum measured values exceeded the estimated values. In September, total rainfall was almost twofold higher than the long-term average, duration of bright sunshine was twofold lower and actual evapotranspiration was above 1 mm d^{-1} only on a few days without rainfall. Further analysis revealed that the measured values smaller than 1 mm d^{-1} were very sensitive to measurement error mainly due to inaccuracy of the precipitation measurements. For instance, the backward calculation of canopy resistance (Section 3.6) failed during days with low evapotranspiration rate.

In the second year of the experiment, 1985 (Fig. 3.7), throughout the measurement period, a very high correlation was achieved between the measured and calculated evapotranspiration (r^2=0.889, RMSE=0.40 mm). An almost perfect fit was achieved for certain periods, e.g. from the 19th June to the 26th June. The measured minimum rate of evapotranspiration was systematically higher than the estimated one, the same conclusion holds also in case of a high rate of evapotranspiration so that ME>0 in all months (overall ME=16.0 mm). The measured peak values of ET_a reached 4.5 mm d^{-1} in May, 4.9 mm d^{-1} in June and 4.7 mm d^{-1} in July. The monthly average values were 2.7, 2.7 and 2.6 mm d^{-1}, respectively.

The biggest discrepancies between the measured and estimated evapotranspiration and the poorest correlation (r^2=0.586, RMSE=0.82 mm, ME=12.6 mm) were found in 1988 (Fig. 3.8, Table 3.3), after installation of the hydraulic pan in a new location at the Polder of Aardla area. During several days measured ET_a remarkably exceeded the calculated values without evident reasons, because this occurred on days without rainfall which could cause error in evapotranspiration measurements. The highest recorded daily ET_a during the whole experiment period also occurred in this year, on the 17th of July reaching 5.7 mm d^{-1}. The monthly average evapotranspiration values were 3.0 mm day^{-1} in July and 1.5 mm d^{-1} in August, respectively. The last figure is explained by low available energy in August, as the observed sunshine duration made up only half of the long-term average (Fig. 3.5).

In the second year in the same location, a good overall correlation was obtained (r^2=0.901) with the lowest mean error (ME=6.7 mm) and root-mean-square error (RMSE=0.39). This is similar to Eerika's experiment when the second year revealed a better fit between the measured and estimated values. In May ET_a was during several days as high as 4 mm d^{-1}, causing higher monthly average of 3.0 mm d^{-1} compared with the Eerika's results in 1985. The corresponding peak and the average values for the following months were: June (4.8 mm d^{-1}, 2.7 mm d^{-1}), July (5.2 mm d^{-1}, 3.3 mm d^{-1}), August (4.0 mm d^{-1}, 1.9 mm d^{-1}), and September (2.5 mm d^{-1}, 1.2 mm d^{-1}), respectively.

The collected data were analyzed also on a monthly basis. The correlation between the measured and calculated evapotranspiration varied in different months and different years (Table 3.3), e.g. in July the coefficient of determination r^2 varied from 0.42 in 1988 to 0.91 in 1989 (Fig. 3.10), which explains the low overall correlation (r^2=0.743). The best correlation was obtained in June (r^2=0.913, Fig. 3.11). Theoretically, the slope of the regression curve should be 1.0 and the intercept 0.0, any deviation from the 1:1 line shows a systematic over or underestimation. In May the intercept of -0.25 was not significantly different from zero, but the slope was significantly different from 1.0 at a 5% level of significance. The same conclusion was valid also for July and August whereas for June and September both the intercept and the slope were significantly different from zero and 1.0, respectively.

The cumulative values of the lysimeter data and those found with the Penman-Monteith method were plotted in the same figure as cumulative precipitation to assess the differences occurring during the course of the experiments. Cumulative actual evapotranspiration tended to be higher than the estimated values, especially in late August and September (Fig. 3.12). This conclusion applied to all years, except for 1984. One theoretical reason to explain this discrepancy is the assumption that the soil heat flux G was set at zero in the calculations, which is strictly not true, as it was found in Chapter 2.

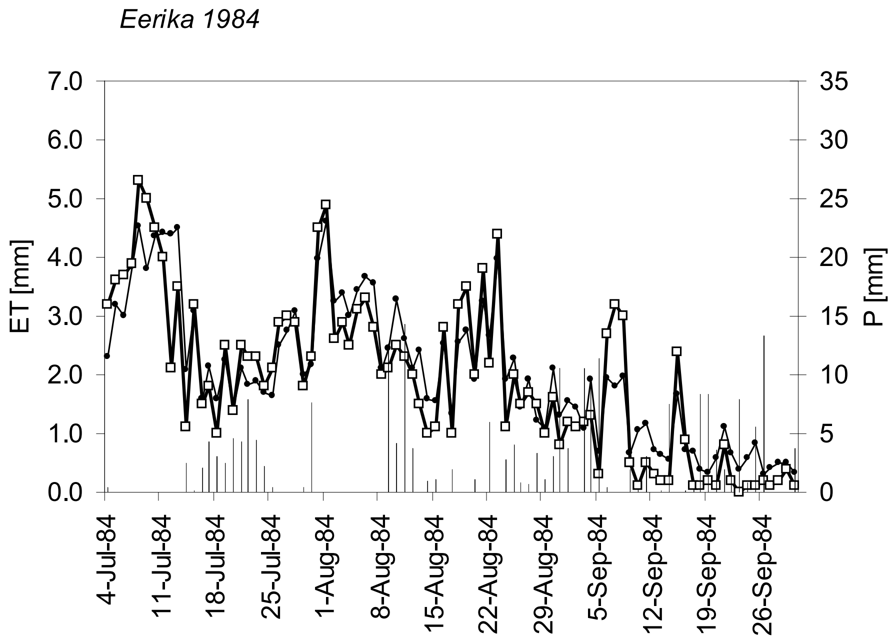

Figure 3.6. Time-series plots of precipitation (bars), measured (thin line with black dots) and estimated (thick line with open squares) evapotranspiration obtained with the Penman-Monteith method at Eerika in 1984.

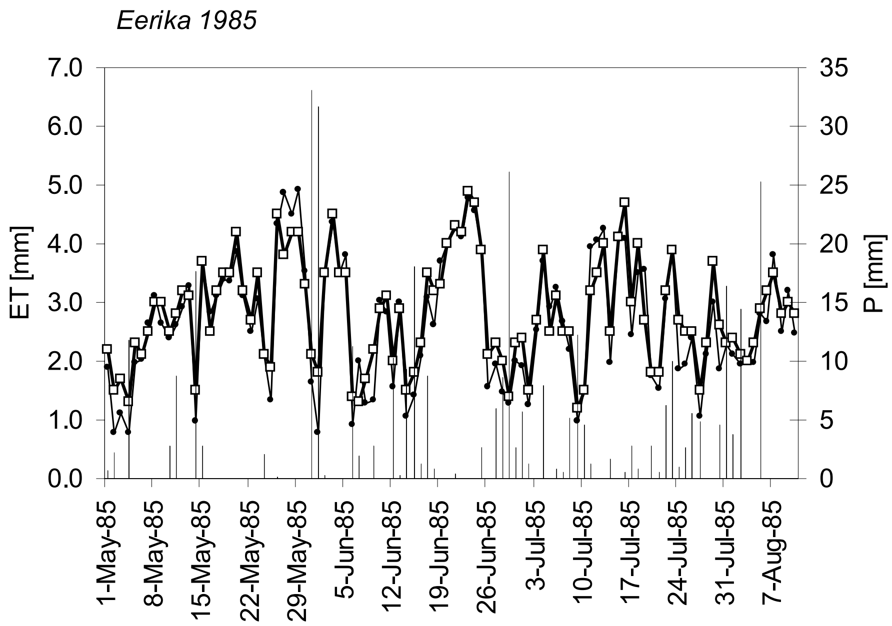

Figure 3.7. Time-series plots of precipitation (bars), measured (thin line with black dots) and estimated (thick line with open squares) evapotranspiration obtained with the Penman-Monteith method at Eerika in 1985.

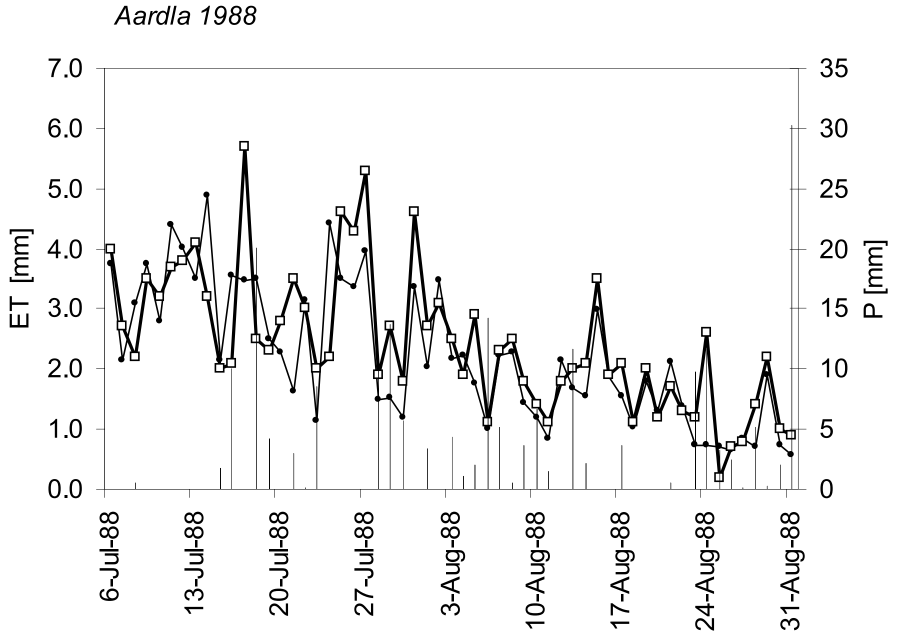

Figure 3.8. Time-series plots of precipitation (bars), measured (thin line with black dots) and estimated (thick line with open squares) evapotranspiration obtained with the Penman-Monteith method at Aardla in 1988.

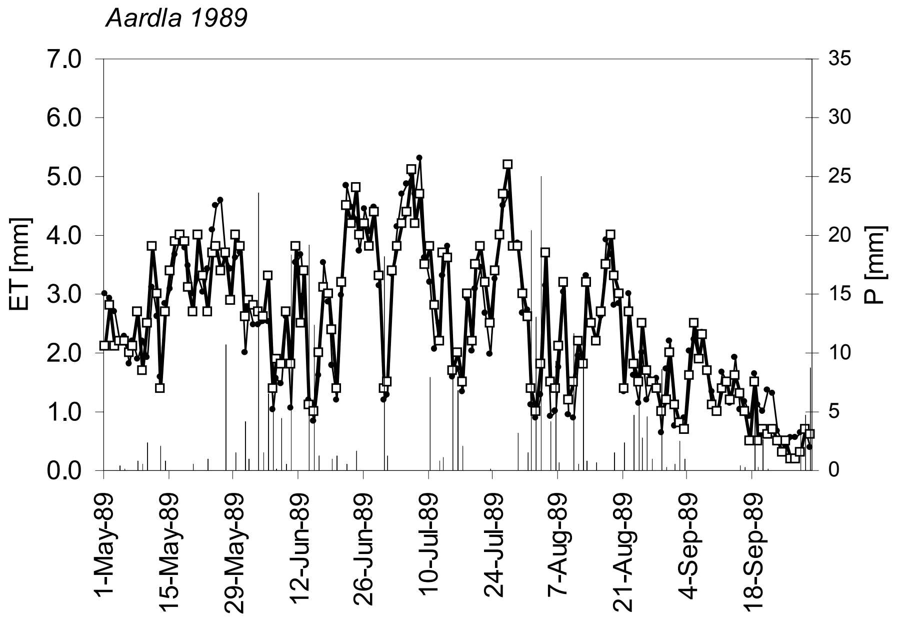

Figure 3.9. Time-series plots of precipitation (bars), measured (thin line with black dots) and estimated (thick line with open squares) evapotranspiration with the Penman-Monteith method at Aardla in 1989.

It is suggested that the heat accumulated in the tank of the hydraulic pan (see the approximately 1.5 m water layer in Fig. (3.1) and (3.2)) during the summer released additional energy in autumn (G<0), which increased available energy for the latent heat flux. However, then lysimeter evapotranspiration must have been less than that estimated in May and June, which was not the case (Fig. 3.12, Table 3.2). Unfortunately, the temperatures of water and of the adjacent soil were not measured. However, as the tank walls were not isolated from the surrounding soil there must have taken place heat exchange reducing the temperature difference. The highest absolute difference between ET_a and ET_{PM} was 16 mm in 1985 (Table 3.2), which is less than 6% of total evapotranspiration.

Table 3.3. Results of statistical analysis for the measured and calculated evapotranspiration values.

	Eerika						Aardla					
	1984			1985			1988			1989		
	r^2	*ME*	*RMSE*	r^2	*ME*	*RMSE*	r^2	*ME*	*RMSE*	r^2	*ME*	*RMSE*
May				0.922	0.1	0.39				0.636	0.0	0.49
June				0.927	0.2	0.41				0.901	0.1	0.41
July	0.659	0.1	0.68	0.820	0.2	0.44	0.421	0.198	1.07	0.912	0.1	0.36
August	0.815	-0.2	0.49	0.820	0.1	0.29	0.645	0.239	0.52	0.896	0.2	0.34
September	0.765	-0.2	0.55							0.796	-0.1	0.31
Overall	*0.832*	-0.1	*0.57*	*0.889*	0.2	*0.40*	*0.586*	0.221	*0.82*	*0.901*	0.0	*0.39*

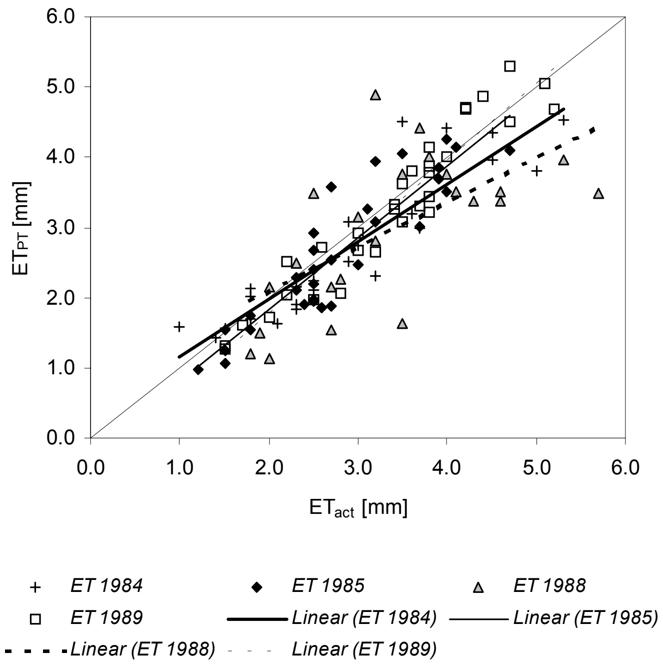

Figure 3.10. Comparison of measured and estimated evapotranspiration in July obtained by the Penman-Monteith method.

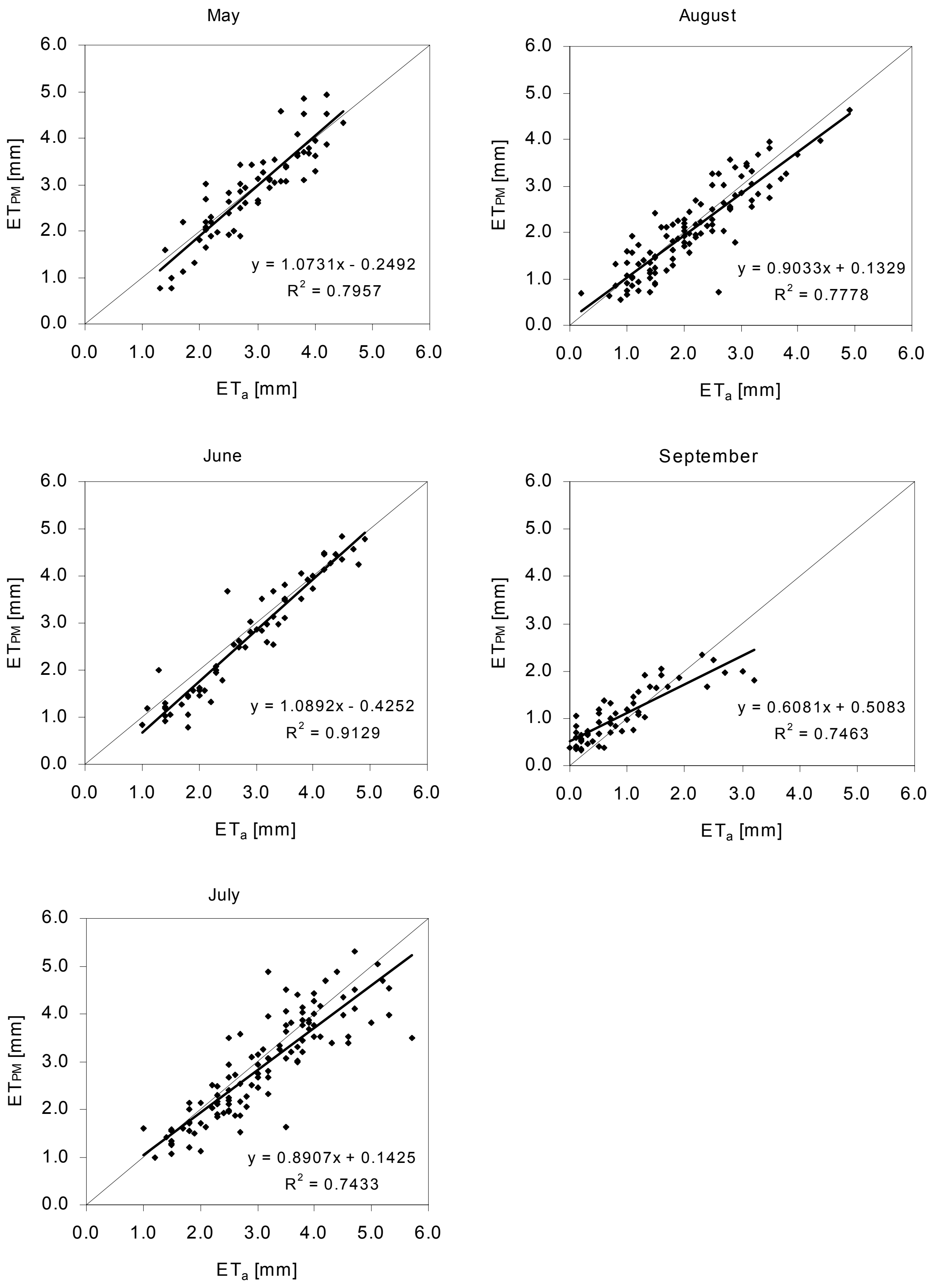

Figure 3.11. Measured and calculated evapotranspiration obtained by the Penman-Monteith method during the four years of the experiment.

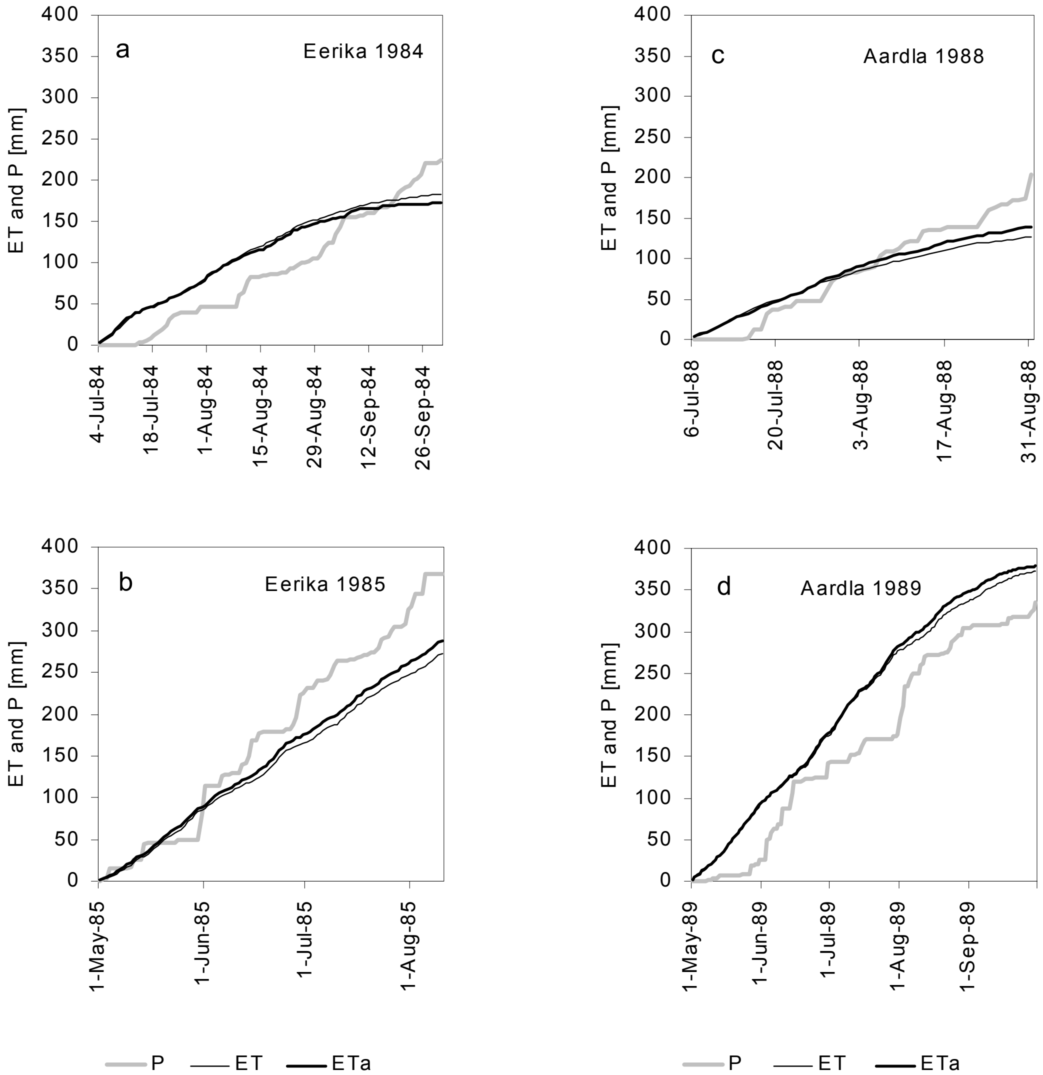

Figure 3.12. Cumulative curves of measured evapotranspiration ET_a, estimated by the Penman-Monteith method ET_{PM}, and precipitation P in the years of the experiment.

3.6 Canopy resistance and aerodynamic resistance

3.6.1 Theoretical background of resistance terms

Monteith (1965) improved the Penman's equation substantially by introducing the canopy resistance r_c and the more general use of the aerodynamic resistance r_a , thus extending the applicability of Penman's equation to describe the evapotranspiration phenomena from cropped surfaces. Canopy resistance comprises the resistance of the vapor flow through the stomata openings of individual leafs and plants, i.e. 'the big leaf' accounts better for the effects of canopy surface on aerodynamic properties. Some authors use stomatal/canopy conductance instead of stomatal/canopy resistance, where one term is the reciprocal of the other. Szeicz and Long (1969) proposed that canopy resistance can be determined as a function of the daily mean stomatal resistance of the single leaves r_s and the leaf area index of the leaves effective in transpiration. These authors assumed that only the surfacial layer (approximately half of the full crop LAI) of the canopy participates effectively in transpiration (e.g. Allen et al. 1989):

$$r_c = \frac{r_s}{LAI_{active}} \tag{3.3}$$

where r_s – is the bulk stomatal resistance of the well-illuminated leaf [s m^{-1}]
LAI_{active} active (sunlit) leaf area index [m^2 (leaf area) m^{-2} (soil surface)],
usually LAI_{active}=0.4…0.5 LAI

Diffusive capacity of the stomata depends on the aperture of the stomata. The bulk stomatal resistance, r_s, is the average resistance of an individual leaf and depends on numerous factors, e.g. crop, meteorological factors and water availability, which will be briefly discussed below.

The transfer of heat and water vapor from the evaporating surface into the air above the canopy is determined by aerodynamic resistance (Allen et al. 1989):

$$r_a = \frac{\ln\left[\frac{z_m - d}{z_{om}}\right]\ln\left[\frac{z_h - d}{z_{oh}}\right]}{k^2 u_z} \tag{3.4}$$

where r_a – is aerodynamic resistance [s m^{-1}]
z_m – is the height of wind measurements [m]
z_h – is height of humidity measurements [m]
d – is zero plane displacement height [m]
z_{om} – is roughness length governing momentum transfer [m]
z_{oh} – is roughness length governing transfer of heat and vapor [m]
k – is von Karman's constant, 0.41 [-]
u_z – is wind speed at height z [m s^{-1}]

Equation (3.4) is based on a more simple equation proposed by Monteith (1965). The equation is restricted to neutral stability conditions, i.e. where temperature, atmospheric pressure, and wind velocity distributions follow nearly adiabatic conditions. The application of the equation for short time periods (hourly or less) may require inclusion of corrections for stability. However, when predicting ET in the well-watered reference surface, heat exchange is small, and therefore stability correction is normally not required.

Many studies have explored the nature of wind regime in plant canopies. Zero displacement heights and roughness lengths have to be considered when the surface is covered by the vegetation. The factors depend upon crop height and architecture. Several empirical equations for the estimation of d, z_{om} and z_{oh} have been developed. The equations recommended by Allen et al. (1989) were used in the present paper to calculate displacement height and roughness lengths:

$$d = \frac{2}{3} z_v = 0.67 z_v \tag{3.5}$$

$$z_{om} = 0.123 z_v \tag{3.6}$$

$$z_{ov} = 0.1 z_{oh} \tag{3.7}$$

where z_v – is canopy height [m]

In general, the effect of soil water deficit, relative humidity, temperature and light are controlling the degree of stomatal opening through different mechanisms that are crop and development stage specific. The physiological effects of a reduction in plant water potential and, consequently, on plant production are very complex and not yet completely clear due to the stochastic nature of the dynamics of these processes as well as due to the complexity of plant responses to water stress (Porporato et al. 2001).

Crop

Canopy resistance has been found to be crop specific and it usually increases as the crop ages and begins to ripen (Allen et al. 1989). There is still lack of adequate information on the values and pattern of changes in r_c over time for the different crops. Monteith and Unsworth (1990) reported that r_c is rarely less than 30 s m^{-1} and many species have a minimum canopy resistance of 100-200 s m^{-1}.

Canopy resistance and stomatal resistance have high diurnal variation as reported by several authors. For example, according to Fowler and Unsworth (1979), daytime minimum values of r_c were 50-100 s m^{-1} for dry and non-senescent wheat canopy, and at night, when stomata are closed r_c ranged between 250-300 s m^{-1}.

Allen et al. (1989) parameterized the indicative value for *reference surface* (clipped grass, where only the upper half is contributing to the surface heat and vapor transfer, i.e. $LAI_{active} = 0.5 \cdot LAI$, crop height of 0.12 m) is approximately 70 s m^{-1}.

Meteorological variables

Many attempts have been made to associate stomatal resistance/conductance with the climatic variables, e.g. solar radiation, leaf or air temperature, vapor pressure deficit, and soil or plant water potential. All these functional relationships are still under debate, as the assumptions that environmental variables act independently of stomatal or canopy resistance (Jarvis-type model, see Jarvis 1976, Kaufmann 1982, Jones 1983, Noilhan and Platon 1989), or that there are strong interactions between these variables (Collatz et al. 1991, Jacobs et al. 1996), have not yet been confirmed. Alves and Pereira (2000) even stated that the assumption about independently acting weather variables is most doubtful.

Generally, the stomata of a leaf are open when exposed to light and remain opened under continuous light unless other factors become limiting (Devlin 1975). Thus, for leaves in their natural environment, the stomatal resistance of a single leaf, r_s, depends significantly on solar radiation and, in the absence of light, stomata are usually closed so that transpiration is effectively zero (Monteith and Unsworth 1990). For example, Alves and Pereira (2000) found for the lettuce crop that r_s depends on radiation with diurnal hysteresis, but for 14:00-20:00 hours the correlation was very high (r^2=0.975), and that there is a linear relationship between r_s and vapor pressure deficit. However, the effect of temperature is less clear as it is difficult to separate it from the effect of the other variables.

As the means for conserving water, the stomata of most plants close as vapor pressure deficit between the leaf and the surrounding air increases, but the nature of this response has been much debated (e.g. Mansfield and Atkinson 1990). Takagi et al. (1998) found that stomatal and bulk canopy conductance in relation to vapor pressure deficit differed from day to day in response to the intensity of vapor pressure deficit of the day.

During rain, drops are intercepted by the foliage and 1-2 mm of water may be retained within the canopy. Subsequently, the rate of evaporation from the wet foliage is faster than transpiration rate, because it is not limited by stomatal resistance, i.e. that for intercepted water r_c=0 (Monteith and Unsworth 1990).

Previous examples showed the effect of weather parameters on canopy resistance, but there exists also an inverse influence when stomatal regulation affects to the partitioning of solar energy, i.e. when decreased evapotranspiration increases the sensible heat.

Soil water availability

The stomatal resistance, r_s, is influenced by soil water availability. Resistance increases when the crop is water-stressed and soil water availability limits its transpiration. Also, the consequence of the reduced stomatal aperture is that less carbon enters stressed leaves, causing reduction in photosynthesis and changes in biochemical reactions, e.g. nitrogen metabolism (Hale and Orcutt 1987). Studies concerning these relationships may be roughly divided into two groups, where in the first case, the effect of soil water depletion on change in stomata closure or, more general, the result of this process, reduction of evapotranspiration, is analyzed, while in the second case, physiological mechanisms (e.g. hormonal changes) are the key interest.

Kelliher et al. (1993) found that the ratio of evaporation to available energy started to linearly decrease when soil water deficit reached to a certain crop specific value. Laboratory experiments conducted by E. -D. Schulze indicated that the stomatal conductance of plants uniformly decline when 60% of soil water available for plants is depleted (cited from E. -D. Sculze et al. 1995). As a consequence of water stress, foliage temperature rises, which may be a stress indicator (Idso et al. 1981, Jackson et al. 1981, Lhomme and Monteny 2000).

In fact, the interrelationship between soil water availability and r_c is even more complex due to the role of accommodation of plants to water shortage, i.e. the extent to which the movement of the root system towards water is able to match the demand imposed by the atmosphere on the foliage (Monteith 1995).

3.6.2 Backward calculation of canopy resistance

The values of the canopy resistance r_c can be obtained by rearranging the Penman-Monteith equation and applying known meteorological parameters and measured evapotranspiration. However, the results of backward calculations must be treated with caution, because the inherent problem is that all measurement and estimation errors are introduced in the estimated parameter, i.e. resistance/conductance values. Regardless of that, several researchers have used this approach (Alves and Pereira 2000, Orlandini 1999, Kustas et al. 1996, Schulze et al. 1994, Menzel 1996, Takagi et al. 1998, Gavin and Agnew 2000). After rearranging Eq. (2.4) canopy resistance can be estimated from the following equation:

$$r_c = \frac{r_a\left[\Delta(R_n - G) + \dfrac{\rho c_p\left(e_a^* - e_a\right)}{r_a} - \Delta\lambda E\right]}{\gamma\lambda E} - r_a \tag{3.8}$$

Equation (3.8) was applied to the present dataset and preliminary analysis revealed that there were a number of days with anomalous r_c values to be excluded from final analysis, i.e. either with extremely high values (>1000 s m^{-1}) or even with negative values. Therefore, the resulting dataset, covering the information over four years, was screened, applying the following quality criteria: 1) the days when measured evapotranspiration was less than 0.4 mm d^{-1}; 2) the days when r_c was below 0; 3) the few remaining days with clear outliers. Actually, the first constraint excluded majority of theoretically ambiguous values indicating that the applied method of back calculation is very sensitive to evapotranspiration rate. After applying the second quality criteria a few days remained when meteorological conditions were similar for several sequential days, but only for one day a high value of r_c (>500 s m^{-1}) was obtained. In fact, based on the theoretical assumption that r_c is zero at a wet canopy, rainy days could be excluded as well, but it was not done namely to check what would the result be for these days. Monteith and Unsworth (1990) suggested that anomalous values of r_c are likely to be obtained in a crop with little foliage if evaporation from the bare soil beneath the leaves makes a substantial contribution to the total flux of water vapor. However, in the present study it was not the case, because the evaporative hydraulic pan was completely covered with a turf of clipped grass.

Considering the good correlation between measured and calculated evapotranspiration (see Section 3.5) it was expected that backward calculated canopy resistance might be used to find out how r_c responses to meteorological conditions. However, the estimated r_c formed a scattered cloud (Fig. 3.13). When examining the response of r_c to vapor pressure deficit then in three years out of four a weak correlation was found between r_c and *VPD*, where canopy resistance tended to increase when *VPD* increased. The highest coefficient of determination was obtained for 1985 (r^2=0.385), whereas in 1989 no correlation was found (Fig. 3.14a, 3.14b). The same conclusion was valid also in case of total radiation and net radiation (Fig. 3.14c, 3.14d) where the highest coefficient of determination was found in 1985 (r^2=0.349). However, the result contradicts the understanding that canopy resistance decreases with increasing total or net radiation. There was no correlation between canopy resistance and the daily rate of evapotranspiration as shown by the scatter diagrams in Figs. (3.14e) and (3.14f).

The average canopy resistance values for different meteorological conditions are summarized in Table 3.4. These results can be compared with those found in literature. Allen et al. (1989) proposed the use of a constant daily value of 70 s m^{-1} for reference grass *ET*. This value has provided very good results in numerous comparative studies (Allen et al. 1989, Jensen et al. 1990, Allen and Fisher 1990). It is also recommended in the FAO guidelines for predicting crop water requirements (Smith et al. 1991). It should be mentioned that in the present experiment, grass was cut three times during the vegetation period, i.e. it differed from the height of 12 cm defined for reference grass. In general, backward calculated r_c was showing higher values for all days and for dry days compared with supposed 70 s m^{-1}. Also, r_c was seldom equal or close to zero on rainy days. The large standard deviation in Table 3.4 implies that canopy resistance deviates a great deal from the average value, thus the influence of different environmental parameters on r_c needs to be further investigated.

Table 3.4. Backward calculated average canopy resistance and standard deviation (denoted with ±) in different meteorological conditions.

Conditions	1984	1985	1988	1989
All days	111±71	65±37	86±88	87±70
Dry days (P=0)	97±60	77±37	100±74	95±65
Rainy days (P>0)	105±59	50±27	57±43	63±48
Rainy days (P>3 mm d^{-1})	111±58	44±24	37±29	47±29

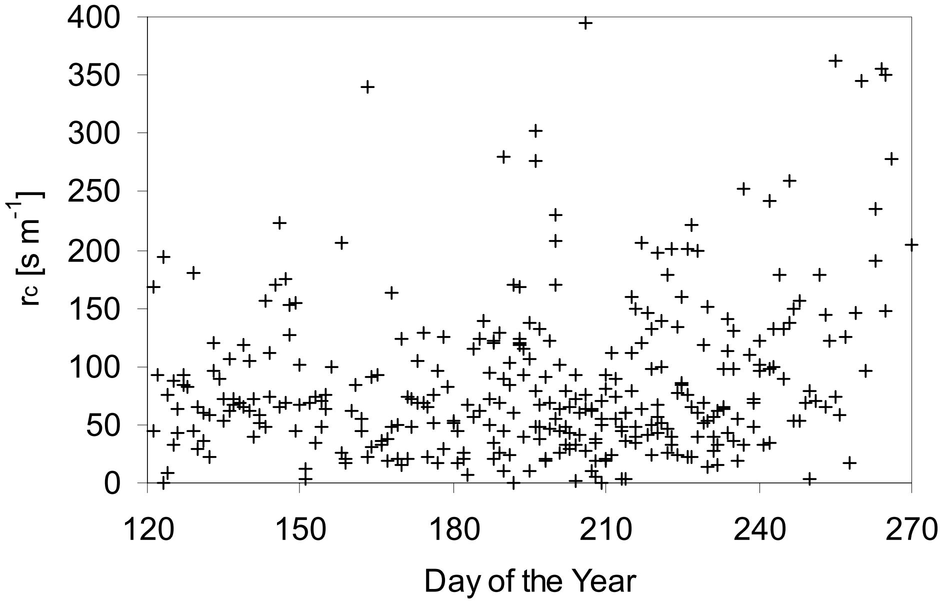

Figure 3.13. Backward calculated daily canopy resistance comprising the data from all years of the experiment.

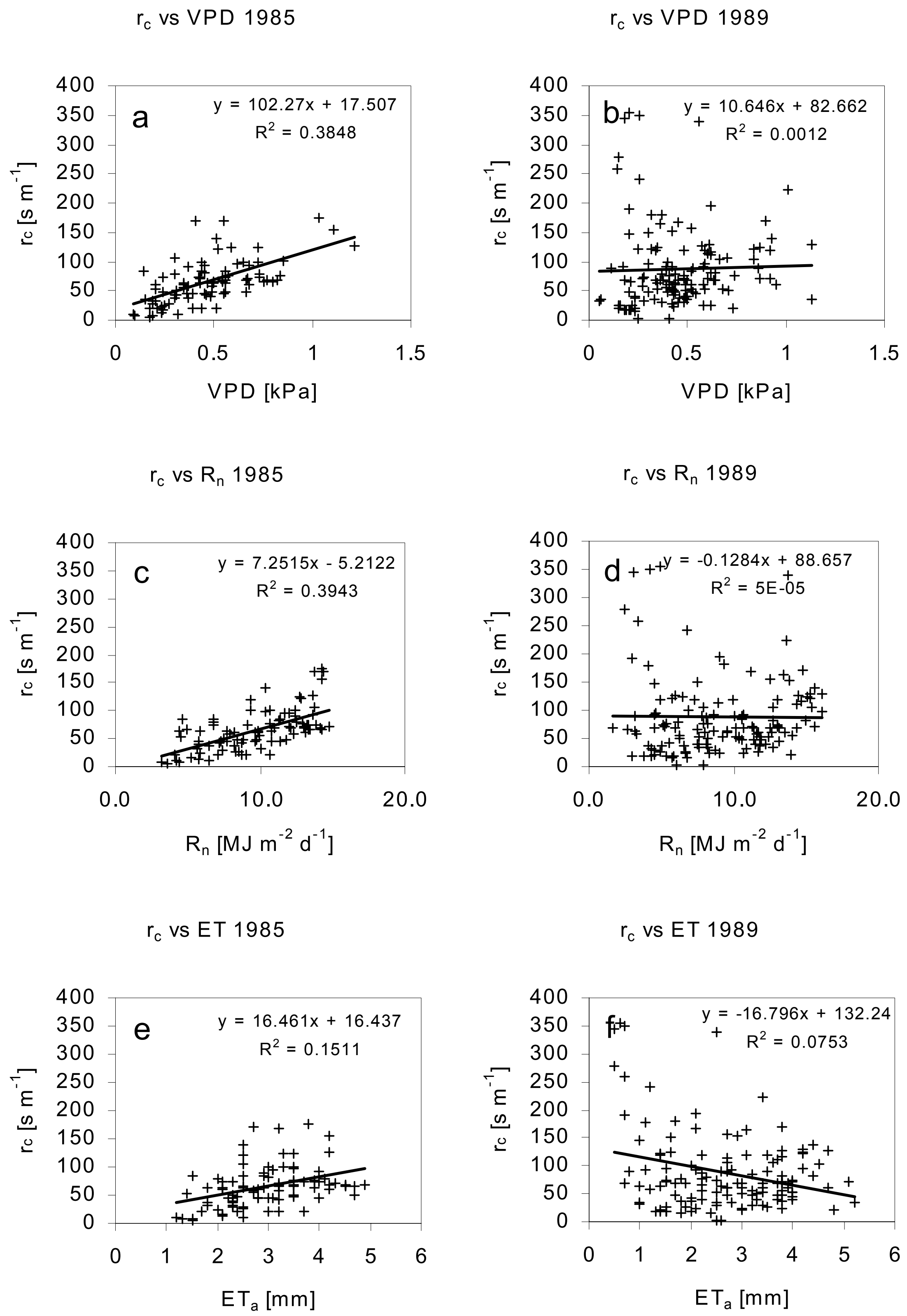

Figure 3.14. Relationship between daily canopy resistance r_c and vapor pressure deficit *VPD*, net radiation R_n, and actual evapotranspiration ET_a in 1985 and 1989.

3.7 Comparison and evaluation of evapotranspiration methods

3.7.1 The interrelationship between meteorological parameters

The disadvantage of Penman's equation is often the missing of data on vapor pressure deficit and wind velocity as well as the Penman-Monteith's necessity to determine aerodynamic and canopy resistance. Thus, it would be attractive to use the Priestley and Taylor equation (1972), since the only variables needed are temperature and net radiation (note that soil heat flux must also be known or else abandoned). The Priestley and Taylor equation (Eq. 2.5) uses only the first, R_n-term, in the Penman-Monteith equation simply multiplying it by factor α with an indicative value of 1.26. The aim of the following analysis was to find out why the P-T equation yields reasonable estimates of *ET*, although it has been criticized due to the ambiguous theoretical background (Monteith and Unsworth 1990).

The Priestley and Taylor method assumes that net radiation is the leading factor for *ET* determination. In case of the present experimentally found *ET*, the correlation between daily *ET* and R_n was high (r^2=0.789, Fig. 3.15a). In case of estimated *ET* obtained by Penman-Monteith equation this correlation was even higher (r^2=0.908, Fig. 3.15b). Thus, correlation analysis revealed that for a grass-covered surface not lacking in water, actual evapotranspiration (in mm) yields an empirical relationship of around 0.3 of net radiation (in MJ m^{-2} d^{-1}) i.e. $ET \cong 0.3\ R_n$.

Among other meteorological variables average temperature (Fig. 3.17e) and wind velocity (Fig 3.15d) did not show an individual correlation with evapotranspiration, but a relatively high relationship was found between VPD and ET_a (r^2=0.648, Fig. 3.15c). It was less than in case of R_n, but VPD itself correlates well with R_n (r^2=0.602, Fig. 3.17f). This result, based on daily data, explains why the Priestley-Taylor method yields good results. In fact, the same result was obtained when monthly data were analyzed as described below.

Net radiation is reflected across the summer solstice in June (Fig. 2.3), while long-term average precipitation on the Estonian territory has an increasing trend from April to August (Fig. 3.3). The increase in precipitation is reflected on increased relative humidity. Using the data of long-term monthly average relative humidity and net radiation (Tartu Tõravere 1955-1989) this relationship was visualized (Fig. 3.16). It was shown that in different months with relatively similar net radiation (e.g. May and July) relative humidity is quite different, which leads to the idea that α-coefficient in the Priestley-Taylor equation must be lower in a month with higher relative humidity, i.e. in July α should be smaller than in May. However, the factor influencing the rate of evapotranspiration is vapor pressure deficit and therefore, the corresponding VPD was calculated. Instead of a strongly hysteretic relationship found in case of RH, an almost non-hysteretic relationship was found in case of VPD (Fig. 3.17). The result was similar to those found with daily data (Fig. 3.15f). It means that VPD correlates well with R_n and on a long–term basis there exists a strong linear relationship between monthly average R_n and *VPD* ($VPD=0.0013\ R_n + 0.088$, where *VPD* [kPa] and R_n [MJ m^{-2} $month^{-1}$], r^2=0.976).

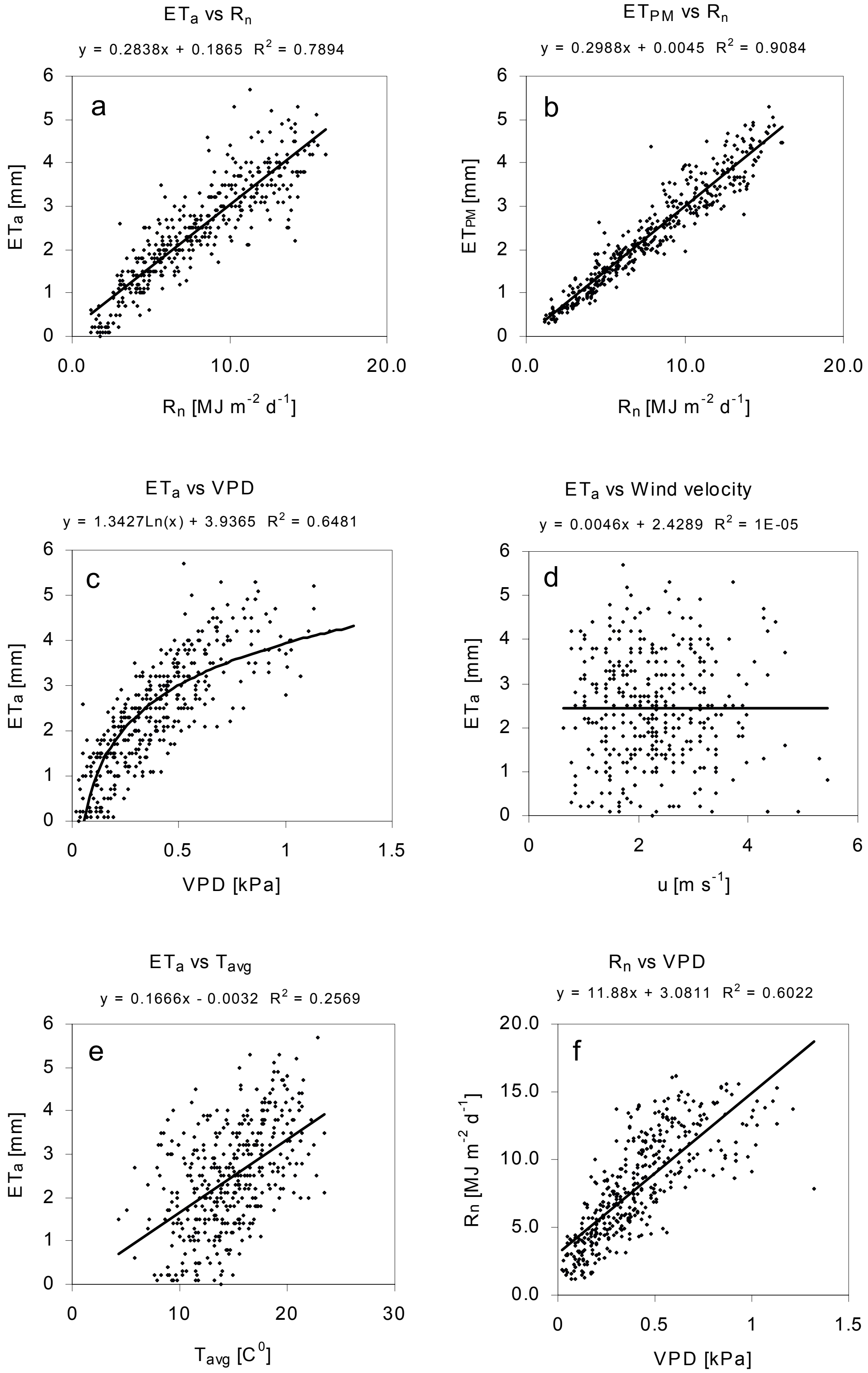

Figure 3.15. Relationships between evapotranspiration and different meteorological parameters.

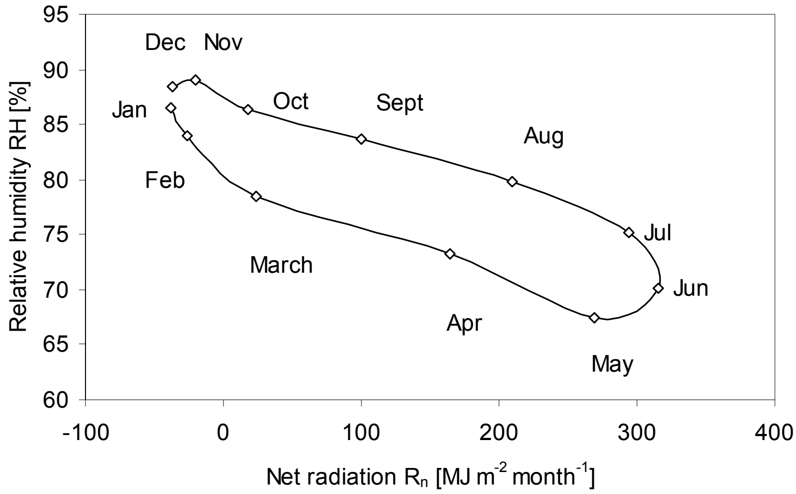

Figure 3.16. Long-term relationship (Tartu Tõravere 1955-1989) between relative humidity *RH* and net radiation R_n.

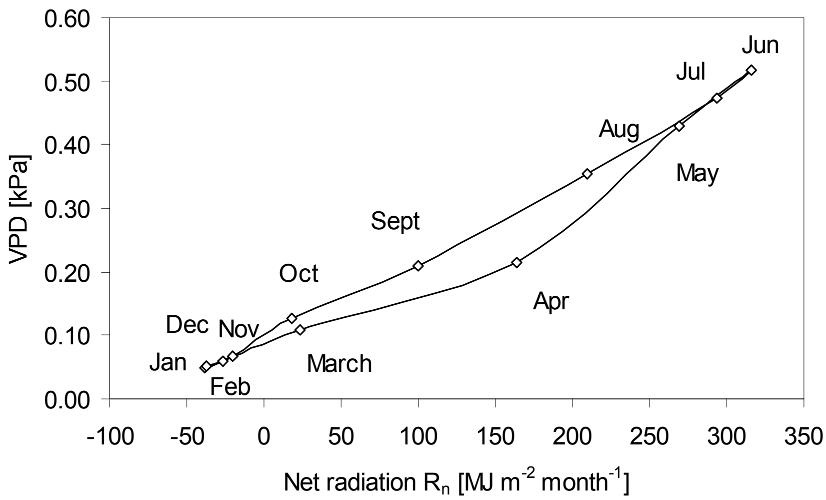

Figure 3.17. Long-term relationship (Tartu Tõravere 1955-1989) between vapor pressure deficit and net radiation R_n.

It is suggested here that the Priestley-Taylor equation implicitly includes the effect of VPD in the following way: in conditions with increasing R_n, VPD also increases and, thus, the relative 'balance' between the effect of radiation and VPD is maintained (in the Penman-Monteith equation the radiation term and the aerodynamic term, respectively). With daily or shorter time steps considerable different conditions can certainly be found. To assess the variability of VPD in different months the following analysis was carried out.

All monthly *pdf*-curves showed an asymmetrical distribution where the mode was less than the average value (Fig. 3.18). In summer months, VPD covers a relatively wide range of values, while in April and September the range around which daily VPD deviation is quite narrow. The implications of the shape of the probability density functions will be discussed in Section 3.7.2.

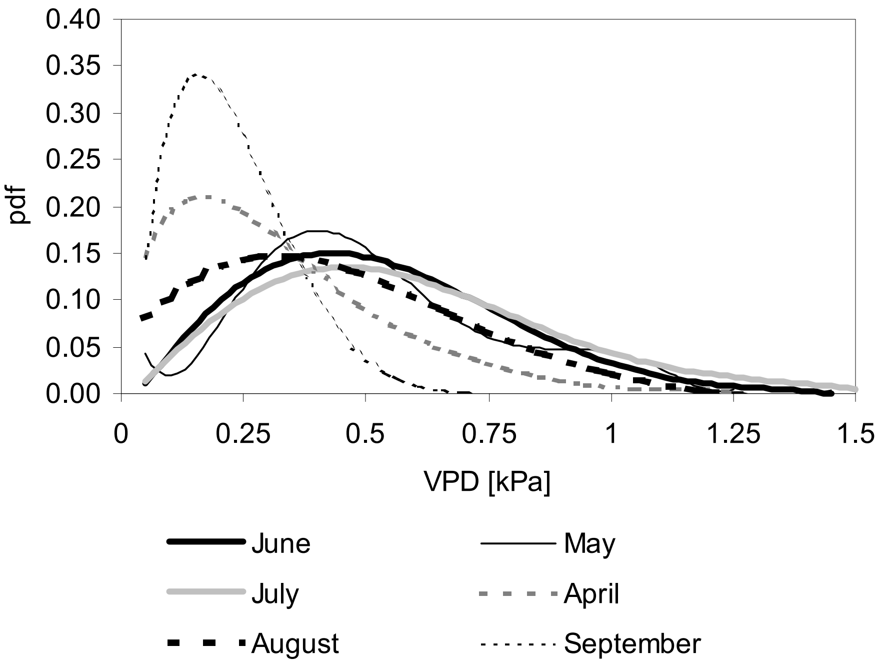

Figure. 3.18. Fitted probability density functions of vapor pressure deficit VPD in different months as based on daily data.

3.7.2 Comparison of the Penman-Monteith and Priestley-Taylor methods

Daily evapotranspiration measured with the hydraulic lysimeter was used to evaluate the Penman-Monteith and Priestley-Taylor methods. In general, the Penman-Monteith method revealed a higher correlation with the measured values than the Priestley-Taylor (Table 3.5). Both methods yielded similar results in August and September when VPD has smaller absolute values and a more narrow range (Fig. 3.18).

Table 3.5. Comparison of the correlations between measured evapotranspiration ET_a and estimated evapotranspiration obtained by the Penman-Monteith ET_{PT} and the Priestley-Taylor ET_{PT} (α=1.26).

Month	Penman-Monteith		Priestley-Taylor	
	$ET_{PM}=f(ET_a)$	r^2	$ET_{PT}=f(ET_a)$	r^2
May	y=1.07x-0.249	0.796	y=1.12x-0.314	0.678
June	y=1.09x-0.425	0.913	y=1.18x-0.312	0.857
July	y=0.89x+0.143	0.743	y=0.89x+0.414	0.671
August	y=0.90x+0.133	0.778	y=0.91x+0.240	0.775
September	y=0.61x+0.508	0.746	y=0.57x+0.500	0.726

In case of the Priestley-Taylor equation the coefficient α was set at 1.26. However, a long debate has been held concerning the 'true' value and character of the empirical parameter of α, since Priestley and Taylor introduced their equation in 1972. The main questions are: 1) should the value of α be essentially constant? and, 2) as an extension of this, under what conditions might differences from the standard value of 1.26 be expected? The Priestley-Taylor equation represents the evapotranspiration rate 'from an extensive wet surface in the absence of advection'. In a number of publications consistency with this value (Davies and Allen 1973, Parlange and Katul 1992, Parlange and Stricker 1996) but also different constants (Barton 1979) have been reported. However, many authors have indicated systematic variations in the value of α depending on the time scale (diurnal and seasonal) (de Bruin and Keijman 1979) or dependency of surface-climatic parameters (Lhomme 1997a, 1997b). Lhomme (1997a) found that the value of α varies in a relatively restricted range which includes the value of 1.26 established experimentally by Priestley and Taylor (1972), and that for typical values of the VPD and aerodynamic resistance of 50 s m^{-1}, which was proposed as a is typical value for grass, α increases with canopy resistance from 1.1 (for r_c=0) to an asymptotic value of about 1.5 (for r_c tending to infinity). In another publication Lhomme (1997b) stated that α is equal to 1.3 for saturated grass surrounded by well-watered grass. Culf (1994) evaluated the value of α for a growing convective boundary layer and found that for realistic atmospheric conditions $1.08 < \alpha < 1.26$. Eichinger et al. (1996) derived theoretically that for typical observed atmospheric conditions $\alpha = 1.26$ and is relatively insensitive to small changes in atmospheric parameters.

When the Priestley-Taylor coefficient was optimized with the present dataset then the calibrated monthly values were as follows: α_{May}=1.18, α_{June}=1.13, α_{July}=1.20, α_{Aug}=1.21, and α_{Sep}=1.21. In fact, these new values only slightly improved r^2 and RMSE. For example, in May RMSE decreased from 0.64 mm to 0.61 mm, in June from 0.59 to 0.48 mm, and in the following months RMSE improved less than 0.3 mm. Thus, the advantage of using monthly adjusted α-values was too small to lose the simplicity of the Priestley-Taylor equation with a single constant value.

3.7.3 Sensitivity of evapotranspiration estimation methods to meteorological and surface parameters

Analysis of the sensitivity of evapotranspiration methods to various climatic and surface dependent parameters has been reported in a number of publications (e.g. McKenny and Rosenberg 1993, Bormann et al. 1996, Qiu et al. 1998, Llasat and Snyder 1998, Tamm 1998a). One reason to carry out this kind of analysis is increasing interest in studies on global climate change (see Intergovernmental Panel on Climate Change – IPCC, 1996) where the expected rise of tropospheric temperature causes changes in other climatic elements as precipitation, cloudiness, humidity and windiness. These changes have a great potential for significant hydrologic impacts. Global circulation models (GCMs) commonly predefine the percentage or magnitude change for eight meteorological parameters (mean temperature, precipitation, amount of clouds, minimum temperature, maximum temperature, mean wind speed, water vapor pressure diurnal range of air temperature) from baseline, which usually comprises a 30-years (Keevallik 1998). However, in several studies, e.g. in Estonia – U.S. Country Studies Program (Punning 1996) and UNEP Country Case Study on Climate Change Impacts and Adaptations Assessments (Tarand and Kallaste 1998) only scenarios for temperature and precipitation were available. Other reasons for knowing parameter sensitivity in evapotranspiration models are that soil-plant-atmosphere models often link the *ET* rate to crop growth models, i.e. potential gross photosynthesis is reduced due to water stress as quantified by relative transpiration (Feddes 1986, van Dam et al. 1997), and also, to obtain information on measurement or estimation accuracy.

The sensitivity analysis of the parameters used in evapotranspiration methods was carried out on the basis of the same 11-year period (1986-1996) as in the case of radiation

(Table 2.7). Only the daily data of June were analyzed for their highest absolute values and the largest differences between the maximum and minimum values. The relative sensitivity coefficients as defined in Section 2.4.7 were calculated for different meteorological and surface dependent parameters separately for the Penman-Monteith and Priestley-Taylor methods. In all cases, the 10% increase was applied to a single parameter's daily value. The results for both evapotranspiration methods are summarized in Table 3.7.

Evapotranspiration appears to be the most sensitive to changes in actual vapor pressure (i.e. changes in relative humidity) when *ET* is estimated with the Penman-Monteith method. The relative sensitivity coefficient S_r was -0.78 (Table 3.7), i.e. when actual vapor pressure e_a increases by 10% then *ET* decreases by 7.8%. Increased e_a caused a decrease in VPD and an increase in relative humidity from 70.3% to 77.4%.

The 10% increase in sunshine duration *n* and mean daily air temperature *T* had approximately the same importance as the relative sensitivity coefficients of 0.37 and 0.28 in the case of the Penman-Monteith method and 0.61 and 0.59 in the case of the Priestley-Taylor method were found, respectively (Table 3.7). The most insensitive among the meteorological parameters was wind velocity with S_r=0.11, i.e. 10% of increased value accounted for 1.1% higher *ET*.

Additionally, the effect of the canopy properties and net radiation were studied. A ten percent taller crop yielded 1.9 percent higher evapotranspiration, while the increased albedo reduced *ET* by 2.7% and 4.4% if *ET* was estimated by the Penman-Monteith and Priestley-Taylor methods, respectively. Both resistance terms revealed low sensitivity where S_r for aerodynamic resistance was in same order that for wind velocity and the canopy resistance appeared to be more than two times more sensitive than aerodynamic resistance.

Table 3.7. Relative sensitivity analysis for the Penman-Monteith and the Priestley-Taylor equations based on the daily data of the June month from 1986-1996.

Parameter	*n* h	*T* C^0	e_a kPa	*u* m s^{-1}	
Base value	9.1	15.2	1.23	2.6	
Relative sensitivity S_r					
Penman-Monteith	0.37	0.28	-0.78	0.11	
Priestley-Taylor	0.61	0.59	0.23	-	
Parameter	Z_v m	*albedo* -	R_n MJ m^{-2} day^{-1}	r_a s m^{-1}	r_c s m^{-1}
Base value	0.15	0.22	10.3	79	75
Relative sensitivity S_r					
Penman-Monteith	0.19	-0.27	0.61	-0.11	-0.27
Priestley-Taylor	-	-0.44	1.0	-	-

The sensitivity coefficients for *n*, *T*, and R_n of the Priestley-Taylor method were nearly twice higher than those of the Penman-Monteith method. For example, the relative sensitivity of net radiation was 1.0 in case of P-T and 0.61 in case of P-M. However, in the P-M equation net radiation influences only the radiative part of evapotranspiration, while in P-T equation it is the main driving force. Based on the 11-year dataset it can be shown that if the radiation term and the aerodynamic term of the P-M equation are calculated separately then nearly 50% of evapotranspiration is caused by radiation and the same amount by atmospheric exchange processes (Fig. 3.19).

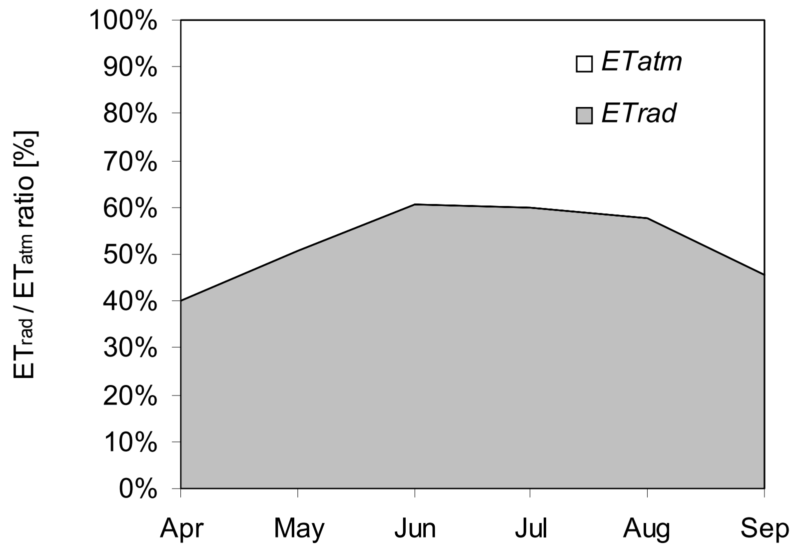

Figure 3.19. The ratio of radiation to turbulent exchange-induced evapotranspiration estimated from the dataset of 1986-1996.

3.7.4 'Typical' weather conditions and the Penman-Monteith equation

In the previous sections the interrelationships between the meteorological variables were already discussed. Even though it is very difficult to draw up these correlations Tamm (1998a) showed that there exist interdependencies in the Tartu's long-term dataset (1949-1995). It was shown that for days with no precipitation (P=0) and for days with recorded precipitation (0<P<1 mm) monthly average relative humidity was statistically significantly different (t-test, p<.0001) for all months from April to September. For example, in May it was 57% for dry days (P=0) and 72% for rainy days (0<P<1 mm). Also, the ratio n/N decreased from 0.63 to 0.34 and wind velocity slightly increased from 3.4 m s^{-1} to 3.7 m s^{-1}. Thus, the sensitivity analysis given in Table 3.7 does not reflect possible actual changes in nature, but the sensitivity of evapotranspiration methods to single parameter changes only. In the nature different meteorological parameters may be weakly correlated, or form more or less typical conditions.

Incremental scenarios, widely used in climate change studies implement, single variable alterations (e.g. -2, -1, 0, +1, +2 C^0 in case of temperature, or a similar percentage change in case of precipitation). It is supposed here that this methodology may result in impossible meteorological conditions. Within the project of UNEP Country Case Study on Climate Change Impacts and Adaptations Assessments (Tarand and Kallaste 1998) it was found that in certain circumstances increased wind speed reduced potential evapotranspiration, which contradicts to the understanding of evaporation phenomena. This interesting finding led to the question whether it is caused by the ambiguity of incremental scenarios or by the character of the Penman-Monteith equation.

The classical form of Penman's equation (Eq. 2.3) allows to divide latent heat into two parts, which are called the radiation term and the atmospheric term. Mathematically, the Penman-Monteith equation can be treated in the same way, but interpretation is more difficult. Rewriting of Eq. (2.4) yields:

$$\lambda E = \frac{\Delta(R_n - G)}{\Delta + \gamma^*} + \frac{\rho c_p \{e_c(T(z)) - e(z)\}/r_a}{\Delta + \gamma^*} \tag{3.9}$$

The first term in Eq. (3.9) can be identified as the diabatic component of latent heat loss associated with the additional supply of heat from radiation, while the second term is the adiabatic component (i.e. temperature and vapor pressure do not change total heat content) (Monteith and Unsworth 1992). It follows that the fraction of R_n, allocated to sensible heat, will be $R_n/(1+\Delta/\gamma^*)$ and the complementary fraction, allocated to latent heat, will be $(\Delta/\gamma^*)R_n/(1+\Delta/\gamma^*)$ (Monteith and Unsworth 1990). The modified psyhrometric constant γ^* is a function of psyhrometric constant γ, aerodynamic resistance and canopy resistance $\gamma^* = \gamma(r_a+r_c)/r_a$. Aerodynamic resistance is a function of wind speed (Eq. 3.4). Note, that due to these functional relationships there can be situations when increased wind speed reduces *ET*. To find out in which theoretical conditions this may occur and if such meteorological conditions occur in the nature, the following analysis was carried out.

The meteorological data for the 11-year period (1986-1996, Tartu), consisting of daily observations of precipitation, duration of bright sunshine, average air temperature, actual vapor pressure and wind speed, were statistically analyzed. Only data from the 1st of June to the 30th of June were selected for analysis. The histograms and the curves of the cumulative probability distribution function were used to select all days that met the following constraints. Three sets were defined: 1) 0-10% probability range as the low level parameter values, 2) 45-55% probability range as the average conditions and, 3) 90-100% probability range as the high parameter values. For example, selected days with VPD<0.25 kPa (0-10%) were called 'wet', days with 0.46<VPD<0.52 (45-55%) were called 'average' and days with VPD>0.87 (90-100%) were called 'dry'. Also, the minimum, maximum and average values were found for all other meteorological parameters. In the same manner 'cold', 'average' and 'warm' days were selected for temperature, 'dark', 'average' and 'sunny' days were selected for the *n/N* ratio, 'calm', and 'average' and 'windy' days were selected for the wind speed.

To study the effect of wind speed, three curves were constructed. Both *n* and *T* were set at the average values in June, 9.1 hours and 15.2 ^{0}C, respectively. Five different wind velocities (0.8, 1.7, 2.6, 4.0, 5.3 m s^{-1}) were set for 'wet' days (VPD=0.05), 'average' days (VPD=0.50) and 'dry' days (VPD=1.32). The resulting curves (Fig. 3.20a) revealed that only on days of low VPD increased wind speed reduced *ET*. This result was compared with the curves obtained from the selected datasets of 'wet', 'average' and 'dry' days. It should be noted that unlike the constructed curves, the selected datasets include the actual observed duration of bright sunshine and air temperatures. Similarly to the constructed curves (Fig. 3.20a), 'dry' days showed increased *ET* (weak correlation, r^2=0.217) when wind speed increased (Fig. 3.20b), 'average' days did not reveal any influence of *u* on *ET*. However, unlike the constructed curves, 'wet' days did not reveal that increased wind speed could diminish evapotranspiration. This result indicates that there may arise problems when the Penman-Monteith equation is used in the incremental scenarios of climate change studies.

An analogous analysis was performed also to study the effect of air temperature and the ratio *n/N*. In the case of air temperature (Fig. 3.21) only a weak correlation was found with 'dry' days (r^2=0.251) while relative duration of bright sunshine (Fig. 3.22) correlated well with 'wet', 'average' and 'dry' days. In both cases the selected datasets were not overlapping.

When the relative duration of bright sunshine was applied as the basis of selection then, surprisingly, the dataset of 'dark' days (n/N<0.1) yielded a linear trend with a negative slope of ET=f(u) relationship (Fig. 3.24). However, the slope was not statistically different from zero ($p<0.05$), i.e. it was not statistically proved that increased wind speed would reduce ET. Completely overlapping datasets were obtained when the data were selected on the basis of wind speed (figures not shown here).

The results show that in the continental climatic conditions of Tartu (approximately 180 km from the sea, see Fig. 1.2) different meteorological parameters may form more or less distinguishable 'typical' meteorological conditions during a certain time period, e.g. in June. The best base to distinguish meteorologically 'typical' conditions is vapor pressure deficit.

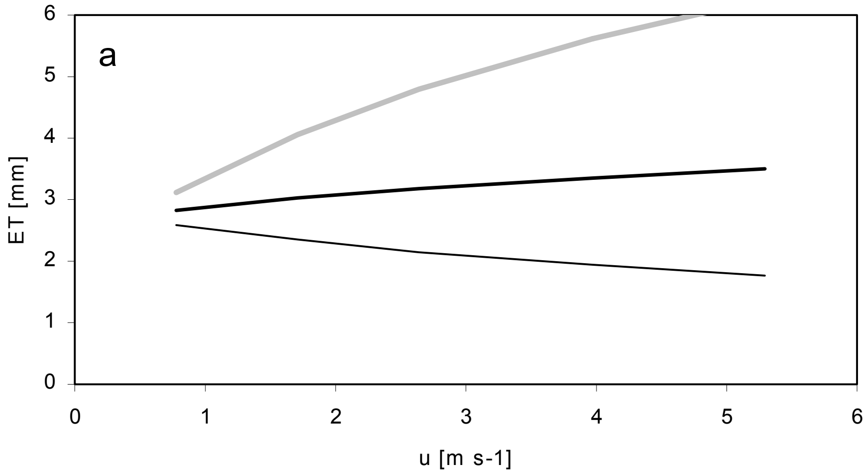

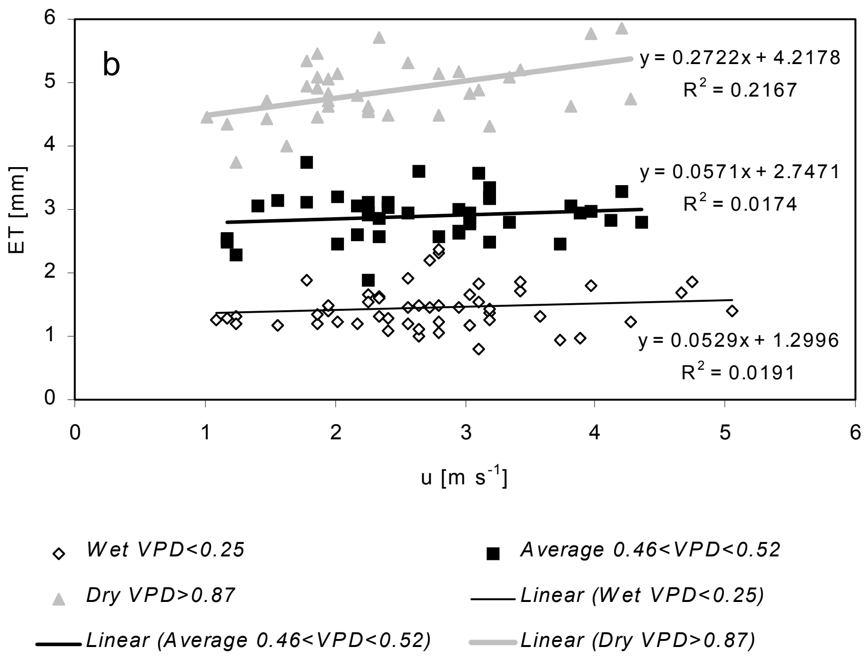

Figure 3.20. The effect of wind speed u on evapotranspiration ET in case of a) constructed curves and b) for selected datasets of 'wet', 'average' and 'dry' days.

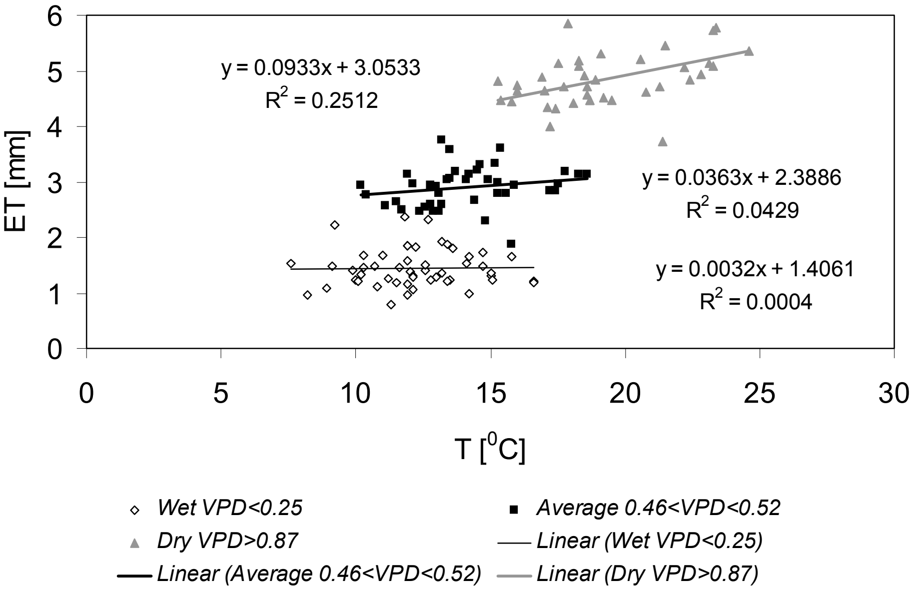

Figure 3.21. The effect of daily average temperature *T* on evapotranspiration *ET* in the datasets for 'wet', 'average' and 'dry' days.

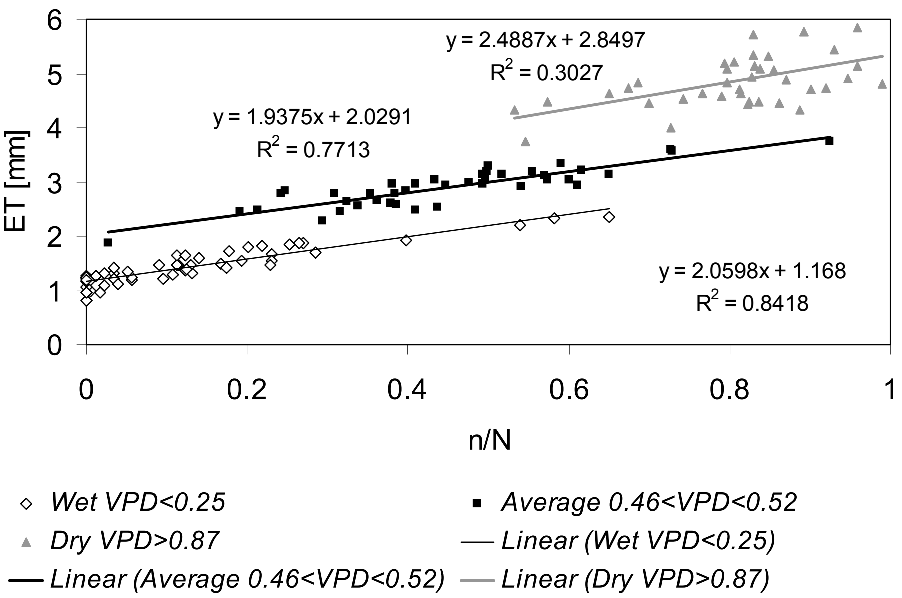

Figure 3.22. The effect of the *n/N* ratio on evapotranspiration *ET* in the datasets for 'wet', 'average' and 'dry' days.

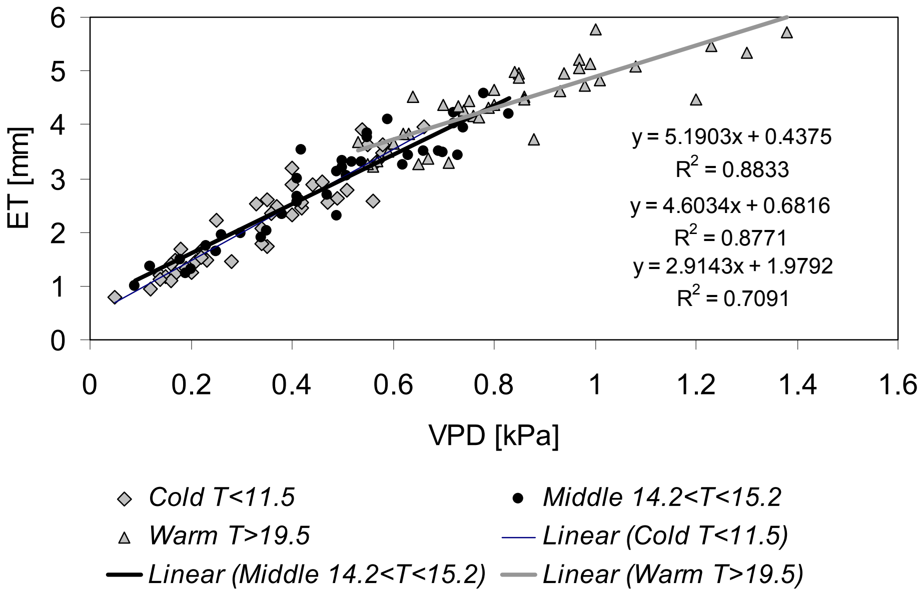

Figure 3.23. The effect of VPD on evapotranspiration *ET* in the datasets for 'cold', 'average' and 'warm' days.

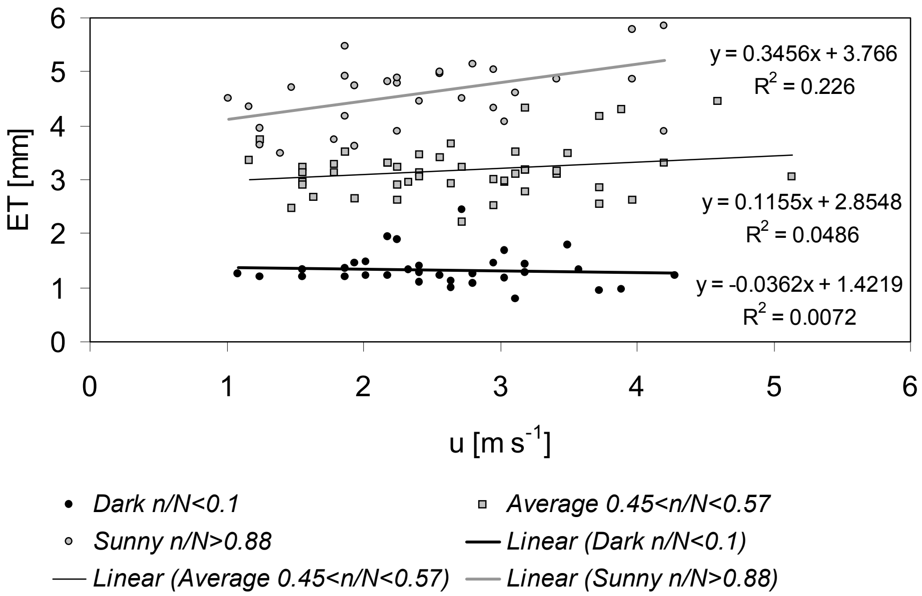

Figure 3.24. The effect of wind velocity on evapotranspiration *ET* in the datasets for 'dark', 'average' and 'sunny' days.

3.8 Conclusions

1. The experimental data of actual evapotranspiration obtained from the hydraulic evaporation pan were used to validate the Penman-Monteith and Priestley-Taylor methods. The Penman-Monteith method yielded good results from three years out of four. The coefficient of determination between measured and estimated *ET* was the highest in June 1985 (r^2=0.927) and the lowest in July 1988 (r^2=0.421). The best overall fit comprising the period from May to September was found in 1989 (r^2=0.901).
2. The Priestley-Taylor method yielded a lower correlation with measured *ET* compared with the Penman-Monteith method, but the difference was relatively small in several months, e.g. in August P-T (r^2=0.775), P-M (r^2=0.778).
3. Canopy resistance found with backward calculation technique showed higher values than the commonly used value of 70 s m^{-1} for dry days. It was seldom equal or close to zero on rainy days and, in general, showed high variation irrespective of the fact how the data were grouped. In spite of the good correlation between measured and estimated *ET*, the backward calculated r_c did not reveal any relevant dependences on the environmental parameters.
4. The calibrated α-coefficients in the Priestley-Taylor method were slightly lower than the common value of 1.26, however, as the monthly calibrated values improved predicted *ET* only slightly, it is suggested to use the standard value of 1.26.
5. It was identified that monthly and daily net radiation correlates well with corresponding vapor pressure deficit, which explains why the Priestley-Taylor performs well in estimation of *ET*.
6. Sensitivity analysis revealed that the Penman-Monteith equation was the most sensitive to VPD, where the 10% increase in VPD increased monthly *ET* (June data from 1986 to 1996) by 6.1%. The Priestley-Taylor equation was nearly twice as sensitive to changes in the parameters used to estimate net radiation as the Penman-Monteith equation.
7. It was showed that when the Penman-Monteith equation was used for certain combinations of meteorological and resistance values (in general, days with very low VPD), increased wind speed reduced *ET*. However, with actual meteorological dataset this finding was not confirmed. Analysis of the data showed that there were weak interdependences between the meteorological variables and that the VPD is the best variable to distinguish 'typical' weather conditions.

Chapter 4

FLOW DOMAIN

4.1 Introduction

A soil profile forms a flow domain that is bounded from the upper end by the soil surface and from the bottom by a flow barrier or a set of predefined boundary conditions. Hillel (1998) defines soil as '*the weathered and fragmented outer layer of the earth's terrestrial surface*'. He adds that '*the soil is anything but a homogeneous entity … with a wide range of attributes*'. The essential source of the complexity of the flow domain is that it consists of three phases of matter: the solid phase, the liquid phase and the gaseous phase. Both the proportions of these three phases and their physical properties undergo continuous variation, depending on the abiotic factors (temperature, precipitation, etc.) and on the biotic factors (vegetation, biological-microbiological activities). These proportions and properties can also be influenced by human activities (e.g. agricultural management). For practical purposes this variability is usually described on spatial and temporal scales.

Accurate prediction of water flow and chemical transport processes in the soil profiles requires the use of simulation models that are able to describe the most important physical, hydrological and chemical processes. Although recent studies have shown the advantage of *two-domain* (also *dual porosity*) models describing the flow in macropore and micropore regions (e.g. Kohler et al. 2001, Larsson 1999), the present part of the paper is focused on the problems related to the *one-domain* models where the water flow is governed by Richards' equation (Richards 1931).

For numerical modeling of the soil water flux using the Richards' equation, the soil hydraulic functions called *the water retention curve* or *pF-curve*, $\Theta(h)$, and *the unsaturated hydraulic conductivity function*, $K(h)$, should be known. These functions can be determined in different ways as discussed in Section 4.2. Although these functions can be given in tabular forms, analytical expressions are more convenient for modeling purposes. Among the large number of soil hydraulic functions those proposed by Brooks and Corey (1964), Mualem (1976) and van Genuchten (1980) are the most popular.

Databases of soil hydraulic properties with a large number of soils are available for the USA (UNSODA, Leij et al. 1996, Nemes et al. 2001) and for Europe (HYPRES, Wösten et al. 1999) while in Estonia there are no published data available. In fact, Estonian soils are pedologically well studied. A comprehensive study 'Estonian Soils' (Kask 1996, *in Estonian*) gives an overview of soil formation and a complete classification of soils, including typical textural fractions and chemical composition. Soil water has been studied by Kitse (1978) who found correlative functions between specific surface area and the hydro-physical parameters as wilting point, field capacity, etc. Roostalu (1978) determined the *pF*-curves for top and sub-soils, which depend only on specific surface area. However, for modeling purposes it was impossible to find necessary h-Θ-K functions either for typical or particular Estonian soils. Therefore, the main purpose of this part of the study was to determine the soil hydraulic functions for a particular soil (see Chapter 5) using different methods, and to discuss the problems related to the selected methods.

4.2 Theory of water flow in soil and soil hydraulic functions

The equation for water flow in unsaturated soils published by Richards' (1931) already more than 70 years ago, is still an important starting point for the analysis of most soil physical problems (Raats 2001). The hydraulic properties of a soil in the Richards' equation are given with the relationships between the volumetric water content Θ, pressure head h and hydraulic conductivity K. A great number of studies have proved the applicability of the Richards' equation for the movement of water in unsaturated soils. Moreover, the solutions of Richards' equation have become useful for inverse methods to determine the physical properties of soils from experimental results. A comprehensive overview of the theory and developments of Richards' equations is given by Raats (2001).

Water flow in soil is caused by the gradient of the hydraulic head and is well described by Darcy's equation for one-dimensional vertical flow:

$$q = -K(h)\frac{\partial (h+z)}{\partial z} \tag{4.1}$$

where q – is soil water flux density [cm d^{-1}], directed positively upwards
K – is hydraulic conductivity [cm d^{-1}]
h – is soil water pressure head [cm]
z – is gravitational head [cm]; also vertical coordinate, with the origin at the soil surface and directed positively upwards
$h+z$ – is hydraulic head [cm]

The water balance of an infinitely small soil volume results in the continuity equation for soil water and representing root water uptake as a sink term is written:

$$\frac{\partial \Theta}{\partial t} = -\frac{\partial q}{\partial z} - S_a(h) \tag{4.2}$$

where Θ – is the volumetric water content [cm^3 cm^{-3}]
t – is time [d]
S_a – is the sink term, i.e. the actual soil water extraction rate by plant roots [cm^3 cm^{-3} d^{-1}]

Combination of Eqs. (4.1) and (4.2) results in the Richards' equation (Richards 1931), which describes water flow in unsaturated or partly saturated soils:

$$\frac{\partial \Theta}{\partial t} = C(h)\frac{\partial h}{\partial t} = \frac{\partial \left[K(h)\left(\frac{\partial h}{\partial z} + 1 \right) \right]}{\partial z} - S_a(h) \tag{4.3}$$

where C – is differential soil water capacity, which is equal to the slope of the soil water retention curve ($d\Theta/dh$) [cm^{-1}]

Equation (4.3) can be solved numerically using finite difference methods (e.g. Feddes et al. 1978, Belmans, et al. 1983, van Dam and Feddes 2000) or a finite element (e.g. Karvonen 1988). For calculations, the initial and boundary conditions as well as the soil hydraulic functions must be known. Thus, it is of utmost importance to successfully describe the flow domain with water retention and hydraulic conductivity functions, however, there are several obstacles to that: missing or insufficient data, difficulties with measuring or estimating the physical parameters, the effect of hysteresis, shrinking and swelling, spatial and temporal variability, etc. Also, these functions should cover all ranges of variability of soil moisture conditions from saturated water to very dry conditions that may occur in the nature.

In general, there are four ways to obtain soil hydraulic functions: 1) laboratory or *in situ* methods, 2) pore-size distribution models, 3) pedotransfer functions, 4) inverse methods. This division is not rigid because: a) laboratory methods may implement inverse methods and widely used pore-size distribution models may have features close to the empirical pedotransfer function, b) some authors classify the pore-size distribution models as a subclass of pedotransfer functions (e.g. Wösten et al. 2001). The second and fourth methods are described in more detail in Section 4.3 and 4.4, respectively.

Laboratory methods

Soil hydraulic functions can be measured using direct or indirect laboratory or *in situ* methods. For example, measurement methods for water retention: sandbox apparatus for the range from -200 cm to 0 cm (Klute 1986), pressure plate method for the range from -20 000 cm to -1000 cm (Klute 1986); constant head method for saturated hydraulic conductivity (Stolte 1977); for unsaturated hydraulic conductivity a) near-saturated conductivity measurements using the crust infiltrometer for the range –50 cm to 0 cm (Booltink et al. 1991), b) evaporation method for the range from -800 cm to 0 cm (Halbertsma and Veerman 1997), c) hot air method for the range from -10000 cm to -100 cm (Al-Soufi 1983, Van Grinsven et al. 1985). In field conditions tension infiltrometers have become popular especially to determine the near-saturation properties (Ankeny et al. 1988, Perroux and White 1988, Jarvis and Messing 1995, Wang et al. 1998). Thus a single method does not cover the complete range of soil moistures occurring in nature. Steady-state methods require restrictive initial and boundary conditions, while transient methods like Wind's evaporation method are more flexible. Thus all methods are time consuming and need a more or less expensive equipment and an experienced laboratory staff.

Pore-size distribution models

Models belonging to this group typically estimate the soil hydraulic functions based on the distribution, connectivity and tortuosity of pores. The models developed by Brooks and Corey (1964), Mualem (1976) and van Genuchten (1980) are very popular among the modelers of soil-water-plant-atmosphere systems. In fact, the laboratory methods or pedotransfer functions, e.g. Vereecken's regression equations (Vereecken et al. 1989, 1990), are often converted into forms of pore-size distribution models.

Based on Brooks and Corey (1964), and Brutsaert (1967) equations Van Genuchten (1980) proposed a more flexible analytical function for water retention which is widely adapted to numerical soil water simulation models:

$$\Theta(h) = \Theta_{res} + \frac{\Theta_{sat} - \Theta_{res}}{\left(1 + |\alpha h|^n\right)^m} \tag{4.4}$$

where Θ_{sat} – is saturated water content [$cm^3\ cm^{-3}$]
Θ_{res} – is the residual water content [$cm^3\ cm^{-3}$]
h - is the soil water pressure head [cm]
α– is an empirical shape factor [cm^{-1}]
n – is an empirical shape factor [-]
m – is an empirical shape factor [-]

Residual water content, Θ_{res}, is the maximum amount of water in the soil that will not contribute to water flow. Mathematically it is defined as $(d\Theta/dh) = 0$. Saturated water content, Θ_{sat}, is maximum soil water content in a soil. In field conditions, Θ_{sat} is usually less than porosity because of entrapped air. Parameter α (>0) is related to the inverse of air entry pressure and determines the relative position of the water retention curve on the water tension axis, parameter n (>1) is a measure of pore-size distribution and characterizes the slope of the $\Theta(h)$ and $K(h)$-functions (van Genuchten 1980, van Genuchten and Nielsen 1985, Durner 1991, the last cited in Messing 1993). Using unsaturated water content, derived from Eq. (4.4), and applying the theory on unsaturated hydraulic conductivity by Mualem (1976), the closed-form function of unsaturated hydraulic conductivity was defined by Van Genuchten (1980) as follows:

$$K(\Theta) = K_{sat}\left(\frac{\Theta-\Theta_{res}}{\Theta_{sat}-\Theta_{res}}\right)^{\lambda}\left[1-\left(1-\left(\frac{\Theta-\Theta_{res}}{\Theta_{sat}-\Theta_{res}}\right)^{\frac{1}{m}}\right)^{m}\right]^{2} \tag{4.5}$$

where K_{sat}– is saturated hydraulic conductivity [$cm\ d^{-1}$]
λ – is an empirical shape factor [-]
m – is an empirical parameter [-]

Soil water content is normalized in Eq. (4.5) by using the term of effective saturation, S_e:

$$S_e(h) = \frac{\Theta(h)-\Theta_{res}}{\Theta_{sat}-\Theta_{res}} \tag{4.6}$$

Equations (4.4) and (4.5) are mostly used in the form where the exponent m is defined as $m=1-1/n$. The exponent λ is a lumped parameter that accounts for pore tortuosity and pore connectivity and provides more flexibility for the $K(\Theta)$-function. Mualem (1976) suggested the value of 0.5 for λ, but several studies have shown that λ may be substantially different ranging: 1) from -16 to 2 (Wösten and van Genuchten 1988), 2) from –9 to 15 (Schuh and Cline 1990), 3) from -3 to 3, with an optimum of $\lambda=-1$ (Schaap and Leij 2000).

Pedotransfer functions

The term *pedotransfer functions* (PTF) was introduced by Bouma (1989) who described PTFs as translating of the data *we have* into the data that *we need*, i.e. PTFs are the predictive functions of certain soil properties from other easily measured properties, e.g. textural fraction, bulk density, organic content, etc. Thus the pedotransfer functions reduce the effort involved in soil sampling and laboratory analysis. The number of publications and reviews concerning PTFs has been growing rapidly during the last couple of years (e.g. Wösten et al. 1995, Pachepsky and Rawls 1999, Minasny et al. 1999, Wösten et al. 2001). However, a different classification of PTFs can be found in literature, which is briefly reviewed and discussed below.

Wösten et al. (1995) divided PTFs into 'class' and 'continuous' PTFs where in the first group, the soil hydraulic characteristics were predicted by texture class and type of the horizon. To facilitate the use of the calculated characteristics in simulation models the analytical equations of Mualem-van Genuchten were implemented. In continuous PTFs the actually measured percentages of the content of clay, silt and organic matter were used, and were described with empirical functions.

Minasny et al. (1999) divided PTFs into three types: 1) point estimation: an empirical function that predicts water content at a pre-defined potential, usually at –10kPa, -33 kPa, and at –1500 kPa (corresponding to permanent wilting point), 2) parametric estimation: closed-form equations, e.g. Brooks and Corey (1964), van Genuchten (1980), 3) physical-empirical models: water retention curves are derived from physical attributes, e.g. Arya and Paris (1981) who translated particle-size distribution into a water-retention curve by converting solid mass fractions to water content, and pore-size distribution into a hydraulic potential by means of a capillary equation.

Wösten et al. (2001) distinguished three types of PTFs: 1) predicting hydraulic characteristics based on a soil structure model (Arya and Paris 1981), 2) point predictions of water retention characteristics (Gupta and Larson 1979, Ahuja et al. 1985), 3) prediction of the parameters used to describe complete hydraulic characteristics. Only the first type has a theoretical background. The techniques used for PTF development are regression analysis, artificial neural network, group method of data processing, etc. (Wösten et al. 2001).

The list of the PTFs that probably best meet Bouma's definition is long, e.g. Campbell (1985), Vereecken et al. (1989, 1990), Rawls and Brakensiek (1989), Wösten (1997), Wösten et al. (1999) (all cited and compared in Wagner et al. 2001).

The method that uses the similarity between particle-size distribution and water retention curves described by Andersson (1990a, 1990b) and modified by Jauhiainen (2000), is described and discussed in more detail in Section 4.4, based on the experimental data.

Inverse methods

Inverse methods combine observed time series of infiltration, evaporation, changes in water content and pressure head with equations of water flux, using optimization algorithms (Kool et al. 1987, Simunek and van Genuchten 1996, Abbaspour et al. 1997, Nützmann et al. 1998, Abbaspour et al. 1999). Wind's evaporation method, which is useful to determine both water retention and hydraulic conductivity functions for one and same soil sample, is described and discussed in more detail in Section 4.3 when analyzing the experimental data.

4.3 Wind's evaporation method

4.3.1 Description of the method

Evaporation method was first introduced by Gardner and Miklich (1962) who used two tensiometers in a soil sample evaporating at one side. Evaporation method to determine both water retention curve and hydraulic conductivity functions on the basis of one sample was improved and extended by Wind (1966). At this time he had to calculate parameters by hand using graphical differentiation. Today, such curves are calculated numerically using computer programs. Wind's evaporation method belongs to a group of methods so-called '*inverse modeling*' methods, where the 'true' values of $\Theta(h)$ are found by a numerical iterative fitting procedure of measured water content and measured soil water pressure head, and where $K(h)$ is estimated from the flux density and the hydraulic head gradients. Inverse modeling of soil hydraulic properties has become popular since the last decade (e.g. van Dam et al. 1994, Abbaspour et al. 1999, Jhorar 2002). Instead of ordinary direct measurements, which need long experimental periods to obtain equilibrium conditions, the inverse technique is much more flexible and quick to perform. However, inverse modeling has certain disadvantages compared with direct measurements, e.g. the estimated parameters will include not only measurement errors but also model error. Moreover, there arises the problem of the uniqueness and stability of the results (van Dam et al. 1994). In case of evaporation method the interval between measurements cannot be too long, which leads to relative increase in the error of the flux densities. Furthermore, the small pressure gradient ($dh/dz \approx -1$) may bias the calculation of hydraulic conductivity (Halbertsma and Veerman 1997, Tamari et al. 1993). The following brief description of Wind's algorithm is given by Halbertsma and Veerman (1997).

Wind's algorithms start from an assumed water retention curve to convert pressure head data into estimated water contents at appropriate depths and continues until the mean measured water content of the soil sample and the mean estimated water content converge. The water retention curve is described up to the sixth-order polynomial that is iteratively changed. Unsaturated hydraulic conductivity is determined from the measured pressure heads and the corresponding water content estimates over depth and time ranges, using instantaneous profile method. Finally, the solving procedure yields maximally $(n\text{-}1)(i\text{-}1)$ data points for $K(\Theta)$ and $K(h)$, where n is the number of measurement scans and i is the number of the compartments of the soil sample. These data sets can be described with a suitable curve.

4.3.2 Experiment

The water retention $h(\Theta)$ and the unsaturated hydraulic conductivity $K(\Theta)$ and $K(h)$ were determined for four soil samples. The methodology of DLO Winand Staring Centre for Integrated Land, Soil and Water Research (SC-DLO) (Halbertsma and Veerman, 1994, Halbertsma and Veerman 1997) was followed. Due to a missing climate chamber, a constant and fixed relative humidity of 50% was not maintained.

Four undisturbed soil samples were taken from the Reola experimental field (see Chapter 5) at MID-plot by pushing the PVC cylinder (height 80 mm and diameter 103 mm) into the soil. One sample represents the average conditions of topsoil (12-20 cm), the next sample represents the layer just below the humus horizon (38-46 cm) and the next two samples represent subsoil (52-60 cm and 70-78 cm). The soil samples were saturated in the exsiccator (slight vacuum around <23 mbar) by placing lower part of the sample into water for 48 hours. Four tensiometers (outer diameter 6 mm, length 55 mm), filled with de-aired water and connected to a pressure transducer unit, were horizontally inserted into pre-bored holes at heights of 10, 30, 50 and 70 mm from the bottom of the soil sample. After that the top was covered with the lid and the samples were allowed to reach an equilibrium between the soil core and the tensiometers. The soil sample inside the PVC-cylinder and the bottom lid were placed into an electronic balance (accuracy 0.1 g). Automatic sampling of soil water pressure and weighing of the sample were completed using specific laboratory equipment model STAR-1 (designed by SC-DLO Winand Staring Centre, Wageningen) (Fig. 4.1). The readings of the pressure transducers and the balance were recorded at regular intervals (60 min for topsoil and 30 min for subsoil). The experiment lasted until the upper tensiometer was 'broken down' i.e. when air entered the ceramic tensiometer. After that the soil was removed from the PVC cylinder, weighed and dried in an oven at 105 °C to determine water content at the end of the experiment and to calculate the bulk density of the soil core. Particle size distribution was measured and the results are given in Table 4.1 and Table 4.2.

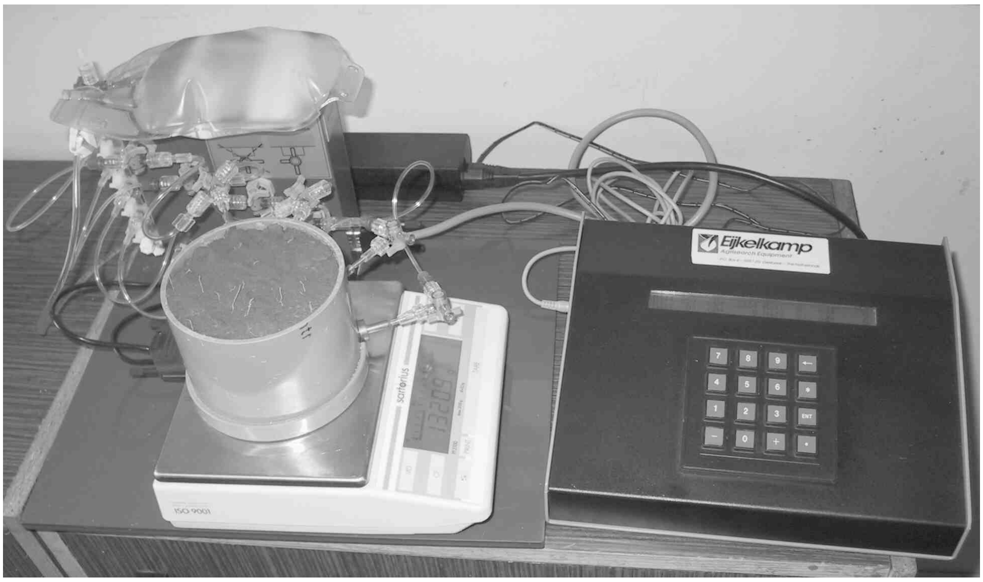

Figure 4.1. Star-1 equipment.

Table 4.1. Particle-size distribution and bulk density of the soil samples used in Wind's evaporation method.

Site	Layer	Particle size distribution									Bulk dens. $g\ cm^{-3}$
		1-2.0	1-0.5	0.5-0.25	0.25-0.1	0.1-0.05	0.05-0.02	0.02-0.005	0.005-0.002	<0.002	
Mid	12-20cm	1.9	7	11.1	31.8	12.9	13.2	13.7	3.3	5.1	1.37
Mid	38-46cm	2.7	5.3	8.2	22.4	12.7	15.9	18.8	4.5	9.6	1.63
Mid	50-58cm	1.6	3.8	8.6	24.1	12.5	15.0	13.3	4.3	16.8	1.73
Mid	70-78cm	0.8	3.7	8.1	26.8	11.0	12.8	13.8	4.9	18.1	1.81

Table 4.2. Textural classes and soil type of the soil samples used in Wind's evaporation method.

Site	Layer	Texture class Sand %	Silt %	Clay %	Soil type
Mid	12-20cm	64.7	30.2	5.1	Sandy loam
Mid	38-46cm	51.3	39.2	9.6	Loam
Mid	50-58cm	50.6	32.6	16.8	Loam
Mid	70-78cm	50.4	31.5	18.1	Loam

For topsoil the measurement lasted 5.3 d and for the following layers only 2.9 d, 2.25 d and 2.75 d, respectively. Average water content decreased from 0.433 to 0.202 m^3 m^{-3} for topsoil and from 0.361 to 0.252 cm^3 cm^{-3}, from 0.362 to 0.273 cm^3 cm^{-3}, from 0.362 to 0.277 cm^3 cm^{-3} for the following layers, respectively. The lowest recorded tensiometer pressure heads were -819 cm for topsoil and -862 cm, -737 cm and -896 cm for subsoil, respectively. The average evaporation rate was around 3-4 mm d^{-1} for topsoil and 2-3 mm d^{-1} for subsoil.

The estimated water retention and hydraulic conductivity values were obtained with the computer program Appia 2.02 (The Winand Staring Centre, Wageningen, The Netherlands) which performs iterative calculations and produces a h-Θ -K dataset. The program Appia was used to calibrate the van Genuchten parameters in Eqs. (4.5) and (4.6). Additionally, a separate spreadsheet solution was written to study differences between tensiometer pairs and an overall dataset. RMSE was also calculated to assess the effect of calibration method on the calibration results. In case of the hydraulic conductivity data the $\log_{10}$-transformation was performed. The parameters Θ_{res} and Θ_{sat} were subject to the constraints 0.0001 (cm^3 cm^{-3}) $< \Theta_{res} < \Theta_{sat}$ and $\alpha > 0.0$. The latter constraint was violated in several cases.

4.3.3 Results

The program Appia allows to use different strategies to calibrate the van Genuchten parameters: 1) simultaneous fit with selected weight factor, usually W1=0.1 (to prefer the water retention curve), 2) predicting K from observed water retention data, 3) predicting $\Theta(h)$ from unsaturated hydraulic conductivity data. In all cases residual moisture content and saturated moisture content were set at estimated and measured values, respectively. Parameter λ was set at 0.5 or was calibrated. The first option was selected as the most appropriate and the corresponding calibration results are shown in Table 4.3 and Fig. (4.2- 4.5).

In general, the estimated Θ-h data pairs formed a rather smooth curve (Fig. 4.2ad, 4.3ad) compared with a scattered cloud of K-h or K-Θ data pairs (Fig. 4.2bcef, 4.3bcef). The last figures revealed that estimated hydraulic conductivity might vary more than by one order of magnitude at particular Θ or h-values. The same conclusion as a striking feature of Wind's method was reported by Larsson et al. (1999). Therefore, the water retention curve can be estimated with higher precision and is better described by analytical expressions compared with the unsaturated hydraulic conductivity function. In spite of a good fit in case of water retention data, visual inspection showed that the shape of the experimental data differed from the expected results. Based on soil texture (Table 4.2), the water retention curves of sandy soils should have a plateau between rapid change of h at the near-saturation region and the second rapid change of h near residual moisture content, as is usually the case with light soils. The experimental results resembled rather the characteristics of the clay soil, which do not exhibit this kind of plateau. One explanation for this is that these results represent the ultimate drying curve, which has a higher tension at the same volumetric water content as the wetting curve. Kool and Parker (1987) and Homaee (1999) proposed that the α parameter in Eq. (4.4) for the wetting curve is two times larger than that of the drying one. When this transformation was applied to the α-values in Table 4.3 the resulting water retention curves were still closer to those for clay soils than to those for loamy soils.

Comparison of the fitted curves represented by the van Genuchten analytical equations revealed that the water retention (Fig. 4.4a) and unsaturated hydraulic conductivity curves (Fig. 4.4bc) for the subsoil layers (52-60 cm and 70-78 cm) resulted in very similar functions, the topsoil curve differed clearly from the subsoil curves, and the intermediate layer (38-46 cm) was transition from topsoil to subsoil. The only deviation seems to be the estimated saturated hydraulic conductivity of the intermediate layer (Fig. 4.4c), which showed a lower value than the other curves. In fact, there was no physical evidence, e.g. soil compaction or clay layer, to cause that result (Table 4.1, 4.2). It is assumed that the shape of the hydraulic conductivity curve is depending greatly on the fact whether K_{sat} is measured independently (or/and set as a fixed value) or is viewed as a fitting parameter, as it was partly done in the present study. Although soil tension was measured at saturated and near-saturated conditions ($\sim+5>h>-10$ cm, i.e. at the beginning of the experiment two lower tensiometers showed positive pressure) the computing program Appia did not estimate the h-Θ-K data pairs for this region due to measurement 'noise' which is larger when the pressure gradient is small (Tamari et al., 1993). The distance between the neighboring tensiometers was only 2 cm and in near-saturated conditions the tension difference was of the same order. The problems related to near-saturated conditions are discussed in more detail in Section 4.4.4.

Another relevant factor affecting the shape of $\Theta(h)$ and $K(h)$-functions is the fitting procedure. Probably the most proper way is to parameterize first the water retention curve (Eq. 4.4, fitting parameters α, n) and thereafter the unsaturated hydraulic conductivity function (Eq. 4.5, λ and K_{sat} if not measured). In the present study five different fitting procedures were compared. The results are shown only in case of topsoil (12-20 cm) because all other soil samples had a similar behavior (Table 4.4, Fig. 4.5). The best way was to use simultaneous fit with the weight coefficient W1=0.1, which yielded a considerably better estimate for $K(h)$-function compared with the case when only $\Theta(h)$ data pairs were used for the prediction of water retention. If the parameter λ was also calibrated then the $K(h)$-function yielded lower RMSE, but in case W1>0.1, fitted λ tended to be less than -15, which resulted in impossible $K(\Theta)$ curves. Interesting results were obtained with a fitting procedure when the water retention curve was estimated from the $K(h)$ dataset. The shape of the $\Theta(h)$ curve was closer to that of typical loamy soils (Fig. 4.5d) than that of the estimated results obtained with the Appia program. Finally, it is concluded that the parameterization of the van Genuchten equations depends not only on the measured or estimated h-Θ-K dataset but also on the choice of fitting procedure.

Table 4.3. Measured* and fitted parameters for the van Genuchten equations depending on the selected calibration method.

Site/layer cm	Θ_{res}	Θ_{sat}	K_{sat}	α	n	λ
	$cm^3\ cm^{-3}$	$cm^3\ cm^{-3}$	$cm\ d^{-1}$	cm^{-1}	-	-
Simultaneous fit, Appia weight coefficient W1=0.1						
Mid 12-20cm	0.04	0.450	51.1	0.0267	1.248	0.5
Mid 38-46 cm	0.04	0.361	0.71	0.0029	1.359	0.5
Mid 52-60 cm	0.04	0.362	5.7	0.0107	1.149	0.5
Mid 70-78 cm	0.04	0.36	15.7	0.0198	1.113	0.5
Simultaneous fit, Appia weight coefficient W1=0.2						
Mid 12-20cm	0.04	0.450	24.7	0.0199	1.283	0.5
Predicting K from observed Θ(h)						
Mid 12-20cm	0.04	0.450	6.0	0.0293	1.239	0.5
Predicting Θ(h) from observed K						
Mid 12-20cm	0.04	0.450	0.22	0.0029	2.522	0.5
Simultaneous fit, Appia weight coefficient W1=0.1, calibrated λ						
Mid 12-20cm	0.04	0.450	7.8	0.0288	1.241	-5.33
Mid 38-46 cm	0.04	0.361	0.335	0.0030	1.345	-4.09
Mid 52-60 cm	0.04	0.362	2.03	0.0100	1.151	-4.99
Mid 70-78 cm	0.04	0.36	4.5	0.0199	1.113	-7.05

*bulk density and Θ_{sat}

Table 4.4. The effect of fitting procedure on RMSE of volumetric moisture content Θ and log_{10}-transformed hydraulic conductivity K in case of topsoil (12-20 cm).

Fitting procedure	$RMSE_{\Theta}$ $cm^3\ cm^{-3}$	$RMSE_K$ $cm\ d^{-1}$
Simultaneous fit, W1=0.1, λ=0.5	0.0028	0.670
Simultaneous fit, W1=0.2, λ=0.5	0.0081	0.641
Predicting K from observed $\Theta(h)$	0.0019	1.242
Predicting $\Theta(h)$ from observed K	0.0665	0.332
Simultaneous fit, W1=0.1, calibrated λ	0.0082	0.447

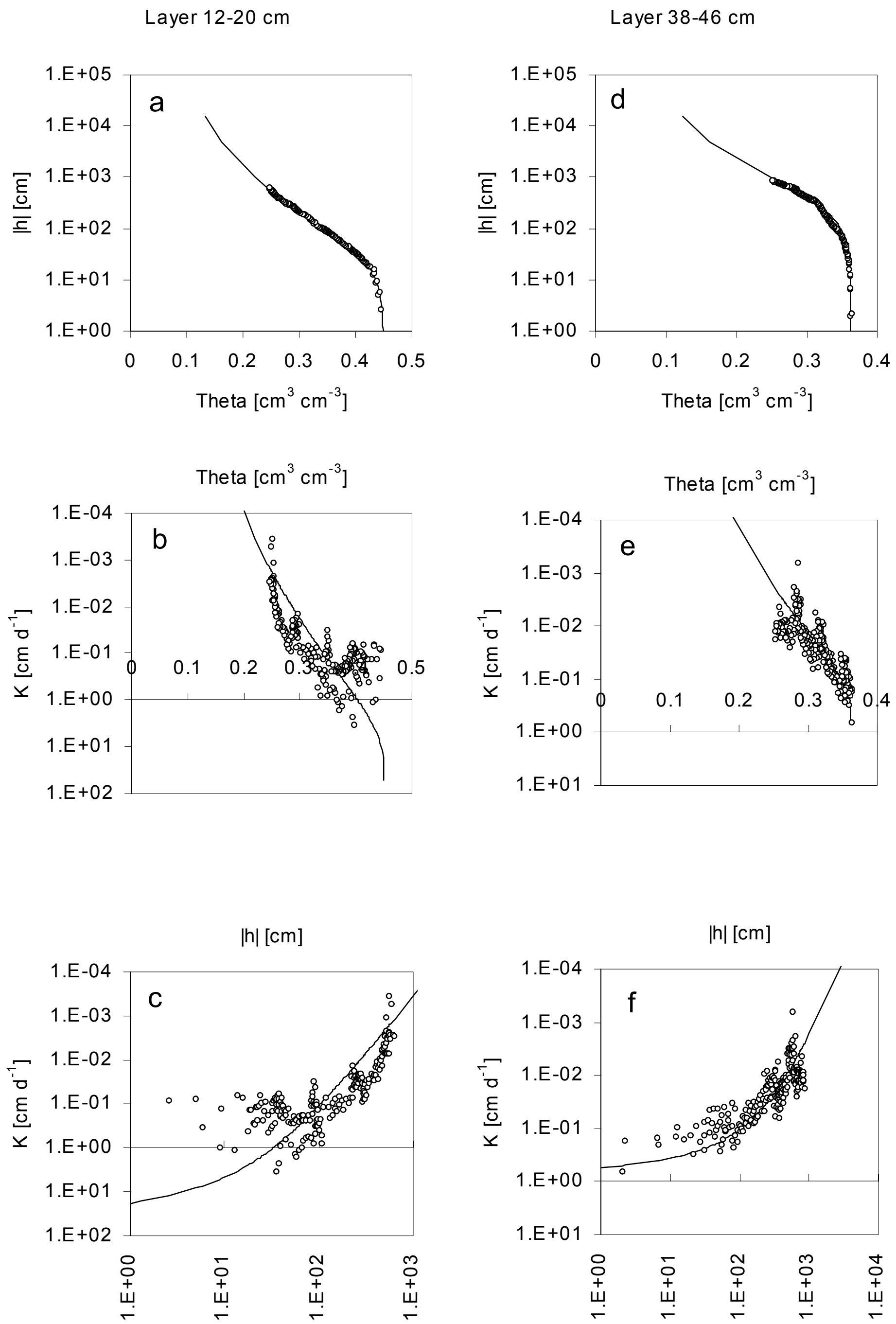

Figure 4.2. The measured (circles) and estimated (lines) water retention curves and unsaturated hydraulic conductivity functions for topsoil (12-20 cm, left column) and for an intermediate soil layer (38-46 cm, right column) at the Mid-site.

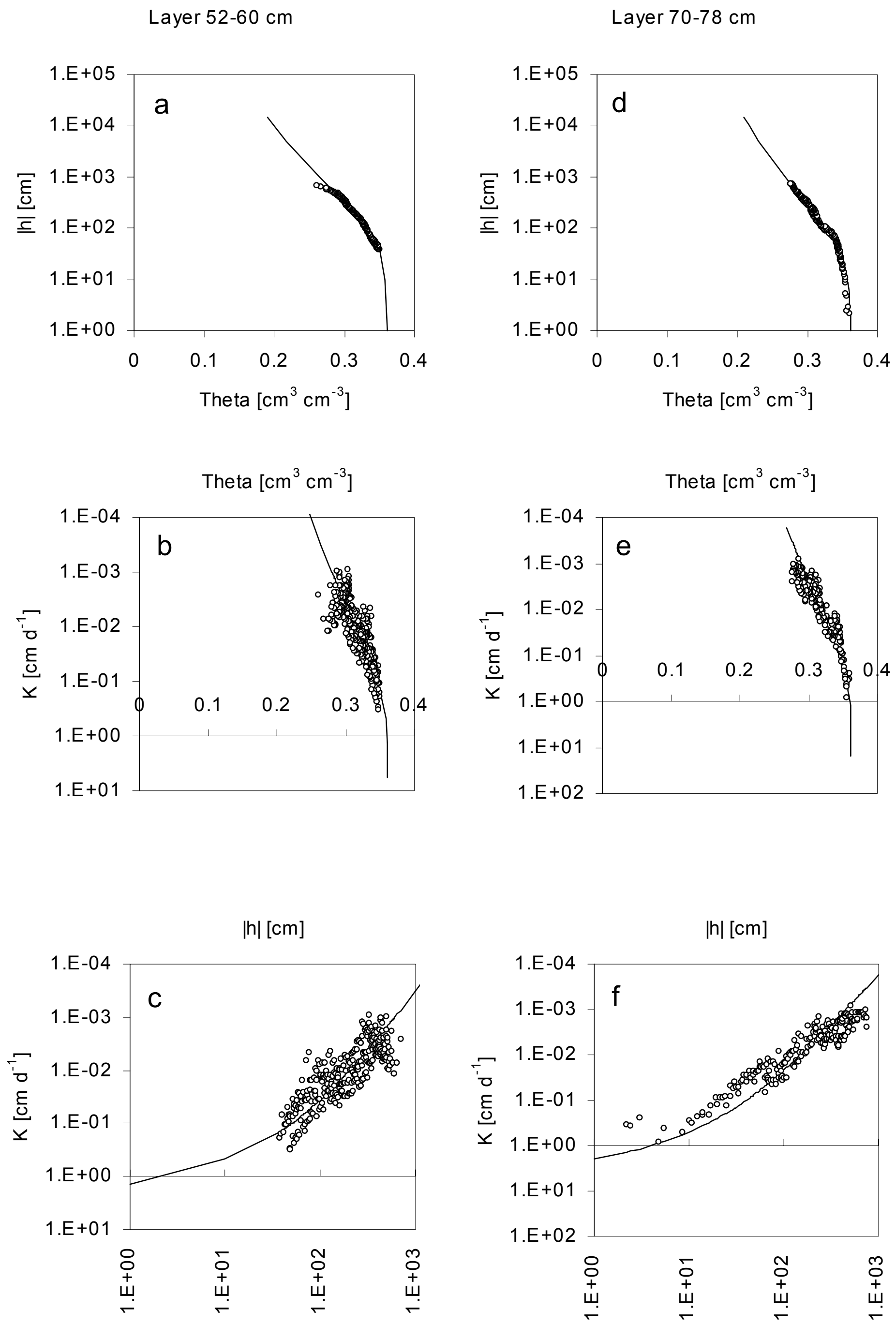

Figure 4.3. The measured (circles) and estimated (lines) water retention curves and unsaturated hydraulic conductivity functions for two subsoil layers (52-60 cm, left column, 70-78 cm, right column).

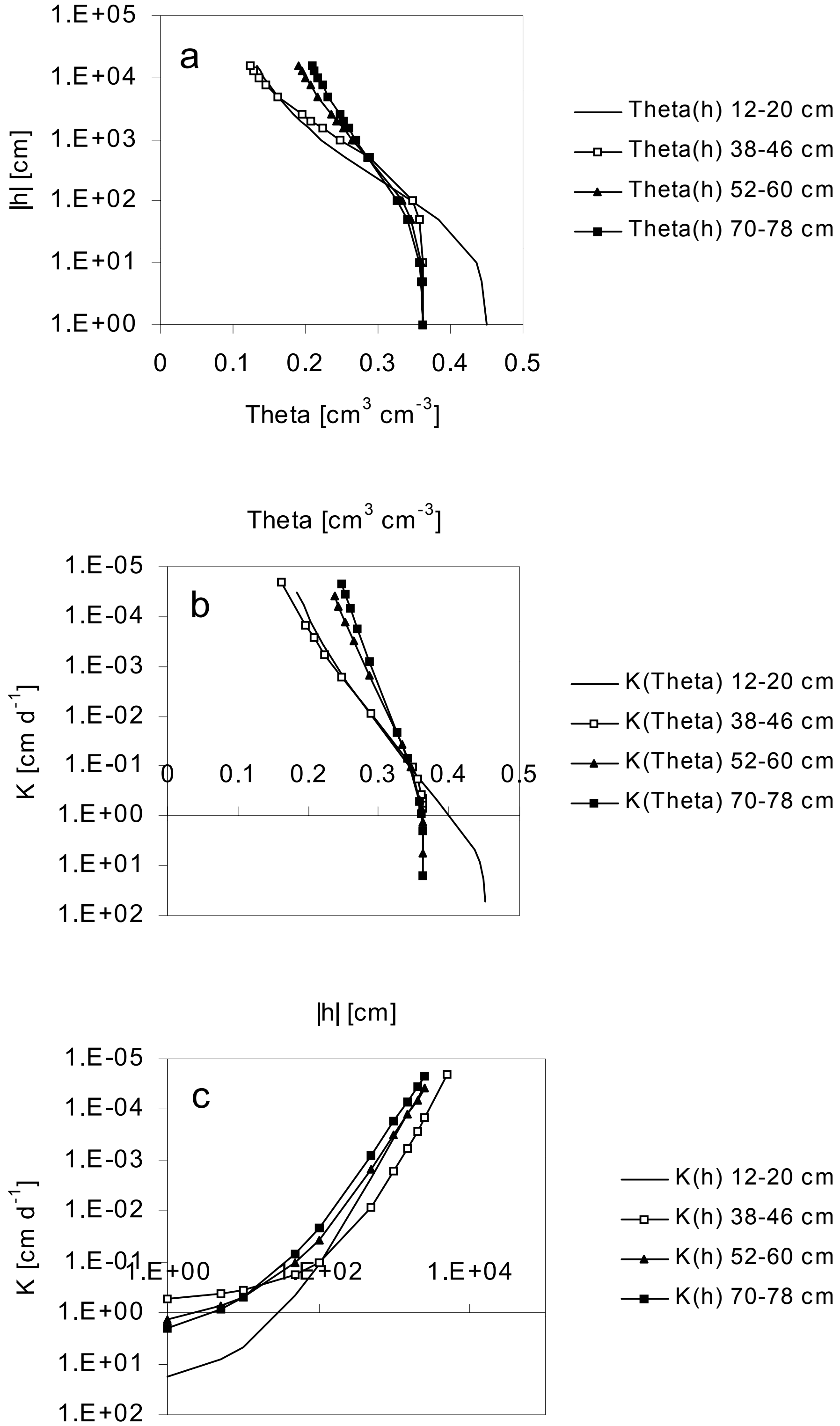

Figure 4.4. Water retention curves and unsaturated hydraulic conductivity functions for four different soil layers at the Mid-site.

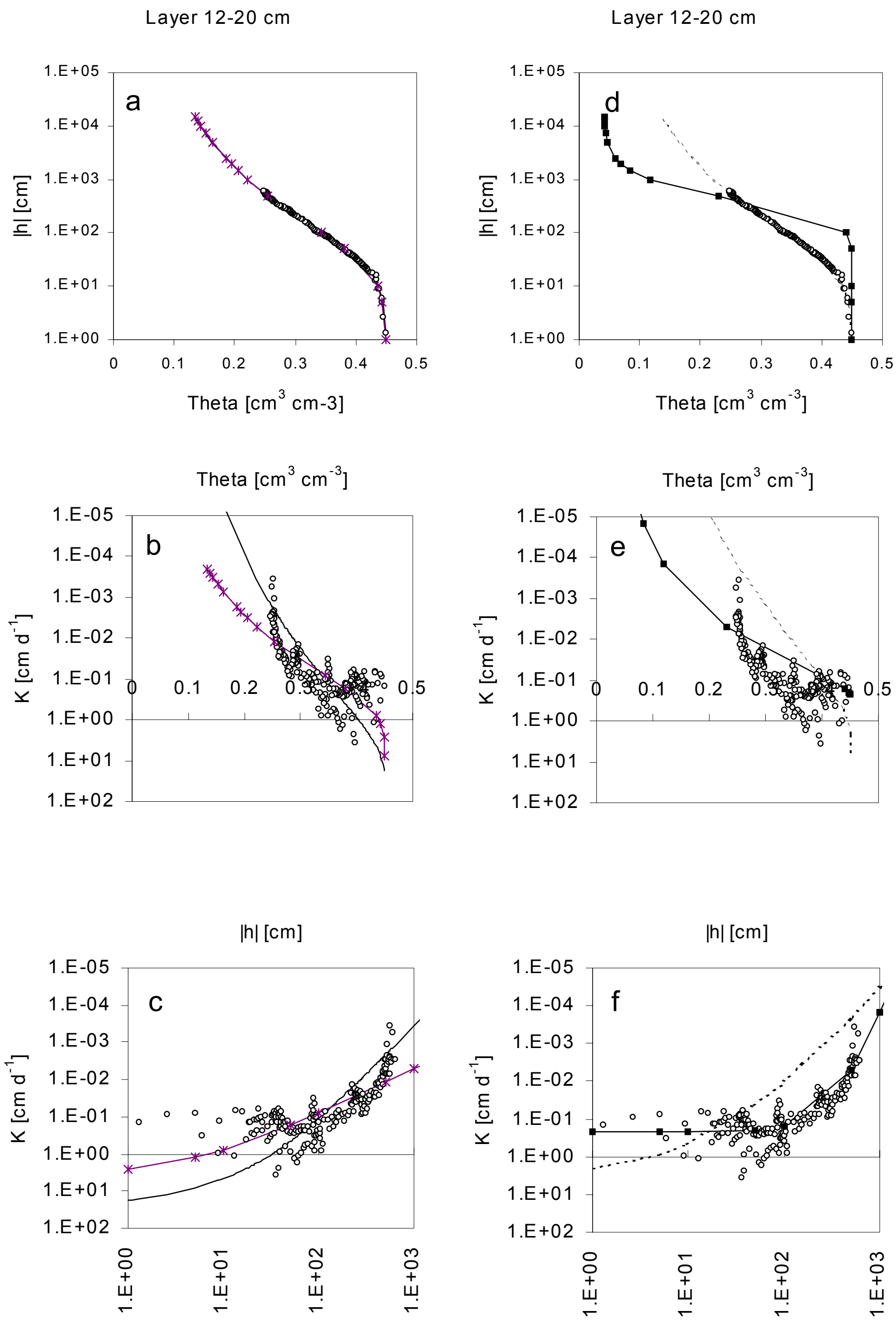

Figure 4.5. The effect of calibration procedure on calibration results on the example of topsoil (12-20 cm) data. Estimated points – circles; (a,b,c) simultaneous fit (W1=0.1, λ=0.5) – line and simultaneous fit (W1=0.1, λ=free) – line with asterisks; (d,e,f) predicting *K* from observed Θ – dashed line and predicting Θ from observed *K* – black dotted line.

4.3.4 Assessment of Wind's evaporation method

The laboratory experiment and the fitting procedure raised a number of problems that might significantly affect the obtained results. These problems may be divided as: a) measurement error, b) representativity of laboratory curves in field conditions, c) bias from the present understanding of the universal character of the van Genuchten parameters both for water retention and hydraulic conductivity, d) problems arising in near-saturated conditions implementing the van Genuchten equation.

Measurement errors

Systematic measurement error occurring during the experiments are classified as follows (Mohrath et al. 1997): a) errors due to the position of the tensiometers, b) errors due to the calibration of the pressure transducers used for pressure head measurements, c) errors due to layering in the soil column. Mohrath et al. (1997) demonstrated the effect of different error sources by a numerical experiment and found that the estimated water retention curves were sensitive only to soil layering, while a small deviation in the position of the tensiometers and in the calibration curve of the pressure transducers had a strong impact influence on the corresponding $K(h)$ *and* $K(\Theta)$ – functions. Moreover, the temperature corrections related to viscosity of liquid water, were large. In the present study, the factory settings for the pressure transducer were used, the deviation from the right position by ± 1 mm was suggested and temperature ranged approximately around 20-25 ^{0}C.

Representativity

The obtained functions represent the desorption curves measured by extracting water from initially saturated soil. In field conditions remarkably different sorption-desorption curves may exist especially after a dry season and heavy rain. De Vos (1997) has pointed out that the pressure heads, corresponding to particular water content measured in the field, are nearly always larger than would be expected on the basis of the laboratory water retention curve. Thus, the first impression that water retention was well determined in comparison with scattered hydraulic conductivity is misleading, as the 'real' curves existing in the field may be considerably different due to air entrapment and hysteresis. It can be added that in field conditions when rainwater infiltrates into the soil K_{sat} is probably much higher than the values estimated by the evaporation method due to macropore flow and, therefore, additional calibration with field data is necessary. Another problem connected with representativity is due to thermal effects on the hydraulic conductivity function, as the kinematic viscosity of water changes from 10 ^{0}C of 1.308×10^{-6} m^2 s^{-1} to 0.801×10^{-6} m^2 s^{-1} at 30 ^{0}C (Lide 1996), respectively. During the laboratory experiment room temperature was around 20-25 degrees, while in field conditions ground temperature changes diurnally and seasonally (see Section 2.5.3). The third problem related to representativity is the size of the soil sample, i.e. whether macropores are well enough represented in small cores (e.g. Bouma 1983, Messing and Jarvis 1995). It is believed that the present sample size was representative for an evaporation experiment, however, for wetting curves the volume may not be sufficient as reported by Anderson and Bouma (1973). The fourth problem is related to the limited range, as Wind's method is performed in the tensiometric range. In the nature, hydraulic conductivity changes several orders of magnitude between saturated moisture content and the wilting point or even lower soil moisture content. However, based on the experimental results (Chapters 5 and 6) prevailing soil moisture conditions fell in the tensiometer range.

Universal character

One reason why the Mualem and van Genuchten equations are widely used in soil water simulation models is that both water retention and hydraulic conductivity functions are described with the same parameters, and that after determining the water retention curve one may expect that these parameters are applicable also for the hydraulic conductivity curve (very often λ is set at 0.5). Additionally, K_{sat} must be known. However, it has also been found that these parameters do not always possess this universal character (e.g. Wang et al. 1998). During the fitting procedure it was found that relatively different calibration results were obtained depending on the fitting procedure. The best results for the water retention curve may yield larger deviation in the case of the unsaturated hydraulic conductivity function compared with a certain 'compromise' between these functions. It should be noted that in the present evaporation experiment K_{sat} was not measured, which added one degree of freedom and probably simplified the calibration procedure of the van Genuchten parameters.

Near-saturation conditions

The water retention and unsaturated hydraulic conductivity functions are usually expressed by the analytical expressions of van Genuchten, as it was done in the present study or like several PTFs do. However, there exists a problem when implementing the van Genuchten Eq. (4.6) in near-saturation conditions, because the equation has analytical ambiguity close to saturation. Estimated hydraulic conductivity may increase tremendously when soil tension is a few centimeters and its value approaches to zero. Similarly, in the nature, in soils with well-developed macropores hydraulic conductivity may also increase very rapidly close to saturation. Probably due to the similarity or 'coherence' of these functions (i.e. analytical and 'true' *K-h*-curves) researchers may expect that the real soil will behave like the analytical equation, i.e. K_{sat} is extrapolated from the unsaturated *K-h*-values. The analysis of the fitting procedure described earlier, combined with the analysis of unsaturated hydraulic conductivity in saturation (h=0) and near-saturation (h=-1 cm … -10 cm) conditions, stimulated to search for relevant discussion in literature.

At first, it can be debated what 'saturated moisture content' means in the nature and where and when the corresponding 'saturated' hydraulic conductivity could be found? In shallow groundwater systems the groundwater table fluctuates continuously in the upper soil zone (in Estonian conditions usually in the upper 1-2 meter layer). After rainstorms the wetting front moves downward and the air may be entrapped in the soil. Most likely saturation may occur when the groundwater level rises and pushes the air out. For example, the soil sample taken from the depth of 70-78 cm and saturated in the exciccator prior to Wind's experiment showed value of Θ_{sat} =0.362 which was never measured in field conditions during the experiment (Θ_{sat} =0.29±0.03, see Chapter 5), although the soil samples were taken below the level of the groundwater table in the piezometers. This discrepancy may be partly explained with measurement error, but it may also imply that in the first case the saturated soil was 'more' saturated than in the latter case, and hence the corresponding saturated hydraulic conductivities must also be different also. Juri (1991) described the complexity of the physics of soil wetting-drying where the order of filling and access to pores is influenced by entrapped air, and found that the drying-wetting loops are not exactly reproducible due to the inherent difficulty of repeating the exact order of pore filling. De Vos (1997) reported that K_{sat} measured in laboratory with a different constant head at the top of the soil sample yielded higher values of K_{sat} at higher hydraulic head gradients. This result conflicts with the common understanding that saturated hydraulic conductivity is constant for a given soil. Dorsey et al. (1990) compared four field methods for measuring hydraulic conductivity and found considerable variability within the same methods as well between different methods.

When Eq. (4.5) with the calibrated van Genuchten parameters was used to calculate near-saturated hydraulic conductivity it revealed that an extremely small change at near-saturated moisture remarkably reduced unsaturated hydraulic conductivity. For example: K_{sat}=51.1 cm d^{-1} and K(-1)=18 cm d^{-1} for topsoil (layer 12-20 cm), and K_{sat} =15.7 cm d^{-1} and K(-1)=2.0 cm d^{-1} for subsoil (layer 70-78 cm). The change in volumetric moisture content was only 0.2% and 0.1%, respectively, i.e. close to measurement accuracy. This difference is more than one order of magnitude smaller than the difference between field and lab measured saturated volumetric moisture content of the same soil described above. In a number of papers similar rapid changes have been reported. Van Dam and Feddes (2000) reported this feature (K_{sat} =15.5 cm d^{-1} and K(-1)=0.73 cm d^{-1} , i.e. about 20 times). Zavaratto et al. (1999) reported measurements with the tension infiltrometer where hydraulic conductivity increased about three orders of magnitude across the pressure head range from -9.1 to -0.4 cm. Jarvis and Messing (1995) reported the measurement of six Swedish tilled soils with a contrasting texture ranging from loamy sand to silty clay, also with tension infiltrometers, where decrease was measured particularly in $0>h>-5$ cm range. They found that estimated saturated hydraulic conductivity was smaller for sandy-textured soils than for finer textured soils and concluded that this result 'presumably reflects the importance of continuous surface-vented macropores for near-saturated water flow in structured field soils'. Finally they stated that K_{sat} estimated by extrapolation from unsaturated hydraulic conductivity measurements is a fitted parameter that depends on the particular model chosen for $K(h)$. However, it was also concluded that direct measurements of K_{sat} in the field at zero or positive pressure heads might not necessarily give more reliable results, because spatial variability in K may be larger at saturation than at small tensions (references in Clothier and White 1981, Perroux and White 1988, Ankeny et al. 1990). Moreover, significant temporal variations in soil hydraulic properties have been found, particularly in the near-saturation region (Messing and Jarvis 1993, Jarvis et al. 1997). Thus, these were only a few examples showing problems involved in determination of saturated hydraulic conductivity.

The analytical ambiguity of Eq. (4.5) occurs, because the derivative of the effective saturation curve is very small in full saturation and near-saturation conditions, which causes exponential decrease in hydraulic conductivity in near-saturation conditions. The magnitude of changes in near-saturated conditions depends on the parameters in the van Genuchten equation, i.e. in certain circumstances the change of K is much less significant than with other sets of parameters. To overcome this problem a certain approximation can be done, e.g. instead of Θ_{sat} in Eq. (4.6) a slightly altered value of $\Theta_{sat}{}^{*}= \Theta_{sat}$-0.01 (or similar) can be used. Another option is to implement the van Genuchten equation up to the tension of a few centimeters close to saturation, thereafter setting it at K_{sat}. In fact, the latter option can be used in dual-domain (dual porosity) models as a rough estimation of the hydraulic conductivity curve. In practice, numerical simulation models (e.g. MACRO, Jarvis and Larsson 1998) divide the pore distribution into macropore and micropore regions applying different flow equations (i.e. gravity-driven or capillary flow, respectively). Thus, the models implementing bi- or multimodal systems can avoid that particular problem inherent in van Genuchten equation.

Nevertheless, there may occur a variety of situations where the whole range of soil moisture conditions can be described with closed form equations. A new comprehensive study by Schaap and Leij (2000), where a dataset of 235 soil samples with retention and unsaturated hydraulic conductivity predictions obtained with the van Genuchten equations, were tested and improved. Instead of K_{sat} in Eq. (4.5) they used K_0 as a matching point to improve the fit for the unsaturated range. Secondly, the parameter λ was allowed to be negative even this contradicts with the interpretation of S_e^{λ} in terms of pore continuity and tortuosity where S_e^{λ} should always be smaller than 1 and hence λ must be positive. Schaap and Leij (2000) found that λ had a clear minimum RMSE for predicted unsaturated hydraulic conductivity at λ=-1 which led to the conclusion that the pore-tortuosity or pore-interaction concept fails. They also found that predicted unsaturated hydraulic conductivity with $K_0 = K_{sat}$ and λ=0.5 yielded RMSE more than one order of magnitude higher than that obtained with fitted K_0 and λ. Finally, Schaap and Leij (2000) concluded that: a) K_0 and λ cannot be interpreted as physically meaningful parameters, b) $K_0 = K_{sat}$ leads to overestimation of saturated hydraulic conductivity, c) fitted K_0 leads to underestimation at or near saturation. Wagner et al. (2001) stated that the use of predicted K_{sat} is in many cases superior to the input of measured K_{sat} as it leads to better fits of $K(h)$ over the full range of the matrix heads. They also found that K_{sat} estimated on the basis of textural parameters might yield values which are more independent of macroporosity and structural properties of soils, which influence K_{sat} but have a rather weak impact on $K(h)$.

In certain circumstances when unsaturated hydraulic conductivity is measured very close to saturation it may be reasonable to set that measured value at K_{sat} instead of extrapolating it, which may lead to a smaller over- or underestimation of the saturated flux. However, inspection of the experimental results of the present study revealed that in case of topsoil this was practically impossible due to the scattered K-h data pair (Fig. 4.2c), however this might prove be reasonable in case of subsoil (Fig. 4.2f).

4.4 Andresson's method

The difficulties related to experimental determination of the water retention characteristics and hydraulic conductivity have given occasion to search for other possibilities, and one option is to use particle size distribution which is much easier to measure. These relationships have been researched by Arya and Paris (1981), Haverkamp and Pralange (1986), Rajkai et al. (1996). Jauhiainen (2000) has tested Andersson's (1990) and Jonasson's (1991) functions for a number of Finnish forest soils.

Similarity between both particle-size distribution and water retention curves described by Andersson (1990a, 1990b) allows to a develop theory which links these curves. The particle-size distribution is given as follows:

$$y = y_0 + b \arctan\left[c \log \frac{x}{x_0} \right] \quad (4.7)$$

where y – is cumulative particle-size distribution function
x – is the corresponding particle diameter
y_0 – is inflection point of the particle size distribution curve corresponding to the particle diameter x_0
b – is the range of the curve in y-direction

c – is the derivative of the curve at the inflection point (x_0, y_0)

The water retention curve is given as follows:

$$\Theta = \Theta_0 - \frac{p}{\pi} \arctan\left[\frac{1}{b_\Theta} \log(\frac{h}{h_{t,0}}) \right] \qquad (4.8)$$

where Θ – is volumetric water content [%]
Θ_0 – is the volumetric water content of the inflection point [%]
$h_{t,0}$ – is the soil matrix potential corresponding to Θ_0 [cm]
p – is the parameter similar to parameter b in Equation 4.8
b_Θ – defines the slope of the water retention curve at the inflection point (Θ_0, $h_{t,0}$)

Combination of the two relationships, $D=0.3/h$ and $D=C_p d_p$, where D is the mean pore diameter [cm] and h is the corresponding matric potential [cm], C_p is transfer function and d_p is the mean particle diameter [cm], gives a relationship between the matric potential and particle size via the transfer function C_p:

$$h = \frac{0.3}{C_p d_p} \qquad (4.9)$$

The transfer functions to parameterize Eq. (4.9), determined by Jauhiainen (2000) were used in the present study.

The particle-size distributions of the four soil samples used in this experiment conducted with Wind's evaporation method were determined in the laboratory. The results shown in Table 4.1. prove the experimental results in Figure (4.4) that the two upper layers and the two lower layers have a similar texture where lighter topsoil (smaller angle of inclination) is lying on subsoil containing more clay (larger angle of inclination). These particle-size distributions were used to estimate the parameters of Andersson's equation (4.8) accounting to the procedure described by Jauhiainen (2000). For estimation of the van Genuchten parameters K_{sat} was set to the value of 20 cm d^{-1} which was taken from the drainage design papers for the field where these soil samples were collected.

Table 4.5. Measured (bulk density, Θ_{sat}) and estimated parameters of the van Genuchten equations for four soil samples fitted with Andersson's *pF*-curve.

Site/ Layer cm	Bulk density g cm^{-3}	Θ_{res} cm^3 cm^{-3}	Θ_{sat} cm^3 cm^{-3}	K_{sat} cm d^{-1}	α cm^{-1}	n -	λ -
Mid 12-20cm	1.37	0.04	0.450	20	0.0228	1.871	0.5
Mid 38-46 cm	1.65	0.04	0.361	20	0.0230	1.649	0.5
Mid 52-60 cm	1.73	0.04	0.362	20	0.0197	1.754	0.5
Mid 70-78 cm	1.80	0.04	0.36	20	0.0212	1.750	0.5

4.5 Comparison of different methods

Comparison of the experimental Θ-h-data points and the following water retention curves estimated with Wind's and Andersson's methods revealed that these two methods resulted in significantly different water retention curves (Fig. 4.6). In fact, Andersson's method yielded more 'expected' results, i.e. sand-type water retention curves with a larger angle of inclination near saturated conditions following the plateau-type part of the curve and a larger inclination angle in the third part of the curve. The experimental results obtained with Wind's method were more typical of heavy soils rather than for light soils. This difference can be partly explained with the hysteretic phenomena, because the evaporation method measures the ultimate drying curve. However, it should be mentioned that Andersson's estimation procedure involved parameters which were estimated from the dataset of Finnish forest soils (Jauhiainen 2000).

An important disadvantage of Wind's evaporation experiment was that soil tension increased very quickly compared with soil moisture change even though the rate of evaporation was reasonable (2-4 mm d^{-1}), as it was described in Section 4.4.2. Thus, the measured soil moisture range is relatively narrow, particularly in case of subsoil samples. The influence of Wind's and Andersson's-based water retention curves and hydraulic conductivity functions on the water balance of the field experiment is shown in Chapter 6. It is concluded that Wind's evaporation method alone may be incapable of describing the soil hydraulic functions due to the character of the method, and, therefore, additional methods describing also wetting curves as use of tension infiltrometers would be desirable.

4.6 Results and conclusions

Soil hydraulic functions for the four soil samples taken from the same soil profile were estimated with two different methods: a) Wind's evaporation method and b) Andersson's method (water retention only). Both methods were reviewed and discussed. The comparison of these methods revealed considerable discrepancies which can be partly explained by the character of these methods. Wind's method yielded a rather smooth curve for q(h) and a scattered cloud for K(h). The shape of the water retention curves were unexpectedly of a 'clay'-type, although the fraction of clay in the samples was small. Andersson's method resulted in 'loamy soil'-type curves. The results of both methods were expressed in the analytical closed-form equations of van Genuchten. It was concluded that parameterization of the van Genuchten equations depends not only on the measured or estimated h-Θ-K dataset but also on the choice of the fitting procedure. The advantages and disadvantages of the van Genuchten equations were discussed. It was found that K_{sat} extrapolated from the van Genuchten analytical $K(h)$-equation might overestimate the 'true' value of K_{sat} due to the analytical ambiguity of the van Genuchten equation in near-saturation conditions.

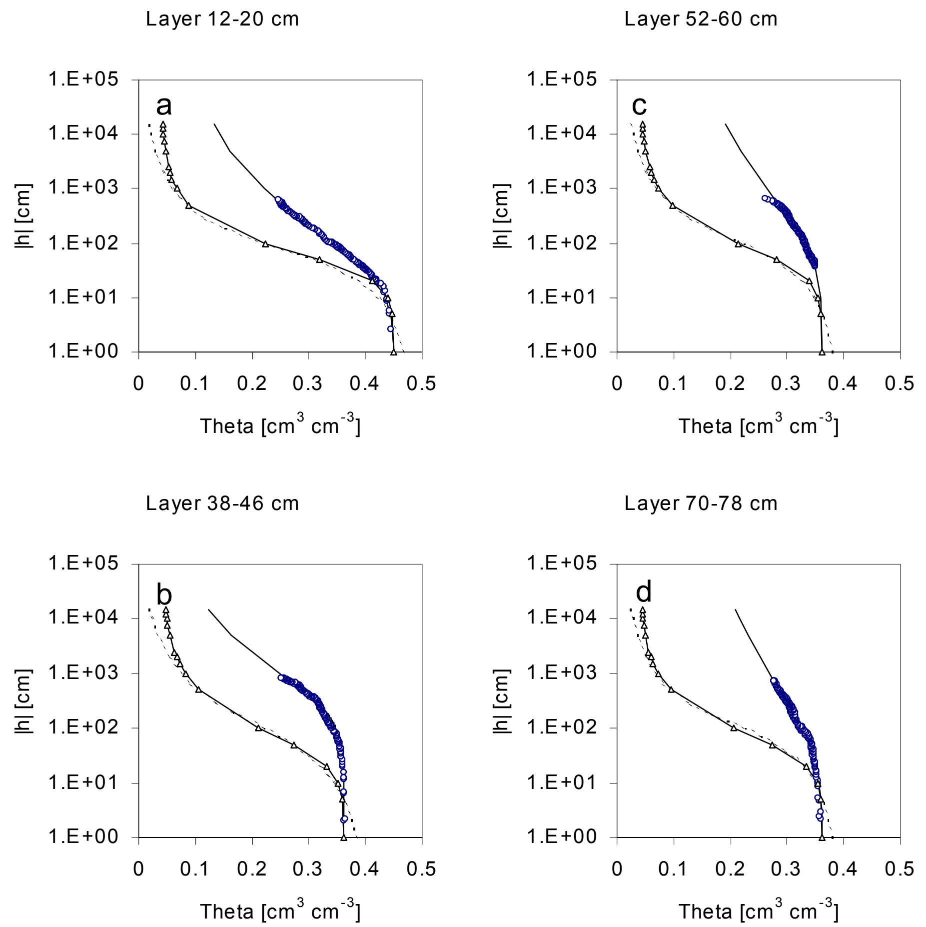

Figure 4.6. Comparison of water retention curves for four soil layers at Reola Mid-site found with Wind's evaporation method (circles – experimental points, line – fitted $\Theta(h)$-curve) and with Andersson's method (dashed line – Andersson's curve, triangles – subsequent van Genuchten curve).

Chapter 5

LOWER BOUNDARY: Case study of controlled drainage experiment

5.1 Introduction

The lower boundary of the soil profile is simpler compared with the upper one. The main process is the outflow or inflow of water, coupled with technical measures (e.g. drainage, subirrigation) and their influence on this process. In humid climate conditions like in Estonia or Finland shallow groundwater is prevailing - groundwater is fluctuating in the upper 1-2 m layer during most of the year. It is closer to soil surface in early spring after melting of snow and in the fall after heavy rainstorms, and it is deeper during the growing season when evapotranspiration usually exceeds precipitation. However, variation of precipitation in different years and within one year will greatly influence the yearly pattern of the groundwater table (see long-term time series in Fig. 7.7). In agriculture, water logging is harmful if the root zone is wetted to the extent where lack of oxygen ceases plant growth, or when trafficability of the field is poor preventing sowing or crop harvest and increasing the hazard of soil compaction. Moreover, wet soil warms up much more slowly than dry soil due to the high specific heat of water compared with the clay minerals (see Section 2.5 Table 2.9). Thus, in the lower boundary the key interest is to lower the groundwater table to the depth that allows field works and creates favourable conditions for plant growth. For this purpose open or sub-surface drainage has been widely used in Estonia.

In Estonia, more than 730 thousand hectares of agricultural land have been drained mostly during the 60's, 70's and 80's. Mainly subsurface drainage was constructed on a total of 650 thousand hectares, while open drainage was applied only 80 thousand hectares (Sustainable water management… 1998). Subsurface drainage systems were preferred due to smaller loss of arable land, lower maintenance expenses and a decreased risk of contamination of surface water. The peak of the drainage works was in the early 70's when approximately 40 thousand hectares of new drainage systems were constructed annually. Almost none of the drainage systems in Estonia have been built with the purpose to manage the water table, e.g. allowing sub-irrigation or control of the ground water level. Only around 9000 hectares of polder areas are provided with dual water control. Unfortunately, in the years of economic decline at the beginning of the 90's majority of these systems became useless.

Field drainage has many important environmental aspects, as it increases water removal and, therefore, increases nutrient and pesticide leaching from agricultural fields (Evans et al. 1989, Stamm 1997). Fertilizers, well dissolved in water, are washed out of topsoil by downward flux into subsoil from where they are discharged into open bodies of water via natural or artificial drainage. The consequence is the eutrophication of rivers, lakes and seas. Nitrogen is by far the most mobile of all the nutrients and subject to the greatest loss from the soil-plant system (Stevenson 1986). In early spring and in the fall when vegetation is absent or in the summer in the case of extreme rainfall the leaching of nitrates may be very intensive (Tamm 2001a, 2001b). Scholefield et al. (1993) found from experiments with and without drainage that drainage volume determined the proportion of leachable nitrogen that remained in the soil after the drainage period. The same was reported by Wesström et al. (2001), who claimed that total reduction in nitrate losses with controlled drainage corresponded to reduced outflow rates.

In certain conditions there occurs denitrification process and gaseous nitrogen compounds are released into the atmosphere, which reduces the amount of nitrate nitrogen ready to discharge from the field. If free oxygen is absent and there is enough carbon, denitrifying bacteria may reduce nitrates and gaseous nitrogen is released. For example, Kalita and Kanvar (1993) observed reduction of NO_3-N concentration at a shallow water table depth, caused by denitrification. Thus, water table management has a dual impact on decreased nitrogen load: a) it substantially reduces the runoff volume (Skaggs and Gilliam 1981, Lalonde et al. 1996, Wesström et al. 2001) and, b) enhances denitrification due to longer time for chemical reactions, poor oxygenation and large content of carbon (Kalita and Kanvar 1993, Kliewer and Gilliam 1995, Kaluli et al. 1999). Klein and Logtestijn (1996) found from laboratory experiments that denitrification rates were very low when soil water-filled porosity decreased below a threshold value equal to field capacity. Stevenson (1986) proposed about two-thirds of field capacity as the corresponding threshold value. On the other hand, Smith and Evans (1998) irrigated agricultural field with swine manure and reported that excessively wet field conditions were prohibitive to nitrification and caused movement of ammonium into groundwater. It can be concluded that bio-chemical reactions in the N-cycle are complicated and that water regime plays an important role.

The concept of controlled drainage makes it possible to vary drainage intensity and thus influence soil moisture regime depending on the interest of farmers (e.g. increasing trafficability for the field works or conserving water supply in the soil). Secondly, it allows to control the amount of outflow from the drainage system and thereby the amount of soluble nutrient losses. Controlled drainage fits better with environmentally sustainable agriculture, as it increases productivity at same time (e.g. Abdirashid 1998, Meija et al. 2000) and reduces plant nutrient leaching (e.g. Wright et al. 1992, Kalita and Kanwar 1993, Lalonde et al. 1996, Brown 1998). Therefore, in certain soil and landscape conditions conventional drainage systems can be improved by applying water table control structures on main drains or ditches. However, even though the denitrification may reduce the contamination of ground and surface water, it represents an economic loss of an essential plant nutrient, and gaseous nitrogen compounds, particularly N_2O, considered as a greenhouse gas, absorb infrared radiation emitted by the Earth's surface and cause the destruction of the stratospheric ozone layer (IPCC 1990, Loaiciga et al. 1996, Roostalu et al. 1996). Thus, the trade-off between increased emissions of greenhouse gases and improved water quality should be achieved.

Controlled drainage experiments in conditions similar to the Estonian climatic and soil conditions have been carried out in Finland (Paasonen-Kivekäs et al. 1996a, 1996b, 1998, 2000) and in Sweden (Wesström et al. 2001). The aim of the present experiment was to investigate the effect of controlled drainage on soil moisture regime as well as on the nitrogen balance in a loamy soil in Estonian conditions. The results concerning the nitrogen balance have been published separately (Timmusk 1996) and were not included in the present analysis.

5.2 Description of the field experiment

5.2.1 Site

A field study was established in 1995 near the Reola village (58⁰18'N, 26⁰34'E), located in South Estonia, about 11 km south of Tartu (Fig. 1.2). The experimental field was drained and bounded from one side with the main ditch of drainage systems discharging into the Porijõgi River. The dynamics of nutrient runoff of the Porijõgi River catchment has been studied in a different study (Mander et al. 2000). One reason why that field was selected was that the Tartu Meteorological Station was located only 2 km away from the experimental field. Meteorological data, except for precipitation, obtained from this station were used in water balance analysis. Before the experiment started the selected field has been used for 5 years as cultural grassland and had been harvested 2-3 times per year. The soil type was sandy loam on loam. Fertilizers, mineral or manure, had not been applied during recent last years. At present, the field belongs to a local farmer.

The experimental field consists of several drainage systems discharging into a main ditch. One drainage system was selected for the current study. In fact, in 1995 a preliminary study was carried out with two drainage systems where the upstream system was dammed up and the downstream system was not. It was necessary to change the experiment layout for the following years, because the difference in groundwater table depth between the treatments was too small to draw up any relevant conclusions. Therefore, data from 1995 were not analysed together with the results for 1996 and 1997.

In 1996 it was decided to use the natural slope of the ground of 5.5‰ to achieve considerably different groundwater depths and hence different soil moisture conditions in various parts of the field. The same idea was implemented, for example, by Kalita and Kanwar (1993). Three subplots were selected perpendicular to the ditch (Fig. 5.1). The first one, close to the main ditch, represents the conditions occurring in the case of controlled drainage (ground level 68.60 m). As the phreatic surface is much closer to the ground level the subplot was called 'Wet'. It should be mentioned that the forest growing on the other side of the ditch might slightly influence the evaporation regime diminishing it compared with the other plots located at a larger distance from the ditch. The next sub-plot, where the effect of inflow from the ditch was weker (ground level 69.10m), was called 'Mid', and the third one without any considerable influence of the controlled water table (ground level 69.5m) was called 'Dry'. As it is seen from Fig. (5.1) the Wet-plot was shifted close to the regulator instead of placing it at the same line with the Mid and Dry-plots. It was decided to additionally use the advantage of the 0.2 m decline of ground level towards the regulator, to obtain bigger differences in the ground water tables of the three study plots.

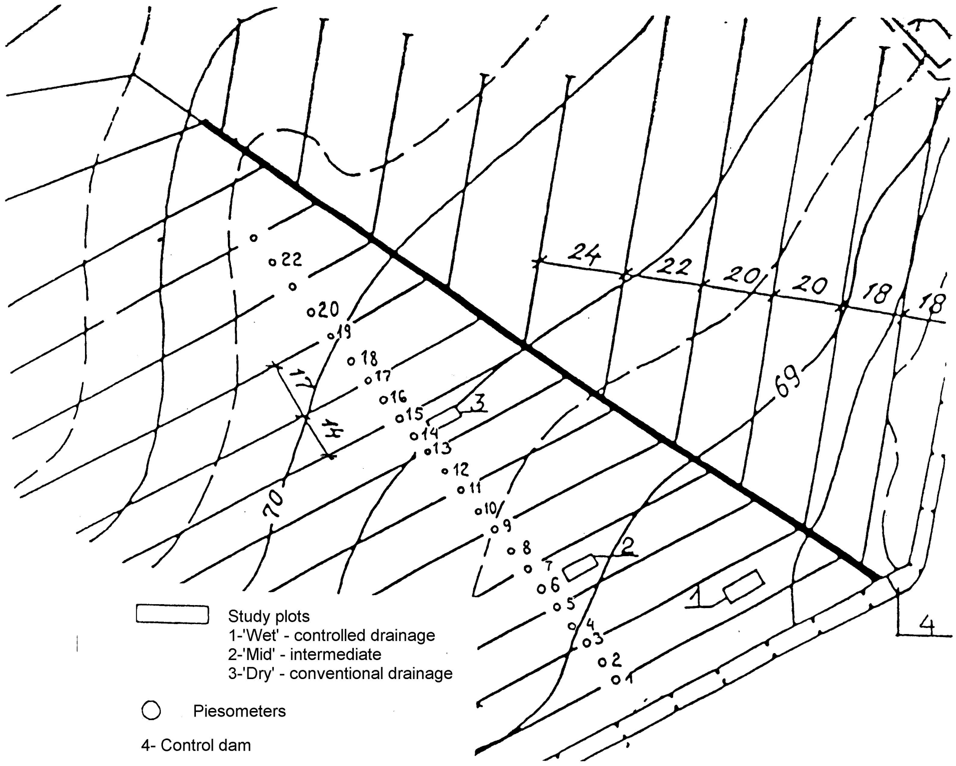

Figure 5.1. Scheme of the experimental field at Reola.

Figure 5.2. Water table regulator on the main ditch.

5.2.2 Drainage design and control weir

The drainage system was built in the mid 70's of clay pipes with a spacing of 14-24 m and average depth of 1.1m. The design of the drainage system in the Reola experimental field was based on the technical norms that consider soil classification both on texture and moisture regime. The design criterion for the drainage system in Estonia is determined as the time (in days) during which the groundwater table has to be lowered, e.g. from soil surface to ploughing depth or from 0.5 m to optimal depth.

The estimated saturated hydraulic conductivity of the drainage design, based on the soil map, was approximately 0.2 m d^{-1}. Tile drains with diameter of 50 mm and length of 30 cm were laid by hand in the drain trench with a design depth of 1.1 m below the soil surface. Drainage pipes were made from burned clay. Water enters the drain through the gap between neighbouring tiles. The collector drains had a larger diameter, 75-100 mm.

The average yearly precipitation at the Tartu Meteorological Station is about 640 mm. Estimated yearly actual evapotranspiration for arable land is about 400 mm. Thus, about 240 mm of water is removed via surface or subsurface runoff. The specific discharge is around 7.61 l s^{-1} km^{-2} (Sustainable water management 1998).

Instead of conventional drainage where drainage runoff depends on hydraulic gradient and the properties of the soil and drainage system, groundwater table management involves regulating devices to control water level (*controlled drainage*) and facilities to supply additional water (*subirrigation*). The water level in ditches may be controlled by adjustable weirs (e.g. Bierkens et al. 1999) and, in subsurface drainage systems, by special control structures (e.g. Lalonde et al. 1996, Wesström 2001) constructed directly on collector drains or drain outlets.

In the present study a very simple and low-cost solution was selected. For a controlled drainage a control weir was built on the ditch. It was made of wooden planks sealed with a plastic sheet at flooded side and reinforced with wooden beams (Fig. 5.2). The sheet was dug into the streambed around 2 m upstream. This kind of simple construction could be practical and very cheap to construct by farmers themselves. One problem might be a seepage barrier, which has to be fixed very carefully to avoid fluxes from the sides and from ditch bottom.

5.2.3 Soil profile

The soil is classified as light pseudopodzolic soil (FAO/ISRIC – Planosol) (Reintam 1995), which is one of the typical soils in South-Estonia. In general, it consists of a homogeneous sandy loam soil profile or a sandy loam topsoil lying on loamy subsoil (Table 5.1). However as soil formation in South-Estonia has historically a glacial character, the whole experimental field is not spatially homogeneous, e.g. the presence of thin loamy sand at the intermediate layer at the Dry-plot. On the other hand, particle size distribution did not reveal large heterogeneity except for the already mentioned loamy sand layer. All other layers, although differently termed, lay relatively close to each other within the soil texture triangle. A detailed soil profile description for the Mid-plot is given in Table 5.2.

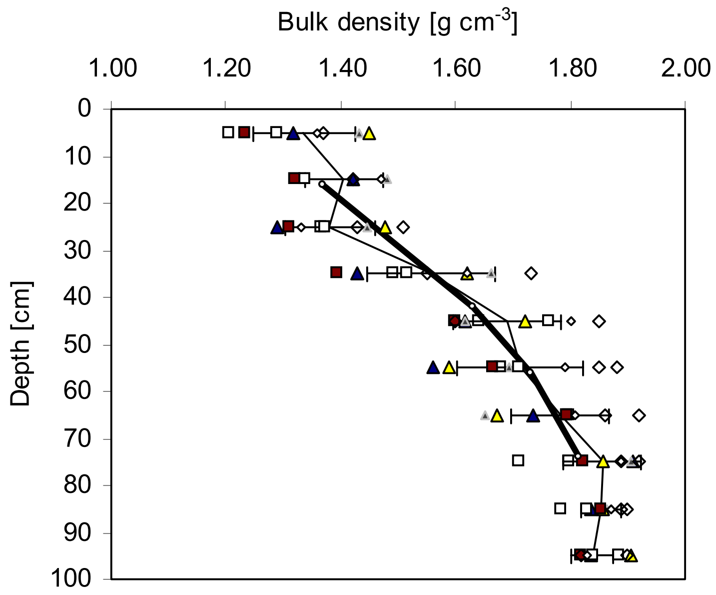

Figure 5.3. Bulk density of different soil layers at the Reola experimental field. Triangles – Dry-plot, diamonds – Mid-plot, squares – Wet-plot, thin line with whiskers – average bulk density with ±standard deviation, thick line – bulk density measured from soil samples used in evaporation method.

Bulk density was measured for every 10 cm layer on all study plots by soil core sampler cylinders with a volume of 50 cm^3 and for the Mid-plot also with a large cylinder used in Wind's evaporation method (volume of 666.5 cm^3). Figure (5.3) reveals the natural variability of bulk density within the experimental field and within a single plot. This variability for topsoil is partly caused by root and worm channels and for subsoil, by the moraine. For subsoil, bulk density reaches the values of 1.8 g cm^{-3} and higher because of the presence of small pieces of moraine.

Table 5.1. Texture classes and corresponding soil types of the Reola experimental field.

Sample	Plot	Layer	Sand % (0.05-2.00mm)	Silt % (0.002-0.05mm)	Clay % (<0.002mm)	Type
1	Wet	0-30 cm	65.8	31.1	3.1	Sandy loam
2	Wet	30-50 cm	63	30.4	6.6	Sandy loam
3	Wet	50-100 cm	57	30.3	12.7	Sandy loam
4	Mid	0-30 cm	66.7	31.1	2.2	Sandy loam
5	Mid	30-50 cm	57.2	31.5	11.3	Sandy loam
6	Mid	50-70 cm	49.6	32.9	17.5	Loam
7	Mid	70-100 cm	45.2	37.4	17.4	Loam
8	Dry	0-30 cm	56.1	41.1	2.8	Sandy loam
9	Dry	30-50 cm	57.4	41	1.6	Sandy loam
10	Dry	50-70 cm	86.7	11.5	1.8	Loamy sand
11	Dry	70-100 cm	62.8	30.6	6.6	Sandy loam

Table 5.2. Detailed description of the soil profile of the Mid-plot.

Layer	Description
A 0-27 (32)	Dark grey, humus content 2%, pH 5-5.5, rough border between following layer
Elg 27 (32) - 45 (80)	In lower part iron ocer, pH 5.5
Btg 45 (80)-95	With blue-grey spots and iron spots, pH 6.0, incl. moraine
C2g 95+	Reddish brown, incl. moraine

5.2.4 Field and laboratory measurement methods

Soil water conditions can vary considerably during the growing season. To follow changes in soil moisture three measurement techniques were used (Fig. 5.4): 1) direct sampling, taking soil samples for obtaining gravimetric soil moisture, 2) indirect sampling, with nylon blocks for measuring electrical resistance, 3) measuring soil tension with tensiometers. Groundwater tubes and piezometers were used to measure fluctuation in the groundwater table. Successful implementation of any of the techniques requires careful installation, operation, and maintenance.

The measurement interval for nylon blocks, tensiometers and the groundwater table was around 5 days. Gravimetric soil samples were taken six times in 1996 (May 7, June 10, July 5, August 8, September 5, October 2), and six times in 1997 (May 8, June 9, June 20, July 21, September 5, October 15).

Gravimetric soil moisture content

Soil sampling is the only direct method for measuring soil water content. When carried out carefully with a sufficient number of samples it is one of the most accurate methods and is often used for calibration of other indirect techniques. Samples were taken with a 1 m soil probe for every 10 cm layer separately from all the three sub-plots. The augering points were located along a line between the drains with a distance of about 1 m between four replicates. Soil samples were stored in the metal water-vapor-proof sample collection cans. In the laboratory, wet soil samples were weighed and opened cans were dried in the oven at temperature of 105°C at least for 24 hours and/or until the weight did not change, and were then weighed for obtaining dry weight. The accuracy of the electronic balance was ±0.01g. The water content on a volumetric basis was converted from gravimetric soil moisture by multiplying by the average soil bulk density.

Tensiometers

Soil water tension or soil water pressure head are the terms describing the energy status of soil water. Soil water pressure head is a measure of the amount of energy with which water is retained in the soil. In the present study jet-fill tensiometers (Soil Moisture Corp.) were used to measure soil tension. One pair of tensiometers was installed into each of three sub-plots at depths of 25 cm and 55 cm. The benefit of jet-fill tensiometers is that they are made from transparent plastic and water can be added when it is necessary, the feature which prolongs the working period of jet-fill tensiometers compared with standard closed-tube systems.

Tensiometers were working well in 1996, however in the following year almost all vacuum gauges of tensiometers were unstable, and therefore the respective data were not included in the current report. The problem of instability was not solved.

Nylon blocs

The most common type of electrical resistance blocks are gypsum blocks, which were compared with nylon blocks in a preliminary study in 1994 (Tamm 1994). According to that study nylon blocks yielded better operational and maintenance results than gypsum blocks and, therefore, were selected for the present study. In the preliminary study gypsum blocks were dissolved after one winter period.

In the present study 10 nylon blocks (type AM-11, *made in* Latvia, Figure 5.5) were installed on each of the three study plots in the middle of every 10 cm interval (i.e. at depth of 5 cm, 15 cm, etc.) up to 1 m depth. The readings of nylon blocks were taken at 8 o'clock p.m. with a gypsum block meter (Eijkelkamp Corp.) that showed readings between 0 and 100, indicating dry and wet, respectively. No corrections were made to account for the temperature effect on resistance. The disadvantage of nylon blocks is that the readings must be converted to soil moisture after calibration with gravimetric soil moisture and that they are relatively insensitive at low soil tension. Therefore, tensiometers and electrical resistance blocks are often used combined to monitor soil water over a wider range of conditions than either can measure alone.

Groundwater table

In the saturated zone, the groundwater table was measured by means of groundwater tubes and piezometers. A line of groundwater tubes was installed perpendicular to the ditch on the drains and between the drains (Fig. 5.1). A total of 23 groundwater tubes and three piezometers were installed directly in a borehole without filter material. Groundwater tubes were 1.1 m long and were made of PVC material and perforated except for the top 50 cm to prevent the lateral infiltration of water into the tube during the periods when topsoil is saturated. Piezometers were 1.5 m long, made of metal and perforated only at the bottom 10 cm.

Groundwater depth was measured with a thin pipe, which was inserted into the tubes, and pushed air into pipe. When the pipe reached the water level the noise of bubbles was noted. Measurement accuracy was estimated to be about +/- 0.5cm.

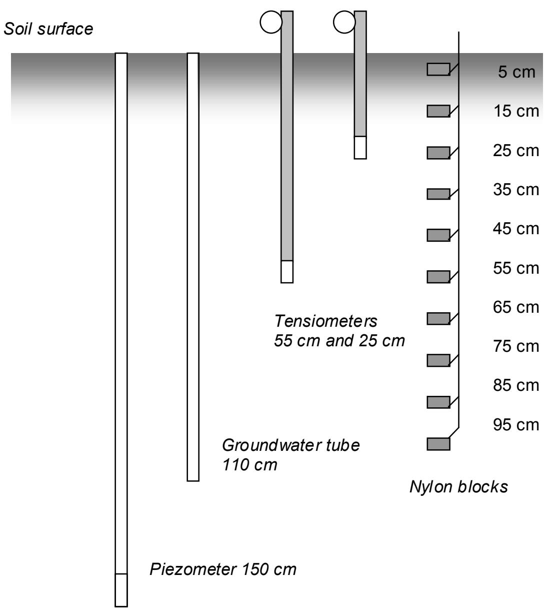

Figure 5.4. Scheme of the study plot on the Reola experimental field.

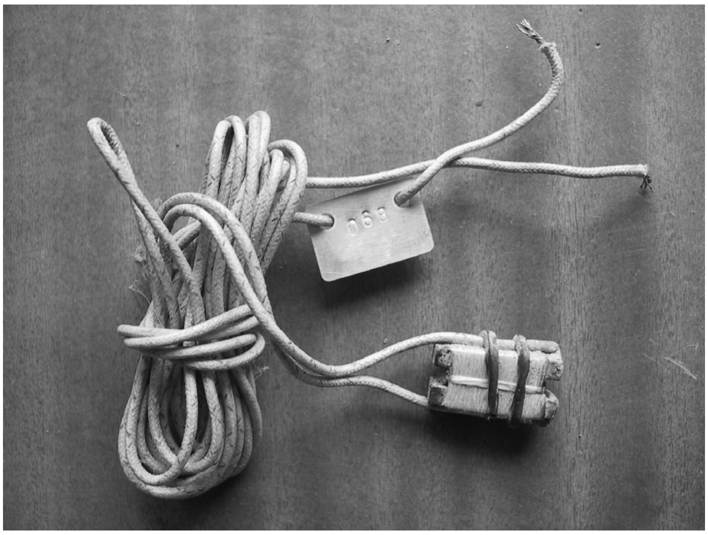

Figure 5.5. Nylon block AM-11.

5.3 Results

5.3.1 Meteorological conditions

Meteorological conditions were measured at the Meteorological Station of Tartu, 2 km from the experimental field. Precipitation *P*, sunshine duration *n*, temperature *T*, moisture deficit *D*, and wind velocity *u* were available on a daily basis. Precipitation was measured also directly at the experimental field with two simple rain gauges with a cross section of 500 cm^2 (GGI-500). The rain gauges were installed at the surface level.

For both years the amount or pattern of precipitation was different from a long-term average. In 1996, the total precipitation for the April-September period of 249 mm was more than 100 mm lower than the average of 374 mm, whereas in 1997, the total precipitation of 359 mm was close to that of a average year. Therefore, 1996 can be classified as a dry year, which could be perfect to achieve the effect of an elevated groundwater table. However, in practice it also revealed that in dry years discharge from the upper watershed might not be sufficient to maintain the desired water level behind the control dam.

In 1996, precipitation was very low in April, only 12 mm, which is approximately one third of the long term average (Fig. 5.6, Table 5.3). Both in May and June, around two thirds of average rainfall was recorded. Fortunately, in July it was slightly wetter than average, but August was extremely dry, actually the driest in this century, with only 12 mm of precipitation, while according to statistical data August is the rainiest month of the year with about 83 mm. Such dryness significantly affected the course of the experiment causing problems with elevating the water table.

In comparison, the spring period in 1997 was moister than the long-term average (Fig. 5.8, Table 5.3) which was more favourable for water table management. Also, June was more wetter than the long-term average, (102 mm and 62 mm, respectively). The following July and August were roughly two times drier than in the average year.

Table 5.3. Meteorological conditions and estimated *ET* in 1996 and 1997.

Month	Average			Sum	
	T	e_a	*u*	*P*	*ET*
	^{0}C	kPa	m s^{-1}	mm	mm
			1996		
April	5.0	0.5	2.9	16	55
May	11.0	0.9	3.4	34	94
June	14.2	1.1	2.8	41	124
July	15.2	1.3	3.2	88	116
August	17.5	1.3	2.2	12	130
September	9.1	0.8	2.6	57	63
Total				249	577
			1997		
April	2.8	0.5	3.0	58	42
May	8.8	0.7	2.6	60	82
June	15.9	1.2	2.1	102	125
July	18.0	1.5	2.0	26	132
August	18.7	1.3	1.9	36	133
September	10.6	1.0	2.8	77	60
Total				359	573

5.3.2 Groundwater table management

Initial conditions and the course of the experiment

In 1996, groundwater table sampling on the Mid-plot was started at the beginning of May and one month later on the other plots, after the piezometers were installed. The control weir was closed on the 26th of May. Due to low inflow from upstream it took almost two weeks to raise the water table in the ditch close to the level of spillway. In the second part of August, inflow ceased and the water table dropped at the ditch.

In 1997 groundwater table sampling was started at the beginning of May and lasted until mid August. The regulator was closed on the 26th of May. Unfortunately, the experiment was terminated because someone had broken the regulator between 10th and 15th of July.

Initial soil moisture conditions were similar in both years (Fig. 5.12a and 5.13a), but in 1997 moister May and June allowed to raise the groundwater table closer to the soil surface compared with 1996. In general, water table management had a significant effect on the groundwater table and a less pronounced effect on the soil moisture conditions in all three study plots.

Groundwater fluctuation measured in deep piezometers

In 1996, the effect of controlled drainage was well investigated in the Wet-plot, 17 m from the ditch, where measured groundwater was around 80 cm below the soil surface during the period when the ditch was dammed up (Fig. 5.7). Lateral inflow into the field stopped further dropping of the groundwater table also in the Mid-plot, 45 m from the ditch. In the Mid-plot the measured groundwater table fluctuated between 120 cm and 90 cm below the soil surface. In the last study plot, the Dry-plot, the piezometer ran empty by the time when the Mid and Wet-plots started to reveal the effect of inflow. Thus, during the period of elevated groundwater the differences in groundwater were approximately 20-40 cm between the Wet-plot and Mid-plot and more than 40 cm between the Mid-plot and Dry-plot.

In 1997, the recorded data revealed that in June and July the average groundwater table was around 60 cm below the soil surface in the Wet-plot, which corresponded approximately to the desired depth (Fig. 5.9). The groundwater table differed around 20 cm between the sub-plots except for the short period from mid June to the beginning of July when both in the Wet and Mid-plots the groundwater table was equally close to the ground. Fortunately, compared with 1996, the groundwater table of the Dry-plot was measurable until mid-August in 1997.

Groundwater fluctuation across the field

Interesting results were received when plotting the measured groundwater table values for the cross-section of the drainage system (Fig. 5.10 and 5.11). In 1996, according to the shape of the measured groundwater table on the 15th of May the drainage system was working only partly, where the 2nd, 3rd and 4th drains were supposed to discharge because the measured water table at midway of these drains was higher than drain depth. As the installation depth of the groundwater tubes and the drainage pipes was equal, it was difficult to determine precisely groundwater level at the depth of the drain bottom, because the lower ends of the groundwater tubes were partly filled (approx. 1-5 cm) with ground and mud. Therefore, when water level was detected in the tube at midway of drains but not in drains then the drains were assumed to discharge and the groundwater table is denoted in figures with a dashed line. In case of adjacent measurements the groundwater table is denoted with a solid line (Fig. 5.10, 5.11).

On the 9th of June the effect of control action is clearly shown as the groundwater table forms a smooth, almost horizontal, line with slight declination towards the field. This declination is even more evident on the 25th of June when the last recorded value of groundwater level in the Mid-plot's piezometer was 18 cm below the water level in the ditch. Between these two dates the recorded precipitation was 32 mm, but for all rainy days, except for the 21st and the 22nd of June (6.0 and 7.2 mm, respectively), potential evapotranspiration by far exceeded rainfall. Thus, the investigated declination of the groundwater table leads to the conclusion that lateral inflow did not compensate for the upward flux of water. During the following sampling period horizontal groundwater level recovered, possibly due to the rainy period at the beginning of July (Fig. 5.10). In August the water table at the ditch decreased and on the 8th of August the water table was measured only in the Mid-plot's piezometer (not shown in Fig 5.10).

At the beginning of May 1997, the drainage was working up to the 9th drain (Fig. 5.11) as the water table was measured in groundwater tubes located between the drain lines, but not in those located along the drain lines. The probable shape of the groundwater table is drawn with a dashed line (Fig. 5.11). On the 15th of May, the first two drains were empty and at least four following drains were working with a low gradient. In case of controlled drainage conditions (on the 20th of June, Figure 5.11) at least the first four drains were submerged, but the following drains were supposed to discharge, as no water table was measured in the groundwater tubes located along the drain lines. The inclination of the groundwater table towards the field was not observed in 1997. However, groundwater level in the Dry-plot's piezometer started to lower already after 20th of June, the Mid-plot's piezometer after 1st of July, and the Wet-plot's piezometer after the regulator was broken (10th-15th of July).

Thus, based on the experimental data of two years it can be concluded that the effect of controlled drainage was well revealed in the Wet-plot, was less significant in the Mid-plot and rather insignificant in the Dry-plot. The main problems involved in that kind of water management measures are: 1) is the lateral hydraulic conductivity sufficient to compensate for withdrawal of water, due to the capillary flux from the water table to the root zone? and 2) is discharge from the upper watershed sufficient to maintain the desired water level behind the control weir?

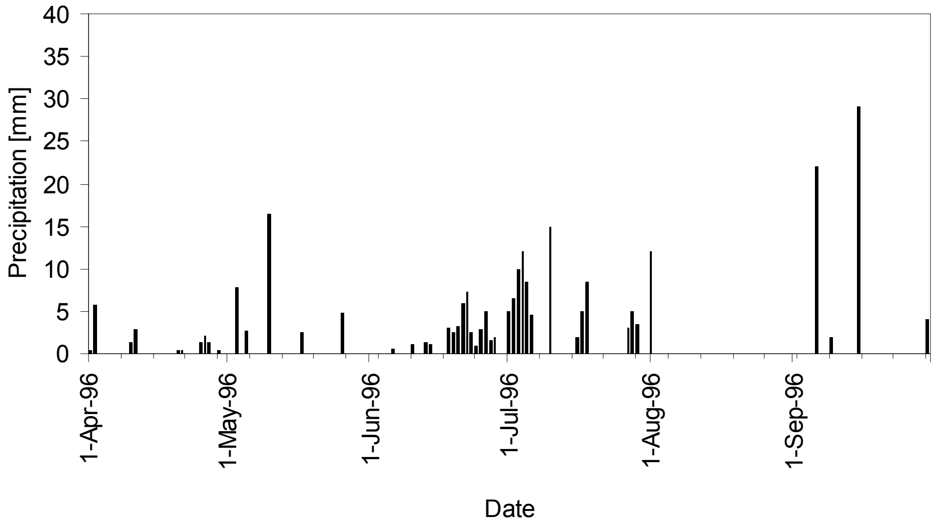

Figure 5.6. Precipitation measured on the Reola experimental field in 1996.

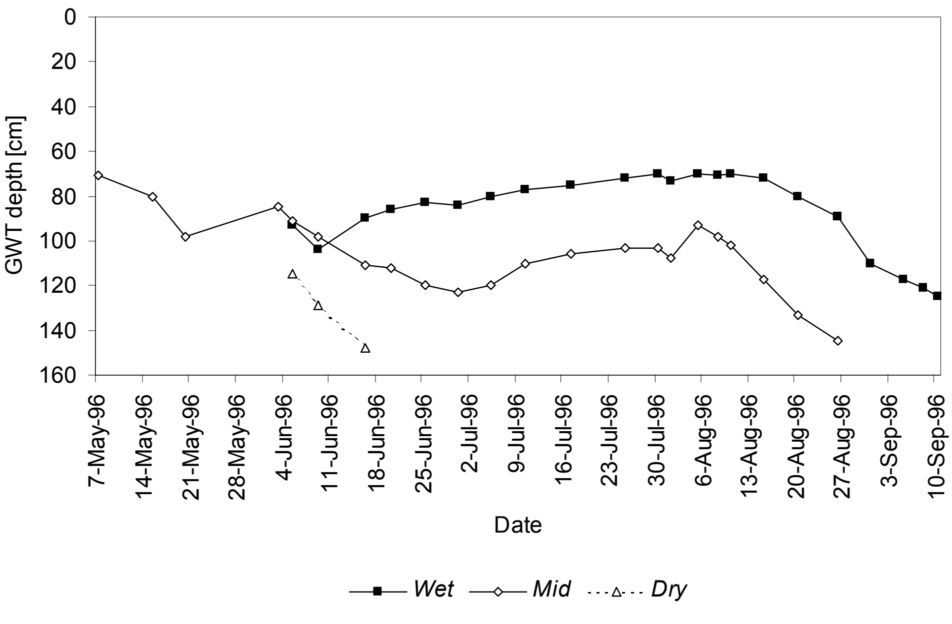

Figure 5.7. Measured water levels in piezometers located below the soil surface in 1996. Triangles denote Dry-plot, diamonds denote Mid-plot and squares denote Wet-plot, respectively.

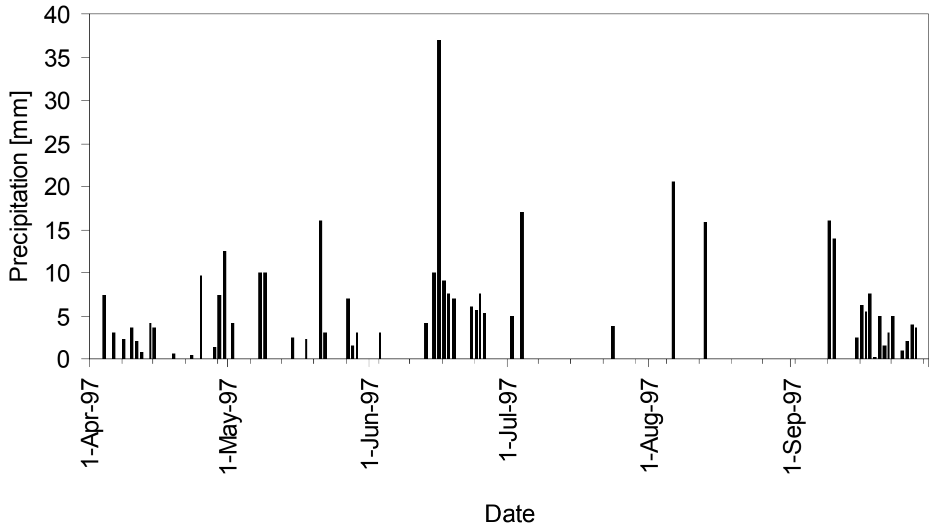

Figure 5.8. Precipitation measured on Reola experimental field in 1997.

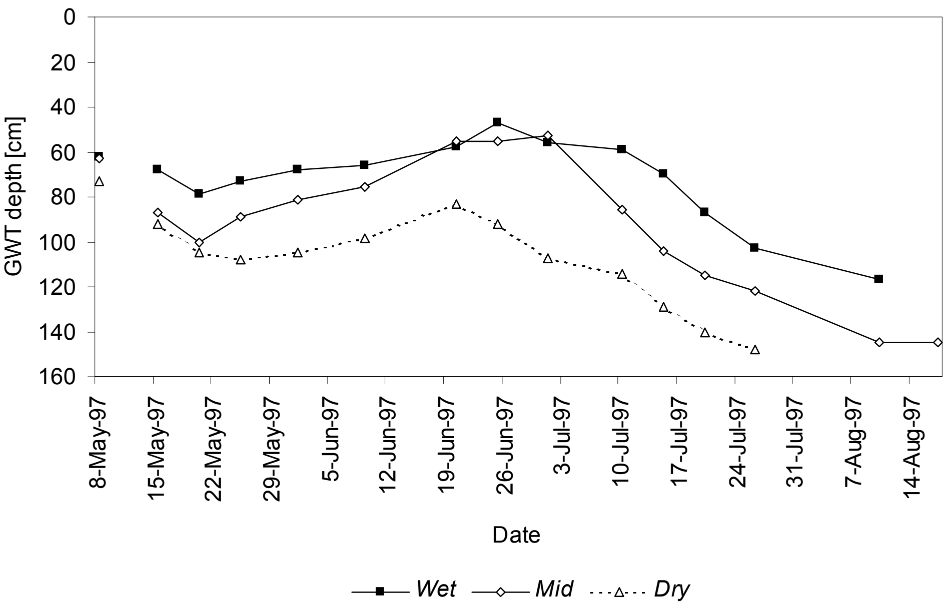

Figure 5.9. Measured water levels in piezometers located below the soil surface in 1997. Triangles denote Dry-plot, diamonds denote Mid-plot and squares denote Wet-plot, respectively.

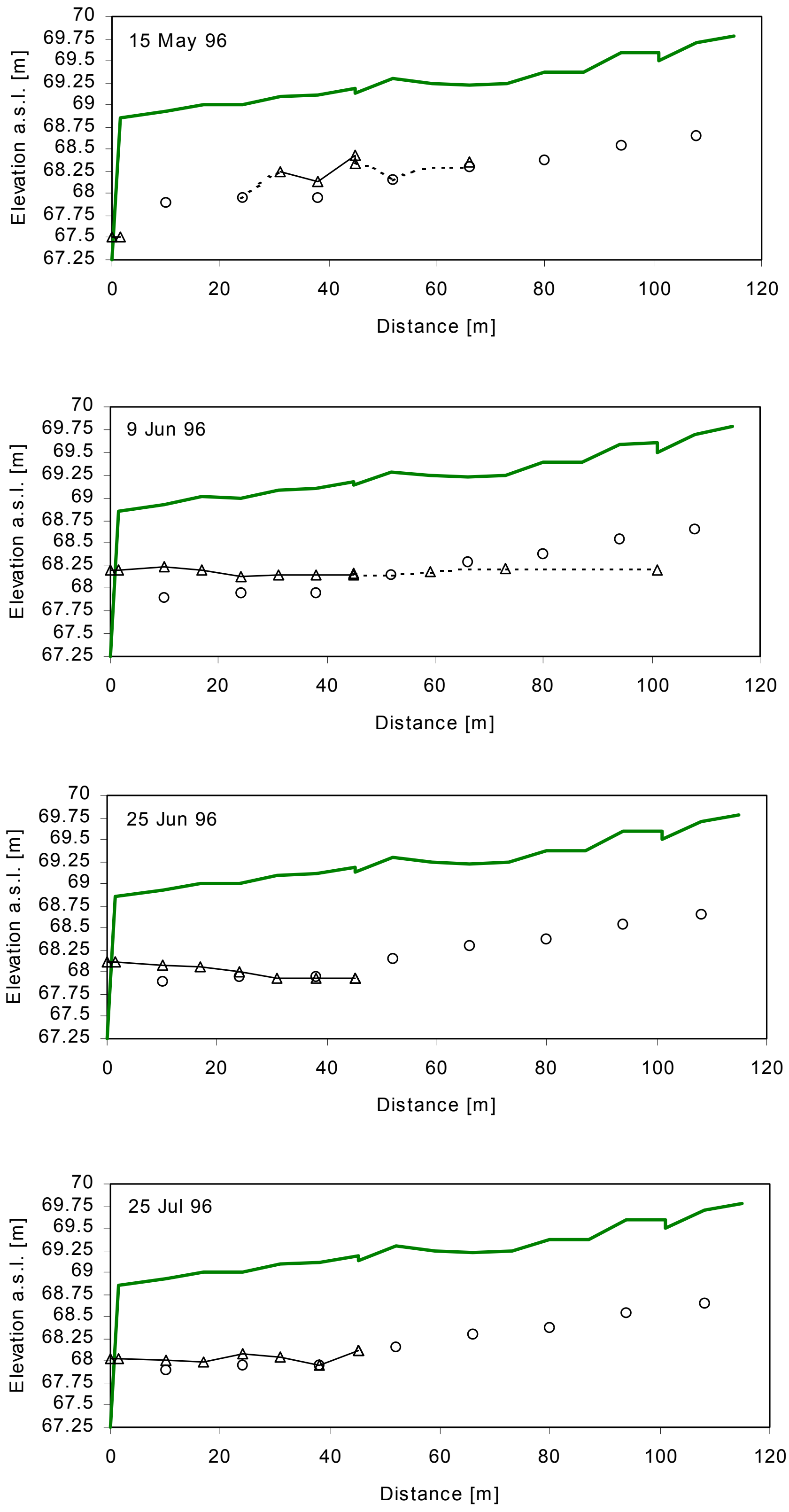

Figure 5.10. Measured groundwater table in 1996. Circles – drainage lines, triangles – water level in groundwater tubes or piezometers, line – groundwater table between the measured values, dashed line – estimated groundwater table.

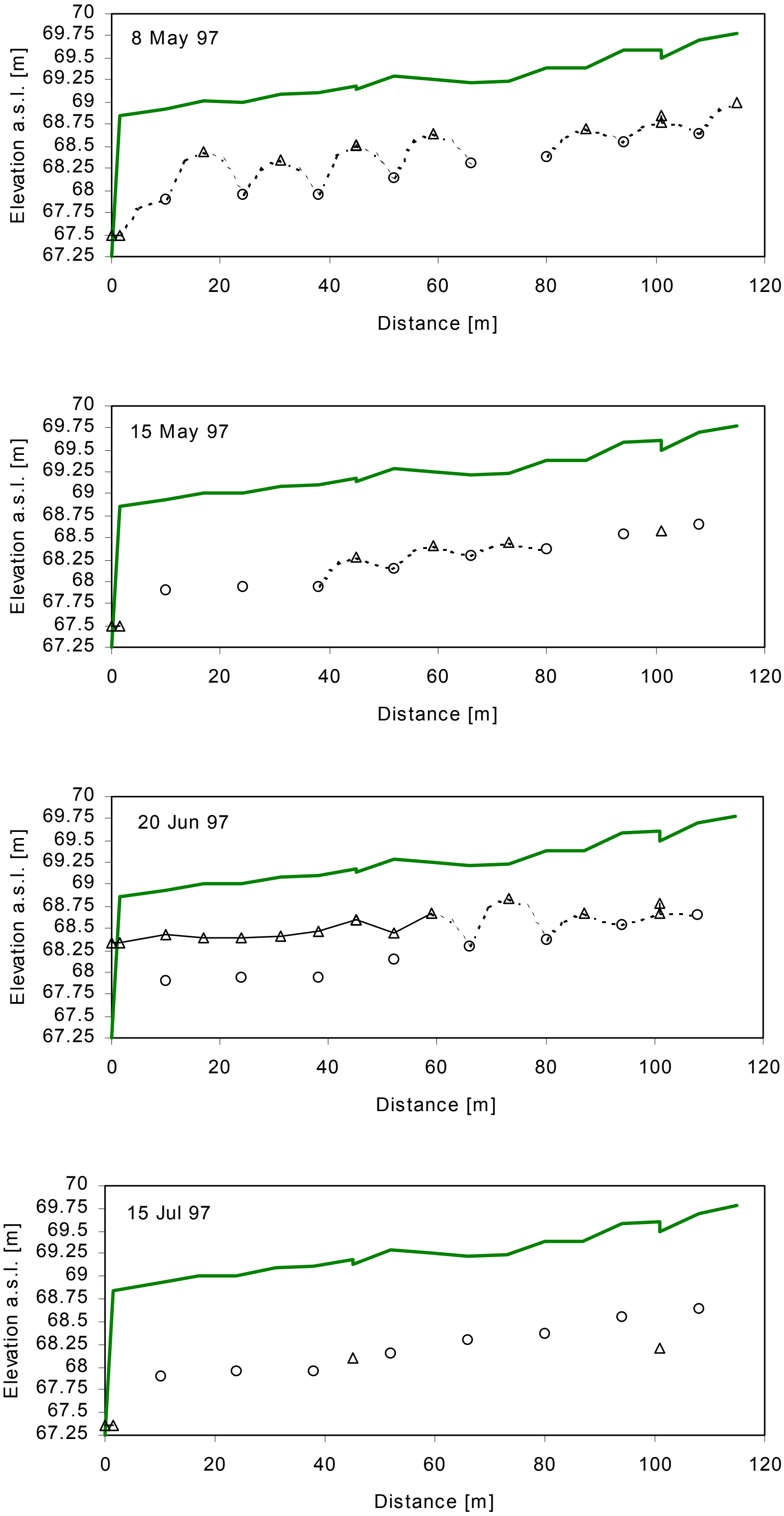

Figure 5.11. Measured groundwater table in 1997. Circles – drainage lines, triangles – water level in groundwater tubes or piezometers, line – groundwater table between the measured values, dashed line – estimated groundwater table.

5.3.3 The effect of water table management on soil moisture regime

According to volumetric soil moisture profiles (Figure 5.12, 5.13) the soil moisture conditions in the Wet-plot were significantly different compared with other sub-plots mainly regarding the higher water content in the upper 50-60 cm zone, not directly depending on the fact whether the groundwater table was elevated or not. It is supposed that the adjacent forest could slightly decrease the rate of evapotranspiration, and the higher initial water content may have been the result of later melting. Secondly, the slightly lower bulk density in the Wet-plot (Figure 5.3) but the same fractional composition as in the other sub-plots (Table 5.1), indicate that the upper zone of the soil profile was probably disturbed when the ditch was dug. In fact, the measured sand-silt-clay percentage was identical at the Wet and Mid-plot (Table 5.1), but the determined bulk density was 1.24 and 1.37 g cm^{-3}, respectively. Thus, the overall conditions in the Wet-plot were assumed to be slightly different than other sub-plots.

In 1996 the initial water content in the 90 cm upper soil layer in the Wet-plot was 317 mm and in the Mid-plot 251 mm, in 1997 the respective values were 329 mm and 262 mm (Fig. 5.14 and 5.15), i.e. the study-plot close to the ditch and forest contained initially 66 mm (67 mm in 1997) more water than the other plots. This difference was generally maintained during the experimental periods in spite of the different course of experiments in both years.

In 1996, between the first and second soil sampling, i.e. on the 8th of May and the 10th of June, total water content decreased, which is in good agreement with the dynamics of the groundwater table (Fig. 5.7). In fact, the water level at the ditch rose already after the 26th of May, when the regulator was closed, but it was not yet reflected by groundwater level measured in the groundwater tubes and piezometers. The following soil sampling events on the 5th of July and the 8th of August coincided with the period when the groundwater tables in the Wet and Mid-plots were rising, which is in good agreement with total water content in both soil profiles (Fig. 5.14). The draught in August caused a low inflow into the ditch, which lowered the water level in the ditch and depleted soil water supply. The wet plot lost 94 mm of water between the sampling events on the 8th of August and the 5th of September, the Mid-plot lost 104 mm and the Dry-plot lost only 71 mm. The rainstorms in September restored total soil water content at all investigated plots close to the value occurring at the beginning of August, as it is seen from the soil sampling results for the 2nd of October. However, groundwater level in the piezometers was not restored yet.

In 1997 the starting conditions where very similar to those of the previous year,.water content being only slightly higher (Fig. 5.15) and the groundwater table being around 10 cm close to the soil surface (Fig. 5.7 and 5.9). During the period between the first and second soil samplings, the 8th of May and the 9th of June, the soil profile in the Wet-plot lost 70 mm of water while the Mid and Dry-plot lost only 36 and 44 mm, respectively. This change was mainly caused by removal of water from the upper zone of the soil profile (Fig. 5.13), as the measured water levels in the piezometers were approximately similar (Fig. 5.9). Between the second and third soil samplings, the 9th and the 20th of June, total water content in the soil profiles increased by 79, 41 and 30 mm in the Wet, Mid and Dry-plots, respectively (Fig. 5.15). At the same time, the water level in the piezometers increased by 8, 20 and 15 cm, respectively. Absolute increase in the groundwater table from a minimum value in May to a maximal value in June in the Wet, Mid and Dry-plots was 37, 47 and 25 cm, respectively.

The second inflection point where the groundwater table started to lower occurred between the third and fourth soil samplings, i.e. between 20th of June and 21st of July. In the Wet-plot this occurred after the regulator was destroyed, and in the plots located further from the ditch, already before that. The following gravimetric soil sampling was carried out on the 5th of September after a long dry period with only two considerable rainfalls (Fig. 5.8) that did not prevent the topsoil from drying near to the wilting point (Fig. 5.13). The last soil sampling in the Mid plot was carried out on the 15th of October, when moisture conditions were almost restored as the measured total water content in the soil profile showed value of 254 mm, which was only 8 mm less than the initial value on the 8th of May.

5.3.4 Complementary measurement techniques – tensiometers and nylon blocks

Tensiometers

Tensiometers (only in 1996) and nylon blocks were complementary techniques used to investigate changes in soil moisture and needed calibration with gravimetric soil water content. Differently from soil sampling, which had four replicates taken randomly along the sampling line, the tensiometers and nylon blocks were measured without replicates. Therefore, in the statistical sense, gravimetric sampling describes changes in soil water status more adequately than other methods. However, for practical convenience it is more appropriate to take readings from a pressure gauge or an analogue-digital device instead of labour-consuming soil sampling, it was considered useful to study the relevance of these techniques.

In general, all tensiometers installed at the same depth showed similar changes in tension on the drying and wetting of soil. Rather fast and uniform drying started at the beginning of August due to the continuous drought (Fig. 5.6 and 5.7) when all tensiometers in topsoil reached the value of air-entry tension (800-900 cm). In case of the Wet-plot, drying was delayed by around 7-10 days. Both tensiometers in the Dry-plot reached the same air-entry value of 780 cm, occurring on the 20th of August in topsoil and on the 5th of September in subsoil. The tensiometers in the Mid and Wet-plots, installed at a depth of 55 cm, registered increased moisture starting from the 5th of September. In fact, on the 4th of September a rainfall of 22 mm was measured.

Measured soil water tension and corresponding soil moisture allows to compare the field-estimated water retention curve with the curves estimated with Wind's and Andersson's methods (Chapter 4). Plotting the tensiometer results on the estimated water retention curves (Fig. 5.18) revealed, that all tensiometer measurements lay between the resulting curves obtained by Wind's evaporation method and Andersson's method. In topsoil three measurements made with the tensiometer installed at 25 cm (Fig. 5.18a) fitted well with Wind's water retention curve and one measurement fitted with with Andersson's-based van Genuchten curve. All other tension values were closer to the results obtained with Andersson's method. The same conclusion is valid also in case with tensiometer installed at a depth of 55 cm (Fig. 5.18b). Unfortunately, there were no tension measurements in 1997 that could add more points for the field-estimated water retention curve.

Taking account the tensiometer results, there were three different methods for estimating the water retention curves, but none of them cannot be treated as faultless. Wind's curve represents the ultimate drying curve; Andersson's method was originally calibrated using Finnish forest soils, and the tensiometer readings represent the spot values that may contain measurement errors due to the effect of temperature or bypass flow (see Buchter et al. 1999).

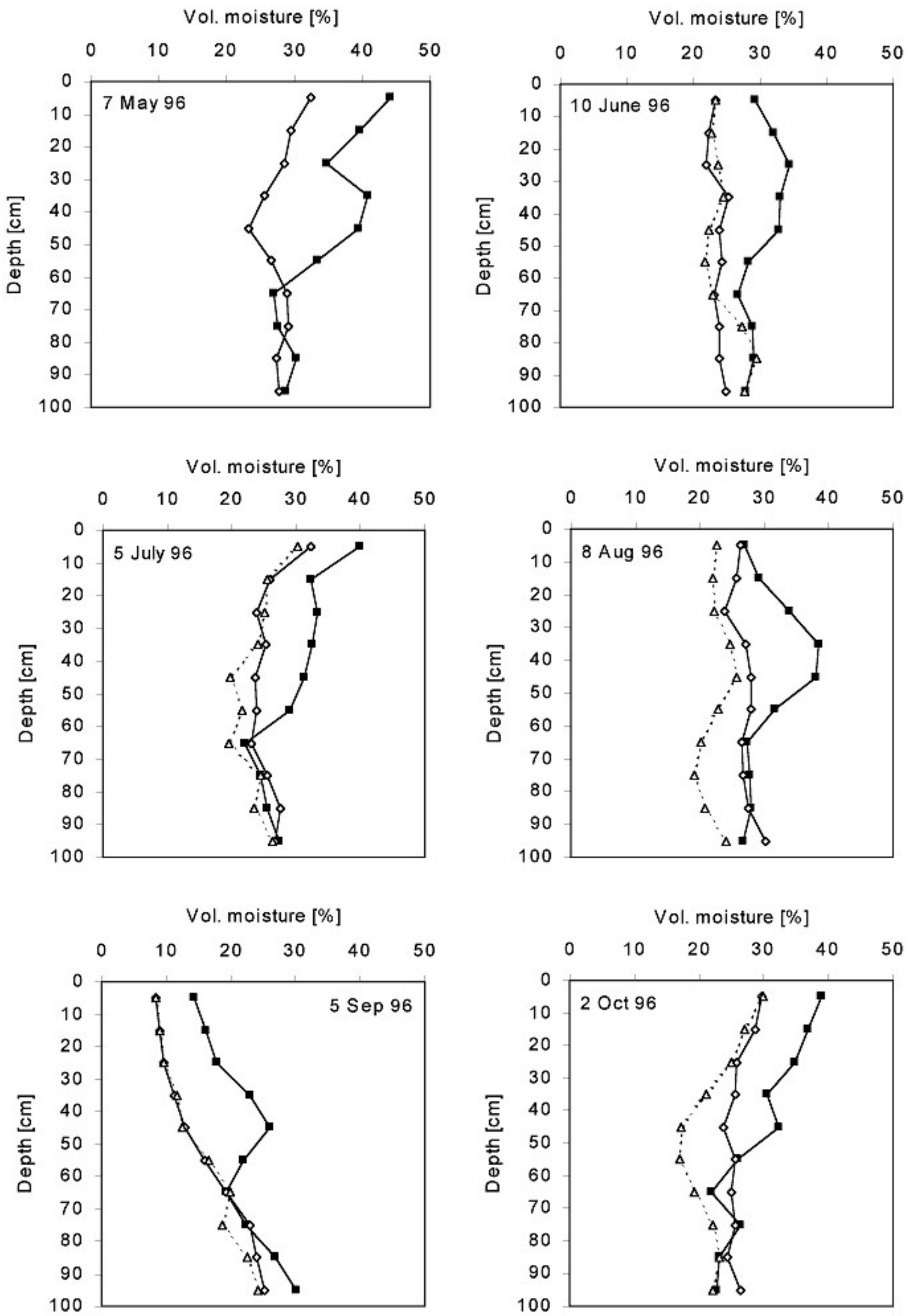

Figure 5.12. The dynamics of volumetric soil moisture in 1996. Triangles denote Dry-plot, diamonds denote Mid-plot and squares denote Wet-plot.

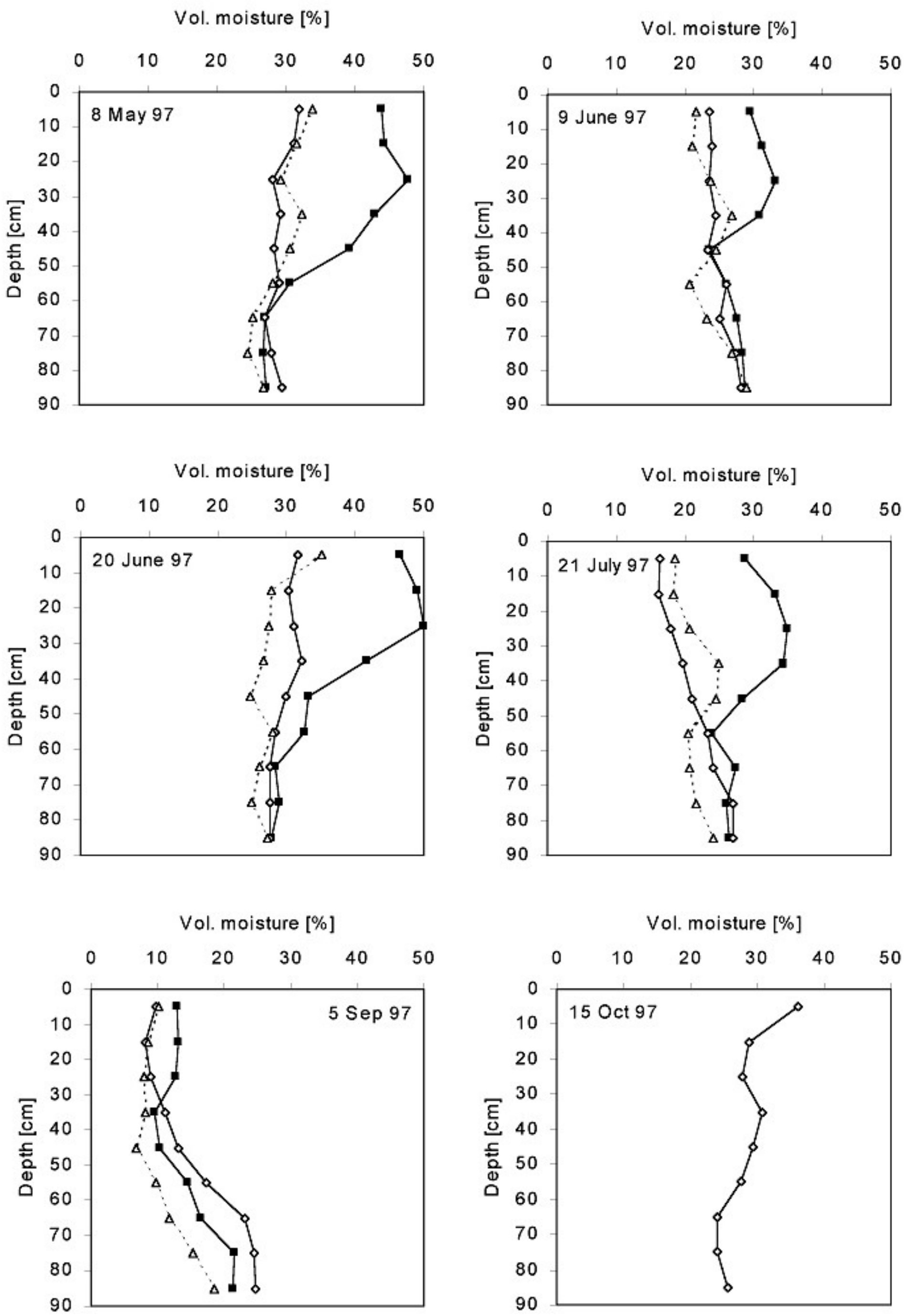

Figure 5.13. The dynamics of volumetric soil moisture in 1997. Triangles denote Dry-plot, diamonds denote Mid-plot and squares denote Wet-plot.

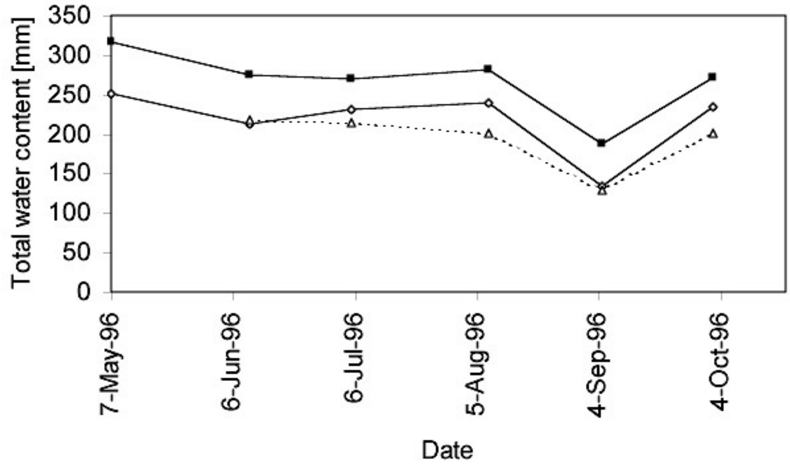

Figure 5.14. Dynamics of total water content in the 90 cm soil profile in 1996. Triangles denote Dry-plot, diamonds denote Mid-plot and squares denote Wet-plot.

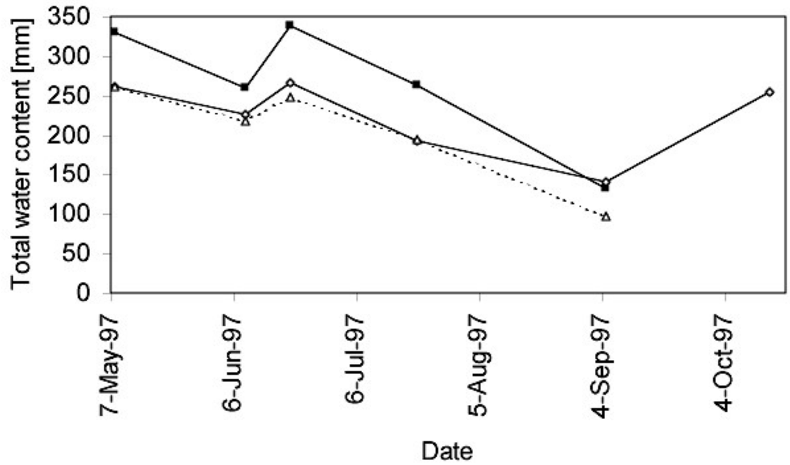

Figure 5.15. Dynamics of total water content in the 90 cm soil profile in 1997. Triangles denote Dry-plot, diamonds denote Mid-plot and squares denote Wet-plot.

Nylon blocks

The correlation between the readings of nylon blocks and soil moisture was analysed assuming the logarithmic relationship, as the manual of nylon blocks describes ($\Theta_{vol}=a\ Ln(c)+b$, where a and b were constants and c was the reading of nylon blocks). Analysis showed that no overall correlation exists for the whole dataset, although the correlation for a single nylon block was high (up to 0.876). For a better comparison with tensiometers only the measurements taken from 25 and 55 cm are shown in Fig. (5.19). A better correlation was obtained for nylon blocks installed in the middle of the 1 m profile. It is assumed that in the case of topsoil the factors affecting the poorer correlation (e.g. r^2 for 5 cm 0.641, 0.812, 0.386) were difficulties with good contact with the soil matrix. In the layers less than 70 cm both the range of moisture changes and that of readings were very narrow and, thus, the measurement error was relatively large. The conclusion is that nylon blocks require individual calibration that reduces their applicability in studies of soil moisture changes.

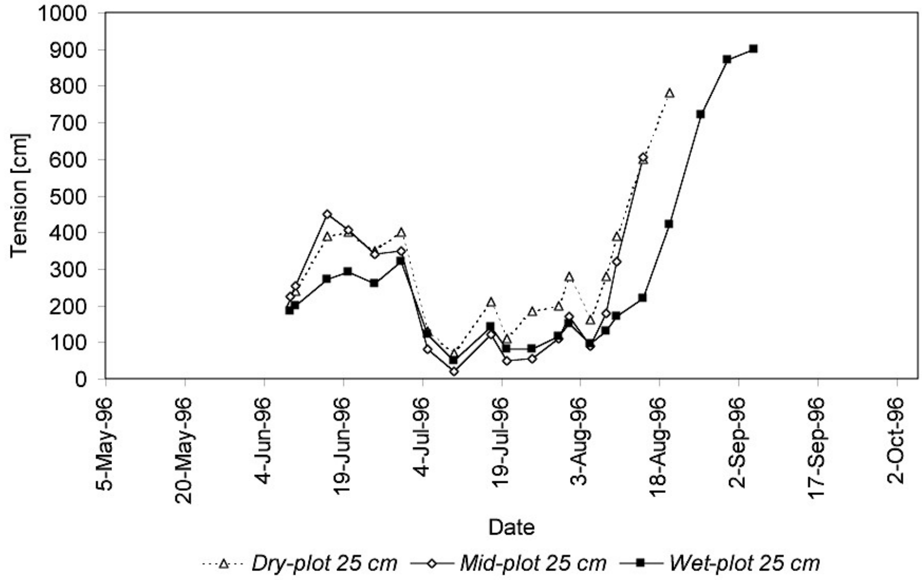

Figure 5.16. Measured soil water tension at a depth of 25 cm in 1996.

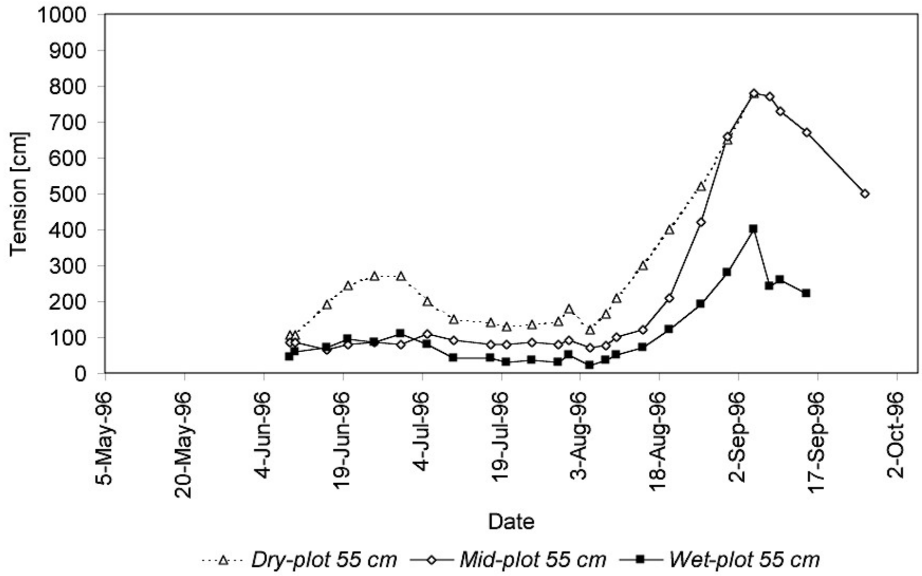

Figure 5.17. Measured soil water tension at a depth of 55 cm in 1996.

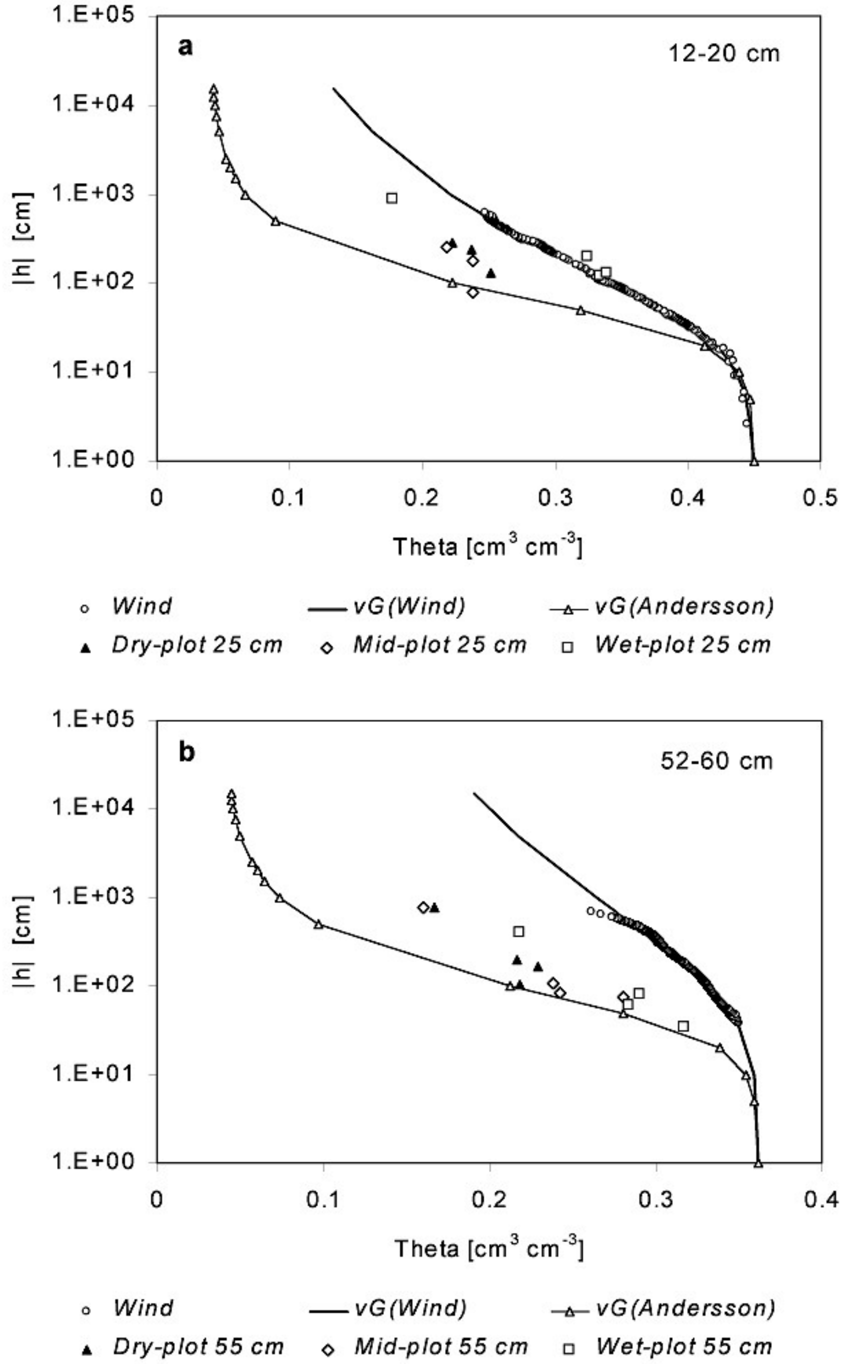

Figure 5.18. Water retention curves estimated with Wind's and Andersson's methods and measured soil water tension at depths a) 25 cm and b) 55 cm. Circles – estimated with Wind's method, line – van Genucten pF-curve estimated with Wind's method, line with triangles - van Genucten pF-curve estimated with Andersson's method, solid triangles – Dry-plot's tensiometer measurements, diamonds – Mid-plot's tensiometer measurements, squares – Wet-plot's tensiometer measurements.

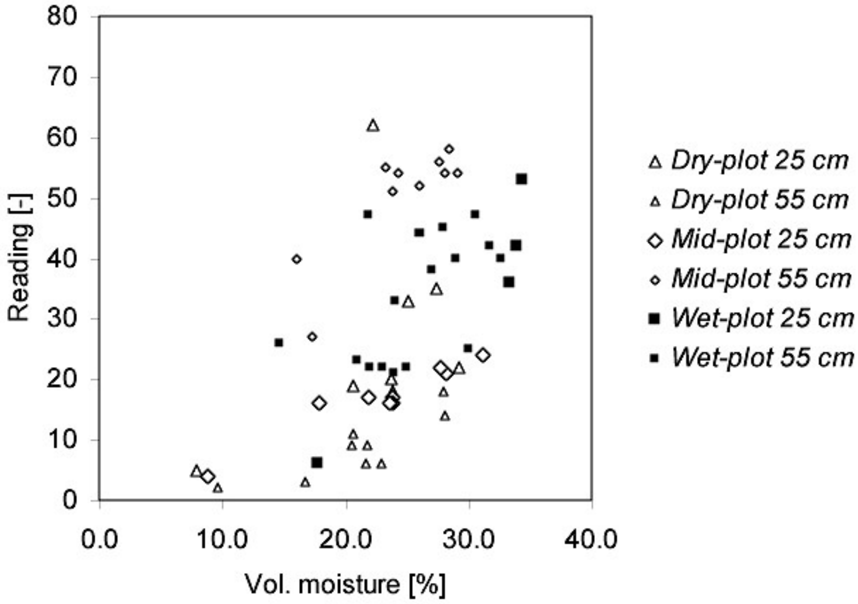

Figure 5.19. Relationship between the readings of nylon blocks and volumetric moisture in 1996-1997.

5.4 Results and conclusions

A controlled drainage experiment was established in 1996 on a field with subsurface drainage and natural slope of the ground of 5.5‰ nearby the Reola village, in South Estonia. For water table management a simple control weir was built on the ditch adjacent to the experimental field. Different soil moisture regimes were investigated in three sub-plots (Wet, Mid and Dry-plots) selected at different distances and elevations from the ditch. The effect of water table management was studied using gravimetric soil sampling, tensiometers and nylon blocks, as well as with measurements of groundwater table across the field using groundwater tubes and piezometers. It was found that:

1. The effect of controlled drainage on the elevated groundwater table on the experimental field was well revealed close to the ditch (18 m, Wet-plot), less at 45 m from the ditch (Mid-plot), while it was rather insignificant at the distance of 101 m (Dry-plot).
2. The effect of controlled drainage on soil moisture regime was less clear, as the Wet-plot had slightly different hydro-physical properties.
3. A very simple construction can be used for water table management, but the effect is strictly depending on lateral hydraulic conductivity which must be large enough to compensate for water withdrawal due to the capillary flux. Also, possibilities to maintain the water table at a desired level may be restricted.
4. Comparison of measurement methods showed that gravimetric soil sampling provides relevant information on spatial and temporal soil moisture, jet-fill tensiometers functioned well during the first year, but completely failed in the second year, while nylon blocks require individual calibration and are thus the least useful method for studies of soil water content.

Chapter 6

LOWER BOUNDARY: Case study of control drainage experiment - Modeling

6.1 Introduction

The flow domain together with complex processes in the upper and lower boundaries forms an entirety that can be described by mathematical expressions. A number of numerical simulation models have been developed to describe water flow in porous medium, which are also necessary for modeling of solute transport, heat flow and crop growth. Physically based models are usually similar regarding implementation of Richards' equation in the model core and solving it with explicit/implicit iterative approximation. Common sub-models included in water balance models are: more or less complex solute transport sub-models describing processes highly sensitive to temperature, soil moisture and microbiological activity (e.g. nitrogen cycle); heat flux models incorporating snow cover or not; crop growth models describing assimilation and actual root-shoot development, including different stress factors and/or yield models. The main programs most widely used in recent years are SOIL and SOILN (Johnsson et al. 1987, Bergström et al. 1991, Jansson 1998), MACRO (Version 4.1, Jarvis and Larsson 1998), SWAP (van Dam et al. 1997, van Dam 2000), LEACHW (Hutson and Wagenet 1992), DRAINMOD (Skaggs 1978, 1980, Skaggs et al. 1988, Fernandez et al. 1998) and in Finland CROPWATN (Karvonen and Kleemola 1995).

The purpose of the present part of the study was to use the SWAP program to simulate the control drainage experiment described in Chapter 5 with different soil hydraulic parameters found in Chapter 4, and also to calibrate and validate the model for further long-term analysis in Chapter 7.

6.2 Agro-hydrological model SWAP – an overview

The agro-hydrological model Soil-Water-Atmosphere-Plant (SWAP) has been developed by a number of scientists in different organizations but mainly at Wageningen University. This model is based on the model SWATR (Feddes et al. 1978) and its derivatives (e.g. Belmans et al. 1983, Kabat et al. 1992). SWAP has been extensively used as the modeling tool in a large number of doctoral theses (pesticide leaching – Groen 1997, water flow and nutrient transport – de Vos 1997, flow and transport in water repellent soils - Ritsema 1998, non-point source pollutants – Tiktak 1999, nitrate leaching – Hack-ten Broeke 2000, SWAP – model concepts – van Dam 2000).

A schematic description of the processes incorporated in SWAP (adapted from van Dam 2000) is presented in Fig. (6.1). SWAP is classified as a one-dimensional model, but saturated flow is treated in a quasi two-dimensional way, which allows to incorporate multi-level ditch systems. This option was found to be very useful to model the case study described in Chapter 5. For the upper boundary, SWAP considers the following processes: potential evapotranspiration (by Monteith 1965 and Allen et al. 1998), potential soil evaporation and plant transpiration (Belmans et al. 1983), actual soil evaporation, actual plant transpiration. In the present studies potential evapotranspiration was estimated independently using the new parameters developed in Chapter 2.

In SWAP, the potential root water extraction rate at a certain depth, $S_p(z)$, is determined by root length density at this depth as fraction of total root length density (van Dam 2000). Too dry or too wet conditions are causing plant stress that reduces transpiration. SWAP implements a well known trapezoidal stress pattern developed by Feddes et al. (1978) that converts potential transpiration into actual transpiration as a function of soil water pressure head.

For one-dimensional vertical flow, the Richards' equation (Eq. 4.3) is numerically solved using a node-centered and variable-weighted Crank-Nicolson finite difference technique. The soil profile may have up to 5 specified soil horizons. The flow domain is divided up to 40 compartments with equal or variable nodal spacing. Soil hydraulic functions are modeled as proposed by Mualem (1976) and Van Genuchten (1980), i.e. Eq. (4.4, 4.5). SWAP allows to model also the hysteresis of water retention function, water repellency and shrinking-swelling soils. SWAP makes distinction between drainage and bottom flux where the first refers to the groundwater flux to or from drainage system (i.e. lateral flow) and the latter refers to the flux at the soil profile's bottom (i.e. vertical flow). The drainage flux density q_{drain} can be calculated from a) groundwater level ϕ_{gwl} and drainage resistance $\gamma_{drain,n}$ where n denotes different drainage fluxes at different drainage levels, e.g. subsurface drains and open ditches, b) a tabular relation between groundwater level and drainage flux, c) analytical drainage equations of Hooghoudt and Ernst for five field drainage conditions. The bottom boundary as defined in SWAP can be set as a) specified groundwater level or pressure head as a function of time, b) specified bottom flux as function of time, c) specified bottom flux as a function of groundwater level. In the present study the first option was implemented. Drainage flux density is calculated as follows:

$$q_{drain} = \frac{\phi_{GWL} - \phi_{drain}}{\gamma_{tot}} \tag{6.1}$$

where q_{drain} – is drainage flux density [cm d^{-1}]
ϕ_{GWL} – is groundwater level [cm]
ϕ_{drain} – is drain level [cm]
γ_{tot} – is total drainage resistance [d]

According to Ernst (1954), flow towards a subsurface drain is described by a vertical flow (from the groundwater level downward to drain level), a horizontal flow towards the vicinity of the drain, a radial flow to the drain and entry of it (Stuyt et al. 2000). Each of these flows is subject to a corresponding resistance (Stuyt et al. 2000). Total resistance can be calculated as follows:

$$\gamma_{tot} = \gamma_{drain} + \frac{L_{drain}}{u_{drain}} \gamma_{entr} \tag{6.2}$$

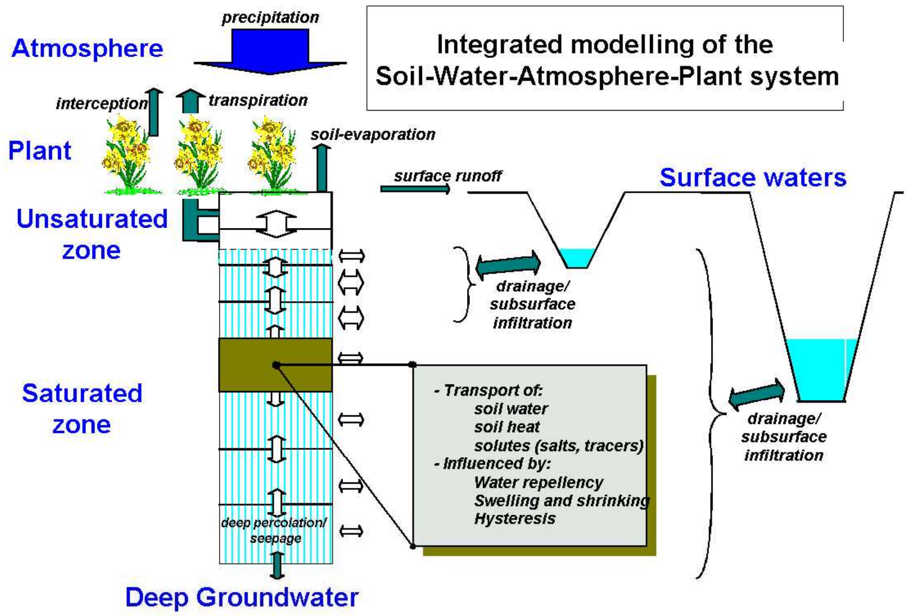

Figure 6.1. A schematized overview of the SWAP model (adapted from Van Dam 2000).

where γ_{tot} – is total drainage resistance [d]
γ_{drain} – is drainage resistance [d]
L_{drain} – is drain spacing [m]
u_{drain} – is wet perimeter of drain [m]
γ_{entr} – is entrance resistance

Drainage resistance can be found from the ratio of distance to drain s and saturated hydraulic conductivity K_{sat}, $\gamma_{drain} = \frac{s}{K_{sat}}$. However, it is rather difficult to parameterize Eq. (6.2). Additional factors such as clogging of flow paths by particle deposition and disturbance of the soil around drainpipes or envelope material may add nonuniformity to the flow field at the drain boundary. Thus it is usually neither possible nor necessary to separate all these individual effects. In field conditions the total entrance head loss [m], consisting of convergence and radial head loss, can be measured and when it is divided by the actual drainage coefficient [m d^{-1}], total entrance resistance is obtained (Vlotman et al. 2000). Entrance resistance may be obtained also from tabulated values, e.g. as in Dierickx (1993), and Smedema and Rycroft (1983). In the present study another option was used: in the first step the drainage flux was calculated according to the Hooghoudt (1940) equation (Eq. 6.3), in the second step total resistance was found from Eq. (6.1) by substituting the calculated drainage flux into Eq. (6.1).

$$q = \frac{8K\,d\,h + 4K\,h^2}{L^2} \tag{6.3}$$

where d – is equivalent depth (less than depth to the impervious layer D)
L – is drain spacing [m]
q – drain discharge [m d^{-1}]
h – is the height of the water table above water level in the drain [m]

SWAP includes different crop growth models from which a simple crop model was selected. Other options like solute transport, heat flow etc., in SWAP are not described here because they were not implemented in the present work.

The hysteresis phenomenon is inherent in the soil-water system, and long drying-wetting periods were observed also during the present experiment. In numerical models of unsaturated flow the effect of hysteresis has been studied by several authors, e.g. Hopmans et al. 1991, Lenhard et al. 1989, Viane et al. 1994, Lehman et al. 1998, Stauffer and Kinzelbach 2001. The last authors reported that simulation without hysteresis, when a 'mean' retention curve was used, yielded nearly as good results as hysteretic simulation. The SWAP has the possibility to set different van Genuchten parameters for desorption and sorption curves, but in this study this option was not used due to missing parameter values.

Unfortunately, SWAP does not include sub-models to calculate accumulation and melting of snow, and it cannot determine the water balance of seasonally frozen soils. Thus, these disadvantages restrict the use of the model for a whole year in Estonian conditions, excluding hence the possibility to implement it in long-term continuous calculations.

6.3 Modeling of soil moisture dynamics and groundwater table at the Mid-plot

6.3.1 Initial and boundary conditions

The control drainage experiment, carried out on the Reola experimental field during the growing period in 1996 and 1997 (see detailed description of the experiment in Chapter 5), was used to assess the applicability of SWAP for Estonian conditions. The modeling period ranged from the 1st of May to the 5th of September in both years. Both years were characterized by warm and dry August and September differing from long-term average conditions. The field was cropped with a mixture of grassland species (e.g. *Trifolium repens L.*, *Lolioum perenne L.*, *Phleum pratense L.*, *Poa pratensis L*). The soil profile was described up to the depth of 300 cm. The upper boundary was flux-controlled, i.e. the driving variables were measured precipitation and estimated potential evapotranspiration. The effect of soil heat flux was not taken into account. The initial values of soil water content were calculated by assuming an equilibrium with groundwater depth (h=0) and linearly decreasing according to equilibrium conditions. The initial groundwater depth was set at 0.5 m, which was appropriate for both years. The bottom boundary was defined as zero flux boundary (Neuman condition). The effect of drainage and outflow to the ditch and inflow from the ditch were considered for the lateral flux.

The soil profile was divided into 4 discrete layers, which were subdivided totally into 26 compartments. Soil layers were parameterized according to the field measurements (see Chapter 4) and the soil hydraulic parameters were based on those found with Wind's evaporation method (Table 4.3) and Andersson's method (Table 4.5). To investigate the effect of the parameters on the soil hydraulic functions, modified parameters were also used. Topsoil was divided into 10 compartments (upper 5 cm into 1 cm compartments, following 25 cm into 5 cm compartments). Subsoil from 30 to 100 cm was divided into 10 cm compartments, from 100 to 200 cm into 25 cm compartments and from 200 to 300 cm into 50 cm compartments.

Variations in leaf area index, displacement height and roughness length were estimated on the basis of annual crop development. Root depth for grass was assumed to increase linearly from the initial value for the date of emergence until the date of flowering. The effect of temperature and soil water shortage or waterlogging was indirectly taken into account by the reduction factors in the water uptake function (Feddes et al. 1978). The critical values for the Feddes model were the same as proposed De Jong and Kabat (1990) for grassland production (e.g. -8000 cm for the wilting point).

6.3.2 Modeling results with Wind's method and with modified soil hydraulic parameters

The simulated dynamics of soil moisture and fluctuation of the groundwater table agreed relatively well with the measurements (Fig. 6.2-6.5). However, consistent differences were found for saturated soil moisture conditions. For example, on the 7th of May 1996 (Fig. 6.2) the groundwater table, measured in the piezometer, showed a value of 71 cm below the ground, while the soil moisture profile measured below that depth was around 0.3 (vol.), i.e. considerably less than the saturated soil moisture of 0.36 (vol.) (Table 4.3) measured in the laboratory. In fact, the same finding was valid for all similar situations in both years. This discrepancy, assuming that the piezometer readings involved no error, may be explained with: 1) measurement error made in gravimetric soil sampling (i.e. part of water was percolated away from the soil samples), 2) measurement error in bulk density, 3) due to entrapped air saturated soil moisture content in field conditions is less than in laboratory conditions. Thus, when measured and modeled results are compared, the errors in measured values should be also taken into account. To show the natural variability in soil moisture content all values in the present Chapter are shown with ± standard deviation.

Another discrepancy that was found pertains to the shape of the measured and modeled soil moisture profiles. If one excludes the conditions of the wetting front (e.g. the 7th of May 1996, the 5th of July 1996, Fig. 6.2) and very dry soil (e.g. the 5th of September 1996, Fig. 6.2, the 5th of September 1997, Fig. 6.3) then measured soil moisture in root zone was rather constant, while the modeled profiles revealed considerable depletion in the upper soil layers. In several papers this kind of deviation is argued to be the result of the inconsistency of the root water uptake algorithm (e.g. Elmaloglou and Malamos 2000) rather than a problem related to the soil hydraulic functions. As it is shown hereafter the uncertainty in the estimation of soil hydraulic properties is most likely the main source of the mentioned discrepancy.

To improve the fitting of the measured and modeled results, the soil hydraulic properties found with Wind's evaporation method were modified with trial-and-error method. At first, saturated soil moisture was reduced from the measured value of 0.36 to a smaller value due to the fact that field measurements showed lower Θ_{sat} than was determined in the laboratory. Afterwards hundreds of combinations of different van Genuchten parameters were studied. To assess the success of fitting the following parameters were calculated: coefficient of determination r^2, root-mean-square-error RMSE, mean residual error ME; also, visual inspection was made. The estimated and modified soil hydraulic properties used in the final comparison are shown in Table 6.1.

Statistical analysis (Table 6.2) revealed that different years were modeled with different success, i.e. the coefficient of determination r^2 for the measured values of soil moisture (vol.) and for those estimated with Wind's method were 0.441 and 0.761 in 1996 and in 1997, respectively. At the same time both, RMSE and ME revealed little difference. Modified parameters increased r^2 as follows: 0.461 and 0.888 in 1996 and in 1997, respectively. It should be emphasized that the groundwater table was calculated and the corresponding errors were reflected in the modeled soil moisture profiles.

Comparison of measured and modeled dynamics of the groundwater table in the Mid plot (Fig. 6.4, 6.5) revealed that, in general, the modeled groundwater table followed the shape of the measured one. Drainage resistances for later fluxes were not calibrated but were calculated on the basis of saturated hydraulic conductivity and the distance to the ditch and drain spacing, as described in Section 6.2. In 1996, the modeled groundwater table started to deviate at the end of May, when the measured values were pertained to same depths as at the beginning of the year, but the estimated results showed a dropping of the groundwater table. During the period when the water table in the ditch was raised, both groundwater tables remained relatively close to the soil surface. In August, when the flux from upstream ceased and the water table was lowered in the ditch, the corresponding lowering was investigated also in the piezometer readings and in the modeled results. In the same period the depletion of soil moisture supply was reflected in smaller values for ET_a (Fig. 6.6).

In 1997, according to visual inspection, the fluctuation of the modeled groundwater table was closer to the measured values than in the previous year although a perfect fit was not achieved. In the second half of June when the water table in the ditch had the highest level and when during a few days (from the 15^{th} to the 18^{th} of June) 63.5 mm of precipitation was recorded then the modeled groundwater table failed to follow the rise in the measured groundwater level. After the control weir was broken between the 10^{th} and the 15^{th} of July both the measured and the modelled groundwater tables started to drop at a very similar speed.

The success of modelling can be judged also by the plotting of measured and estimated tension in the same figure. Figure (6.7) represents the results obtained with a dataset of soil hydraulic properties found by Wind's method. Large discrepancies between the measured and modelled values imply that there exist problems with the estimated water retention curves. In fact, these discrepancies could be caused by a number of reasons, e.g. inappropriately determined soil hydraulic properties, particular root water uptake model, as well as problems with measurement of soil water tension. Unfortunately, soil tension cannot be compared for the second year of the experiment when overall modelling was more successful due to lack of tension measurements.

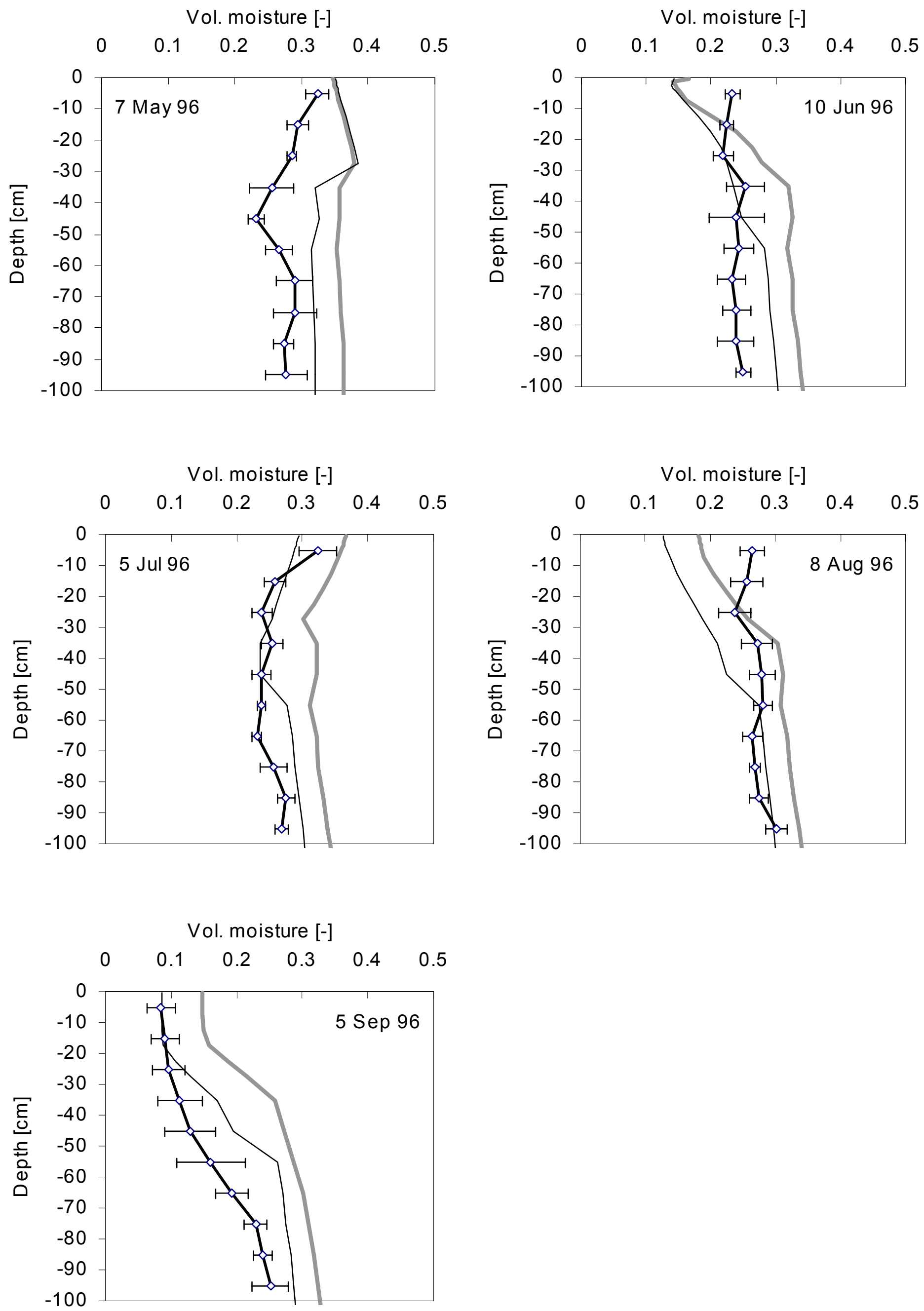

Figure 6.2. Measured and calculated soil moisture (vol.) profiles for the Mid-plot obtained with Wind's method in 1996. Thick line – measured moisture profile (whickers denote ± standard deviation), gray thick line – modeled moisture profile with the parameters of Wind's method, thin line - modeled moisture profile with modified parameters.

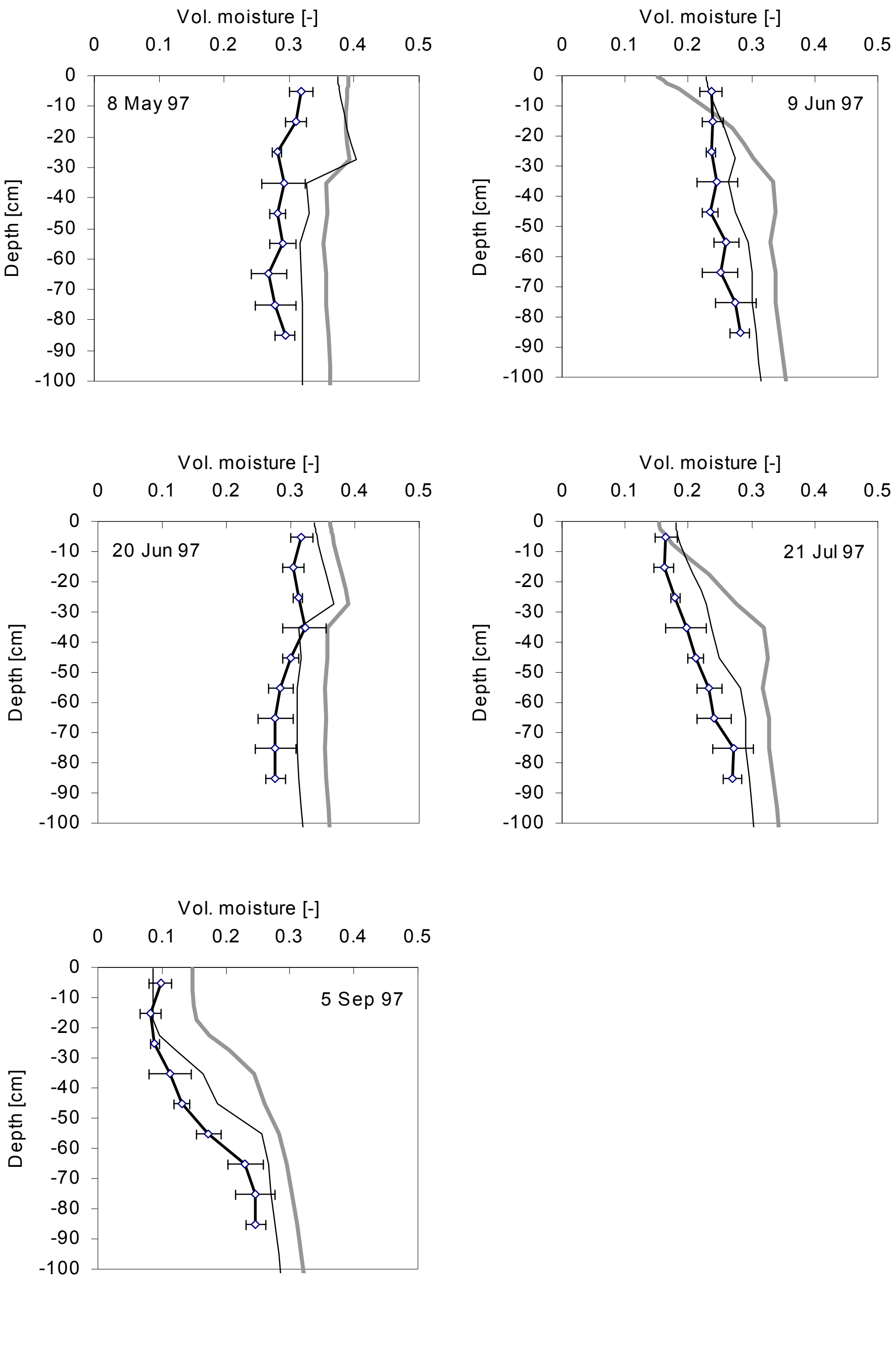

Figure 6.3. Measured and estimated soil moisture (vol.) profiles for the Mid-plot obtained with Wind's method in 1997. Thick line – measured moisture profile (whickers denote ± standard deviation), gray thick line – modeled moisture profile with the parameters of Wind's method, thin line - modeled moisture profile with modified parameters.

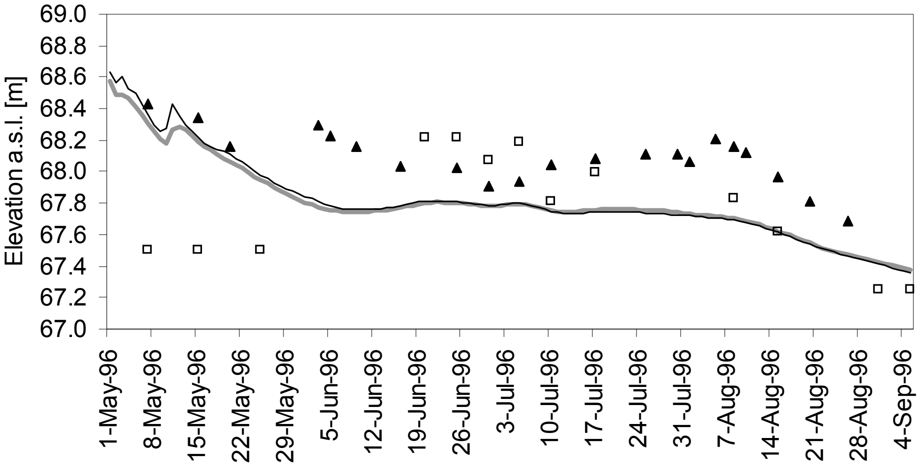

Figure 6.4. Measured and calculated water table dynamics for the Mid-plot obtained with Wind's method in 1996. Gray thick line – estimated groundwater table with soil hydraulic properties of Wind's method, thin line – estimated groundwater table with modified soil hydraulic properties, triangles – measured groundwater table in the Mid-plot's piezometer, squares – elevation of water table in the ditch.

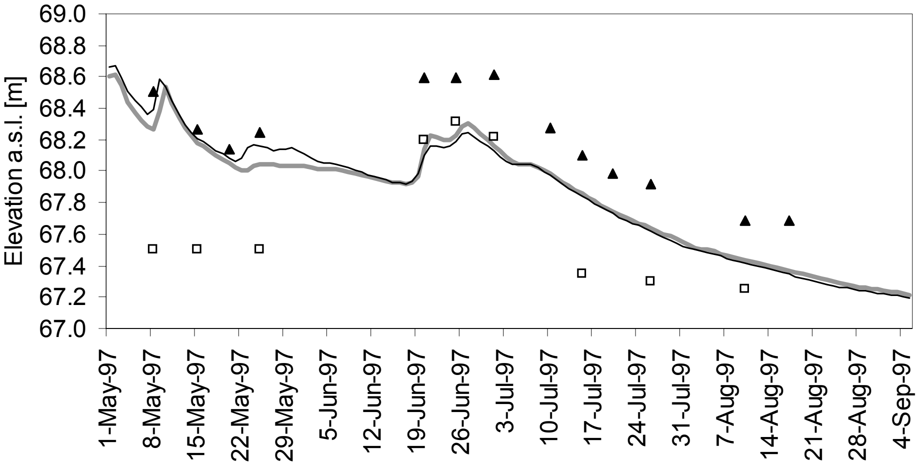

Figure 6.5. Measured and calculated water table dynamics for the Mid-plot obtained with Wind's method in 1997. Gray thick line – estimated groundwater table with soil hydraulic properties of Wind's method, thin line – estimated groundwater table with modified soil hydraulic properties, triangles – measured groundwater table in the Mid-plot's piezometer, squares – elevation of water table in the ditch.

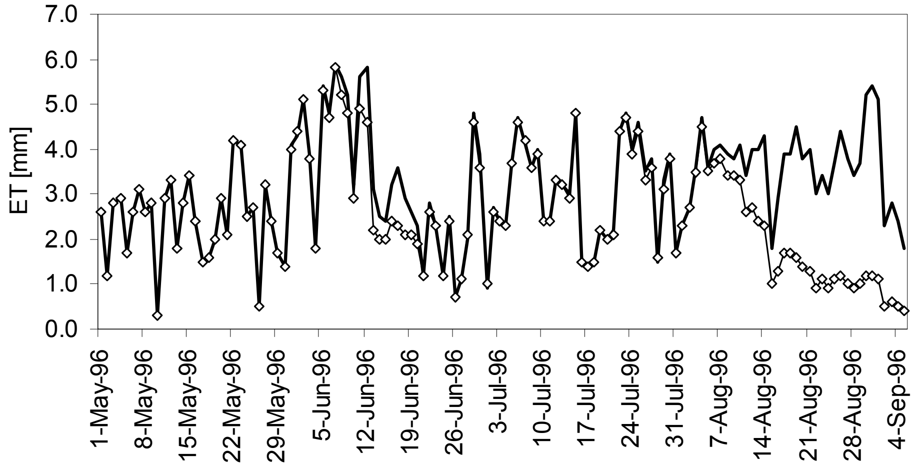

Figure 6.6. Daily potential and actual evapotranspiration in 1996. Thick line – potential evapotranspiration, thin line with white diamonds – actual evapotranspiration found with the soil hydraulic parameters of Wind's method.

Figure 6.7. Modeled and measured soil water tension for the Mid-plot in 1996. White diamonds – measured tension at a depth of 25 cm, black diamonds – tension at a depth of 55 cm, thin line – modeled tension at a depth of 25 cm, thick line – modeled tension at a depth of 55 cm.

6.3.3 Modeling results obtained with Andersson's method and with modified soil hydraulic parameters

Analogously to Section 6.3.2 the modeling of the control drainage experiment was carried out with the soil parameters found by Andersson's method. The main findings were the same as in the previous section: measured water content in the layers under the groundwater table was lower than the estimated values; measured moisture content in the root zone was rather constant, while the modeled moisture content tended to decrease towards depth (Fig. 6.8, 6.9).

In 1996 the modeled soil moisture profile had almost a perfect fit on the 5^{th} of July and on the 5^{th} of September, but failed on other measurement dates (Fig. 6.8). In 1997 the best fit was achieved on the 21^{st} of July, whereas on other measurement dates deviation between the measured and modeled values were more or less significant (Fig. 6.9). In general, like in the case of Wind's method the second year of the experiment yielded a better correlation than the previous year, i.e. r^2 was 0.725 in 1997 and only 0.416 in 1996 (Table 6.2). Compared to Wind's method the overall correlation was lower, but both RMSE and ME yielded lower values in case of Andersson's method (Table 6.1).

Like in the case of Wind's method it was studied how the modification of the soil hydraulic parameters will improve the correlation between the measured and the modeled soil moisture profiles. As the similar fitting procedure would have led to the results similar to those obtained with Wind's method, a different idea of modification was applied. Different soil hydraulic properties for adjacent soil layers may cause a considerably different moisture content in these layers. Thus, in this case it was studied how well the present experimental data can be modeled with a constant set of the van Genuchten parameters for the whole soil profile. One set of parameters that yielded a higher correlation compared with that obtained with the original values of Andersson's method (Table 6.1) is plotted in Fig. (6.8) and in Fig. (6.9). In fact, constant parameters yielded larger and sharper changes in water content than variable parameters, which pointed to the need for differentiating soil layer properties. Nevertheless, modified parameters yielded a better correlation than the original results obtained with Andersson's method, i.e. r^2 was 0.501 in 1996 and 0.760 in 1997 (Table 6.2, Figs. 6.8, 6.9).

The modeled groundwater table calculated with Andersson's method appeared to be closer to the measured values than that obtained with Wind's method, particularly for the beginning of the experiments and for the falling water table in July and August in 1997 (Fig. 6.10, 6.11). Modified parameters accelerated the removal of water from the soil profile. The modeled groundwater table did not achieve the level of the measured groundwater table during the period when the water table in the ditch was raised.

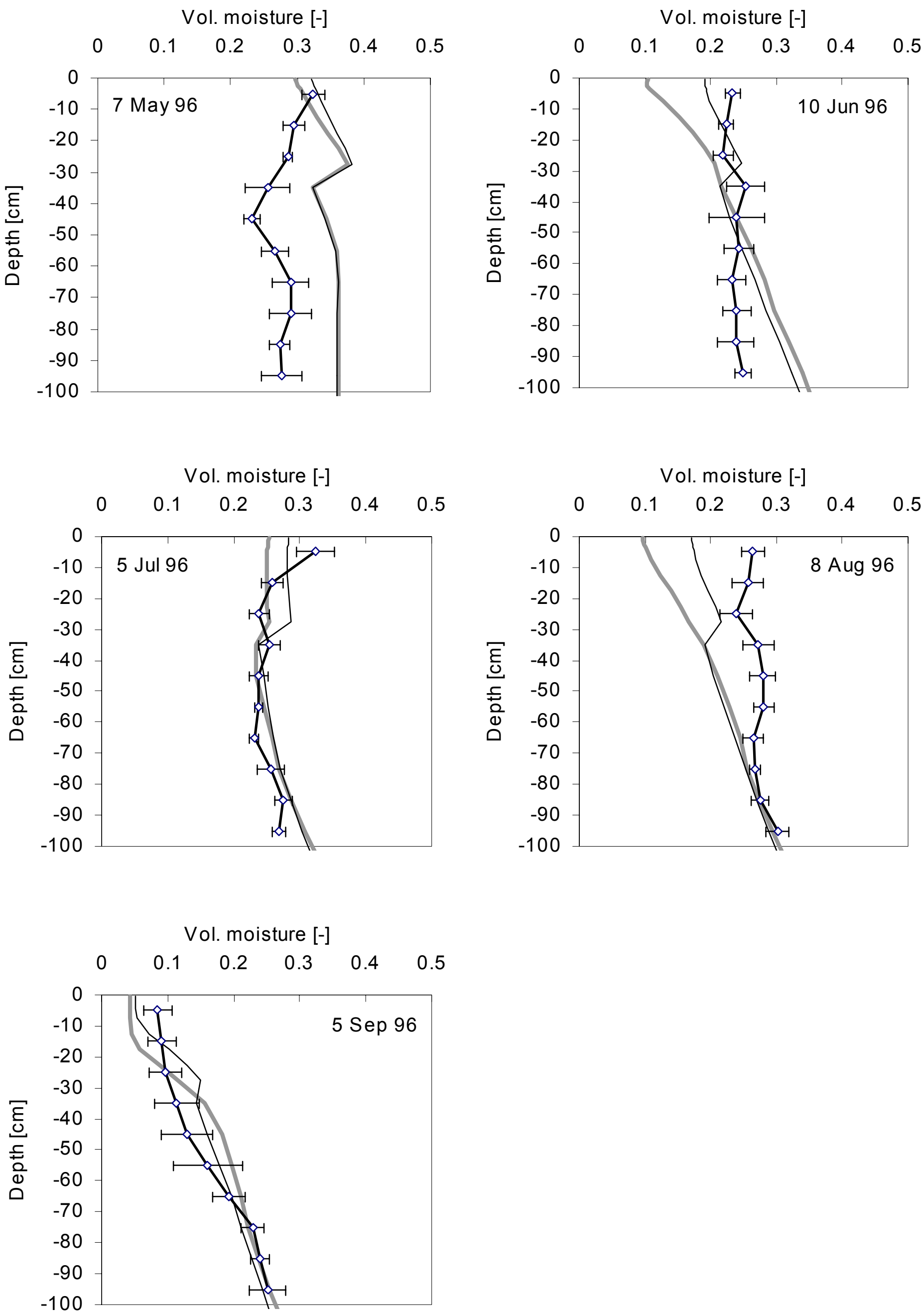

Figure 6.8. Measured and calculated soil moisture (vol.) profiles for the Mid-plot obtained with Andersson's method in 1996. Thick line – measured moisture profile (whickers denote ± standard deviation), gray thick line – modeled moisture profile with the parameters of Andersson's method, thin line - modeled moisture profile with modified parameters.

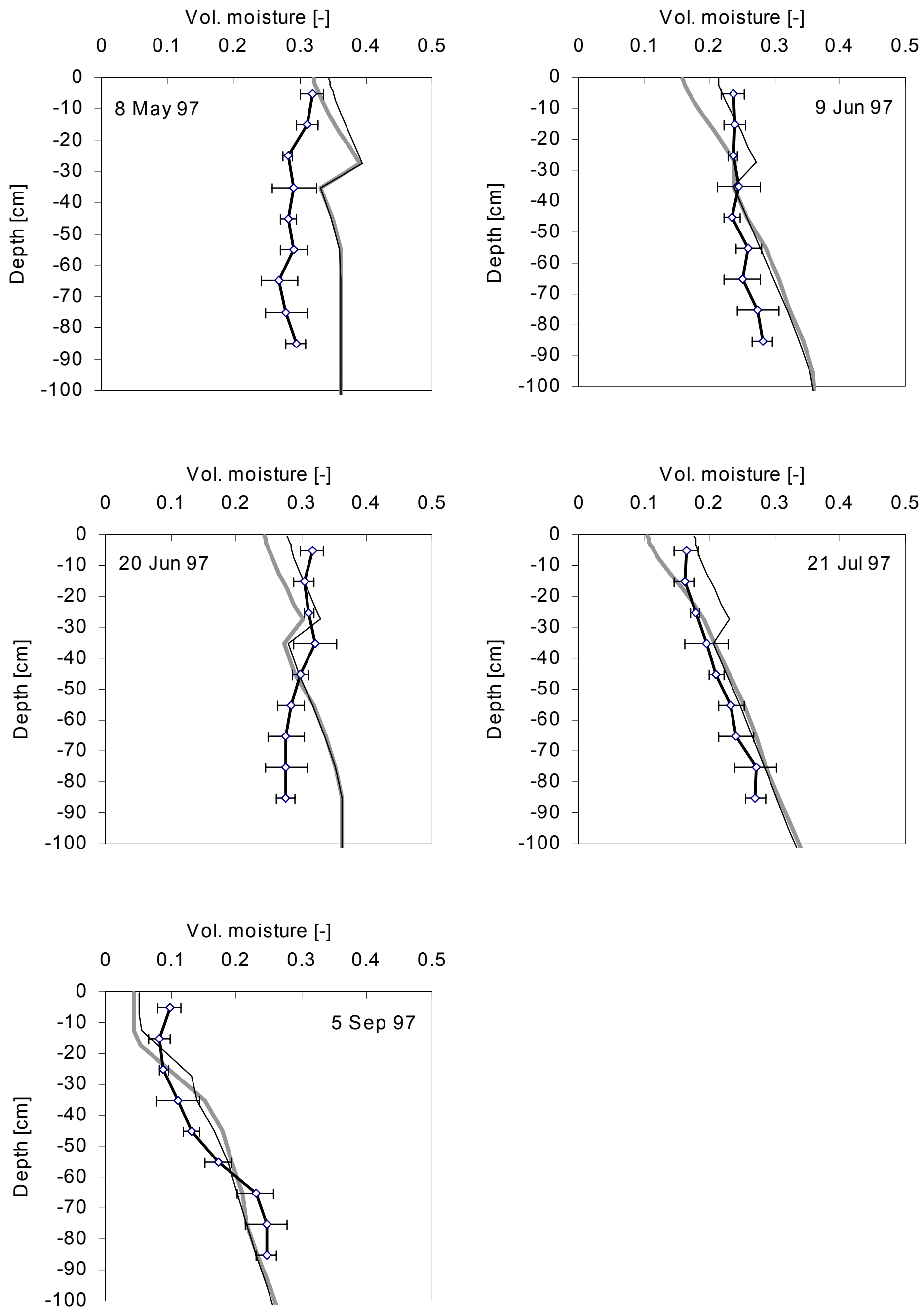

Figure 6.9. Measured and calculated soil moisture (vol.) profiles for the Mid-plot obtained with Andersson's method in 1997. Thick line – measured moisture profile (whickers denote ± standard deviation), gray thick line – modeled moisture profile with the parameters of Andersson's method, thin line - modeled moisture profile with modified parameters.

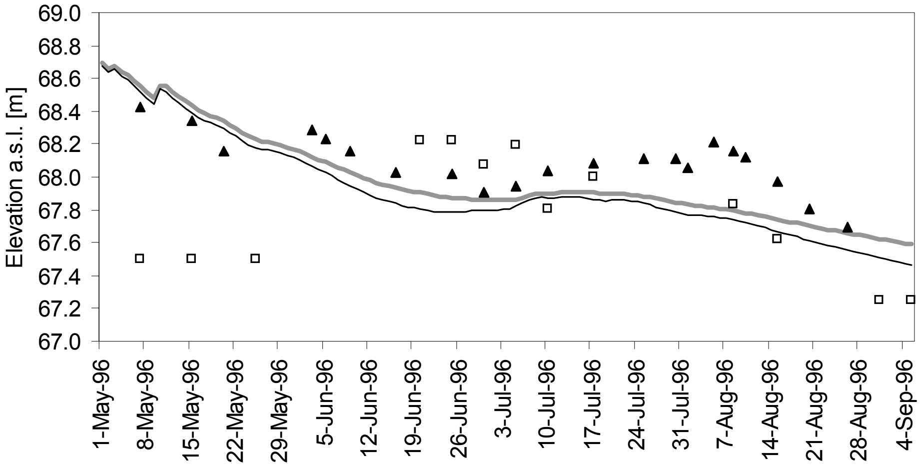

Figure 6.10. Measured and calculated water table dynamics at the Mid-plot with Andersson's method in 1996. Gray thick line – estimated groundwater table with soil hydraulic properties of Andersson's method, thin line – estimated groundwater table with modified soil hydraulic properties, triangles – measured groundwater table in the Mid-plot's piezometer, squares – elevation of the water table in the ditch.

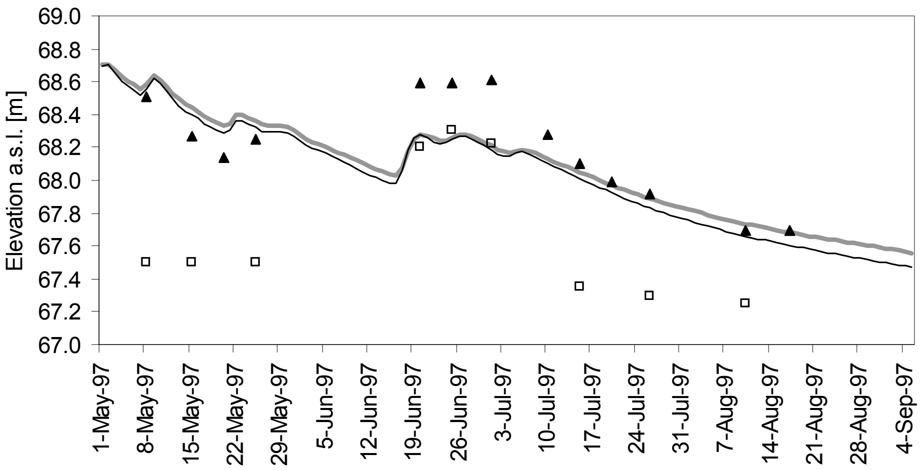

Figure 6.11. Measured and estimated water table dynamics for the Mid-plot in 1997. Gray thick line – estimated groundwater table with the soil hydraulic properties of Andersson's method, thin line – estimated groundwater table with modified soil hydraulic properties, triangles – measured groundwater table in the Mid-plot's piezometer, squares – elevation of the water table in the ditch.

Table 6.1. Estimated and modified soil hydraulic properties used in SWAP for modeling soil moisture dynamics at the Mid-plot.

Site/layer cm	Θ_{res}	Θ_{sat}	K_{sat}	α	n	λ
	$cm^3\ cm^{-3}$	$cm^3\ cm^{-3}$	$cm\ d^{-1}$	cm^{-1}	-	-
Wind's method Simultaneous fit, Appia weight coefficient W1=0.1						
Mid 0-30cm	0.04	0.450	51.1	0.0267	1.248	0.5
Mid 30-50 cm	0.04	0.361	0.71	0.0029	1.359	0.5
Mid 50-70 cm	0.04	0.362	5.7	0.0107	1.149	0.5
Mid 70+ cm	0.04	0.36	15.7	0.0198	1.113	0.5
Modified parameters based on Wind's method						
Mid 0-30cm	0.04	0.450	51.1	0.0167	1.448	0.5
Mid 30-50 cm	0.04	0.341	7.1	0.0107	1.359	0.5
Mid 50-70 cm	0.04	0.32	5.7	0.0107	1.149	0.5
Mid 70+ cm	0.04	0.32	15.7	0.0198	1.113	0.5
Andersson's method						
Mid 0-30cm	0.04	0.450	50.0	0.0228	1.871	0.5
Mid 30-50 cm	0.04	0.361	20.0	0.0230	1.649	0.5
Mid 50-70 cm	0.04	0.362	20.0	0.0197	1.754	0.5
Mid 70+ cm	0.04	0.36	20.0	0.0212	1.750	0.5
Modified parameters based on Andersson's method						
Mid 0-30cm	0.04	0.450	50.0	0.02	1.7	0.5
Mid 30-50 cm	0.04	0.361	20.0	0.02	1.7	0.5
Mid 50-70 cm	0.04	0.362	20.0	0.02	1.7	0.5
Mid 70+ cm	0.04	0.36	20.0	0.02	1.7	0.5

Table 6.2. Fitting results and actual evapotranspiration with different sets of soil hydraulic properties.

Name of the set	Year	r^2 -	RMSE $cm^3\ cm^{-3}$	ME $cm^3\ cm^{-3}$	ET_a* mm
Wind's method	1996	0.441	0.0809	-0.0666	303
	1997	0.761	0.0803	-0.0735	334
Modified parameters based on Wind's method	1996	0.461	0.0512	-0.0173	328
	1997	0.888	0.0437	-0.0367	358
Andersson's method	1996	0.416	0.0659	-0.0103	357
	1997	0.725	0.0514	-0.0205	384
Modified parameters based on Andersson's method	1996	0.501	0.0571	-0.0167	381
	1997	0.760	0.0483	-0.0278	398

*in 1996 ET=381 mm, in 1997 ET=402 mm for a period from 1st of May to 5th of September

6.4 Modeling of soil moisture dynamics and the groundwater table in the Dry plot and Wet-plot

Both the Dry-plot and Wet-plot were subject to modeling as the Mid-plot described in Section 6.3. Differently from the Mid-plot the soil hydraulic parameters were available only from the set of parameters found by Andersson's method. The initial and boundary conditions were the same as described in Section 6.3.1 except for groundwater depth that was set at 0.7 m for the Dry-plot and at 0.5 m for the Wet-plot. These depths were appropriate for both years of the experiment. The soil profile of the Dry-plot was divided into four layers where all layers except for the third layer located at a depth of 50 to 70 cm, were determined to be sandy loam with respect to composition and the thin third layer was found to be loamy sand. The soil profile of the Wet-plot was divided into three layers all of which were of the same soil type, sandy loam. The particle-size distribution and bulk density of the Dry-plot and the Wet-plot are given in Table 6.3, textural classes and soil types in Table 6.4. The soil hydraulic properties found with Andersson's method as well as modified properties are given in Table 6.5.

According to the statistical analysis and visual inspection the best modeling results were obtained for the Dry-plot. In 1996, the coefficient of determination was 0.588 with the soil hydraulic parameters found by Andersson's method and 0.684 with the modified parameters. In 1997 the respective values were 0.720 and 0.787 (Table 6.6). When these results were compared with those obtained for the Mid-plot then it appeared that the results were better especially for 1996. The modeled soil moisture profiles were similar to the measured ones. In fact, the soil hydraulic properties found by Andersson's method yielded modeling results that were very close to the measured values on the 5th of July 1996, on the 5th of September 1996, on the 9th of June 1997, on the 21st of July 1997 and on the 5th of September 1997 (Figs. 6.12, 6.13). The largest deviation was found on the 8th of August 1996 when the measured soil moisture profile was much moister than the modeled one. According to meteorological conditions it seemed that the modeled results were even more appropriate than the measured ones, because the weather was warm and dry for a long period before that particular soil sampling event. In fact, during the previous three weeks only 23.5 mm of precipitation was recorded, while the estimated potential evapotranspiration was 82 mm. The modified soil hydraulic properties improved fitting with the measured results (Table 6.6).

It is difficult to assess how well the groundwater table was modeled in 1996 because only three measurements of the water table were made in the Dry-plot's piezometer. The last sampling date was the 17th of June, after which the water table was continuously lower that the depth of the piezometer, 150 cm. In 1997 the estimated groundwater table was very close to that with the measured values. In general, it can be concluded that the piezometer length of 150 cm was insufficient for measurements of groundwater fluctuation in the Dry-plot.

Table 6.3. Particle-size distribution and bulk density for the Dry and Wet-plots.

		Particle size distribution									Bulk dens.
Site	Layer	1-2.0	1-0.5	0.5-0.25	0.25-0.1	0.1-0.05	0.05-0.02	0.02-0.005	0.005-0.002	<0.002	$g\ cm^{-3}$
Dry	0-30 cm	1.4	3	9.1	25.9	16.7	21.1	14.5	5.5	2.8	1.37
Dry	30-50 cm	1.6	1.6	5.6	26.2	22.4	22.6	7.8	10.6	1.6	1.47
Dry	50-70 cm	4.2	6.6	18.3	43.4	14.2	7.7	3.7	0.1	1.8	1.73
Dry	70-100 cm	2.5	5.1	12.3	29.1	13.8	14.6	11.2	4.8	6.6	1.81
Wet	0-30 cm	1.3	3.3	8.1	33	20.1	17.1	10.8	3.2	3.1	1.28
Wet	30-60 cm	2.7	4.6	9.3	26.2	20.2	15.8	10.4	4.2	6.6	1.48
Wet	60-100 cm	3.2	4.8	11.1	22.7	15.2	15.5	11	3.8	12.7	1.79

Table 6.4. Textural classes and soil types of the soil samples of the Dry and Wet-plots.

		Texture class			
Site	Layer	Sand %	Silt %	Clay %	Soil type
Dry	0-30 cm	56.1	41.1	2.8	Sandy loam
Dry	30-50 cm	57.4	41	1.6	Sandy loam
Dry	50-70 cm	86.7	11.5	1.8	Loamy sand
Dry	70-100 cm	62.8	30.6	6.6	Sandy loam
Wet	0-30 cm	65.8	31.1	3.1	Sandy loam
Wet	30-60 cm	63	30.4	6.6	Sandy loam
Wet	60-100 cm	57	30.3	12.7	Sandy loam

The modeling results for the Wet-plot were the poorest compared with the other plots. Both statistical analysis and visual inspection of the soil moisture profiles revealed large deviations between measured and modeled volumetric soil moisture contents (Table 6.6, Figs. 6.16, 6.17). Soil moisture content for the upper half-meter tended to be moister than that estimated with SWAP. In fact, the quality of data of the Wet-plot was lower than that of the other plots, if the magnitude of their standard deviations was compared. It was also found that the overall moisture regime in the Wet-plot was considerably different from that of the other plots (see results in Chapter 5). In 1996, there was a very low correlation between the measured and modeled soil moisture profiles (r^2=0.154), and the modified soil hydraulic properties improved the results only slightly (r^2=0.230) (Table 6.6). In 1997 the results were comparable with those obtained for the Mid and Dry-plots (r^2=0.568) and hence modified soil hydraulic properties improved the correlation (r^2=0.748). The last result was almost as high as it was in case of the Dry-plot, however, visual inspection revealed large deviations which were confirmed with almost two times as large RMSE-values for the Wet-plot.

The dynamics of the groundwater table of the Wet-plot was relatively well estimated. Comparison of the measured water table in the Wet-plot's piezometer with the modeling results revealed that the soil hydraulic properties found with Andersson's method and with modified parameters yielded similar results. It is difficult to make preferences because for different time periods one or the other set of parameters yielded better results. For example, in 1996, the Andersson's set of soil parameters gave smoother dynamics of the groundwater table compared with the results obtained with the modified parameters (Fig. 6.16). In 1997, the Andersson's set of soil parameters gave a better estimate before and after the water was raised in the adjacent ditch, while the modified parameters yielded a better estimate of the effect of the elevation of the water table (Fig. 6.17).

An interesting result was obtained when the water retention curves found with the modified soil hydraulic parameters were plotted in the same figure as those found with Wind's and Andersson's methods, together with the tensiometer readings (see Fig. 5.18). The resulting new figure (Fig. 6.20, only the modified Mid-plot curve is shown, the other plots resulted in very close curves) revealed that the modified water retention curves were located between Wind's-curve and Andersson's-curve. Moreover, the modified curves were close to points which had been obtained by plotting the tensiometer readings and the corresponding volumetric soil water content in Fig. (6.20).

Table 6.5. Estimated and modified soil hydraulic properties used in SWAP for modeling soil moisture dynamics for the Dry and Wet-plots.

Site/layer cm	Θ_{res}	Θ_{sat}	K_{sat}	α	n	λ
	$cm^3\ cm^{-3}$	$cm^3\ cm^{-3}$	$cm\ d^{-1}$	cm^{-1}	-	-
Andersson's method in the Dry-plot						
Dry 0-30cm	0.04	0.450	50.0	0.017	1.812	0.5
Dry 30-50 cm	0.04	0.36	20.0	0.015	1.915	0.5
Dry 50-70 cm	0.04	0.36	20.0	0.021	2.387	0.5
Dry 70+ cm	0.04	0.36	20.0	0.021	1.831	0.5
Modified parameters based on Andersson's method in the Dry-plot						
Dry 0-30cm	0.04	0.450	50.0	0.017	1.5	0.5
Dry 30-50 cm	0.04	0.36	20.0	0.015	1.7	0.5
Dry 50-70 cm	0.04	0.342	50.0	0.02	1.7	0.5
Dry 70+ cm	0.04	0.32	20.0	0.02	1.7	0.5
Andersson's method in the Wet-plot						
Wet 0-30cm	0.04	0.450	50.0	0.019	2.030	0.5
Wet 30-60 cm	0.04	0.36	20.0	0.017	2.129	0.5
Wet 60+ cm	0.04	0.36	20.0	0.020	1.785	0.5
Modified parameters based on Andersson's method in the Wet-plot						
Wet 0-30cm	0.04	0.450	50.0	0.02	1.5	0.5
Wet 30-60 cm	0.04	0.36	20.0	0.015	1.7	0.5
Wet 60+ cm	0.04	0.32	20.0	0.02	1.7	0.5

Table 6.6. Fitting results and actual evapotranspiration with different sets of soil hydraulic properties for the Dry and Wet plot.

Name of the set	Year	r^2	RMSE	ME	ET_a*
		-	$cm^3\ cm^{-3}$	$cm^3\ cm^{-3}$	mm
Andersson's method at the Dry-plot	1996	0.588	0.0536	0.0344	342
	1997	0.720	0.0458	-0.0156	389
Modified parameters based on Andersson's method at Dry-plot	1996	0.684	0.0341	0.0154	357
	1997	0.787	0.0376	-0.0169	391
Andersson's method at the Wet-plot	1996	0.154	0.0673	0.0266	381
	1997	0.568	0.0808	0.0454	378
Modified parameters based on Andersson's method at the Wet-plot	1996	0.230	0.0893	0.0558	381
	1997	0.748	0.0607	0.0273	394

*in 1996 ET=381 mm, in 1997 ET=402 mm for a period from 1st of May to 5th of September

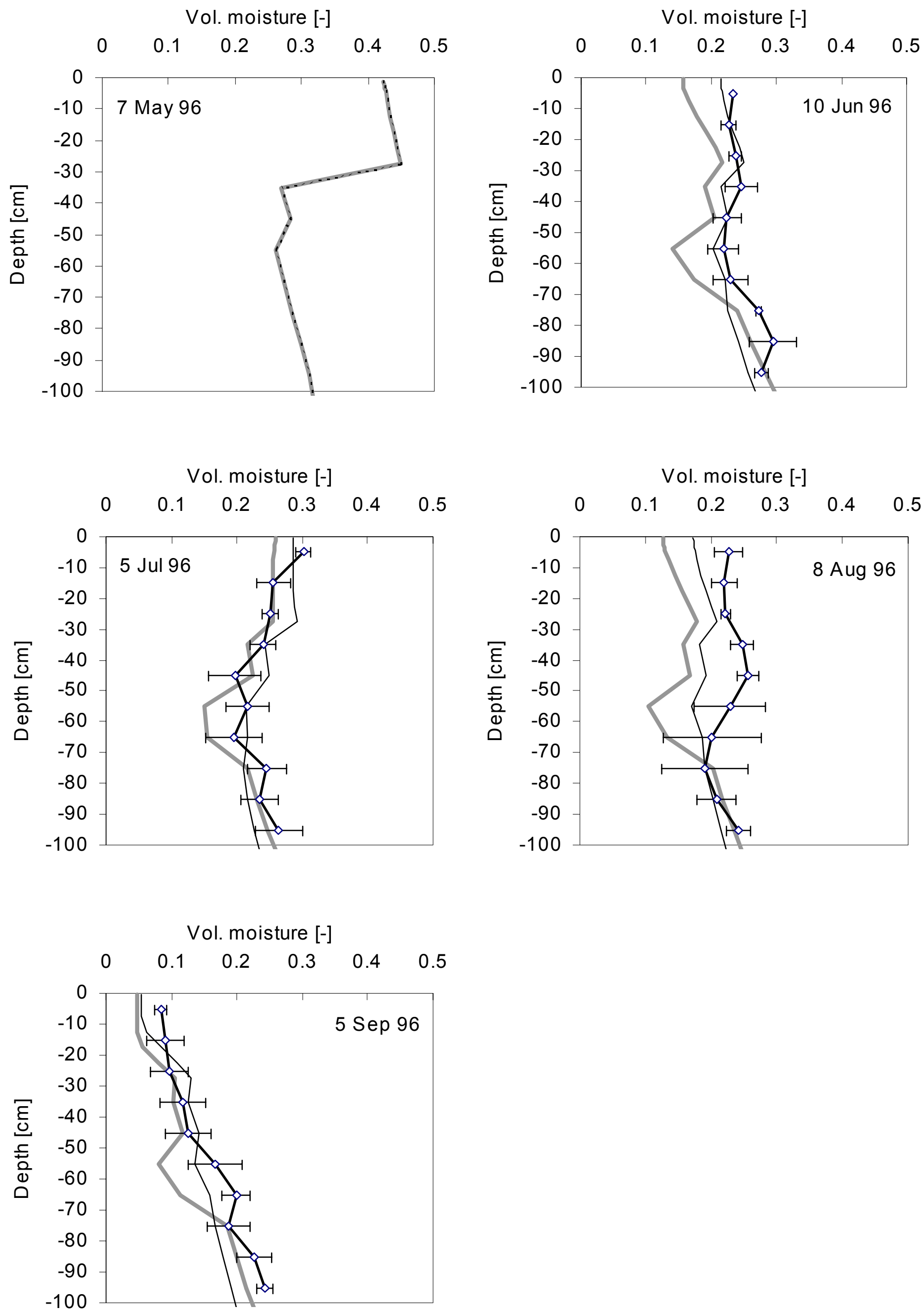

Figure 6.12. Measured and estimated soil moisture (vol.) profiles for the Dry-plot in 1996. Thick line – measured moisture profile (whickers denote ± standard deviation), gray thick line – modeled moisture profile with the parameters of Andersson's method, thin line - modeled moisture profile with modified parameters.

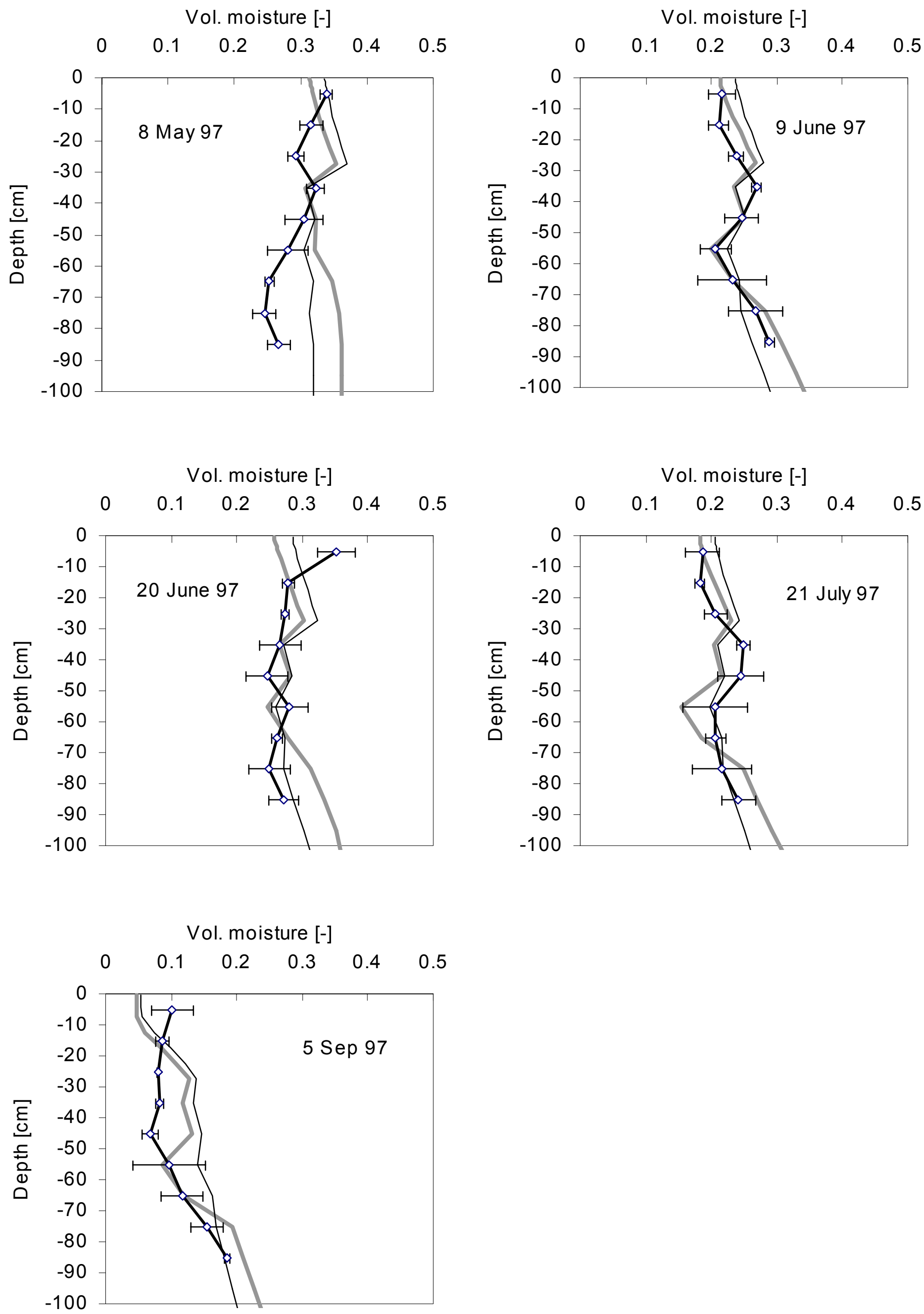

Figure 6.13. Measured and estimated soil moisture (vol.) profiles for the Dry-plot in 1997. Thick line – measured moisture profile (whickers denote ± standard deviation), gray thick line – modeled moisture profile with the parameters of Andersson's method, thick line - modeled moisture profile with modified parameters.

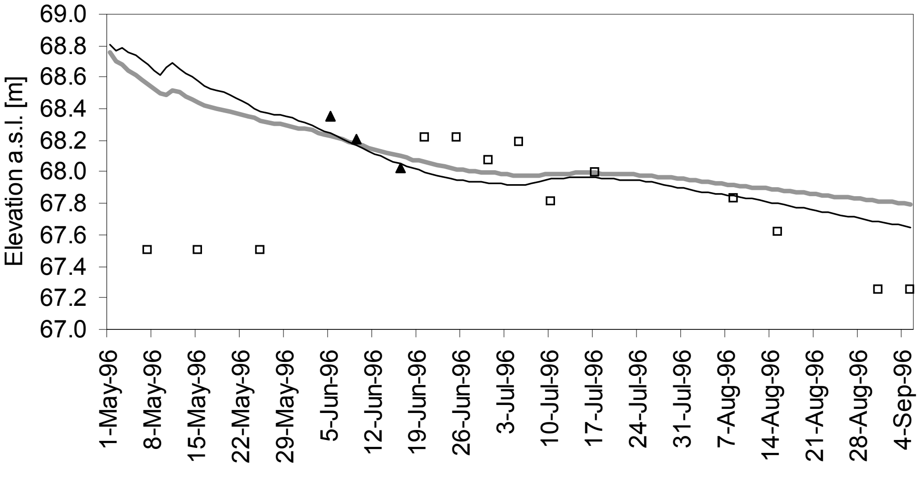

Figure 6.14. Measured and estimated water table dynamics for the Dry-plot in 1996. Gray thick line – estimated groundwater table with the soil hydraulic properties of Andersson's method, thin line – estimated groundwater table with modified soil hydraulic properties, triangles – measured groundwater table in the Dry-plot piezometer, squares – elevation of the water table in the ditch.

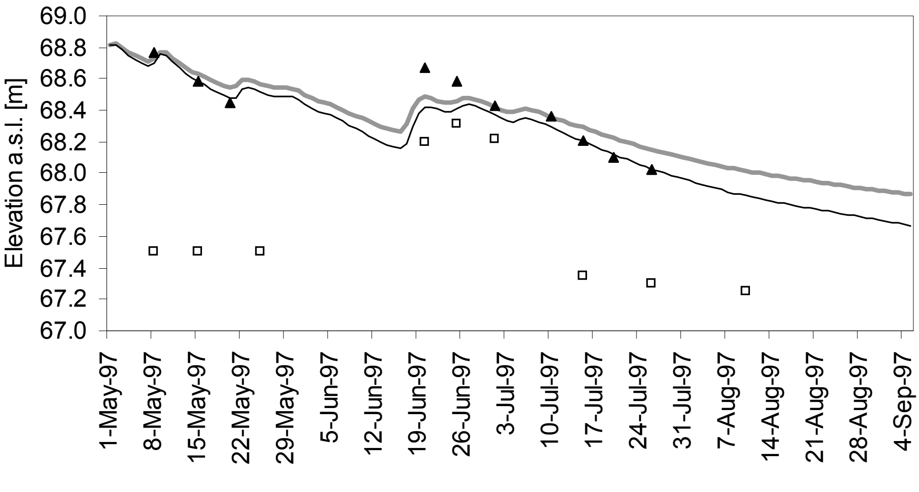

Figure 6.15. Measured and estimated water table dynamics for the Dry-plot in 1997. Gray thick line – estimated groundwater table with the soil hydraulic properties of Andersson's method, thin line – estimated groundwater table with modified soil hydraulic properties, triangles – measured groundwater table in the Dry-plot piezometer, squares – elevation of the water table in the ditch.

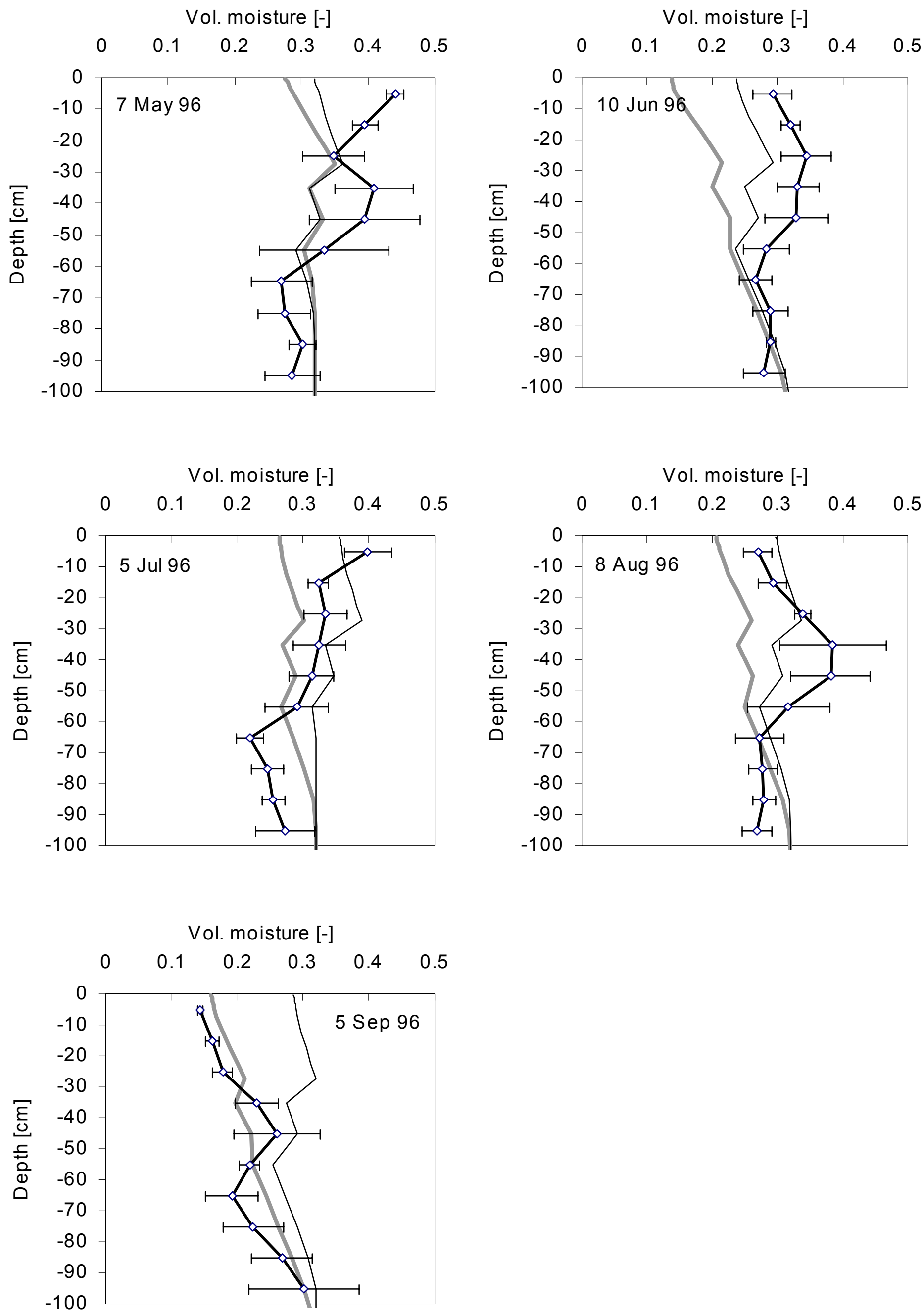

Figure 6.16. Measured and estimated soil moisture (vol.) profiles for the Wet-plot in 1996. Thick line – measured moisture profile (whickers denote ± standard deviation), gray thick line – modeled moisture profile with the parameters of Andersson's method, thin line - modeled moisture profile with modified parameters.

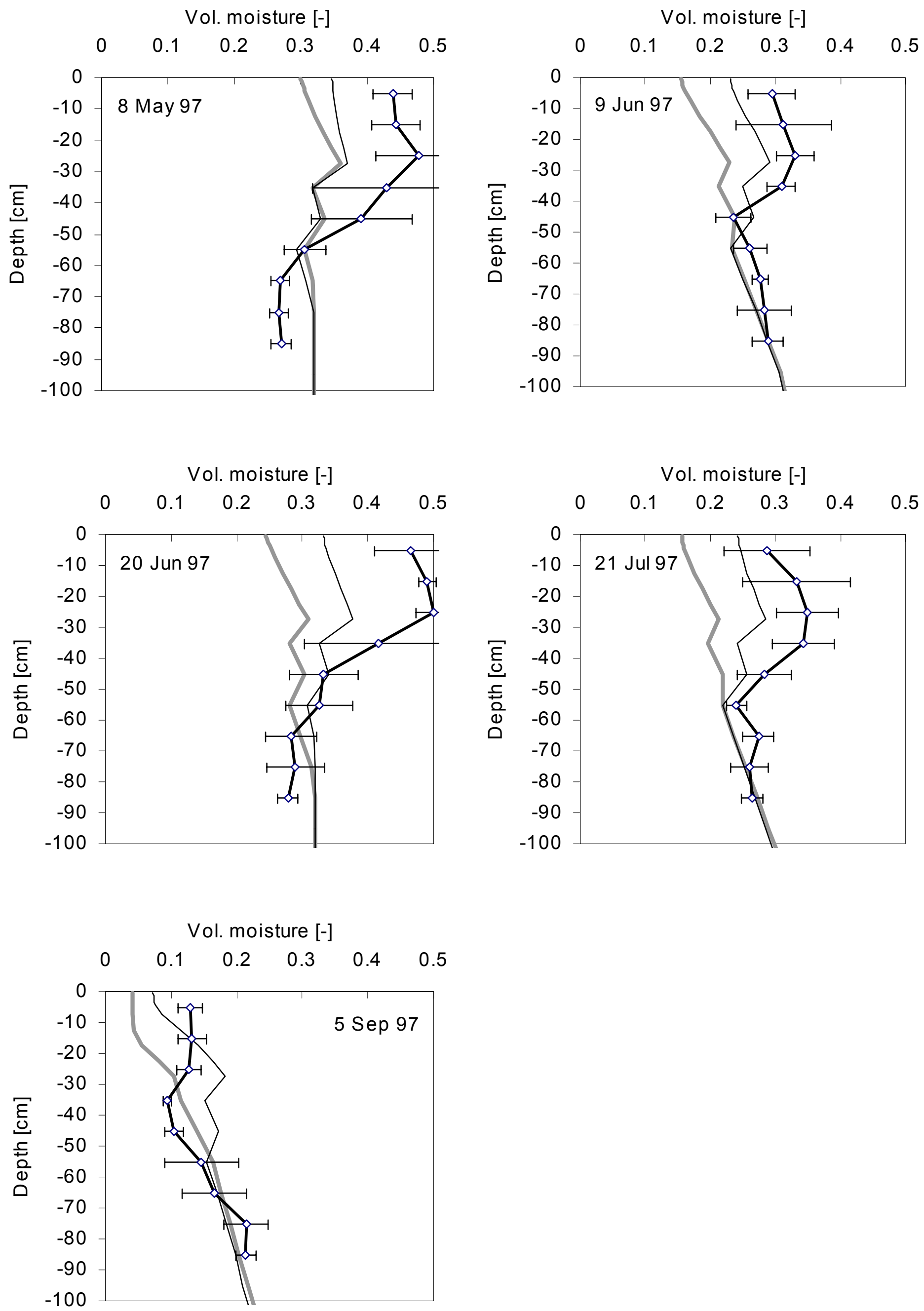

Figure 6.17. Measured and estimated soil moisture (vol.) profiles for the Wet-plot in 1997. Thick line – measured moisture profile (whickers denote ± standard deviation), gray thick line – modeled moisture profile with the parameters of Andersson's method, thin line - modeled moisture profile with modified parameters.

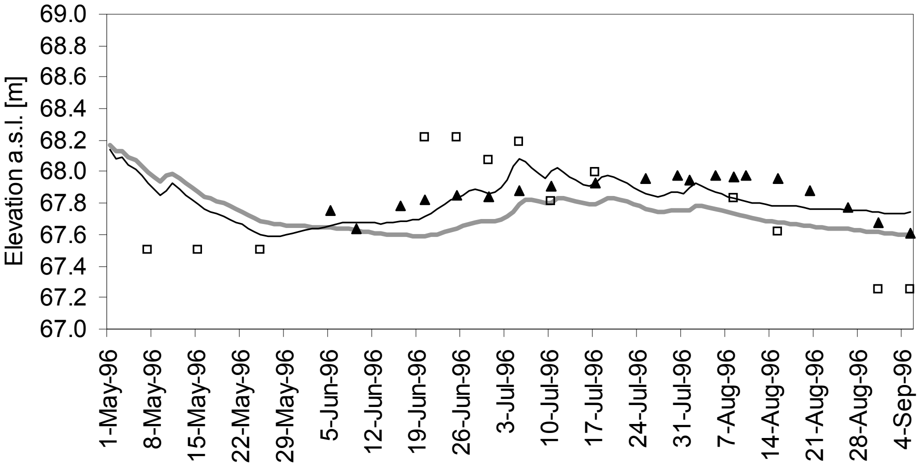

Figure 6.18. Measured and estimated water table dynamics for the Wet-plot in 1996. Gray thick line – estimated groundwater table with the soil hydraulic properties of Andersson's method, thin line – estimated groundwater table with modified soil hydraulic properties, triangles – measured groundwater table in the Wet-plot's piezometer, squares – elevation of the water table in the ditch.

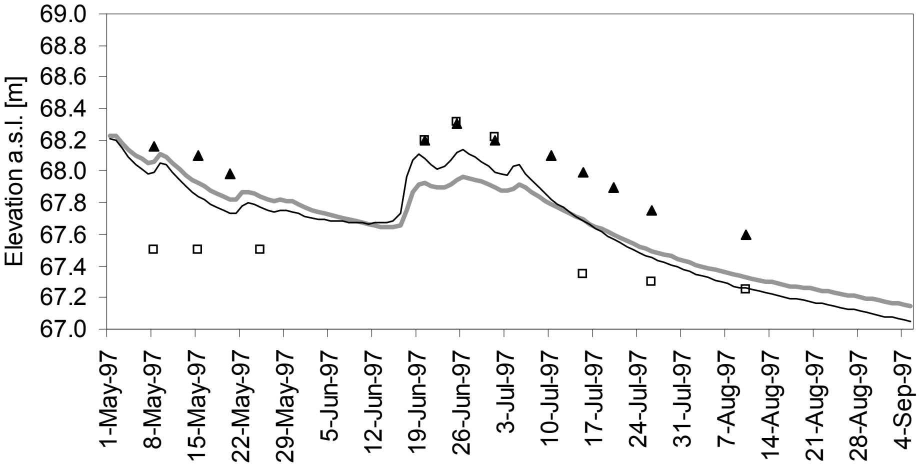

Figure 6.19. Measured and estimated water table dynamics for the Wet-plot in 1997. Gray thick line – estimated groundwater table with the soil hydraulic properties of Andersson's method, thin line – estimated groundwater table with modified soil hydraulic properties, triangles – measured groundwater table in the Wet-plot's piezometer, squares – elevation of the water table in the ditch.

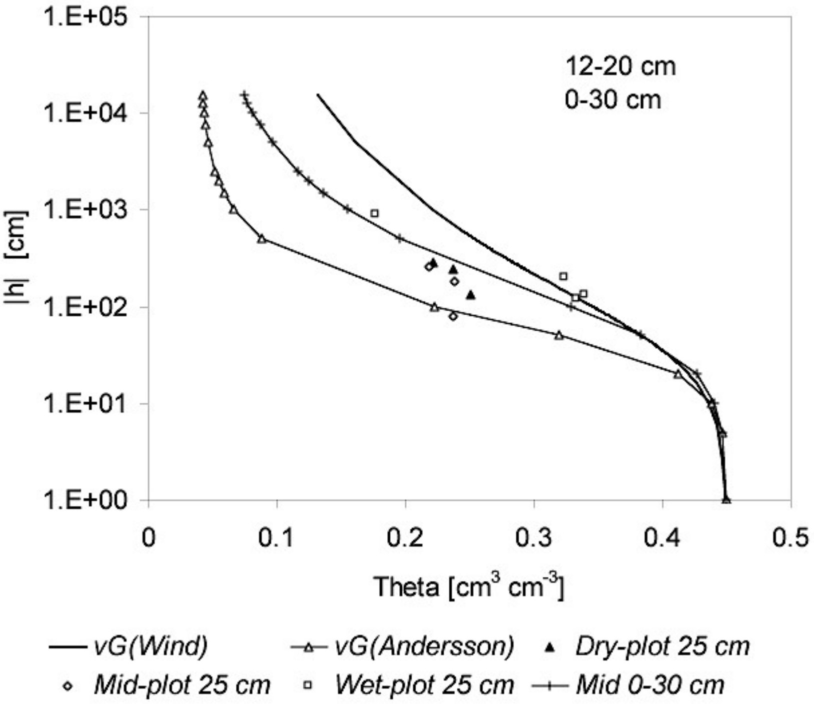

Figure 6.20. Estimated water retention curves obtained with Wind's and Andersson's methods, measured soil water tension at a depth of 25 cm and modified water retention curve. Line – van Genuchten pF-curve estimated with Wind's method, line with triangles - van Genuchten pF-curve estimated with Andersson's method, solid triangles – Dry-plot's tensiometer measurements, diamonds – Mid-plot's tensiometer readings, squares – Wet-plot's tensiometer readings, lines with crossing marks – modified water retention curve for the Mid-plot's soil layer of 0-30 cm.

6.5 Conclusions and discussion

The agro-hydrological model Soil-Water-Atmosphere-Plant (SWAP) was used to model the control drainage experiment carried out at Reola, near Tartu. Model runs were made for two years and for three sub-plots located at different distances from the ditch. Thus, the experimental data of the three study plots, named by the prevailing moisture regime as Wet, Mid and Dry plot, were used to evaluate how well SWAP may be implemented in Estonian conditions. The Mid-plot was modeled with soil hydraulic properties estimated with Wind's evaporation method and with Andersson's method. The other study plots were modeled only with the latter method. To obtain better correlation between measured soil water content and the modeled one, all three study plots were modeled also with modified soil hydraulic properties. In general, it is difficult to judge which method yielded the best results, because the overall modeling results tended to improve with distance from the ditch and were significantly different for different years. In the case of the Mid-plot, the Wind's method yielded higher coefficient of determination, but also with higher RMSE. Calibrated soil hydraulic parameters increased the fit between the measured and modeled values, however none of these sets can be treated as unique. The water retention curves of the modified soil hydraulic properties fell between the 'boundary curves' found with Wind's evaporation method and Andersson's method and were surprisingly close to the results obtained with tensiometers.

A comparison of the measured and modeled soil moisture profiles at the root zone provided the following conclusions: the measured soil moisture tended to be more 'constant' than the modeled one and the correctness of the root-water-uptake model may be judged only after the soil hydraulic properties are well determined due to their significant effect on the soil water distribution.

The agro-hydrological program SWAP can be used as a tool to model field-scale hydrological processes in Estonian conditions for studies concerning the growing period. For studies comprising continuous simulation of hydrological processes over a period of several years it is necessary to use models that take into account the influence of seasonally frozen soil and accumulation and melting of snow cover.

Chapter 7

LONG-TERM NUMERICAL EXPERIMENTS

7.1 Introduction

Simulation modeling is an important tool in evaluating the economic and environmental effects of different water management practices on groundwater regime, runoff volume, crop yield, and other quantity and quality processes. However, the time period must be representative, i.e. it must cover a wide range of climatic conditions including very dry years and very wet years. It is considered here that as climate change studies in the world and in Estonia often operate with a 30-year time period (Keevallik 1998, Järvet 1998, Tamm 1998b) then this period would be also be proper for the present study.

In Chapter 6 the measured groundwater table and soil moisture profiles of the field experiment were used to calibrate the model that could be used in long-term calculations. Unfortunately, the present version of the agro-hydrological model SWAP has two disadvantages: 1) it does not calculate the influence of seasonally frozen soil which is necessary to consider in northern latitudes, 2) it does not allow easily perform sequential computations. Therefore the model CROPWATN (Karvonen and Kleemola 1995), developed in Finland, was used in the present study to carry out long-term simulations.

The aim of the present chapter was to compare SWAP and CROPWATN, as well as to implement CROPWATN in long-term hydrological simulations. The analysis included the period 1966-1995 and incorporated available meteorological data obtained from the Tartu Meteorological Station of the Estonian Meteorological and Hydrological Institute.

7.2 Time-series of meteorological values from 1966 to 1995

The time-series of meteorological parameters from 1966 to 1995 were analyzed to find out possible trends in climatic conditions. Only linear trends were analyzed. As the coefficient of determination was negligible in all cases the trends were judged mainly on the basis of the slope, i.e. when the slope was positive then the parameter revealed an increasing trend and *vice versa*. The most noteworthy trends were noted in case of yearly precipitation and average air temperature (Fig. 7.1a and 7.1b). An additional analysis was carried out to find out more details pertinent to the characteristics of these changes. The cumulative curve of the difference P_i-P_{avg}, where P_i was annual precipitation of *i*'s year and P_{avg} was the average for the entire period, revealed successive dry years (decreasing curve) and wet years (increasing curve). Thus, it was found that from 1966 to 1976 all years were characterized by less precipitation than the average for the whole period (P_{avg}=606 mm) and that the wet period started in 1977 (Fig. 7.2).

Annual average temperatures also showed an increasing trend where the difference between the beginning and the end of the trendline was 1.5 C^0 (Fig. 7.1b). *VPD* and R_n did not reveal any trends (Fig. 7.1c), while the estimated potential evapotranspiration *ET* increased slightly (Fig. 7.1a), probably due to increased wind speed ($y = 0.01009x + 2.934$, r^2=0.200). However, it is still not clear how much these changes influence hydrological processes in agricultural fields. To study these effects simulation models can be used.

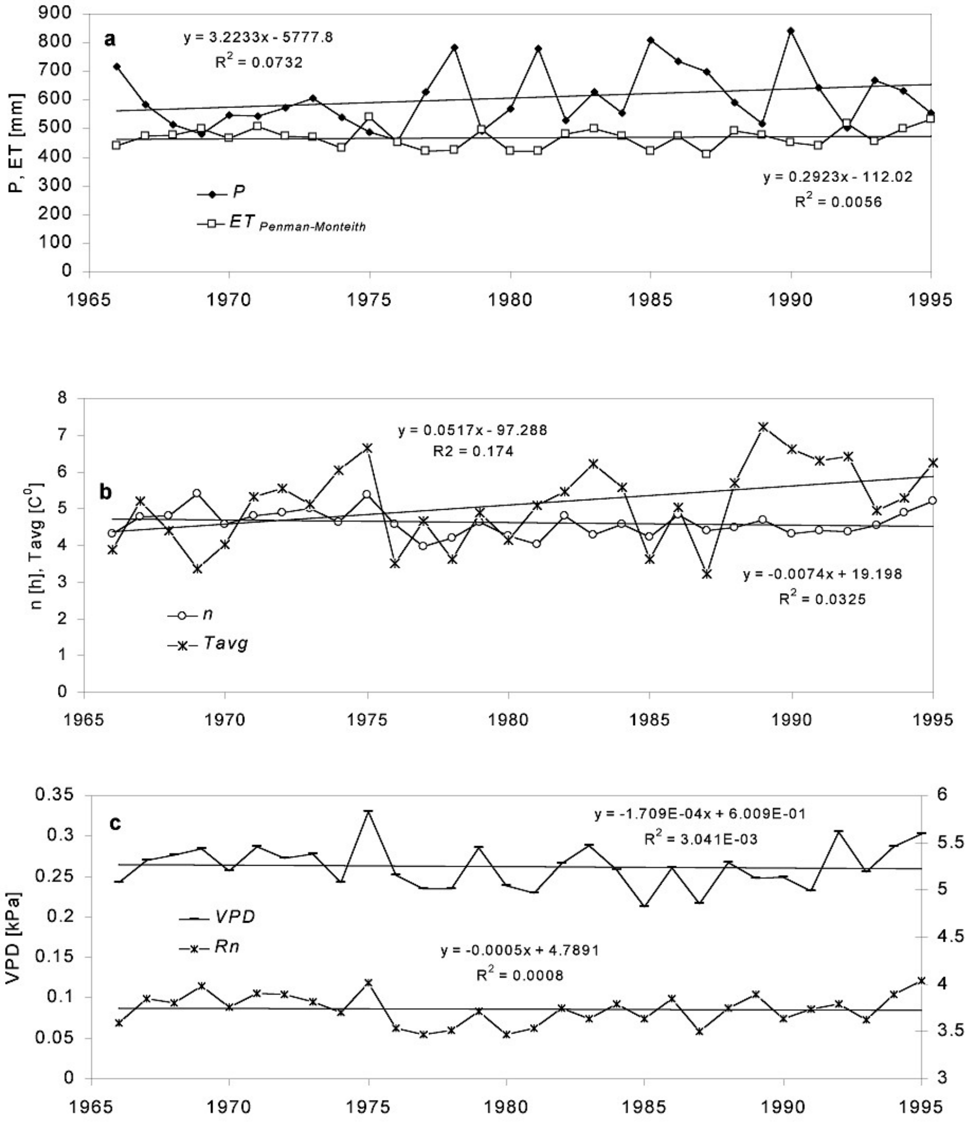

Figure 7.1. Time-series and linear approximation of annual values of a) precipitation *P* and evapotranspiration *ET* estimated with the Penman-Monteith equation, b) yearly average duration of bright sunshine *n* and daily average temperature T_{avg}, and c) vapor pressure deficit *VPD* and net radiation R_n data from 1966 to 1995 observed at the Tartu Meteorological Station.

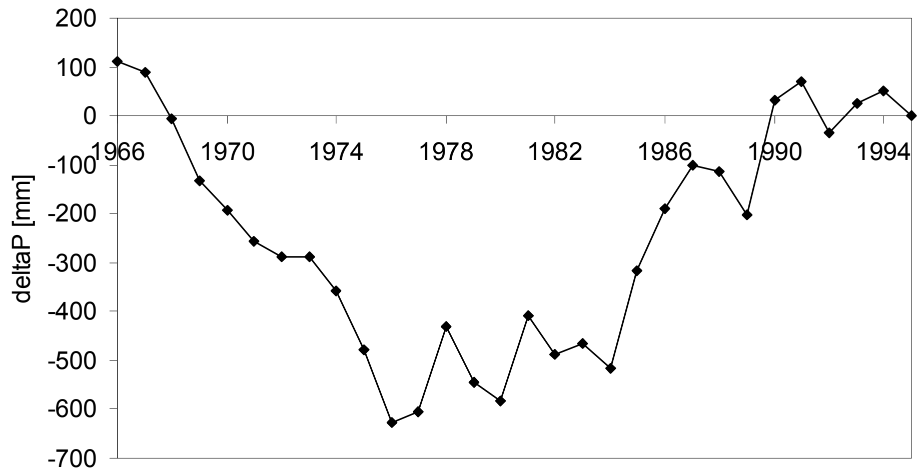

Figure 7.2. Cumulative curve of the difference $\Delta P=P_i-P_{avg}$ showing dry years (negative slope) and wet years (positive slope) on the basis of annual precipitation observed at the Tartu Meteorological Station.

7.3 Comparison of SWAP and CROPWATN

7.3.1 Description of CROPWATN

To study the effect of long-term meteorological conditions on the fluctuation of the groundwater table, drainage runoff and the ratio ET_a/ET the simulation model CROPWATN was used. Analogously to SWAP, the model CROPWATN (Karvonen and Kleemola 1995) focuses on water and crop production on a daily basis, implementing Richards' equation in the model core and solving it by explicit/implicit iterative approximation. Additionally, it includes a frost model (Karvonen 1988) and calculates nitrogen limited crop production and field-scale solute transport in the unsaturated zone (Karvonen et al. 1989a, 1989b).

7.3.2 Comparative calculations with SWAP and CROPWATN

Both SWAP and CROPWATN were initialized with the same values of the soil hydraulic properties (Table 6.1, Mid-plot, modified Andersson's method). From among the available meteorological data, the years with different precipitation data were selected including the driest year 1992 (precipitation 223.9 mm during the period from the 1st of April to the 30th of September) and the wettest year 1985 (618.9 mm). As CROPWATN was originally developed for potato growth then it was adapted to grass covered surfaces by changing the leaf area indices. Calculations were started on the 1st of April with the initial groundwater table at a depth of 100 cm. The results are shown in Fig. (7.3) and Table (7.1).

Cumulative curves revealed that both models yielded very similar results. In 1992 (Figure 7.3a) CROPWATN showed a slightly lower groundwater table at the end of the calculation period due to larger evapotranspiration and the drainage flux (Table 7.1). Similar results were obtained in all selected years, however, the difference decreased with increased precipitation. The main reason for the difference between the results is that crop models calculate the stage of crop development in a slightly different way, which influences actual evapotranspiration rate. Moreover, the root sink term used in CROPWATN is different from that used in SWAP. In CROPWATN, root water uptake is based on a minimum of the work done by plant roots, which may lead to slightly different soil moisture profiles compared with SWAP. In general, the results of both models were satisfactorily close to each other, which allows to assume that the results of long-term calculations made with both CROPWATN and SWAP would be acceptable.

Table 7.1. Comparison of evapotranspiration and the groundwater table at the end of the calculation period and cumulative drainage flux, calculated with CROPWATN and SWAP in selected years.

Year	P mm	Evapotranspiration ET mm	ET_a CROPWATN mm	ET_a SWAP mm	Groundwater table GWL CROPWATN cm	GWL SWAP cm	Drainage flux q CROPWATN mm	q SWAP mm
1992	224	577	399.5	385.3	205.4	200	19.28	18.9
1975	278	585	471.2	460.9	201.4	196.5	20.63	19.4
1973	419	503	477.8	460.8	148.8	144.1	13.86	12.8
1966	484	406	404.2	394.5	85.3	83.9	57.13	53.2
1978	547	459	449.6	440	79.1	76.1	63.8	59.6
1985	619	457	456.5	443.7	78.6	74.6	129.9	124.1

7.4 Long-term calculations with CROPWATN

CROPWATN was used in long-term calculations to study the effect of drainage and soil parameters on the groundwater table, drainage runoff and evapotranspiration. Continuous calculations from 1966 to 1995 were performed with different values of drainage spacing and depth (Table 7.2), also with three different water table management practices: conventional drainage, controlled drainage (applying weir crest at a depth of 80 cm) and subirrigation (adding water to maintain groundwater level at 80 cm during May-August). The soil properties (i.e. parameters of the van Genuchten model) were set at those determined for the Mid-plot (Table 6.1, modified Andersson's method). Drain spacing was based on the Mid-plot's parameters (i.e. 14 m) and both smaller drain spacing, indicating over-drainage (7 m and 10 m), and larger spacing, indicating under-drainage (18 m, 28 m, 42 m), were used in the computations. Drain depth was set at 80 cm to 130 cm with 10 cm intervals. The results of the calculations were plotted as surface graphs (Fig. 7.4-7.6). Additionally, the effect of the saturated hydraulic conductivity of subsoil was studied. K_{sat} was set at 20 cm d^{-1}, 10 cm d^{-1} and 2 cm d^{-1}, where the larger value was equal to that estimated in Table 6.1 and the lowest value was approximately equal to the one determined with Wind's method (Fig. 4.3f).

Table 7.2. Drainage system parameters used in long-term calculations with CROPWATN.

Parameter	Values					
Drainage spacing [m]	7	10	14	18	28	42
Drainage depth [cm]	80	90	100	110	120	130
K_{sat} subsoil [cm d^{-1}]	20	10	2			

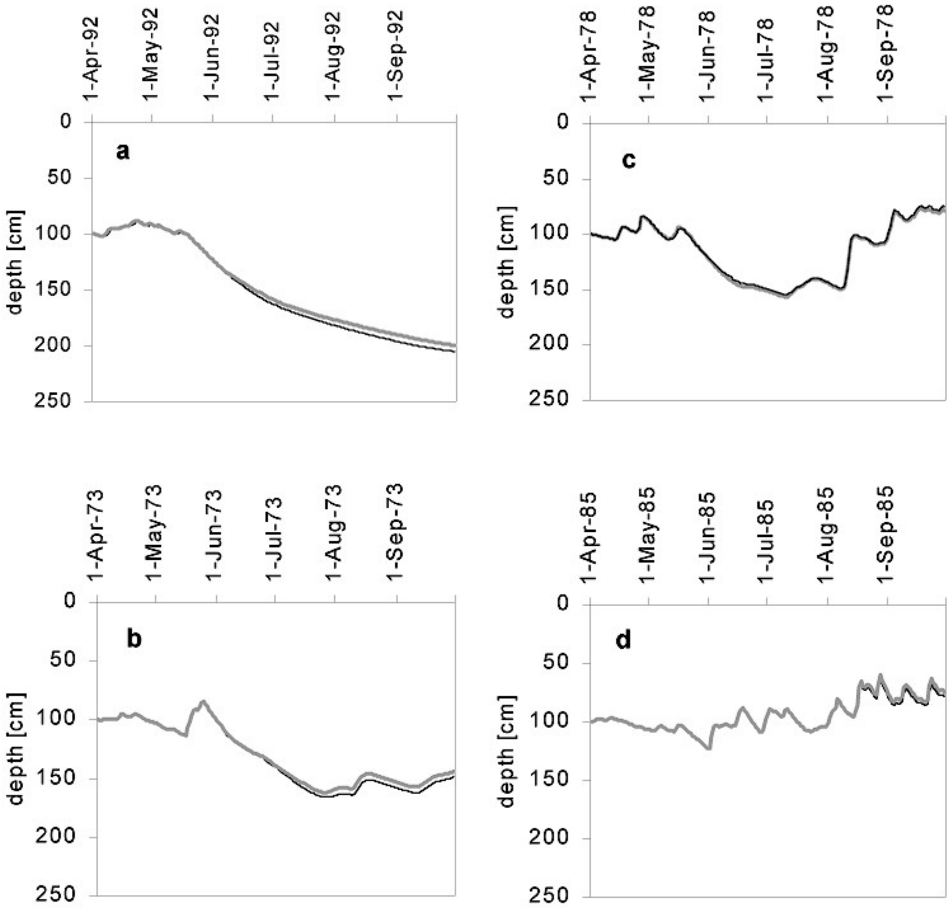

Figure 7.3. Groundwater table in different years calculated with SWAP (thick gray line) and CROPWATN (thin black line).

Figure (7.4) shows that with the present drainage design parameters and K_{sat}=20 cm d^{-1} the yearly average groundwater table was below drainage depth (Fig. 7.4a) and when two drains out of three failured, i.e. L_{drain}=42 m then the yearly average groundwater table was close to drainage depth but still below it. When subsoil's hydraulic conductivity was considered to be lower, i.e. 10 cm d^{-1} and 2 cm d^{-1}, then the yearly average groundwater table was close to drainage depth or above that (Fig. 7.4b,c).

Drainage runoff was almost the same when K_{sat}=20 cm d^{-1} or K_{sat}=10 cm d^{-1} and L_{drain}<=14 m and decreased rapidly with drainage failure (Fig. 7.5a,b). When K_{sat} was set at 2 cm d^{-1} then the effect of drainage spacing and installation depth on drainage runoff was more significant (Fig. 7.5c).

The ratio of actual to potential evapotranspiration revealed water stress either due to water logging or water scarcity. It was found that with selected soil hydraulic properties (i.e. water retention curves and unsaturated hydraulic conductivity curves) and crop (i.e. grassland) the reduction in ET_a/ET was relatively small and the ratio ET_a/ET showed values between 0.92-1.0. In the case of K_{sat}=20 cm d^{-1} the shape of the graph indicated over-drainage, i.e. only the largest spacing and the smallest drainage depth yielded a value close to 1.0 (Fig. 7.6a). In the case of K_{sat}=10 cm d^{-1}, the effect of water logging became also evident (Fig. 7.6b, L_{drain}=42 m and depth=80 cm) and in the case of K_{sat}=2 cm d^{-1}, both types of water stresses were clearly revealed (Fig. 7.6c). According to Fig. (7.6c) the present drainage design is slightly over-sized, i.e. wider drainage spacing will not decrease productivity. In fact, the grassland's ET_a/ET ratio is not very sensitive, as it was almost the same with the spacing range 10 to 28 m. Considerably deeper drainage with smaller spacing would lead to water shortage, and lower drain depth and larger spacing would lead to water logging.

The calculated time series of the groundwater table (Fig. 7.7) showed the influence of dry and wet periods, already described above (see description of Fig. 7.2). During the dry period (years 1967-1972) the groundwater table was lowered below drainage installation depth and during wet years 1972 and 1973 it was raised back to level approximately 1 m below the soil surface. Two dry years, 1975 and 1976, lowered the groundwater table again. The effect of very wet years (1978 - 781 mm, 1985 - 807 mm, 1990 - 840 mm) can also be identified. In long-term simulation it is clearly evident that the influence of the previous year can be significant in many cases. Although in 1989 there was only 518 mm of precipitation, the effect of dryness is less marked due to the effects of previous wet years. One conclusion that can be drawn is that if models are aimed at facilitating strategic (long-term) decision making, it is crucial that simulations are continuous over the calculation period so that the effect of successive wet (or dry) years can be taken into account properly. In other words, long-term simulations should not be carried out for individual years where the same initial condition is the starting point for each year.

Finally, the capacity of CROPWATN to consider different drainage management strategies was demonstrated. Besides conventional drainage, the effect of controlled drainage and subirrigation was analyzed. Figure (7.8) presents the results of a drainage system with drainage depth of 1.0 m and K_{sat} for a subsoil of 20 cm d^{-1}. Similar figures could be easily drawn up for all combinations of K_{sat} and drainage design parameters as described above. The results obtained with the present drainage parameters showed that drainage volume was almost equal in case of conventional and controlled drainage (Fig. 7.8a), which implies that control structures alone cannot create considerable effect on field water regime. This conclusion was validated also by the results of ET_a/ET (Fig. 7.8b) and by the estimates of the average groundwater table (Fig. 7.8c). In case of subirrigation soil water conditions were more favorable, i.e. evapotranspiration occurred at a potential rate. It can be concluded that groundwater modeling serves as a valuable source of information for the long-term sustainability of drainage systems, providing useful data on drainage design, including also possible risks of over-drainage and water logging.

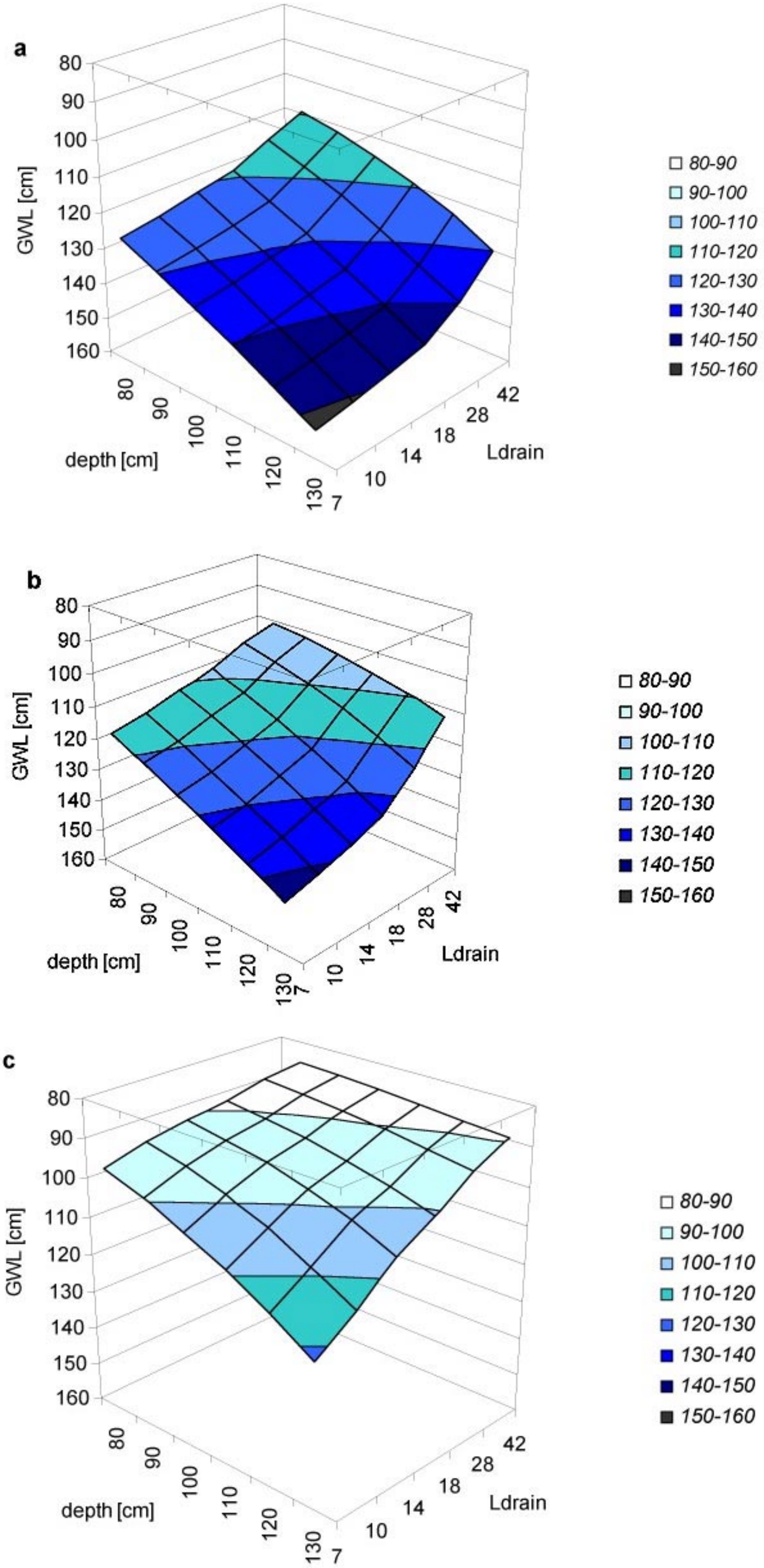

Figure 7.4. The effect of drainage parameters (drain spacing L_{drain} and drain depth) and the value of K_{sat} on the yearly average groundwater table. a) K_{sat} = 20 cm d^{-1}, b) K_{sat} = 10 cm d^{-1}, c) K_{sat} = 2 cm d^{-1} .

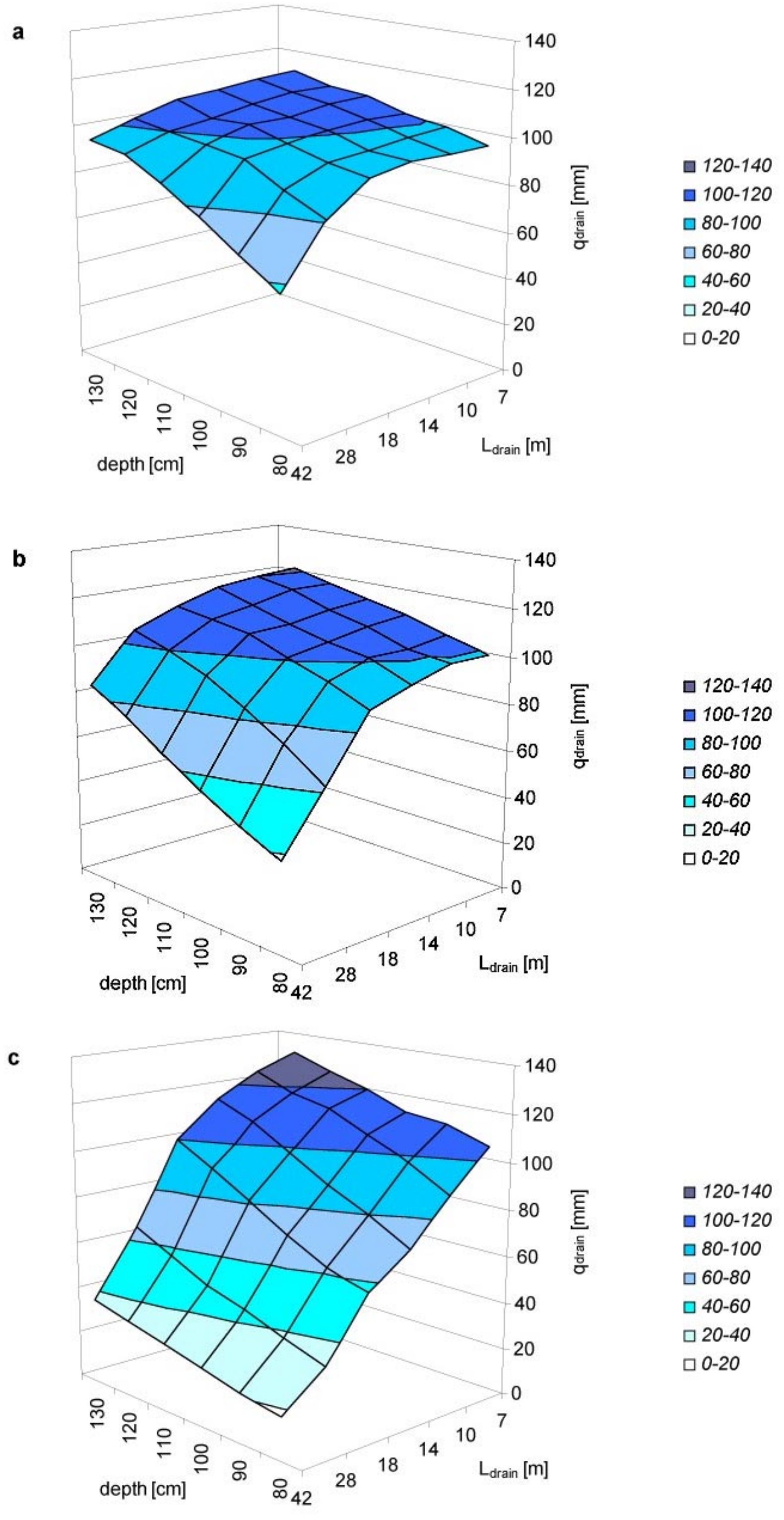

Figure 7.5. The effect of drainage parameters (drain spacing L_{drain} and drain depth) and the value of K_{sat} on yearly drainage runoff. a) K_{sat} = 20 cm d^{-1}, b) K_{sat} = 10 cm d^{-1} c) K_{sat} = 2 cm d^{-1}.

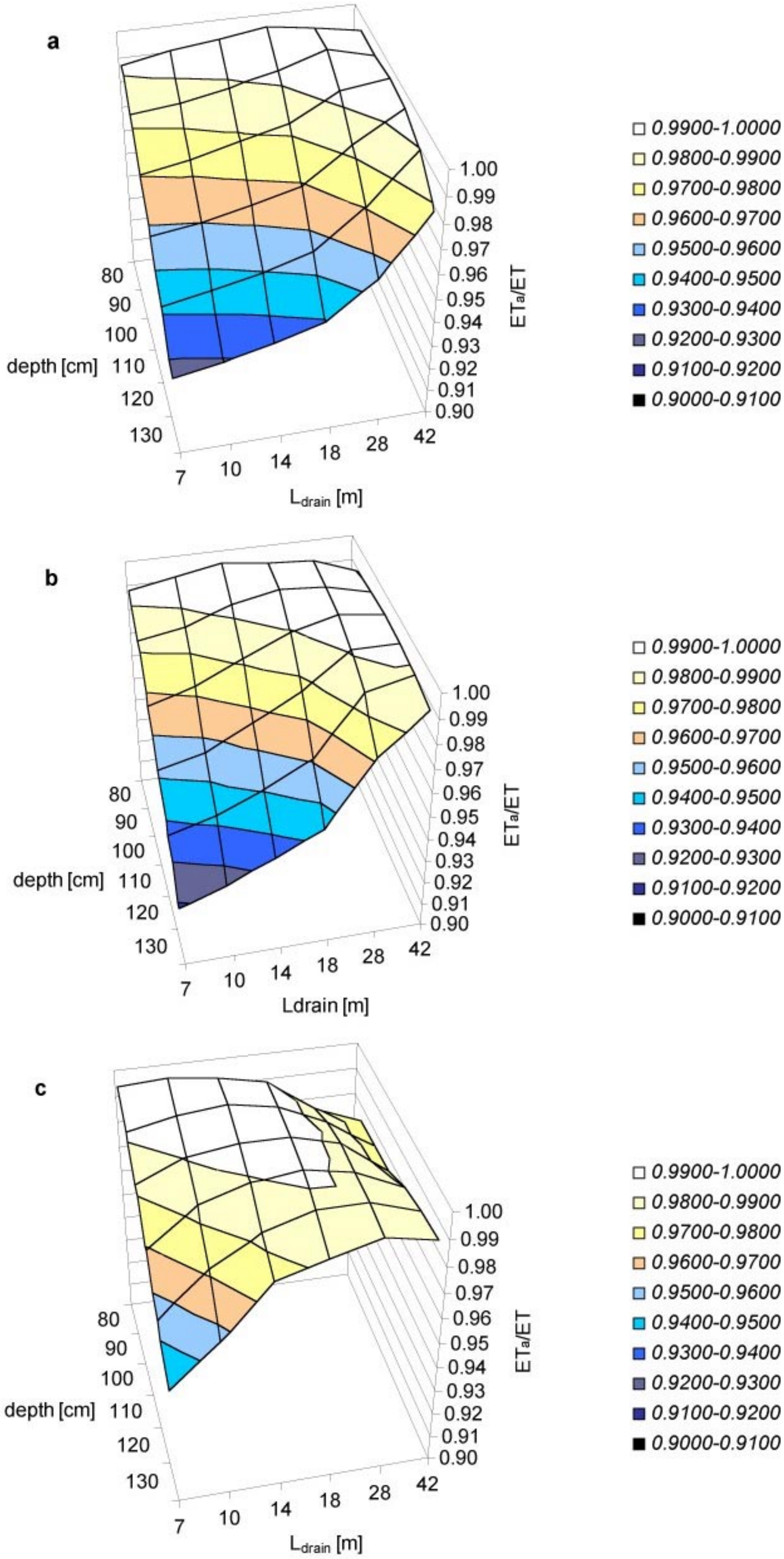

Figure 7.6. The effect of drainage parameters (drain spacing L_{drain} and drain depth) and the value of K_{sat} on the ratio of relative evapotranspiration. a) K_{sat} = 20 cm d^{-1}, b) K_{sat} = 10 cm d^{-1}, c) K_{sat} = 2 cm d^{-1}.

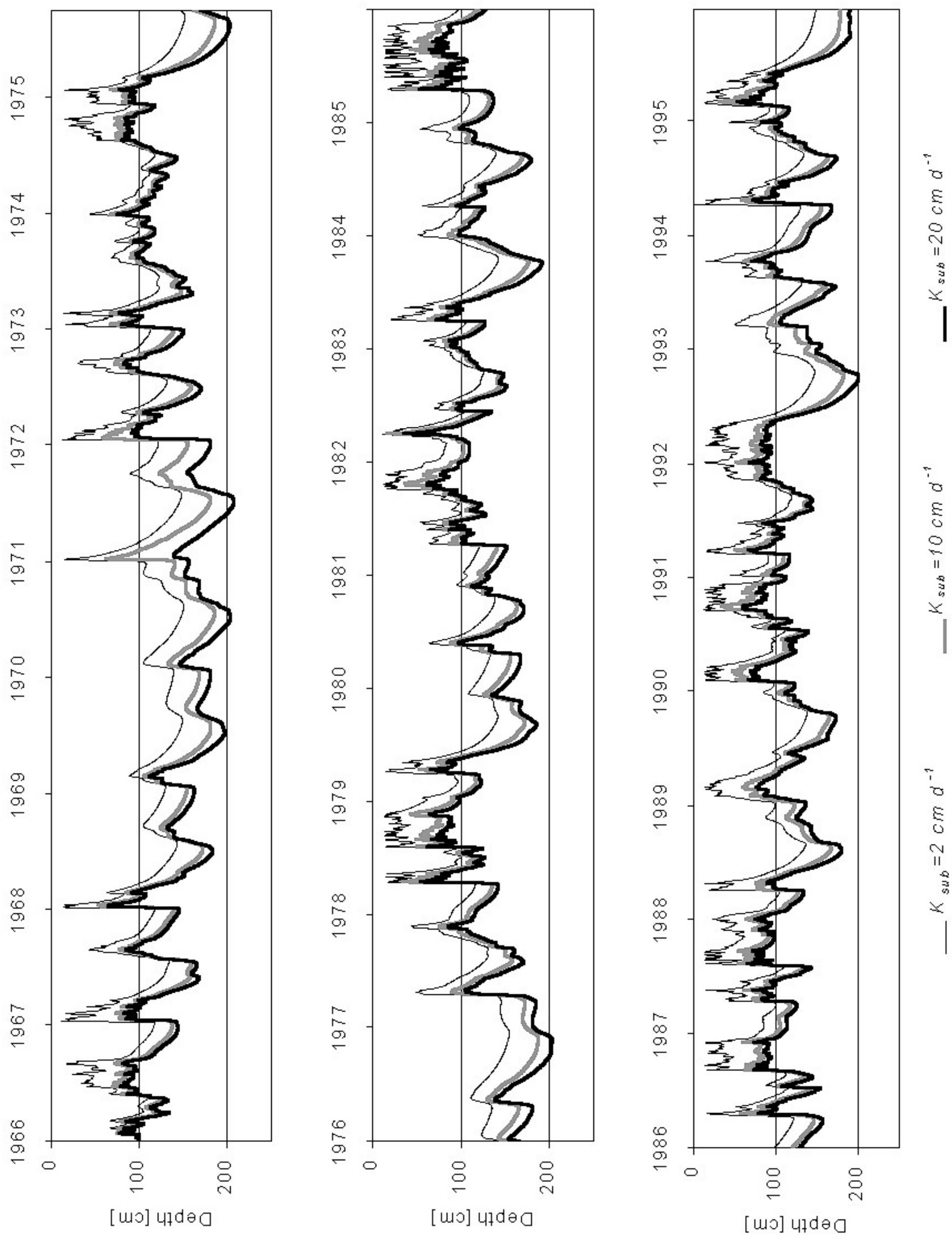

Figure 7.7. Modeled time-series of the groundwater table obtained by CROPWATN, based on long-term meteorological conditions (1966-1995) observed at the Tartu Meteorological Station.

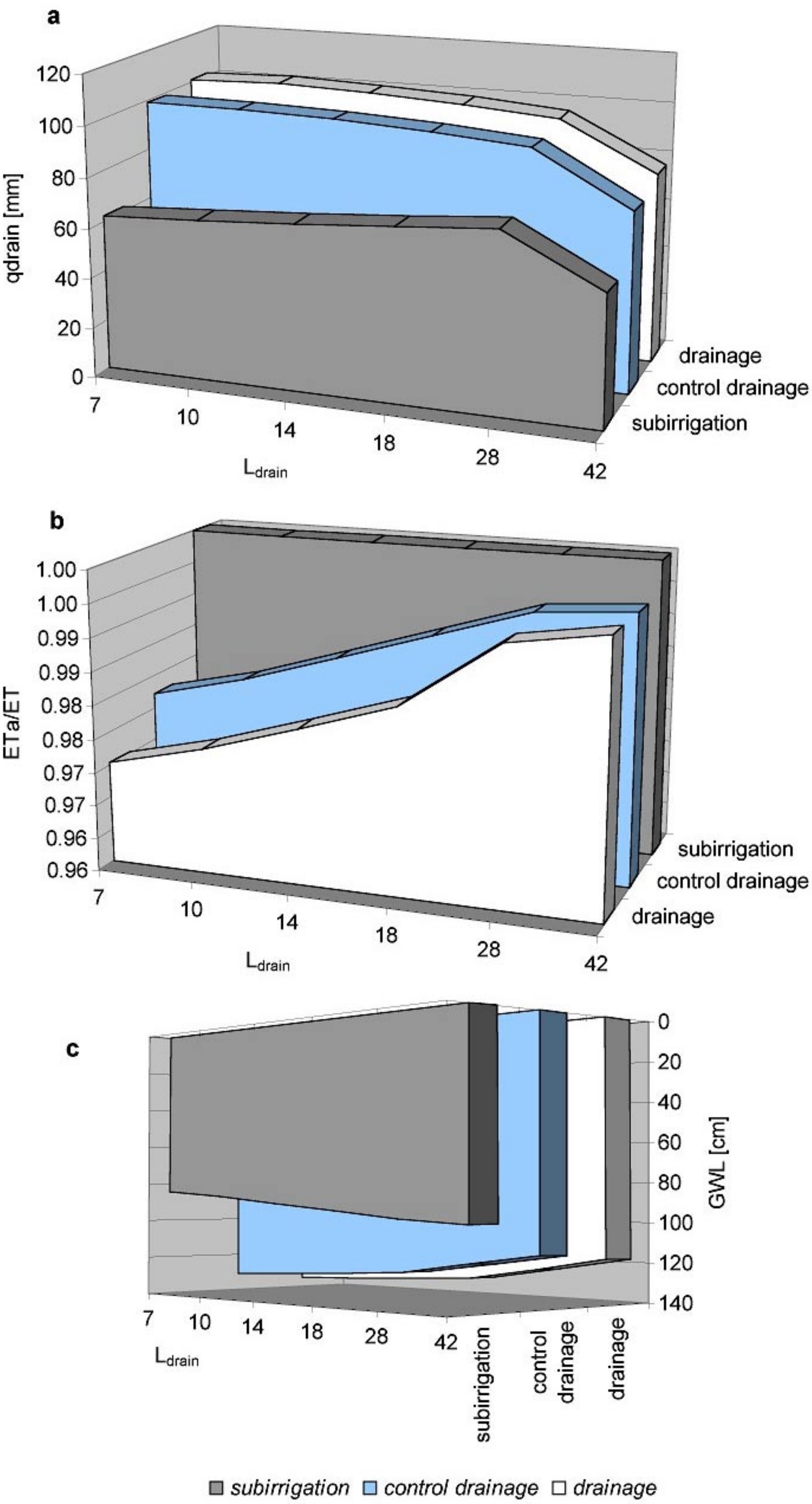

Figure 7.8. Effect of conventional drainage, controlled drainage and subirrigation on a) drainage flux, b) ratio ET_a/ET, and c) average depth of the groundwater table from May to August. K_{sat}=20 cm d^{-1} , drain depth 100 cm.

7.5 Conclusions

Long-term time series of meteorological variables combined with simulation models can provide useful information to be considered in water management studies and in practical designing. It was found that:

1. For the vegetation period the simulation model CROPWATN yields results very similar to those obtained with SWAP. Due to its better properties for making sequential calculations and suitability for a cold climate, CROPWATN can be a useful tool for modeling long-term water balance and crop growth in Estonian conditions.
2. Long-term calculations with several combinations of drain spacing and drain depth can provide useful information about drainage design parameters including the possible risks of over-drainage and waterlogging.
3. Hydrological models aimed at facilitating decision making should simulate continuous long-term time periods in order to take into account the effect of the previous years and, particularly, the effects of successive wet or dry years.

Chapter 8

SUMMARY

1. The standard procedure for estimating net radiation was parameterized with new values to improve the fit with observed radiation in Estonia. The commonly used set of parameters were found to systematically overestimate net radiation during the summer months and underestimate in the winter months. New equations for the net long-wave radiation that may also be used in the Priestley-Taylor equation were developed. Function for calculating clear day total radiation was also developed.
2. Soil heat flux was estimated numerically for both bare soil and grass covered soil. Estimated soil temperatures compared very well with the measured values. The soil heat flux from grass-covered surfaces was less than 10% of the net radiation during the March-September period. The highest soil heat flux, in June (21 MJ m^{-2} $month^{-1}$), was equal to 5.8% of net radiation. The largest relative value, in October (-13.7 MJ m^{-2} $month^{-1}$), was equal to -173.4% of the net radiation.
3. Measured evapotranspiration obtained from the hydraulic pan covered with a clipped grass canopy was used to validate the Penman-Monteith equation in Estonian conditions. In three out of four years the results were very good. The highest coefficient of determination was obtained in May 1985 (r^2=0.922), and the lowest in July 1988 (r^2=0.421). On a monthly basis comprising all years of experimentation the correlation was the best in June (r^2=0.913).
4. It was shown that vapor pressure deficit correlated well with net radiation both on a daily basis (r^2=0.602) and on a long-term monthly basis (r^2=0.976). These results validate the use of the Priestly-Taylor equation in Estonian conditions. A comparison of the measured and estimated evapotranspiration revealed a higher r^2 with the Penman-Monteith method. However the difference between the two methods was small to negligible in several months.
5. Measured evapotranspiration obtained from the hydraulic pan was used to back calculate the canopy resistance. Estimated values showed higher canopy resistance than the commonly used value of 40-70 s m^{-1} for dry days. Estimated canopy resistance was seldom equal or close to zero in rainy days. According to statistical analysis, r_c was not correlated with single meteorological parameters.
6. It was shown on example of June that meteorological variables may have a weak interdependences, i.e. 'typical' conditions, which may be violated in the case of incremental changes. In certain combinations of meteorological and resistance values (in general, days with very low VPD) the Penman-Monteith method may lead to ambiguous results.
7. Water retention curves that were determined with two methods, Wind's evaporation method and Andersson's method, yielded different shapes for water retention curves. In the case of Wind's method the water retention curves were

unexpectedly of a 'clay'-type, although the fraction of clay in the soil samples was small. Andersson's method resulted in 'loamy soil'-type curves.

8. It was found that parameterization of the van Genuchten equations depends not only on the measured or estimated h-Θ-K dataset but also on the choice of the fitting procedure.
9. It was shown that K_{sat} extrapolated from the van Genuchten analytical $K(h)$-equation might overestimate the 'true' value of K_{sat} due to the analytical ambiguity of the van Genuchten equation in near-saturation conditions.
10. The experiment of controlled drainage by raising the water table at a nearby ditch showed that with very simple and low-cost hydraulic structures the water regime in an adjacent field could be affected. The effect of controlled drainage on soil moisture content and groundwater table is strictly depending on the lateral hydraulic conductivity that has to be large enough to compensate the water withdrawal due to capillary flux. Also possibilities to maintain water table in a desired level may be restricted, e.g. due to insufficient discharge from the upper watershed.
11. The agro-hydrological model, SWAP, was used to simulate the controlled drainage experiment. Soil hydraulic functions were parameterized using the results of both Wind's and Andersson's methods. In general, it was difficult to judge which method yielded the best results, because the overall modeling results tended to improve with distance from the ditch and were significantly different for different years. However, Andersson's method produced slightly more accurate results for predicting the soil moisture profiles and for the fluctuation of the groundwater table.
12. The modified soil hydraulic functions that were based on Wind's and Andersson's methods improved the modeling results. The modified water retention curves were very close to the points which were obtained by plotting the tensiometer readings and corresponding volumetric soil water content into the same figure with Wind's and Andersson's curves. This implies that in the present case the use of tensiometers to determine $\Theta(h)$-curve in the field conditions could be possible.
13. Calculated depths of the groundwater table and drainage flux using SWAP and CROPWATN (developed in Finland) were almost identical. However, CROPWATN has an advantage as it includes a frost model that is necessary for the long-term continuous simulations in Estonian conditions.
14. CROPWATN was used to calculate continuous simulations comprising a 30-year period. The effect of long-term meteorological conditions revealed that hydrological models aimed at facilitating decision making should simulate continuous long-term time periods in order to take into account the effect of the previous years, and particularly the effects of successive wet or dry years.
15. Continuous simulation with CROPWATN over a period of 30 years using different drainage design parameters, soil properties and water management strategies allowed to evaluate corresponding effects on hydrological processes in the agricultural fields.

References

Abbaspour, K.C., M.Th. van Genuchten, R. Schulin and E. Schläppi (1997). A sequential uncertainty domain inverse procedure for estimating subsurface flow and transport parameters. Water Resour. Res. 33:1879-1892.

Abbaspour, K.C., M.A. Sonnleitner and R. Schulin (1999). Uncertainty in estimation of soil hydraulic parameters by inverse modeling: example lysimeter experiment. Soil Sci. Soc. Am. J. 63:501-509.

Abdirashid, A.E, M.H. Egeh, C.A. Madramootoo and C. Hamel (1998). Water table and N-fertilizer rate management effect on water quality and corn yield. In: Drainage in the 21st Century: Food Production and the Environment. Proceedings of the Seventh International Drainage Symposium. 8-10 March 1998, Orlando, Florida, Larry C. Brown (Ed.) Published by American Society of Agricultural Engineers, USA, pp. 380-386.

Abtew, W. (1996). Evapotranspiration measurements and modeling for three wetland systems in south Florida. Wat. Res. Bulletin. 32(3):445-473.

Abtew, W. and J. Obeysekera (1995). Lysimeter study of evapotranspiration of cattails and comparison of three estimation methods. Trans. ASAE 38(1):121-129.

Ahuja, L.R., J.W. Naney and R.D. Williams (1985). Estimating soil water characteristics from simpler properties or limited data. Soil. Sci. Soc. Am. J. 49:1100-1105.

Allen, R.G. and D.K. Fisher (1990). Low cost electronic weighing lysimeters. Trans. ASAE 122(2):97-106.

Allen, R.G., M.E. Jensen, J.L. Wright and R.D. Burman (1989). Operational estimates of evapotranspiration. Agron. J. 81:650-662.

Allen, R.G., L.S. Pereira, D. Raes and M. Smith (1998). Crop evapotranspiration - Guidelines for computing crop water requirements - FAO Irrigation and drainage paper 56. Food and Agriculture Organization of the United Nations, Rome.

Al-Soufi, R. (1983). Unsaturated hydraulic conductivity. Thesis for the degree of Licenciate in Technology. Helsinki University of Technology, Laboratory of Water Resources, 77 pp.

Alves, I. and L.S. Pereira (2000). Modelling surface resistance from climatic variables? Agric. Water Manage. 42:371-385.

Anderson, J.L. and J. Bouma (1973). Relationship between saturated hydrauic conductivity nd morphometric data of an agrillic horizon. Soil Sci. Soc. Am. J. 37:408-413.

Andersson, S. (1990a). Markfysikaliska undersökningar i odlad jord, XXVII Kornkurvor, Teoretiska exempel, analys och kommentarer. Sweriges Lantbruksuniversitet, Uppsala, 155 pp.

Andersson, S. (1990b). Markfysikaliska undersökningar i odlad jord, XXVIII Bindningskurvor, por- och kornkurvor, En matemetiskt strukturerad model. Sveriges Lantbruksuniversitet, Uppsala, 155 pp.

Ångström, A. (1924). Solar and terrestrial radiation. Q.J.R. Meteorol. Soc. 50:121-125.

Ankeny, M.D., T.C. Kaspar and R. Horton (1988). Design for an automated tension infiltrometer. Soil Sci. Soc. Am. J. 52:893-895.

Ankeny, M.D., T.C. Kaspar and R. Horton (1990). Characterization of tillage and traffic effects on unconfined infiltration measurements. Soil Sci. Soc. Am. J. 54:837-840.

Arya, L.M. and J.F. Paris (1981). A physioempirical model to predict the soil moisture characteristics from particle-size distribution and bulk density data. Soil Sci. Soc. Am. J. 45:1023-1030.

Barton, I.J. (1979). A parameterization of the evaporation from a nonsaturated surface. J. Appl. Meteorol. (18):43-47.

Belmans, C., J.G. Wesseling and R.A. Feddes (1983). Simulation of the water balance of a cropped soil:SWATRE. J. Hydrol. 63:271-286.

Bergström, L., H. Johansson and G. Torstensson (1991). Simulation of soil nitrogen dynamics using the SOILN model. Fert. Res. 27:181-188.

Beven, K. (1979). A sensitivity analysis of the Penman-Monteith actual evapotranspiration estimates. J. Hydrol. 44:169-190.

Bierkens, M.F.P., P.J.T. van Bakel and J.G. Wesseling (1999). Comparison of two modes of surface water control using a soil water model and surface elevation data. Geoderma 89:149-175.

Bihele, Z., H. Moldau and J. Ross (1980). 'Matematitsheskoe modelirovanie transpiratsii i fotosinteza rastenii pri nedostatke potshvennoi vlagi' (*in Russian*) - 'Matematical modeling of transpiration and photosynthesis in case of insufficient soil moisture conditions'. Leningrad, 209 pp.

Booltink, H.W.G., J. Bouma and D. Gimenez (1991). A suction crust infiltrometer for measuring hydraulic conductivity of unsaturated soils near saturation. Soil Sci. Soc. Am. J. 55:566–568.

Bormann, H., B. Diekkrüger and O. Richter (1996). Effects of data availability on estimation of evapotranspiration. Phys. Chem. Earth 21(3):171-175.

Bouma, J. (1983). Use of soil survey data to select measurement techniques for hydraulic conductivity. Agric. Water Manage. 6:177-190.

Bouma, J. (1989). Using soil survey data for quantitative land evaluation. Adv. Soil Sci. 9:177-213.

Brady, N.C. (1984). The nature and properties of soils. Ninth edition, 750 pp.

Brooks, R.H. and A.T. Corey (1964). Hydraulic properties of porous media. Hydrology paper 3, Colorado State University, 27 pp.

Brown, L.C. (Ed.) (1998). Drainage in the 21st Century: Food Production and the Environment. Proceedings of the Seventh International Drainage Symposium. 8-10 March 1998, Orlando, Florida, Published by ASAE, USA, 738 pp.

Brutsaert, W. (1967). Some methods of calculating unsaturated permeability. Trans. ASAE 10:400-404.

Buchter, B., C. Hinz, H. Wydler and H. Flühler (1999). Evaluation of temperature and bypass flow sensitivity of tensiometers in a field soil. Geoderma 87:281-291.

Burman, R.D. and L. O. Pochop (1994). Evaporation, Evapotranspiration and Climatic Data. Elsevier Science, 302 pp.

Campbell G.S. (1985). Soil Physics with Basics. Elsevier, New York.

Camuffo, D. and A. Bernardi (1982). An observational study of heat flux and the relationship with net radiation. Boundary-Layer Meteorol. 23:359-368.

Carslaw, H.S. and J.C. Jaeger (1959). Conduction of heat in Solids. Oxford University Press, London.

Climate of Tartu and its changes during the recent decades (1980). Est. Academy of Sciences, Inst. of Astrophysics and Atmospheric Physics (*in Estonian* with English summaries), 182 pp.

Clothier, B.E. and I. White (1981). Measurements of sorptivity and soil water diffusivity in the field. Soil Sci. Soc. Am. J. 45:241-245.

Clothier, B.E. and K.R.J. Smettem (1990). Combining laboratory and field measurements to define the hydraulic properties of soil. Soil Sci. Soc. Am. J. 54:299-304.

Collatz, G.J., J.T. Ball, C. Grivet and J.A. Berry (1991). Physiological and environmental regulation of stomatal conductance, photosynthesis and transpiration: a model that includes a laminar boundary layer. Agric. For. Meteorol. 54: 107-136.

Crago, R.D. (1996). Comparison of the evaporative fraction and the Priestley-Taylor a for parameterizing daitime evaporation. Water Res. Research. 32(5): 1403-1409.

Culf, A.D. (1994). Equilibrium evaporation beneath a growing convective boundary layer. Boundary-Layer Meteorol. 70:37-49.

Dam, J.C. van, J. Huygen, J.G. Wesseling, R.A. Feddes, P.Kabat, P.E.V. van Walsum, P. Groenendijk and C.A. van Diepen (1997). Theory of SWAP version 2.0. Simulation of water flow, solute transport and plant growth in the Soil-Water-Atmosphere-Plant environment. Wageningen Agricultural University and DLO Winand Staring Centre. Technical Document 45. 168 pp.

Dam, J.C. van (2000). Field-scale water flow and solute transport. SWAP model concepts, parameter estimation, and case studies. PhD-thesis, Wageningen University, Wageningen, The Netherlands, 167 pp.

Dam, J.C. van and R.A. Feddes (2000). Numerical simulation of infiltration, evaporation and shallow groundwater levels with the Richards equation. J. Hydrol. 233:72-85.

Dam, J.C. van, J.N.M. Stricer and P. Droogers (1994). Inverse method to determine soil hydraulic functions from multistep outflow experiment. Soil Sci. Soc. Am. J. 58:647-652.

Davies, J.A. and C.D. Allen (1973). Equilibrium, potential and actual evaporation from cropped surfaces in Southern Ontario. J. Appl. Meteorol. 12(4):649-657.

de Bruin, H.A.R. and J.O. Keijman (1979). The Priestley-Taylor model applied to a large shallow lake in the Netherlands. J. Appl. Meteorol. 18:898-903.

De Jong, R. and P. Kabat (1990). Modeling water balance and grass production. Soil Sci. Soc. Am. J. 54:1725-1732.

Devlin, R. (1975). Plant Physiology 3rd edition, Van Nostrand Reinhold ltd./Canada.

Dierickx, W. (1993). Research and developments in selecting subsurface drainage materials. Irrig. and Drain. Systems 6:291-310.

Doorenbos, J. and W.O. Pruitt (1977). Guidelines for predicting crop water requirements, Food and Agriculture Organization United Nations, FAO Irrigation and Drainage Paper 24, 2nd Ed., Rome, 156 pp.

Dorsey, J.D., A.D. Ward, N.R. Fausey and E.S. Bair (1990). A comparison of four field methods for measuring saturated hydraulic conductivity. Trans. ASAE 33(6):1925-1931.

Durand, R. (1975). Estimation du rayonnement global apartir de la durée d'insolation. Ann. Agron. 25:779-795.

Durner, W. (1991). Vorhersage der hydraulischen Leitfähigkeit strukturierter Böden. Bayreuther Bodenkundliche Berichte, Band 20. Bayreuth.

Eichinger W.E., M.B. Parlange and H. Sticker (1996). On the concept of equilibrium evaporation and the value of the Priestley-Taylor coefficient. Water Resour. Res. 32(1):161-164.

Elmaloglou, St. and N. Malamos (2000). Simulation of soil moisture content of a prairie field with SWAP93. Agric. Water Manage. 43:139-149.

Ernst, L.F. (1954). Het berekenen van stationaire groundwaterstromingen, welke in een verikaal vlak afgebeeld kunnen worden [The computation of steady state groundwater flows, which can be projected in the vertical plane]. Rapport IV. Landbouwproefstation en Bodemk. Inst. T.N.O. Groningen, The Netherlands.

Evans, R.O., J.W. Gilliam and R.W. Skaggs (1989). Effect of agricultural water table management on drainage water quality. Report 237 of the Water Resource Research Institute of the University of North Carolina.

Feddes, R.A., P.J. Kowalik and H. Zaradny (1978). Simulation of field water use and crop yield. Simulation Monographs, Pudoc, Wageningen, 189 pp.

Feddes, R.A. (1986). Modelling and simulation in hydrologic systems related to agricultural development: state of the art. Intern. symp. 'Water management for agricultural development', Athens, 7-11 April. In: EWRA-publ. 1:131-146.

Feddes, R.A., R.W.R Koopmans and J.C. van Dam (1997). Agrohydrology. Wageningen University, Department of Environmental Sciences, the Netherlands.

Fernandez, G.P, G.M.Chescheir and R.W. Skaggs (1998). DRAINMOD 5.0:A windows version that considers crop yield, nitrogen and salinity. In: Drainage in the 21st Century: Food Production and the Environment. Proceedings of the Seventh International Drainage Symposium. 8-10 March 1998, Orlando, Florida, Larry C. Brown (Ed.) Published by American Society of Agricultural Engineers, USA, pp. 220-226.

Fowler, D. and M.H. Unsworth (1979). Turbulent transfer of sulphur dioxide to a wheat crop. Q. J. R. Meteorol. Soc. 105:767-783.

Gardner, W.R. and F.J. Miklich (1962). Unsaturated conductivity and diffusivity measurements by a constant flux method. Soil Sci. 93:271-274.

Gates, D.M. (1980). Biophysical Ecology. Springner-Verlag, New York.

Genuchten, M. Th. van (1980). A closed form equation for predicting the hydraulic conductivity of unsaturated soils. Soil Sci. Soc. Am. J. 44:892-898.

Gavin. H. and C.T. Agnew (2000). Estimating evaporation and surface resistance from a wet grassland. Phys. Chem. Earth (B) 25(7-8):599-603.

Genuchten, M. Th. van and D.R. Nielsen (1985). On describing and predicting the hydraulic properties of unsaturated soils. Ann. Geophysicae 3:615-628.

Glover, J. and J.S.G. McCulloch (1958). The empirical relation between solar radiation and hours of sunshine. Q. J. R. Meteorol. Soc. 84:172-175.

Grinsven, J.J.M. van, C. Dirksen and W. Bouten (1985). Evaluation of hot air method for measuring soil water diffusivity. Soil Sci. Soc. Am. J. 49:1093-1099.

Groen, K.P. (1997). Pesticide leaching in polders. Field and model studies on cracked clays and loamy sand. PhD-thesis, Wageningen University, 296 pp.

Gupta, S.C and W.E. Larson (1979). Estimating soil water characteristics from particle size distribution, organic matter percent, and bulk density. Water Resour. Res. 15:1633-1635.

Gupta, S.C, J.K. Radke and W.E. Larson (1981). Predicting temperatures of bare and residue covered soils with and without a corn crop. Soil. Sci. Soc. Am. J. 45:405-412.

Haan, C.T., B. Allred, D.E. Storm, G.J. Sabbagh and S. Prabhu (1995). Statistical procedure for evaluating hydrologic/water quality models. Trans. ASAE 38(3):725-733.

Hack-ten Broeke, M.J.D. (2000). Nitrate leaching from dairy farming on sandy soils. Case studies for experimental farm De Marke. PhD-thesis, Wageningen University, 145 pp.

Halbertsma, J.M. and G.J. Veerman (1994). A new calculation procedure and simple set-up for the evaporation method to determine soil hydraulic functions. Wageningen (The Netherlands), DLO Winand Staring Centre, Report 88, 25 pp.

Halbertsma, J.M. and G.J. Veerman (1997). Determination of the unsaturated conductivity and water retention characteristics using the Wind's evaporation method. In: Manual for soil physical measurements, J. Stolte (ed.). Wageningen, DLO Winand Staring Centre, Technical Document 37:47-55.

Hale, M.G. and D.M. Orcutt (1987). The physiology of plants under stress. A Wiley-interscience publication.

Halldin, S. (1988). Swedish evaporation research. A review. Nordic Hydrol. 19:303-340.

Hanna, L.W. and M. Siam (1981) The empirical relation between sunshine and radiation and its use in estimating evaporation in North-East England. J. Climatol. 1:11-19.

Hargreaves, G.H. and Z.A. Samani (1982). Estimating potential evapotranspiration. J. Irrig. and Drain. Eng., ASCE, 108(3):223-230.

Haverkamp, R. and J.-Y. Pralange (1986). Predicting the water-retention curve from particle-size distribution: 1. Sandy soils without organic matter. Soil Sci. 142:325-339.

Hillel, D. (1998). Environmenrtal soil physics. Academic Press, 757 pp.

Homaee, M. (1999). Root water uptake under non-uniform transient salinity and water stress. Ph.D. Thesis, Wageningen Agricultural University, 171 pp.

Hooghoudt, S.B. (1940). Algemeene beschouwing van het probleem van de detailontwatering en de infiltratie door middle van parallel loopende drains, greppels, slooten, en kanalen. Versl. Landbouwk. Onderz. 46 (14)B. Algemeene Landsdrukkerij,'s-Gravenhage, 193 pp.

Hopmans, J. W., K.C., Roy and W.W. Wallender (1991). Irrigation water management and soil-water hysteresis – a computer modeling study with stochastic soil hydraulic properties. Trans. ASAE, 34(2):449-459.

Howell, T.A, J.L. Steiner, A.D.Schneider and S.R. Evett (1995). Evapotranspiration of irrigated winter wheat – southern high plains. Trans. ASAE, 38(3):745-759.

Howell, T.A, S.R. Evett, A.D. Schneider, R.W. Todd and J.A. Tolk (1998). Evapotranspiration of irrigated fescue grass in a semi-arid environment. An ASAE Annual International Meeting, Orlando, Florida, July 12-16, 1988. Paper No. 982117.

Hussein, A.S.A. (1999). Grass ET estimates using Penman-type equations in central Sudan. J. Irrig. and Drain. Eng., ASCE, 125(6):324-329.

Hutson, J.L. and R.J. Wagenet (1992). LEACHM. Leaching Estimation And CHemistry Model: A process based model of water and solute movement, transformations, plant uptake and chemical reactions in the unsaturated zone. Version 3. Dept of Agronomy, Cornell University, Ithaca, NY.

Idso, S.B., R.D. Jackson, P.J. Pinter, G.J. Reginato and J.L. Hatfield (1981). Normalizing the stress-degree-day parameter for environmental variability. Agric. Meteorol. 24:45-55.

IPCC, (Intergovernmental Panel on Climate Change) (1990). Climate Change, The IPCC Scientific Assessment. (Eds) J.T. Houghton, G.J. Jenkins and J.J. Ephraums. Cambridge University Press, Cambridge, UK.

IPCC, (Intergovernmental Panel on Climate Change) (1996). Climate change 1995: The science of climate change. Eds. J.T. Houghton, L.G. Meira Filho, B.A. Callander, N. Harris, A. Kattenberg, and K. Maskell. Cambridge Univerity Press, Cambridge, UK.

Jackson, R.D., S.B. Idso, R.J. Reginato and P.J. Pinter (1981). Canopy temperature as a crop stress indicator. Water Resour. Res. 17:1133-1138.

Jacobs, C.M.J., B.J.J.M van den Hurk, and H.A.R. de Bruin (1996). Stomatal behaviour and photosynthetic rate of unstressed grapevines in semi-arid conditions. Agric. For. Meteorol. 80:11-134.

Jansson, P.-E. (1998). Simulation model for soil water and heat conductions. Description of the SOIL model. Dept. of Soil Sciences. Swedish Univ. of Agric. Sci. 76 pp.

Jarvis, H.G. (1976) The interpretation of the variations in leaf water potential and stomatal conductance found in canopies in the field. Phil. Trans. R. Soc. Lon. B. 273:595-610.

Jarvis, N.L. and I. Messing (1995). Near-saturated hydraulic conductivity in soils of contrasting texture measured by tension infiltrometers. Soil Sci. Soc. Am. J. 59:27-34.

Jarvis, N.L., I. Messing and M.H.Larsson (1997). Measurement and prediction of near-saturated hydraulic conductivity for use in dual-porosity models. In: Characterization and measurement of the hydraulic properties of unsaturated porous media. (Eds.) M.Th. van Genuchten, F.J. Leij, L. Wu. Proceddings of the International Workshop on Characterization and measurement of the hydraulic properties of unsaturated porous media. Riverside, California, October 22-24, 1997, pp. 839-850.

Jarvis, N.L. and M.H. Larsson (1998). The MACRO model (Version 4.1). Technical description. http://130.238.110.134:80/bgf/Macrohtm/macro.htm

Jauhiainen, M. (2000). Hydraulic properties of Finnish forest soils. Licentiate's thesis. University of Helsinki, Dept of For. Ecol.

Jensen, M.E., R.D. Burman and R.G. Allen (1990). Evapotranspiration and irrigation water requirements. ASCE Manuals and Reports on Engineering Practice No. 70, 332 pp.

Jhorar, R.K., W.G.M Bastiaanssen, R.A. Feddes, and J.C. van Dam (2002). Inversely estimating soil hydraulic functions using evapotranspiration fluxes. J. Hydrol. 258:198-213.

Johnsson, H., L. Bergström, P-E. Jansson and K. Paustian (1987). Simulated nitrogen dynamics and losses in a layered agricultural soil. Agric. Ecosyst. Environ. 18:333-356.

Jonasson, S.A. (1991). Estimation of soil water retention for natural sediments from grain size distribution and bulk density. Geologiska institutionen CTH/GU, Publ. A 62. Goteborg, Sweden.

Jones, H.G. (1983). Plants and microclimate: a quantitative approach to environmental plant physiology. Cambridge University Press, Cambridge.

Jury, W.A. (1991). Soil physics. John Wiley and Sons, Inc. Chapter 2. pp. 34-70.

Järvet, A. (1998). An assessment of the climatic change impact on groundwater regime. In: Climate Change Studies in Estonia, Eds. T.Kallaste and P.Kuldna. Tallinn. pp. 111-116.

Kabat, P., B.J. van der Broek and R.A. Feddes (1992). SWACROP: A water management and crop production simulation model. ICID Bulletin 92, vol. 41, no. 2:61-84.

Kalita, P.K. and R.S. Kanwar (1993). Effect of water-table management practices on the transport of nitrate-N to shallow groundwater. Trans. ASAE 36(2):413-422.

Kaluli, J.W, C.A. Madramootoo, X. Zhou, A.F. MacKenzie and D. L. Smith (1999). Subirrigation systems to minimize nitrate leaching. J. Irrig. and Drain. Eng. 125(2):52-58.

Karvonen, T. (1988). A model for predicting the effect of drainage on soil moisture, soil temperature and crop yield. PhD-thesis. In Finnish. Helsinki University of Technology, Otaniemi. 215 pp.

Karvonen, T. and J. Kleemola (1995). Chapter IV-6: CROPWATN: prediction of water and nitrogen limited potato production. In: P. Kabat, B. Marshall, B.J. van der Broek, J. Vos and H. van Keulen (Eds): Modelling and parameterization of the Soil-Plant-Atmosphere system. A comparison of potato growth models. Wageningen Pers. pp. 335-369.

Karvonen, T., H. Laurila, J. Kleemola, A. Ilola and J. Poikselkä (1989a). Interactive simulation programs for teaching and research, Program I: Computation of potential crop production on a daily basis. University of Helsinki, Department of Crop Husbandry, Publication No. 21, 52 pp.

Karvonen, T., M. Paasonen-Kivekäs and P. Vakkilainen (1989b). Nitrogen movement, transformation and uptake by plant roots. University of Helsinki, Research Report 1989, 5 pp.

Kask, R. (1996). Eesti mullad (*in Estonian*, Estonian soils), 239 pp.

Kashyap, P.S. and R.K. Panda (2001). Evaluation of evapotranspiration estimation methods and development of crop-coefficients for potato crop in a sub-humid region. Agric Wat. Manage. 50:9-25.

Kaufmann, M.R. (1982). Leaf conductance as a function of photosynthetic photon flux density and absolute humidity difference from leaf to air. Plant Physiol. 69:1018-1022.

Keevallik, S. (1998). Climate change scenarios for Estonia. In: Climate Change Studies in Estonia, Eds T.Kallaste and P.Kuldna. Tallinn, pp. 1-6.

Kelliher, F.M., R. Leuning and E.-D. Shulze (1993). Evaporation and canopy characteristics of coniferous forests and grasslands. Oecologia 95:153-163.

Kincaid, D.C. and D.F Heermannn (1974). Scheduling irrigation using a programmable calculator, USDA ARS-NC-12

Kitse, E. (1978). Mullavesi (*in Estonian*, Soil water), 142 pp.

Kirkham, D. and W.L. Powers (1972). Advanced Soil Physics. John Wiley & Sons, Inc., New York.

Klein de, C.A.M and R.S.P. van Logtestijn (1996). Denitrification in grassland soils in the Netherlands in relation to irrigation, N-application rate, soil water content and soil temperature. Soil Biol. Biohem. Vol. 28 No. 2:231-237.

Kliewer, B.A. and J.W. Gilliam (1995). Water table management effects on denitrification and nitrous oxide Evolution. Soil. Sci. Soc. Am. J. 59:1694-1701.

Klute, A. (1986). Water retention: laboratory methods. In: Methods of soil analysis; Part 1; Physical and Minearological methods, A. Klute (Ed.), Agronomy series no 9, ASA and SSSA, Madison, Wisconsin, pp. 635-662.

Kohler, A., K.C. Abbaspour, M. Fritsch, M. Th. van Genuchten and R. Schulin (2001). Simulating unsaturated flow and transport in a macroporous soil to tile drains subject to an entrance head: model development and preliminary evaluation. J. Hydrol. 245:67-81.

Kolyasev, F.E. and A.I. Gupalo (1958). On the correlation of heat and moisture properties of soils. Publication No. 629 (Special Report No. 40) Highway Res. Bd, Nat. Acad. Sci., Washington, pp. 106-112.

Kool, J.B. and J.C. Parker (1987). Development and evaluation of closed form expressions for hysteretic soil hydraulic properties. Water Resour. Res. 23:105-114.

Kool, J.B., J.C. Parker, and M.Th. van Genuchten (1987) Parameter estimation for unsaturated flow and transport models – a review. J. Hydrol. 91:255-293.

Kustas, P.W., D.I. Stannard and K. J. Allwine (1996). Variability in surface energy flux partitioning during Washita '92: Resulting effects on Penman-Monteith and Prietley-Taylor parameters. Agric. For. Meteorol. 82:171-193.

Lalonde, V., C.A. Madramootoo, L. Tenholm and R.S. Broughton (1996). Effects of controlled drainage on nitrate concentrations in subsurface drain discharge. Agric. Water Manage. 29:178-199

Larsson M.H., N.J. Jarvis, G. Torstensson and R. Kasteel (1999). Quantifying the impact of preferential flow on solute transport to tile drains in a sandy field soil. J. Hydrol. 215:116-134.

Larsson, M. (1999). Quantifying macropore flow effects on nitrate and pesticide leaching in a structured clay soil. Field experiments and modeling with the MACRO and SOILN models. PhD-thesis. Swedish Univ. of Agric. Sci.

Lehman, P., F. Stauffer, C. Hinz, O. Dury and H. Flühler (1998). Effect of hysteresis on water flow in a sand column with a fluctuating capillary fringe. J. Contam. Hydrol. 33:81-100.

Lenhard, R.J., J.C. Parker and J.J. Kaluarachchi (1989). A model for hysteretic constitutive relations governing multiphase flow. 3. Refinements and numerical simulations. Water Resour. Res. 25:1727-1736.

Lewan, E. (1993). Evaporation and discharge from arable land with cropped or bare soils during winter. Measurements and simulations. Agric. For. Meteorol. 64:131-159.

Lhomme, J.-P. (1997a). An examination of the Priestley-Taylor equation using a convective boundary layer model. Water Resour. Res. 33(11):2571-2578.

Lhomme, J.-P. (1997b). A theoretical basis for the Priestley-Taylor coefficient. Boundary-Layer Meteorol. 82 (2):179-191.

Lhomme, J.-P. and B. Monteny (2000). Theoretical relationship between stomatal resistance and surface temperatures in sparce vegetation. Agric. For. Meteorol. 104(2):85-170.

Leij, F.J., W.J. Alves, M.Th. van Genuchten and J.R. Williams (1996). Unsaturated Soil Hydraulic Database, UNSODA 1.0 User's Manual. U.S. Environmental Protection Agency, Ada, Oklahoma, Report EPA/600/R-96/095, 103 pp.

Lide, D.R. (ed) (1996). Handbook of chemistry and physics. 76th ed. CRC Press, Boca Raton, FL.

Lindsey, S.D. and R.K. Farnsworth (1997). Sources of solar radiation estimates and their effect on daily potential evaporation for use in streamflow modeling. J. Hydrol. 201:348-366.

Liu, C., X. Zhang and Y. Zhang (2002). Determination of daily evaporation and evapotranspiration of winter wheat and maize by large-scale weighing lysimeter and micro-lysimeter. Agric. For. Meteorol. 111:109–120.

Llasat, M.C. and R.L. Snyder (1998). Data error effects on net radiation and evapotranspiration estimation. Agric. For. Meteorol. 91:209-221.

Loaiciga, H.A., J.B. Valdes, R. Vogel, J. Garvey and H. Schwarz (1996). Global warming and the hydrologic cycle. J. Hydrol. 174:83-127.

Mahdian, M.H. and J. Gallichand (1995). Validation of the SUBSTOR model for simulating soil water content. Trans. ASAE 38(2):513-520.

Mander, Ü., A. Kull, V. Kuusemets and T. Tamm (2000). Nutrient runoff dynamics in a rural catchment: influence of land-use changes, climatic fluctuations and ecotechnological measures. Ecol. Eng. 14:405-417.

Mansfield, T.A and C.J. Atkinson (1990). Stomatal Behaviour in Water Stressed Plants. In: Alscher, R. G. & Cumming, J. R. (eds.). Stress Responses in Plants : Adaptation and Acclimation Mechanisms. New York : Wiley-Liss. pp. 241-264.

Marshall, T.J., J.W. Homes and C.W. Rose (1996). Soil Physics. Third Edition (Reprinted 1999). Cambridge: Cambridge University Press. 453 pp.

Martinez-Lozano, J.A., F. Tena, J.E. Onrubia and J. De La Rubia (1984). Agric. For. Meteorol. 33:109-128.

McEntee, M.A. (1980). A revision of the equation relating sunshine hours to radiation income for Ireland. Irish J. Agric. Res. 19:119-125.

McKenney, M.S. and N.J. Rosenberg (1993). Sensitivity of some potential evapotranspiration estimation methods to climate change. Agric. For. Meteorol. 64:81-110.

Meija M.N., C.A. Madramotoo and R.S. Broughton (2000). Influence of water table management on corn and soybean yields. Agric. Water Manage. 46:73-89.

Mendez, J., L.D. Hinzman and D.L. Kane (1998). Evapotranspiration from a wetland complex on the arctic coastal plain of Alaska. Nordic Hydrol. 29(4/5):303-330.

Menzel, L. (1996). Modelling canopy resistances and transpiration of grassland. Phys. Chem. Earth. Vol.21(3):123-129.

Messing, I. (1993). Saturated and near-saturated hydraulic conductivity in clay soils. Measurement and prediction in field and laboratory. PhD-thesis. Swedish University of Agricultural Sciences, Uppsala, Sweden.

Messing, I. and N.J. Jarvis (1995). A comparison of near-saturated hydraulic properties measured in small cores and large monoliths in a clay soil. Soil Technol. 7:291-302.

Messing, I. and N.J. Jarvis (1993). Temporal variation in the hydraulic conductivity of a tilled clay soil as measured by tension infiltrometers. J. Soil Sci. 44:11-24.

Minasny, B., A. B. McBratney and K.L. Bristow (1999). Comparison of different approaches to the development of pedotransfer functions for water-retention curves. Geoderma 93:225-253.

Moench, A.F. and D.D. Evans (1970). Thermal conductivity and diffusivity of soil using a cylindrical heat source. Soil Sci. Soc. Am. Proc. 34:377-381.

Mohrath, D., L. Bruckler, P. Bertuzzi, J.C. Gaudu and M. Bourlet (1997). Error analysis of an evaporation method for determining hydrodynamic properties in unsaturated soil. Soil Sci. Soc. Am. J. 61:725-735.

Monteith, J.L. (1965). Evaporation and the Environment. Symp.Soc.Expl.Biol. 19:205-234.

Monteith, J.L. and M.H. Unsworth (1990). Principles of environmental physics, 2nd ed. 287 pp.

Monteith, J.L. (1995). Accommodation between transpiring vegetation and the convective boundary layer. J. Hydrol. 166:251-263.

Mualem, Y. (1976). A new model for predicting the hydraulic conductivityof unsaturated porous media. Water. Resour. Res. 12:513-522.

Mustonen, S.E. (1964). Potentiaalisen evapotranspiraation määrittämisestä. (in Finnish), Acta Agric. Fennica. 102:2.

Nemes, A., M.G. Schaap, F.J. Leij and J.H.M. Wösten (2001). Description of the unsaturated soil hydraulic database UNSODA version 2.0. J. Hydrol. 251:151-162.

Neuwirth, F. (1980). The estimation of global and sky radiation in Austria. Sol. Energy 24:421-426.

Niinemets, Ü., W. Bilger, O. Kull and J.D. Tenhunen (1999a). Responses of foliar photosynthetic electron transport, pigment stoichiometry, and stomatal conductance to interacting environmental factors in a mixed species forest canopy. Tree Physiol. 19:839-852.

Niinemets, Ü., A. Sõber, O. Kull, W. Hartung and J.D. Tenhunen (1999b). Apparent controls on leaf conductance by soil water availability and via light-acclimation of foliage structural and physiological properties in a mixed deciduous, temperate forest. Int. J. Plant Sci. 160:707-721.

Noilham J. and S. Platon (1989). A simple parameterization of land surface processes for meteorological models. Mon. Wea. Rev. 117:536-549.

Nützmann, G., M. Thiele, S. Maciejewski and K. Joswig. (1998). Inverse modelling techniques for determining hydraulic properties of coarse-textured porous media by transient outflow methods. Adv. Water Resour. 22 (3):273-284.

Oldekop, E. (1911). 'Ob isparenii iz poverhnosti petchnix basseinov' (*in Russian*) – 'On the evaporation from river watersheds'. Jurjew (present Tartu), 197 pp.

Orlandini, S. (1999). Two-layer model of near-surface soil drying for time-continuos hydrologic simulations. J. Hydrol. Engineering 4(2): 91-99.

Ortega-Farias, S.O., R.H. Cuenca and M. Ek (1996). Daytime variation of sensible heat flux estimated by the bulk aerodynamic method over a grass canopy. Agric. For. Meteorol. 81:131-143.

Paasonen-Kivekäs, M., T. Karvonen and P. Vakkilainen (2000). Impact of water table management on nutrient losses in agricultural fields. (in Finnish). In: Vakkilainen, P (Ed.) Peltoviljelyn ravinnehuuhtoutumien vähentäminen pellon vesitaloutta säätämällä. Salaojituksen Tutkimusyhdistys RY:n tiedote N:o 25, pp. 8-40.

Paasonen-Kivekäs, M., T. Karvonen, P. Vakkilainen, N. Sepahi, J. Kleemola and M. Teittinen. (1996a). Field studies on controlled drainage and recycling irrigation-drainage for reduction of nutrient loading from arable land. Water Sci. Tech. 33(4-5):333-339.

Paasonen-Kivekäs, M., M. Teittinen, J. Kleemola and T. Karvonen. (1996b). Water table management in crop production - case studies in Finland. Proc of the 6th Drainage Workshop on Drainage and Environment. ICID- Ljubljana, Slovenia, April 21-29, 1996, pp. 583-588.

Paasonen-Kivekäs, M., T. Karvonen, P. Vakkilainen, M. Teittinen and J. Kleemola (1998). Potential of water table management for abatement of nutrient load. In: Drainage in the 21st Century: Food Production and the Environment. Proceedings of the Seventh International Drainage Symposium. 8-10 March 1998, Orlando, Florida, Larry C. Brown (Ed.) Published by American Society of Agricultural Engineers, USA, pp. 370-379.

Pachepsky, Ya.,A. and W.J. Rawls (1999). Accuracy and reliability of pedotransfer functions as affected by grouping soils. Soil Sci. Soc. Am. J. 63:1748-1757.

Parlange M.B. and H. Stricker (1996). On the concept of equilibrium evaporation and the value of the Priestley-Taylor coefficient. Water Resour. Res. 32(1):161-164.

Parlange, M.B. and G.G. Katul (1992). Estimation of the diurnal variation of potential evapotranspiration from a wet bare-soil surface. J. Hydrol. (132):71-89.

Penman, H.L. (1948). Natural evaporation from open water, bare soil and grass. Proc. R. Soc. London, Ser. A, 194:120-145.

Pereira, L.S., A. Perrier, R.G. Allen and I.Alves (1999). Evapotranspiration: Concepts and future trends. J. Irr. Drain. Eng. 125(2):45- 51.

Perroux, K.M. and I. White (1988). Designs for disc permeameters. Soil Sci. SocAm. J. 52:1205-1215.

Porporato, A., F. Laio, L. Ridolfi and I. Rodriguez-Iturbe (2001). Plants in water-controlled ecosystems:active role in hydrologic processes and response to water stress III. Vegetation water stress. Adv. Water Resour. 24:725-744.

Prescott, J.A. (1940). Evaporation from a water surface in relation to solar radiation. Trans. R. Soc. Sci. Autralia 64:114-125.

Priestley, C.H.B. and R.J.Taylor (1972). On the assessment of surface heat flux and evaporation using large-scale parameters. Monthly Weather Rev. 100:81-92.

Punning. J.-M. (Ed.) (1996). Estonia in the system of global climate change. Institute of Ecology, Tallinn, Estonia, 206 pp.

Qiu G.Y., T. Yano and K. Momii (1998). An improved methodology to measure evaporation from bare soil based on comparison of surface temperature with a dry soil surface. J. Hydrol. 210:93-105.

Raats, P.A.C. (2001). Developments in soil-water physics since the mid 1960s. Geoderma 100:355-387.

Raijkai, K., S. Kabos, M.Th. van Genuchten and P.-E. Jansson (1996). Estimation of water-retention characteristics from the bulk density and particle-size distribution of Swedish soils. Soil Sci. 161:832-845.

Rawls, W.J. and D.L. Brakensiek (1989). Estimation of soil water retention and hydraulic properties. In: Morel_Seytoux, H.J. (Ed.), Unsaturated Flow in Hydrologic Modeling – Theory and Practice. Kluwe Academic Publishing, Dordrecht, pp. 275-300.

Reicosky, D.C. and D.B. Peters (1977). A portable chamber for rapid evapotranspiration measurements on field plots. Agron. J. 69:729-732.

Reintam, L. (1995). Soils in Estonia. In: Boguslavski, E.v., Limberg, P. et al. (Eds.). Boden und Düngung. Mitt. der Internat. Arbeitsgemeinschaft f. Bodenfruchtgarkeit d. IBG. Tartu, S. 122-131.

Revfeim, K.J.A. (1997). On relationship between radiation and mean daily sunshine. Agric. For. Meteorol. 86:183-191.

Revheim K.J.A. and R.B. Jordan (1976). Precision of evaporation measurements using the Bowen ratio. Boundary Layer Meteorol. 10:97-111.

Richards, L.A. (1931). Capillary conduction of liquids in porous mediums. Physics. 1:318-333.

Rietveld, M.R. (1978). A new method for estimating the regression coefficients in the formula relating solar radiation to sunshine. Agric. Meteorol., 19:243-252.

Rijtema, P.E. (1965). An analysis of actual evapotranspiration. Verlagen landbouwkundige Onderzoekingen (Agricultural Research Reports), 659, Centre for Agricultural Publishing and Documentation (Pudoc), Wageningen, the Netherlands, 107 pp.

Ritsema, C.J. (1998). Flow and transport in water repellent sandy soils. PhD-thesis. Wageningen University, 213 pp.

Roostalu, H. (1978). Hyrological and physical characteristics and the watersupplying capacity of different soils (*in Russian*). EMMTUI, XLII:48-60.

Roostalu, H., P. Kasearu and M.Rei (1996). Emissions in Estonia's agriculture and animal husbandry. In: Estonia in the system of global climate change. (Ed.) J.-M. Punning. Institute of Ecology. Tallinn. Publication 4:17-25.

Rose, C.W. and M.L. Sharma (1984). Summary and recommendations of the workshop on evapotranspiration of plant communities. Agric. Water Manage. 8:325-342.

Rosset, M., M. Riedo, A. Grub, M. Geissmann and J. Fuhrer (1997). Seasonal variation in radiation and energy balances of permanent pastures at different altitudes. Agric. For. Meteorol. 86:245-258.

Russak, V., A. Jõeveer and A. Kallis (1997). Atmospheric transmittance and its long-term changes in Estonia. Meteorol. Zeitschrift, N.F. 6:137-141

Russak, V. (1998). Seasonal peculiarities of long-term changes in radiation regime in Estonia. In: Climate Change Studies in Estonia, Eds. T.Kallaste and P.Kuldna. Tallinn, pp. 13-20.

Russak, V.K. (1990). Trends of solar radiation, cloudiness and atmospheric transparency during recent decades in Estonia. Tellus 42B:206-210.

Sandsborg, J. and B. Olofsson (1980). Observation on the water balance for winter wheat, barley and fallow. Swedish J. Agric. Res. 10:17-23.

Saugier, B. and E.A. Ripley (1978). Evaluation of the aerodynamic method of determination fluxes over natural grassland. Q. J. Roy. Meteorol. Soc. 104:257-270.

Schaap, M.G. and F.J. Leij (2000). Improved prediction of unsaturated hydraulic conductivity with the Mualem-van Genuchten model. Soil Soc. Am. J. 64:843-851.

Scholefield, D., K.C. Tyson, E.A. Garwood, A.C. Armstrong, J. Hawkins and A.C. Stone (1993). Nitrate leaching from grased grassland lysimeters:effect of fertilizer input, field drainage, age of sward and patterns of wather. J. Soil Sci. 44:601-613.

Schuh, W.M. and R.L. Cline (1990). Effect of soil properties on unsaturated hydraulic conductivity pore-interaction factors. Soil Sci. Soc. Am. J. 54:1509-1519.

Sculze, E.-D., R. Leuning and F.M. Kelliher (1995). Environmental regulation of surface conductance for evaporation from vegetation. Vegetatio 121:79-87.

Szeicz, G. and I.F.Long (1969). Surface resistance of crop canopies. Water Resour. Res. 5:622–633.

Shuttleworth, W.J. (1992). Chapter 4, Evaporation. In Handbook of Hydrology, D.R. Maidment (ed.), McGRAW-HILL, INC.

Shuttleworth, W.J. and J.S. Gurney (1990). The theoretical relationship between foliage temperature and canopy resistance in sparse crops. Q.J.R. Meteorol. Soc. 116:497-519.

Shuttleworth, W.J. and J.S. Wallace (1985). Evaporation from sparce crops - an energy combination theory. Q.J.R. Meteorol. Soc. 111:839-855.

Simunek, J. and M.Th. van Genuchten (1996). Estimating unsaturated soil hydraulic properties from tension disc infiltrometer data by numerical inversion. Water Resour. Res. 32:2683-2696.

Skaggs, R.W. (1978). A water management model for shallow water table soils. Report No. 134, Water Resources Research Institute, North Carolina state University, Raleigh.

Skaggs, R.W. (1980). DRAINMOD – Reference report: Methods for design and evaluation of drainage – water management systems for soils with high watertables. USDA-SCS, SouthNational Technical Center, Fort Worth, TX.

Skaggs, R.W. and J.W. Gilliam (1981). Effect of drainage system design and operation on nitrate transport. Trans. ASAE 24:929-934.

Skaggs, R.W., J.E. Parsons and K.D. Konyha (1988). DRAINMOD version 4.0 – An overview. ASAE Paper No. 88-2563. St. Joseph, MI: ASAE.

Smedema L.K. and D.W. Rycroft (1983). Land Drainage: Planning and Design of Agricultural Drainage System. Batsford Academic and Educational Ltd. London, 376 pp.

Smith, M, R.G. Allen, J.L. Monteith, A. Perrier, L.S. Pereira and A. Segeren (1991). Report of the expert consultation on procedures for revision of FAO guidelines for prediction of crop water requirements. FAO, Food and Agricultural Organization of the United Nations, Rome.

Smith, J.T. and R.O. Evans (1998). Evaluation of BMPs to improve drainage water quality from agricultural land irrigated with swine lagoon effluent. In: Brown, L. C.(Ed.) (1998). Drainage in the 21st Century: Food Production and the Environment. Proceedings of the Seventh International Drainage Symposium. 8-10 March 1998, Orlando, Florida, Published by ASAE, USA, pp. 9-16.

Souch, C., C. Wolfe and C.S.B. Grimmond (1996). Wetland evaporation and energy partitioning:Indiana Dunes National Lakeshore. J. Hydrol. 184:189-208.

Spinnanger, G. (1968). Global radiation and duration of sunshine in Northern Norway and Spitsbergen. Meteorol. Ann. 5:3.

Stranhill, G. (1965). A comparison of four methods of estimating solar radiation. Arid Zone Res. 25: 55-61.

Stamm, C. (1997). Rapid transport of phosphorus in drained grassland soils. PhD Dissertation No. 12486, Swiss Federal Institute of Technology Zürich.

Stauffer, F. and W. Kinzelbach (2001). Cyclic hysteretic flow in porous medium column: model, experiment, and simulations. J. Hydrol. 240:264-275

Steiner, J.L., T.A. Howell and A.D. Schneir (1991). Lysimetric evaluation of daily potential evapotranspiration models for grain sorghum. Agronomy J. 83:240-247.

Stevenson, F.J. (1986). Chapter 4, The nitrogen cycle in soil: global and ecological aspects. In: F.J. Stevenson. Cycles of soil. A Wiley-Interscience publication. pp. 106-180.

Stewart, R.B. and W.R Rouse (1977). Substantiation of the Priestly and Taylor parameter a=1.26 for potential evaporation at high latitudes. J. Appl. Meteorol. 16:649-650.

Stokmans, J.A. (1971). The empirical relation between global radiation and duration of sunshine for several European meteorological stations. Dpt. Irrigation and Civil Engineering, Agric. Univ., Wageningen. (Rietveld, 1978).

Stolte, J. (1977). Determination of the saturated hydraulic conductivity using the constant head method. In: Manual for soil physical measurements, J. Stolte (ed.). Wageningen, DLO Winand Staring Centre, Technical Document 37:27-32.

Stuyt, L.C.P.M, W. Dierickx and J.M. Beltrán (2000). Materials for subsurface land drainage systems. FAO irrigation and drainage paper 60. Rome.

Sulev, M. (1990). Actinometrical instruments. In Climate of Tartu and its changes during the recent decades. Est. Academy of Science, pp. 23-34.

Sustainable water management strategies for the land drainage and irrigation sector (1998). Estonia, TCP/EST/5612. Field document. Food and Agriculture Organization of the United Nations, Rome, 1998, 117 pp.

Takagi, K., T. Tsuboya and H. Takahashi (1998). Diurnal hysteresis of stomatal and bulk surface conductances in relation to vapor pressure deficit in a cool-temperate wetland. Agric. For. Meteorol. 91:177-191.

Tamari, S., L. Bruckler, J. Halbertsma and J Chadoeuf (1993). A simple method for determing soil hydraulic properties in the laboratory. Soil Sci. Soc. Am. J. 5:642-651.

Tamm, T. (1994). Field experiments on the dynamics of soil moisture. In: (Eds. Kettunen, J., Granlund, K. Paasonen-Kivekäs, M. and H. Sirviö) Spatial and temporal variability and interdependencies among hydrological processes. Prceedings of a Nordic Seminar Kirkkonummi, Finland, pp. 14-16.

Tamm, T. (1998a). Parameters of evapotranspiration in case of altered climatic conditions. In: Proc. of The Second International Conference on Climate and Water, Espoo, Finland, 17-20 August 1998, 2:719- 728.

Tamm, T. (1998b). Assessment of climate change impact on areal evapotranspiration. In: Climate Change Studies in Estonia, Eds T.Kallaste and P.Kuldna. Tallinn. pp. 127-132.

Tamm, T. (1988c). Impact of climate change on drained land. In: Country Case Study on Climate Change Impacts and Adaptation Assessments in the Republic of Estonia, Eds. A.Tarand and T.Kallaste. Tallinn, Ch. 5.7.4, pp. 93-95.

Tamm, T. (2001a). Typical pattern for nitrate leaching from agricultural land in Estonia. In: 'Environmental Impact and Water Management in a Catchment Area Perspective'. Proceedings of the Syposium dedicated to the 40th Anniversary of Institute of Environmental Engineering at Tallinn Technical University. 24-26 September, 2001, Tallinn, Estonia, pp. 89-93.

Tamm, T. (2001b). Nitrate leaching from agricultural land in Estonia: two case studies. In: 'First Baltic Syposium on Environmental Chemistry.' Abstracts. 26-29 September, 2001, Tartu, Estonia, pp. 93-94.

Tamm, V. (1975). Vihmutatavate kultuuride veetarve ja kastmire•iim Eesti NSV mineraalmuldadel (*in Estonian*, Water demand and irrigation regime of the irrigated agricultural crops in mineral soils of Estonian SSR). Tartu, Estonian Agricultural Academy, 247 pp.

Tamm, V. (1994). Estimating evapotranspiration from grassland in Estonia. Proc.NJF Seminar No 247, Uppsala, pp. 90-92.

Tarand, A. and T. Kallaste (Eds.) (1998). Country Case Study on Climate Change Impacts and Adaptations Assessments in the Republic of Estonia. UNEP/GEF Report, Tallinn, Estonia, 146 pp.

Thornton, P.E. and S.W. Running (1999). An improved algorithm for estimating incident daily solar radiation from measurements of temperature, humidity, and precipitation. Agric. For.. Meteorol. 93:211-228.

Thunholm, B. (1990). A comparison of measured and simulated soil temperature using air temperature and soil surface energy balance as boundary conditions. Agric. Forest Meteorol. 53:59-72.

Tiktak, A. (1999). Modeling non-point source pollutants in soils. Application to the leaching and accumulation of pesticides and cadmium. PhD-thesis. Wageningen University, 232 pp.

Timmusk, T. (1996). Effects of controlled drainage on nitrate nitrogen in the soil profile. (*In Estonian*). Trans. Estonian Agric. Univ. 186:47-55.

Todd, R.W., Klocke, N.L., Hergert, G.W. and A.M. Parkhurst (1991). Evaporation from soil influenced by crop shading, crop residue, and wetting regime. Trans. ASAE 34(2):461- 466.

Vakkilainen, P. (1982). 'Maa-alueelta tapahtuvan haihdunnan arvioinnista' (in Finnish) – 'On the estimation of evapotranspiration'. Ph.D Paper. Oulun Yliopisto, 146 pp.

Vereecken, H., J. Feyen, J. Maes and P. Darius (1989). Estimating the soil moisture retention characterisic from texture, bulk density, and carbon content. Soil Sci. 148:389-403.

Vereecken, H., J. Maes and J. Feyen (1990). Estimating unsaturated hydraulic conductivity from easily measured soil properties. Soil Sci. 149:1-12.

Viane, P., H. Vereecken, J. Diels and J. Feyen (1994). A statistical analysis of six hysteresis models for the moisture retention characteristics. Soil. Sci. 157:345-355.

Viiralt, R. (1996). Rohumaade bioproduktsiooni formeerumine ning aineringed (muld-rohustu-loom) ja ainete bilansid rohumaal (*in Estonian*, Bioproduction, nutrient cycles (soil-plant-animal) and balance at grassland). ETF grandiprojekt nr. 198.

Vlotman F.W., L.S. Willardson and W. Dierickx (2000). Chapter 5. Design of drain envelopes:theory and testing. In:Envelope design for subsurface drains. ILRI publication 56. Wageningen, The Netherlands, pp. 121-246.

Vos, J.A. de (1997). Water flow and nutrient transport in a layered silt loam soil. PhD-thesis, Wageningen University, 284 pp.

Vörösmarty, C.J., C.A. Federer and A.L. Schloss (1998). Potential evaporation functions compared on US watersheds: Possible implications for global-scale water balance and terrestrial ecosystem modeling. J. Hydrol. 207:147-169.

Wagner, B., V.R. Tarnawski, V. Hennings, U. Müller, G. Wessolek and R. Plagge (2001). Evaluation of pedo-tranfer functions for unsaturated soil hydraulic conductivity using an independent data set. Geoderma 102:275-297.

Wallace, J.S. (1995). Calculation evaporation: resistance to factors. Argic. For. Meteorol. 73:353-366.

Wang, D., S.R.Yates and F.F. Ernst (1998). Determining soil hydraulic properties using tension infiltrometers, time domain reflectrometry, and tensiometers. Soil Sci. Soc. Am. J. 62:318-325.

Wesström, I., I. Messing, H. Linnér and J. Lindström (2001). Controlled drainage - effects on drain outflow and water quality. Agric. Water Manage. 47:85-100.

Wijk, W.R. van and D.A. De Vries (1963). Periodic temperature variations. In Physics of Plant Environment, ed. Van Wijk, W.R., North-Holland Publishing Company, Amsterdam.

Wind, G.P. (1966). Capillary conductivity data estimated by a simple method. In: P.E. Rijtema and H. Wassink (Eds), Water in the unsaturated zone. Proceedings of the Wageningen symposium, June 1966, Vol. 1. IASH Gentgrugge/ Unesco Paris, pp. 181-191.

WMO (1966). Measurement and estimation of evaporation and evapotranspiration. World Meteorological Organization, Geneva, Technical Note 83.

Wright, J.A., A. Shirmohammadi, W.L.Magette, J.L. Fouss, R.L. Bengtson and J.E. Parsons (1992). Water table management practice effects on water quality. Trans. ASAE 35 (3):823-830.

Wright, J.L. (1982). New evapotranspiration crop co-efficients. J.Irrig.Drain. Eng., ASCE 108(IR2):57-74.

Wright, J.L. and M.E Jensen (1972). Peak water requirements of (15) crops in Southern Idaho. J.Irrig. Drain. Eng., ASCE 24(IR1):193-201.

Wösten, J.H.M. and M.Th. van Genuchten (1988). Using texture and other soil properties to predict the unsaturated soil hydraulic functions. Soil Sci. Soc. Am. J. 52:1762-1770.

Wösten, J.H.M., P.A. Finke and M.J.W. Jansen (1995). Comparison of class and continuous pedotransfer functions to generate soil hydraulic characteristics. Geoderma 66:227-237.

Wösten, J.H.M. (1997). Pedotransfer functions to evaluate soil quality. In: Gregorich, E.G., Carter, M.R. (Eds.), Soil Quality for Crop Production and Ecosystem Health. Developments in Soils Science, vol. 25, Elsevier, Amsterdam, pp. 221-245.

Wösten, J.H.M., A. Lilly, A. Nemes, and C. Le Bas (1999). Development and use of a database of hydraulic properties of European soils. Geoderma 90:169-185.

Wösten, J.H.M., Ya.A. Pachepsky and W.J. Rawls (2001). Pedotransfer functions: bridging the gap between available basic soil data and missing soil hydraulic characteristics.

Wösten, J.H.M., A. Lilly, A. Nemes and C. Le Bas (1999). Development and use of a database of hydraulic properties of European soils. Geoderma 90:169-185.

Zavaratto, L., N. Jarvis, and L. Persson (1999). Use of similar media scaling to characterize spatial dependence of near-saturated hydraulic conductivity. Soil Sci. Soc. Am. J. 64:486-492.